Integrating Non-viral Gene Therapy and 3D Bioprinting for Bone, Cartilage and Osteochondral Tissue Engineering

Tomas Gonzalez Fernandez, B.Sc., M.Sc.

A thesis submitted to the University of Dublin in partial fulfilment of the requirements for the degree of

Doctor in Philosophy

Trinity College Dublin, December 2017

Supervisors: Prof. Daniel J. Kelly and Prof Fergal J. O'Brien

Internal examiner: Prof. Conor T. Buckley

External examiner: Prof. Magali Cucchiarini Madry

Abstract

INTEGRATING NON-VIRAL GENE THERAPY AND 3D BIOPRINTING FOR BONE, CARTILAGE AND OSTEOCHONDRAL TISSUE ENGINEERING
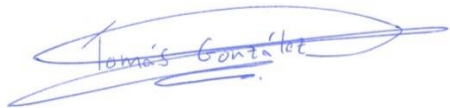
PhD thesis by

Tomas Gonzalez Fernandez

The repair of osteochondral defects, affecting both the articular cartilage and the underlying subchondral bone, is key for the effective recovery of joint homeostasis and the prevention of further cartilage degeneration and the onset of osteoarthritis (OA). Although important advances have been made in the field of tissue engineering to regenerate these injuries, the traditional approaches based on the formation of homogenous tissues fail to recapitulate the spatial complexity of the osteochondral unit. The objective of this thesis was to engineer a multiphasic tissue suitable for osteochondral defect regeneration by combining 3D bioprinting and non-viral gene delivery to spatially regulate the differentiation of mesenchymal stem cells (MSCs). Realising this objective first required (1) optimisation of the non-viral gene delivery vector, (2) the identification of suitable therapeutic gene combinations to direct MSC differentiation and (3) the development of printable biomaterials, also known as bioinks, which were supportive of non-viral gene delivery both *in vitro* and *in vivo*. These gene activated bioinks were capable of spatially directing MSC fate towards either the osteogenic or chondrogenic pathway. In turn, this enabled the printing of mechanically robust biphasic osteochondral constructs with zonally confined gene delivery and spatially defined stem cell differentiation and matrix deposition. *In vivo*, these printed constructs promoted the development of tissue mimicking key aspects of the osteochondral unit. In conclusion, this thesis highlights a promising and novel approach for the incorporation of gene delivery for 3D bioprinting ande engineering of therapeutically relevant and structurally complex musculoskeletal tissues.

Declaration

I declare that this thesis has not been submitted as an exercise for a degree at this or any other university and it is entirely my own work.

I agree to deposit this thesis in the University's open access institutional repository or allow the Library to do so on my behalf, subject to Irish Copyright Legislation and Trinity College Library conditions of use and acknowledgement.

Tomas Gonzalez Fernandez

Dublin, 19th of December, 2017

Summary

Articular cartilage injuries can cause pain and disability and show poor capacity for self-repair. In addition, if not treated, they can predispose patients for osteoarthritis (OA). OA is a prevalent joint disease and affects both the articular cartilage and the underlying subchondral bone, and results in severe joint degradation, pain and loss of function. At present, there is no cure for OA and most current therapies for cartilage repair and regeneration, such as microfracture, osteochondral autografts and autologous chondrocyte implantation, are limited and only suitable for treating focal defects of the joint surface. This has motivated the field of cartilage and osteochondral tissue engineering (TE) to find new approaches to regenerate damaged joints and thus, prevent the onset of OA. Traditional tissue engineering approaches typically involve the homogenous distribution of cells (e.g. mesenchymal stem cells) and growth factors in mechanically weak biomaterials, in an attempt to produce uniform tissues that are not suitable for treating large osteochondral defects. It is evident that new strategies are required to recapitulate the complexity of interfacial tissues such as the osteochondral unit.

Novel biofabrication techniques such as 3D bioprinting of cells and growth factors in hydrogel bioinks could be a potential solution, as this approach offers precise layer-by-layer spatial control and could allow for zonal phenotypic regulation of host and transplanted cells to guide tissue and organ regeneration. However, the spatial presentation of signalling molecules such as recombinant growth factors can be challenging, as such proteins can easily diffuse through the hydrogels that are commonly used as bioinks, thereby preventing the spatial confinement of such cues to required regions of the printed construct. Engineering cells to locally produce growth and transcription factors through the incorporation of non-viral gene delivery into a 3D printable material might offer a promising alternative for localised and sustained gene delivery of growth and transcription factors. This thesis aimed to investigate the combination of nanoparticle-based non-viral gene delivery and biofabrication techniques for the development of a new generation of 3D bioprinted gene activated constructs for osteochondral TE.

Firstly, the capacity of nanohydroxyapatite (nHA) to deliver reporter and therapeutic genes to mesenchymal stem cells (MSCs) encapsulated in alginate hydrogels was explored. Successful sustained transfection and overexpression of therapeutic genes offered by this gene activated alginate hydrogels led to either chondrogenic or osteogenic differentiation of MSCs depending of the delivered gene combination. The osteogenic potential of this approach confirmed the relevance of nHA-mediated transfection in alginate gels for endochondral bone tissue engineering. However, the possible osteoinductivity of nHA could limit its use as gene carrier for stable cartilage tissue engineering.

The success of non-viral gene delivery ultimately depends on the choice of gene delivery vector. Recognizing the inherent osteogenicity of nHA, novel and stablished non-viral gene delivery vectors were compared for their capacity to support chondrogenesis and osteogenesis of MSCs. The differences found in cell viability, morphology, gene transcription and MSC fate between the use of polyethylenimine (PEI), nHA and the RALA amphipathic peptide (RALA) as nanoparticle-based gene carriers demonstrated that the differentiation of MSCs through the application of non-viral gene delivery strategies depends not only on the gene delivered, but also on the delivery vector itself. When delivering the same genetic cargo, nHA vectors promoted mineralization and MSC hypertrophy, while RALA transfected cells promoted a more stable cartilage phenotype.

After identifying nHA-mediated gene delivery for the osseous layer of a multiphasic osteochondral construct, MSC transfection using the RALA peptide was assessed for stable chondrogenic differentiation and the formation of *de novo* hyaline cartilage. Parameters for RALA-mediated gene delivery to MSCs were optimized and combinatorial gene delivery of chondrogenic growth and transcription factors was shown to promote chondrogenesis of MSCs and suppress their progression towards the endochondral route.

As this thesis progressed, and once the best combinations of non-viral gene delivery vectors and therapeutic genes for either chondrogenesis or osteogenesis of MSCs were identified, we sought to incorporate these nanoparticle-pDNA complexes into alginate-based bioinks to gain spatiotemporal control over gene delivery within 3D

5

printed constructs. nHA-plasmid DNA (pDNA) complexes entrapped into calcium chloride (CaCl$_2$) pre-crosslinked alginate hydrogels were used to co-print polycaprolactone (PCL) fibre reinforced constructs able to drive bone formation *in vivo*. In addition, the incorporation of RALA-mediated gene delivery of chondrogenic factors in alginate-methylcellulose (ALG-MC) hybrid gels resulted in pore-forming bioinks capable of *in vivo* cartilage tissue formation.

Finally these developed gene activated bioinks were used to engineer mechanically robust, bi-phasic osteochondral constructs capable of zonal MSC differentiation and the recapitulation of certain key biochemical gradients found in the native osteochondral unit.

In conclusion, this thesis describes the development of a novel strategy for the engineering of multiphasic gene activated osteochondral constructs able to direct MSC phenotype to generate spatially complex tissues. This work highlights the synergies that can be achieved by combining 3D bioprinting and non-viral combinatorial gene delivery, particularly for the engineering of complex musculoskeletal interface tissues.

Acknowledgements

Having arrived to this final stage of my PhD means the last steps of an unexpected journey that started five years ago when my supervisor Daniel Kelly opend me the gates of Trinity College to work with him as a summer intern after my Erasmus year. He didn´t only opened me the gates of this excellent institution, but also opened my mind and intellect to scientific research. So the first person I would like to thank is my supervisor Daniel Kelly for being an excellent mentor, guide and colleague during all these years.

I also would like to acknowledge my second supervisor Fergal O'Brien who has been always welcoming and available to share his knowledge and advice.

Although without Fergal and Danny the scientific work in this thesis would not have been possible, without the unconditional support of my family and the guidance of my father Victor and my mother Amaya this thesis would not have been possible.

Massive thanks to current and previous postdocs, Grainne, Binu, Erica, Swetha and Fiona, your help and attention made this work a reality and I can´t thank you enough, everyone in Trinity Centre for Bioengineering and in the Tissue Engineering Research Group in Royal College of Surgeons, and all my collaborators all over the world, as Redl Heinz said to me once, Art is I but Science is we.

I would like to make a special mention to my friends and colleagues Lara, Pedro, Andy, Susan and Dinorath who started this adventure with me and have been there in the lab, in the pub or at home to make my PhD and unforgettable experience that will always be engraved in my heart.

I also want to acknowledge Trinity College Dublin and the country of Ireland for adopting me and giving me the opportunity and all the facilities to develop this work, although it was always rainy, my memories of my time here could not be warmer.

Contents

List of Figures

18

of the pellets after 28 days of *in vitro* culture. Scale bar = 100 μm for the 20x images and 1 mm for the 4x images. (*) Denotes significance (n=4, p<0.05) to the CTRL- and pGFP groups; (***)

Percentage of living cells in the printed gels 1 day after fabrication. Quantification of DNA/ww (D), GAG/ww (E), collagen/ww (F) and calcium/ww (G) in the 3D printed gels after 28 days of *in vitro* culture in chondrogenic media. (H) Histological and immunohistochemical analysis of the 3D printed gels after 28 days of *in vitro* culture. (Scale bar = 0.5 mm). (*) Denotes significance (n=4, p<0.05); (**) denotes significance (n=4, p<0.01).

Fig.7.4. Characterization of temporal RALA-pDNA release and transfection of encapsulated MCS in the alginate and ALG-MC gels. (A) CryoSEM images of the encapsulated RALA-pDNA complexes in the alginate and ALG-MC (1:1 and 1:2) gels. Scale bar = 200 μm. (B) Encapsulation efficiency of the RALA-pDNA complexes in the different gels. (C) Percentage of the released RALA-pDNA complexes in the different gels at 12 h, 24 h, day 3, 7 and 10. (D) GFP positive encapsulated MSCs in the alginate and ALG-MC containing RALA-pGFP complexes at day 1, 3, 7 and 10 after fabrication. Scale bar = 250 μm. (E) Luciferase quantification in the media of cell laden alginate and ALG-MC gels containing RALA-pLUC complexes at day 1, 3, 7 and 11. (D) DNA quantification in the cell laden alginate and ALG-MC gels containing RALA-pLUC complexes at day 1, 3, 7 and 11. (*) Denotes significance (n=4, p<0.05) in comparison to the rest of the groups at the same time point; (**) denotes significance (n=4, p<0.01) in comparison to the rest of the groups at the same time point; (ns) denotes no significance (n=4, p>0.05).

Fig.7.5. *In vitro* RALA-mediated gene delivery in 3D printed ALG-CA and ALG-MC gels. (A) Schematic of the encapsulation of MSCs and RALA-pLUC complexes into the alginate-based bioinks and 3D printing to produced gene activated constructs in which transfection could be monitored through measuring the luciferase in the culture media. (B) Macroscopic pictures of the 3D printed gene activated gels. Live/dead staining in the ALG-Ca control (CTRL) (C), ALG-Ca RALA-pLUC (RALA-pLUC Ca) containing gels (D) and ALG-MC RALA-pLUC (RALA-pLUC MC) containing gels (E) 1 day after fabrication. Scale bar = 1 mm for the large magnification pictures and 250 μm for the higher magnification. (F) DNA quantification in the CTRL, RALA-pLUC Ca and RALA-pLUC MC gels at different time points. (G) Luciferase quantification in the culture media of the tested gels at day 1, 3, 7 and 14 after fabrication. (*) Denotes significance (n=4, p<0.05) in comparison to the rest of the groups at the same time point; (**) denotes significance (n=4, p<0.01) in comparison to the rest of the groups at the same time point; (***) denotes significance (n=4, p<0.001) in comparison to the rest of the groups at the same time point.

List of tables

Nomenclature

°C	Degrees Celsius
2D	2 dimensional
3D	3 dimensional
A	Appendix
AB	Antibody
ACAN	Aggrecan
ACI	Autologous chondrocyte implantation
ADAMT	Desintegrin and metalloprotease with thrombospondin motifs
ALG-MC	Alginate-methylcellulose
ALP	Alkaline phosphatase
ANOVA	Analysis of variance
AR	Alizarin red
ASC	Adipose-derived stem cell
Au-NP	Gold nanoparticle
BMP	Bone morphogenic protein
BMSC	Bone marrow-derived mesenchymal stem cell
BSA	Bovine serum albumin
$CaCl_2$	Calcium chloride
CaP	Calcium phosphate
CDM	Chemically defined medium
CDMP	Cartilage derived morphogenic protein
CHM1	Chondromodulin 1
CNT	Carbon nanotube
CO_2	Carbon dioxide
COMP	Cartilage oligomeric matrix protein
CPP	Cell penetrating peptide
cryo-SEM	Cryogenic scanning electron microscopy
cT	Comparative threshold
CTRL	Control
DKK1	Cickkopf 1 homolog
DMEM	Culbecco´s modified eagle medium
DMMB	Dimethylmethylene
DNA	Deoxyribonucleic acid
ECM	Extracellular matrix
EDTA	Ethylenediaminetetraacetic acid
ELISA	Enzyme-linked immunosorbent assay
FBS	Foetal bovine serum
FDA	Food and drug administration
FDM	Fused depostion modelling
FGF	Fibroblast growth factor

FRZB	Frizzled related protein
GAB	Gene activated bioink
GAG	Glycosaminoglycan
GAM	Gene activated matrix
GAPDH	Glyceraldehyde-3-phosphate dehydrogenase
GELMA	Gelatinmethacryloyl
GFP	Green florescent protein
GREM1	Gremlin 1
H&E	Hematoxylin and eosin
HA	Hydroxyapatite
HCl	Hydrochloric acid
HDAC4	Histone deacetilase 4
HIF-1α	Hypoxia inducible factor 1 alpha
HIV	Human immunodeficiency virus
HPRA	Health products regulatory authority
HUVEC	Human umbilical vein endothelial cell
HyA	Hyaluronic acid
i.e.	*Id est*
IGF	Insulin growth factor
IHH	Indian hedgehog
IL-1	Interleukin 1
IL-1Ra	Interleukin 1 receptor antagonist
ITS	Insulin transferring selenium
LB	Luria Bertani
LUC	Luciferase
MAPK	Mitogen-activated protein kinase
microCT	Micro computed tomography
miRNA	Micro RNA
MMP	Matrix metalloprotease
MNP	Magnetic nanoparticle
MSC	Mesenchymal stem cell
NGF	Nerve growth factor
nHA	Nanohydroxyapatite
O_2	Oxygen
OA	Osteoarthtitis
OPF	Oligo[poly(ethyleneglycol)fumarate]
ORO	Oil-red-o
PBS	Phosphate buffered saline
PCL	Polycrapolactone
PCM	Pericellular matrix
PCR	Polymerase chain reaction

PDF	Platelet derived factor
PDMS	Polydimethylsiloxan
pDNA	Plasmid DNA
PEG	Polyetyleneglycol
PEI	Polyethilenimine
PFA	Paraformaldehyde
PLG	Poly(lactide-co-glycolide)
PLGA	Polyglycolic acid
PLL-PA	Poly(L-lysine)-palmitic acid
pO_2	Oxygen pressure
PTD	Peptide transduction domain
PTH	Parathyroid hormone
PTHrP	Parathyroid hormone receptor protein
rAAV	Recombinant adeno-associated virus
RALA	RALA peptide
RFP	Red fluorescent protein
RM	Regenerative medicine
RNA	Ribonucleic acid
RPHPLC	Reversed-phase high-performance liquid chromatography
RPM	Revolutions per minute
RT	Room temperature
RUNX2	Runt-related transcription factor 2
SEM	Scanning electron microscopy
siRNA	Small interfering RNA
SMAD	Mothers against DPP homolog
SOX	Sex-determining region Y
SV40	Simian virus 40
TAPP	Tiacrylate/amine polycationic polymer
TE	Tissue engineering
TEM	Transmission electron microscopy
TetOn	Tracycline-on
TGF-β	Transforming growth factor beta
TIMP	Tissue inhibitors of metalloprotease
TMC	N,N,N-trimethyl chitosan chloride
TNFα	Tumor necrosis factor alpha
UPW	Ultrapure water
VEGF	Vascular endothelyal growth factor
WW	Wet weight
α2M	Alpha 2 macroglobulin
β-TCP	Beta tricalcium phosphate

Publications

Journal articles

Gonzalez-Fernandez T., Tierney E.G., Cunniffe G.M., O'Brien F.J., Kelly D.J., 2016. Gene Delivery of TGF-β3 and BMP2 in an MSC-Laden Alginate Hydrogel for Articular Cartilage and Endochondral Bone Tissue Engineering. Tissue Engineering Part A 22 (9-10), 776-787.

Gonzalez-Fernandez T., Cunniffe G.M., Daly A.C., Sathy B.N., Jeon O., Alsberg E., Kelly D.J., 2017. Three-Dimensional Bioprinting of Polycaprolactone Reinforced Gene Activated Bioinks for Bone Tissue Engineering. Tissue Engineering Part A 23 (17-18), 891-900.

Gonzalez-Fernandez T., Sathy B.N., Hobbs C., Cunniffe G.M., McCarthy H.O., Dunne N.J., Nicolosi V., O'Brien F.J., Kelly D.J., 2017. Mesenchymal Stem Cell Fate Following Non-viral Gene Transfection Strongly Depends on the Choice of Delivery Vector. Acta Biomaterialia 55, 226-238.

Conference abstracts

Gonzalez-Fernandez T., Tierney E.G., O'Brien F.J., Kelly D.J. Gene-activated Alginate Hydrogels for Cartilage tissue engineering. Proceedings of the 20th Annual Conference of the Section of Bioengineering of the Royal Academy of Medicine in Ireland, January 2014, Limerick, Ireland.

Gonzalez-Fernandez T., Tierney E.G., O'Brien F.J., Kelly D.J. Alginate Hydrogels as a 3D Gene Delivery Platform for Cartilage Tissue Engineering. Tissue Engineering International and Regenerative Medicine Society (TERMIS), European Chapter, June 2014, Italy, Genoa.

Gonzalez-Fernandez T., Tierney E.G., O'Brien F.J., Kelly D.J. Gene-activated Alginate Hydrogels for Articular Cartilage and Endochondral Bone Tissue Engineering. 4th TERMIS World Congress, September 2015, Boston, USA.

Gonzalez-Fernandez T., Sathy B.N., O'Doherty M., McCarthy H.O., Dunne N.J., O'Brien F.J., Kelly D.J. MSC fate following non-viral transfection with therapeutic genes strongly depends on the choice of gene delivery vector. Proceedings of the 22nd Annual Conference of the Section of Bioengineering of the Royal Academy of Medicine in Ireland, January 2016, Galway, Ireland.

Gonzalez-Fernandez T., Sathy B.N., McCarthy H.O., Dunne N.J., O'Brien F.J., Kelly D.J. Alginate hydrogels incorporating cell penetrating peptide-mediated gene delivery for cartilage tissue engineering. Tissue Engineering and Regenerative Medicine International Society (TERMIS), European Chapter, June 2016, Uppsala, Sweden.

Gonzalez-Fernandez T., Sathy B.N., McCarthy H.O., Dunne N.J., O'Brien F.J., Kelly D.J. MSC fate following non-viral transfection with therapeutic genes strongly depends on the choice of gene delivery vector. Tissue Engineering and Regenerative Medicine International Society (TERMIS), European Chapter, June 2016, Uppsala, Sweden.

Gonzalez-Fernandez T., Daly A.C., Freeman F., Jeon O., Alsberg E., Dunne N.J., McCarthy H.O., O'Brien F.J., Kelly D.J. Gene Activated Bioinks for Spatial Gene Delivery in Osteochondral Tissue Engineering. Proceedings of the 23rd Annual Conference of the Section of Bioengineering of the Royal Academy of Medicine in Ireland, January 2017, Belfast, U.K.

Gonzalez-Fernandez T., Sathy B.N., Hobbs C., Cunniffe G.M., McCarthy H.O., Dunne N.J., Nicolosi V., O´Brien F.J., Kelly D.J. Mesenchymal Stem Cell Fate Following Nanoparticle-based Gene Transfection Strongly Depends on the Choice of Delivery Vector. International Society for Stem Cell Research (ISSCR) Annual Meeting, June 2017, Boston, U.S.A.

Gonzalez-Fernandez T., Freeman F., Daly A., Jeon O., Alsberg E., Dunne N.J., McCarthy H.O., O'Brien F.J., Kelly D.J. Zonal 3D Printing of Cell-laden Gene Activated Bioinks for Interface Tissue Engineering. International Society for Stem Cell Research (ISSCR) Annual Meeting, June 2017, Boston, U.S.A.

Gonzalez-Fernandez T., Freeman F., Daly A., Jeon O., Alsberg E., Dunne N.J., McCarthy H.O., O'Brien F.J., Kelly D.J. Spatial Deposition of Gene Activated Bioinks For Osteochondral Tissue Engineering. Tissue Engineering and Regenerative Medicine International Society (TERMIS), European Chapter, July 2016, Davos, Switzerland.

CHAPTER 1

Introduction

1.1. Cartilage damage and osteoarthritis: pathology, treatment and social burden

Focal articular cartilage defects are a common pathology of the knee joint. These lesions originate due to trauma and/or high physical activity, are associated with intense pain and disability and show poor capacity for self-repair due to the avascular nature of cartilage and the low mitotic activity of chondrocytes, the resident cell type within the tissue. Furthermore, chondral and osteochondral (defects that affect both the articular cartilage and the underlying subchondral bone) can predispose patients to osteoarthritis (Buckwalter and Mankin, 1998).

Osteoarthritis (OA) is the most prevalent chronic joint disease and is associated with intense pain and loss of function in the affected joint (Bijlsma et al., 2011). It affects 10% of men and 18% of women over 60 years of age (Woolf and Pfleger, 2003), generating a high socio-economic burden in developed countries (Reginster, 2002; Woolf and Pfleger, 2003). The medical care expenditures associated with OA patients in the United States exceeds $185 billion annually (Kotlarz et al., 2009), and as the population ages and gains weight, the costs and prevalence of OA are expected to exponentially increase in future years (Brooks, 2002; Jackson et al., 2001; Wallace et al., 2017). By the year 2030 arthritis will affect the 25% of the US adult population (Hootman and Helmick, 2006).

OA pathology involves a complex and multifactorial process which affects the whole joint, producing changes in the composition and structure of the articular cartilage and the subchondral bone which eventually result in severe degradation and inflammation. At present, there is no cure for OA and most current therapies for articular cartilage repair and regeneration show many limitations.

The treatment of knee OA has traditionally focused on symptom control and prevention strategies (Fibel et al., 2015). Current surgical therapies for the treatment of focal cartilage or osteochondral defects, such as bone marrow stimulation and mosaicplasty, aim to promote joint tissue regeneration and hence, limit the onset and progression of OA. These surgical techniques suffer from many limitations such as donor site morbidity and fibrocartilage tissue formation (Buckwalter and Martin, 2006). If joint damage progresses to end stage OA, the only clinical option is total joint arthroplasty, but this surgical procedure is constrained by a poor functional outcome in some patients and the lifespan of prostheses (Glyn-Jones et al., 2015), with ten year revision rates reported to be as high as 12% (Labek et al., 2011).

This has led to a significant progress in the field of cartilage and osteochondral tissue engineering (TE), in order to find new approaches to regenerate damaged joints and prevent the onset of OA.

1.2. Non-viral gene delivery in mesenchymal stem cell based TE strategies

TE approaches, involving the combination of cells, carrier biomaterials and bioactive factors, have been investigated as a promising alternative that can provide a durable and stable repair without the problems and limitations associated with current therapies. Different cell sources, biomaterials and signals have been proposed for this purpose. Mesenchymal stem cells (MSCs) are a promising cell source for cartilage and bone regeneration due to their multipotent differentiation capacity and putative immunomodulatory properties (Tuan et al., 2003; Uccelli et al., 2008).

MSC fate can be modulated through the introduction of exogenous genes for the cell-mediated synthesis of specific proteins, which might be preferable over the delivery of recombinant growth factors due to their short-half life, fast body clearance, lower therapeutic effect in comparison to natural proteins and the need of supraphysiological doses that might lead to unexpected side-effects (Evans, 2014; Santos et al., 2011; Zara et al., 2011).

In this context, non-viral gene therapy offers a promising approach for the delivery of plasmid DNA (pDNA) encoding for growth and transcription factors for MSC based TE strategies. The transient over expression associated with these gene carriers, and the ease of fabrication and incorporation into 3D matrices for localised transfection, highlight the value of these vectors for TE. In comparison to their viral counterparts which due to their immunogenicity, risk of insertional mutagenesis that can result in oncogene transactivation, and high levels of expression that can cause adverse pathologies, might not be ideal for their application into regenerative medicine (RM) (Mi et al., 2003; Williams and Thrasher, 2014; Yin et al., 2014).

The importance of the combination of 3D matrices or scaffolds with gene delivery for TE lies in a more prolonged and localised effect of the transgene overexpression, overcoming the limitations of 2D transfection (Dinser et al., 2001; Madry et al., 2003) and direct injection, which is not appropriate for targeting a specific tissue (Madry and Cucchiarini, 2014). Gene activated matrices (GAMs) are the result of this strategy, in which a gene and its carrier are contained in a biodegradable scaffold, which offers structural support, cell attachment, retention of new tissue formation, and confined gene delivery for an *in situ* effect. GAMs typically aim to deliver a single gene homogenously to cells within the scaffold. This approach is not suitable for engineering complex tissue interfaces such as the osteochondral unit, which consists of articular cartilage, calcified cartilage and the underlying subchondral bone. Another limitation of the current GAM approaches lies in the use of mechanically weak substrates that might not be able to withstand the high levels of compressive and shear loading that will be present in an articulating joint upon implantation.

Due to the aforementioned issues, biofabrication techniques involving a layer-by-layer spatial patterning of genetic gradients in 3D might be a promising strategy for the recapitulation of the native organization of the osteochondral unit.

1.3. 3D printing to enable musculoskeletal TE

3D bioprinting allows for the precise spatial positioning of biomaterials, cells and bioactive compounds to fabricate 3D constructs with biological properties suitable for clinical restauration of tissue and organ function (Murphy and Atala, 2014). However, the biomaterials used for this purpose, also known as bioinks, offer limited biological activity and poor control of cellular processes such as MSC differentiation and specific matrix production. To overcome these limitations, the use of growth factor presentation to promote lineage-specific differentiation of stem cells has been explored, but this approach can be challenging due to the diffusive transport characteristics of the hydrogels typically used as bioinks.

A potential way to overcome this limitation could be through nucleic acid delivery, *via* genes encoding for key signaling factors. For example, the physical encapsulation of pDNA complexed with non-viral nanoparticulate carriers into printable cell-laden bioinks might allow for the zonal printing of different vectors and pDNAs with limited diffusion of gene products between layers. In addition, the printing of polymer reinforced hydrogel composites enable the fabrication of constructs with mechanical properties similar to those of native cartilage while maintaining their biological functionality (Daly et al., 2017).

1.4. Objectives of this thesis

The main aim of this thesis is to explore the combination of nanoparticle-based non-viral gene delivery and biofabrication techniques for the development of a new generation of 3D bioprinted gene activated constructs for osteochondral TE. Specifically, we sought to develop a range of gene activated hydrogel based bioinks (GAB) that were supportive of either cartilage or bone development. We then sought to use these GABs to 3D bioprint spatially defined and mechanically reinforced constructs suitable for osteochondral TE. To this end, the following specific objectives were defined:

1. **Explore the capacity of nanohydroxyapatite to transfect MSCs encapsulated in alginate hydrogels for bone and cartilage TE**. The success of a gene delivery strategy ultimately depends on the gene delivery mechanism to maximize nucleic acid uptake and, consequently, downstream protein production. Inorganic nanoparticles made of calcium phosphate (CaP), gold or silica, have been drawing attention in TE due to their biocompatibility, wider availability, long-term stability, ease of preparation and low toxicity (Wagner and Bhaduri, 2012). CaP in the form of nanohydroxyapatite (nHA), has been shown to allow sustained MSC transfection in 3D collagen scaffolds and promote bone formation *in vivo* (Curtin et al., 2015). Developing a bioink for osteochondral TE first requires identification of a hydrogel that can support both cartilage and bone development. Alginate is a naturally occurring anionic polymer that is ideally suited to cartilage and bone TE due to its biocompatibility, tailorable degradation kinetics, and low toxicity (Lee and Mooney, 2012). Encapsulation of MSCs in alginate hydrogels has demonstrated potential for both cartilage and bone regeneration *in vitro* and *in vivo* (Igarashi et al., 2010; Sheehy et al., 2014a; Simmons et al., 2004). Furthermore, alginate can be used as a bioink for the 3D printing of MSCs supporting robust chondrogenesis in comparison to other hydrogel-based bioinks such as gelatin methacryloyl (GelMa) and BioINK^{TM} (Daly et al., 2016a). With the view towards using alginate as the biomaterial element of a gene-activated bioink (GAB) and nHA as gene carrier, *the first objective of this thesis will explore the capacity of nHA to transfect MSCs encapsulated in alginate hydrogels for bone and cartilage TE.*

2. **Compare novel and stablished non-viral vectors for chondrogenic and osteogenic differentiation of MSCs.** Although nHA is highly biocompatible and has been shown to offer superior transfection efficiencies to other commercially available vectors (Curtin et al., 2012), it has also been shown to be inherently highly osteogenic and osteoinductive (Cunniffe et al., 2016a). A synergistic effect between the osteogenic stimulus provided by nHA and the overexpression of the delivered genes has been also reported, which translated in significantly higher bone repair *in vivo* in comparison to the use of polyethilenaimine (PEI) as vector, despite PEI supporting higher transgene expression (Curtin et al., 2015). Recognizing that nHA might not be

the optimal gene carrier for engineering stable hyaline cartilage engineering, *the second objective of this thesis compares novel and stablished non-viral vectors for chondrogenic and osteogenic differentiation of MSCs.*

3. **Determine the best gene combination and culture conditions for the promotion of a stable hyaline cartilage phenotype.** As stated previously in this introduction, MSCs are a promising cell source for cartilage and bone regeneration due to their multipotent differentiation capacity. Engineering phenotypically stable articular cartilage using MSCs remains a significant challenge in the field. The intrinsic endochondral ossification potential of Bone marrow-derived MSCs (BMSCs) can result in a hypertrophic phenotype which is not ideal for articular cartilage repair (Somoza et al., 2014). In order to suppress hypertrophic differentiation of MSCs, delivery of genes encoding for a diverse range of growth and transcription factors has been explored (Gurusinghe and Strappe, 2014). In addition, MSC expansion and culture conditions such as oxygen tension play a key role in regulating MSC chondrogenic differentiation (Sheehy et al., 2012). Having identified the RALA amphipathic peptide as the suitable vector for MSC chondrogenesis, *the third objective of this thesis sought to determine the best gene combination (chondrogenic and antihypertrophic factors) and culture conditions (hypoxia and normoxia) for the promotion of a stable hyaline cartilage phenotype.*

4. **Investigate the use of the developed GABs for the 3D printing of mechanically robust constructs for bone TE.** Previous research exploring the use of alginate hydrogels as a gene delivery system for bone applications have been limited by the mechanical weakness of the constructs and limited bone formation *in vivo* (Krebs et al., 2010; Loozen et al., 2013). Co-printing of hydrogel-based bioinks and Polycaprolactone (PCL) have been previously explored for enhancing the mechanical properties and integrity of the construct (Daly et al., 2016b). This approach might be clinically relevant for the treatment load bearing cartilage and bone defects. The inclusion of non-viral gene delivery into the hydrogel component of these composites might allow for the bioprinting of "off-the-shelf" mechanically robust constructs able of inducing therapeutic protein overexpression *in vivo* to accelerate tissue repair. Having developed nHA-gene activated alginate hydrogels capable of

osteogenesis of MSCs *in vitro, the fourth objective of this thesis investigates the use of these hydrogels as gene activated bioinks (GABs) for the 3D printing of mechanically robust constructs for bone TE which can be relevant for the regeneration of the subchondral bone layer in an osteochondral defect.*

5. **Explore the development of pore-forming GABs for enhanced gene delivery, and assess the capacity of these constructs to support cartilage and bone development.** Hybrid multicomponent gels are a promising candidate for bioink development (Armstrong et al., 2016). Methylcellulose has previously been added to alginate to produce viscous bioinks suitable for 3D printing of high fidelity constructs (Schütz et al., 2015). Additionally, after ionic crosslinking of the printed constructs, the methylcellulose was released from the scaffold acting as a sacrificial material that enhanced the microporosity of the bulk alginate gel, with no negative effect on cell viability (Markstedt et al., 2015; Schütz et al., 2015). Alginate-methylcellulose bioinks have also been shown to support the chondrogenic potential of encapsulated chondrocytes (Müller et al., 2017). The modulation of alginate microporous structure through the incorporation of methylcellulose could not only be beneficial for the chondrogenic capacity of MSCs but also to increase gene transfection in a GAB approach. The opening of micro-pores in alginate hydrogels through the application of ultrasound pulses was shown to facilitate the on-demand release of encapsulated PEI-pDNA complexes (Huebsch et al., 2014). *The fifth objective of this thesis explores the development of gene-activated pore-forming bionks for enhanced gene delivery, and assess the capacity of these constructs to support cartilage and bone development.*

6. **Develop 3D printed biphasic gene activated constructs for zonal differentiation of MSCs in which both layers are mechanically interlocked and possess mechanical properties similar to those in native cartilage.** Osteochondral defects affect both the articular cartilage and the underlying subchondral bone. A successful tissue engineering strategy must regenerate both tissue types and ensure integration of both layers to avoid delamination of the construct *in vivo* when joint forces are applied (Nooeaid et al., 2012). Having identified the optimal combination of vector, genes and printable material for the bone and the cartilage layers, *the final objective*

of this thesis is to develop a 3D printed biphasic gene activated construct for zonal differentiation of MSCs in which both layers are mechanically interlocked and possess mechanical properties similar to those in native cartilage.

In summary, the objectives of this thesis are:

1. To incorporate non-viral gene delivery to alginate hydrogels for cartilage and bone TE strategies.

2. To compare the effects of different non-viral nanoparticle-based gene delivery vectors on MSC fate.

3. To assess the optimal culture conditions and gene combination for the chondrogenic differentiation of MSCs.

4. To 3D print mechanically reinforced gene activated constructs for bone TE.

5. To explore the modulation of alginate-based bioink microporosity for enhanced gene delivery and promotion of chondrogenesis of MSCs.

6. To 3D print a mechanically reinforced, bi-phasic gene activated construct for osteochondral TE.

CHAPTER 2

Literature review

Controlled Non-viral Gene Delivery in Cartilage and Bone Orthopaedic
Tissue Engineering: Current Strategies and Future Directions

Abstract

Non-viral gene delivery for orthopaedic tissue engineering might offer a superior option to recombinant protein administration and viral gene transduction approaches, due to a more physiological and controlled expression of growth and transcription factors that could effectively enhance tissue repair. The ease of incorporation of this approach into 3D materials for the generation of gene-activated matrices, highlights the importance of non-viral gene therapy for *in situ* transfection and the regeneration of damaged organs. This review aims to analyse the different modalities of non-viral gene delivery used for the repair of bone and cartilage, and explore the current challenges for the recapitulation of tissue development, repair and architecture, that still exist for the engineering of functional orthopaedic tissues.

2.1. Introduction

In 2011, more than 102 million of US inhabitants reported musculoskeletal conditions, meaning 21 million hospital admission, 2.1 billion drug prescriptions, and an aggregate economic impact of $796.3 (Yelin et al., 2016). Since the 1990's the treatment of orthopaedic conditions has experienced a great refinement fostered by the close collaborative efforts of surgeons, biologists and engineers. Due to the limitations of mechanical stabilization and biomechanical analysis of operative techniques for the treatment of orthopaedic lesions, processes inspired in the native healing and organ development have been investigated to enhance regeneration (Huard and Fu, 2000). Cytokines, growth factors, inflammatory reactions and protein interactions have been widely investigated for this purpose showing promising results for the healing of soft and hard tissues into the clinics (Fisher et al., 2013; Huard and Fu, 2000; Huard et al., 2003).

Although this promising scenario, the delivery of morphogens in the form of recombinant growth factors for tissue regeneration remains challenging. Due to their short half-life, fast body clearance and lower therapeutic effect in comparison with natural proteins (Evans, 2014; Heyde et al., 2007; Santos et al., 2011), supra-physiological concentrations of these proteins are required to exert a biological effect, which might impair tissue repair and cause off-target effects (Baldo, 2014; Carragee et al., 2011; Zara et al., 2011) such as ectopic bone formation seen with Medtronic's INFUSE bone graft (Carragee et al., 2011). Due to these limitations, controlled release systems based in non-covalent (surface adsorption, physical entrapment, affinity binding and ionic complexation) or covalent (chemical conjugation) immobilization (Schliephake, 2010; Vo et al., 2012) of proteins into carrier materials have been investigated. Despite the research efforts devoted to this end, many of the pre-existing challenges remain when using these systems. In addition, quick release kinetics, low loading efficiencies and difficulty for spatiotemporal control of simultaneous and sequential presentation of different factors hamper the successful of these approaches that have resulted in low regenerative outputs in vivo. In comparison to the controlled release of proteins, gene therapy is a more elegant approach for inducing the cell-

mediated expression of the desired factor in a physiological, localised and sustained manner (Fig.2.1).
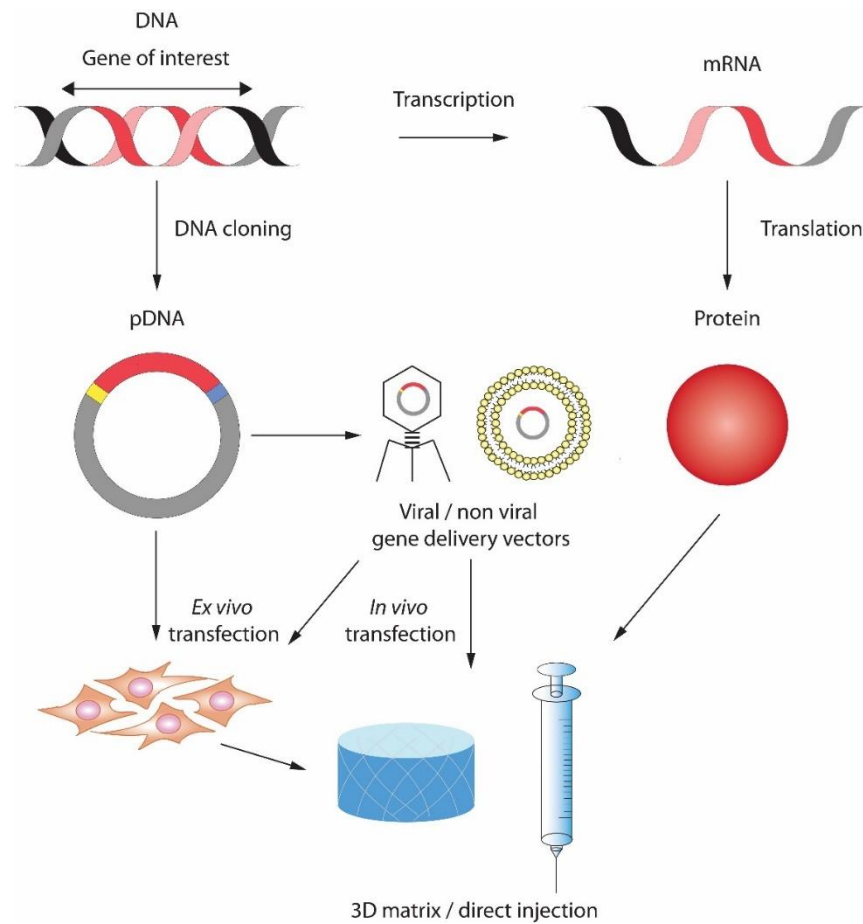
Fig.2.1. Protein and gene delivery for TE and RM of orthopaedic tissues. The DNA is transcribed into RNA and then translated into a protein that can be delivered in vivo suing a 3D matrix or direct injection to enhance tissue repair. The DNA sequence encoding for a gene of interest can also be cloned into a pDNA which can be delivered to MSCs in an ex vivo approach by viral and non-viral approaches. Either the pDNA or the transfected MSCs can also be delivered in vivo through 3D biomaterials and direct injection to produce a therapeutic effect.

Gene transfer allows for the sustained synthesis of native proteins in the site of injury. It is also superior in comparison to traditional approaches for the delivery of transcription factors, and receptor proteins which are localised in specific cellular compartments (Evans and Huard, 2015). It also could target the treatment of orthopaedic genetic diseases such as Ducheme muscular dystrophy and osteogenesis imperfecta which current treatments are only symptomatic and a curative approaches are needed (Huard and Fu, 2000). But most importantly, gene therapy could be a more

physiological and compatible approach with wound healing and tissue regeneration processes (Bonadio et al., 1999)

Since the 1980's the field of gene therapy has matured with more than 35,000 papers, 16,000 US patents and 1,800 clinical trials (Ledley et al., 2014) and Glybera, the first human gene therapy product approved for use in Europe by the European Commission in 2012 (Ylä-Herttuala, 2012). But despite these encouraging developments, no FDA-approved product exists in orthopedic gene therapy and only a few products have been moved into clinical trials and completed Phase II (Elmallah et al., 2015; Mease et al., 2010). More recently, a cell-mediated gene therapy for degenerative arthritis, Invossa, has been approved by south Korean regulators for the treatment of osteoarthritis by a single intra-articular injection of chondrocytes overexpressing transforming growth factor β1 (TGFβ-1) (Cho et al., 2016).

This review summarises the past and current efforts in the use of non-viral gene therapy for the regeneration of orthopaedic tissues, focusing in its application to tissue engineering strategies and its potential for the translation into the clinics to broaden the field of gene therapy from the treatment of rare genetic diseases to its presence in the daily life of millions of people suffering from degenerative diseases such as osteoarthritis (OA).

2.2. Gene therapy in orthopaedic tissue engineering

2.2.3. Types of gene delivery

Gene delivery faces many cellular barriers that need to be overcome for the efficient expression of the gene of interest. Nucleic acids require its uptake by the cells and, passing through the cell membrane and its transport inside the cell cytoplasm, avoiding degradation, arrive to the nucleus where the transcription takes place (Wang et al., 2013). A key component of gene therapy is the choice of the gene delivery vector, i.e. the vehicle that can effectively deliver the DNA molecule, also called plasmid DNA (pDNA), encoding for the gene of interest to the target tissue or cell type ensuring a suitable expression profile of the transgene. The principal division between gene delivery vectors is whether they are viral or non-viral (Table 2.1).

Non-viral gene delivery can be divided in physical (or vector free) and chemical. While physical transfection methods rely on the delivery of the pDNA through the temporal disruption of the cell membrane, chemical methods consist of the complexation of the pDNA to different types of macromolecules which protect the pDNA from degradation and facilitate its transport to the cell nucleus. Viral vectors are often classified according to their viral family and their delivery mechanism is based in their inherent ability to translocate their own genetic material into the host's genome in a process known as transduction.

2.2.4. Viral gene therapy vs non-viral gene therapy in the tissue engineering context

Viral vectors are preferred generally in gene therapies (Saraf and Mikos, 2006) due to their high cell transfection efficiencies of around 80-90%. More than 70% of gene therapy clinical trials carried out so far have used viral vectors (Yin et al., 2014). Also, the three gene delivery therapies in the field of orthopedic/musculoskeletal medicine that have successfully completed phase II clinical trials utilized viral gene delivery approaches (Cho et al., 2016; Elmallah et al., 2015; Mease et al., 2010). The main concerns associated with viral vectors relate to their potential immunogenicity, the risk of insertional mutagenesis that can result in oncogene transactivation and leukemia, and difficulties in their production (Williams and Thrasher, 2014; Yin et al., 2014) (Table 2.1). Despite the huge amount of work focused on the development of safer viral vectors over the last decade, safety concerns still prevail. Lentiviral (based on viruses of the family *Retroviridae*) and adenoviral (based on viruses of the family *Adenoviridae*) approaches have been developed for cartilage and bone regeneration, but their use in orthopedic tissue engineering is hindered by the difficulties of linking the viruses to 3D matrices for localised transfection (Brunger et al., 2014; Cao et al., 2011; Feeley et al., 2006; Gelse et al., 2008; Glass et al., 2014; Pascher et al., 2004; Ueblacker et al., 2007). One approach to address this issue is to use the poly-L-lysine-mediated immobilization of lentiviruses in polycaprolactone (PCL) 3D matrices (Brunger et al., 2014; Glass et al., 2014), which can provide spatial control of gene transfection in a mechanically functional scaffold.

Another alternative is to adsorb adenoviruses into natural polymeric scaffolds such as collagen–glycosaminoglycan (GAG), however this approach can lead to the leakage of the viral vector to the surrounding tissue (Pascher et al., 2004). Also, recently, recombinant adeno-associated viruses (rAAV) have been investigated for regenerative medicine as a promising viral vector to overcome the limitations associated with retroviruses and adenoviral vectors. These show reduced host immune response due to the removal of the immunogenic sequences in the viral genome and no risk of insertional mutagenesis as their genetic material is kept as an episome, similar to non-viral pDNA delivery (Frisch et al., 2017; Venkatesan et al., 2012). In addition, rAAV vectors have been combined with hydrogels for temporally sustained gene transfection of MSCs, highlighting their potential for tissue engineering (Rey-Rico et al., 2017).

Ex vivo viral gene transduction and posterior seeding of transfected cells in 3D constructs has been shown to be an easier and more successful approach, but it depends on cell survival upon implantation. The use of adenoviruses for the delivery of sex determining region Y box 9 (SOX9) (Cao et al., 2011) and bone morphogenic protein 2 (BMP2) (Gelse et al., 2008) genes and subsequent incorporation of the transfected cells into polyglycolic acid (PGA) matrices has been shown to enhance the regeneration of large partial-thickness and full thickness cartilage defects.

While viral vectors offer more stable and higher levels of expression than non-viral approaches, non-viral gene carriers might be more suitable for tissue engineering strategies where the final goal is enhanced matrix formation and cell differentiation. This is due to do their ease of production, safety, low immunogenicity (Yin et al., 2014) and potential to be incorporated into 3D matrices (Table 2.1).

One of the main concerns of the use of viral vectors in orthopedic tissue engineering applications is the effect of the long-term overexpression of high levels of growth factors which might impair the regenerative and tissue repair processes (Fig.2.2.A). The adenoviral delivery of TGF-β1 through intra-articular administration into arthritic rabbit knee joints resulted in successful transgene overexpression that caused pathological changes in the knee and the surrounding muscle tissue stimulating cartilage degradation, muscle edema and fibrogenesis instead of repair (Mi et al., 2003)

(Fig.2.2.B). These results suggest that high levels of expression can cause adverse pathologies and a more controlled transfection and transgene expression is preferable (Bonadio et al., 1999; Mi et al., 2003). Also, in a study comparing *ex vivo* bone marrow-derived MSCs (BMSCs) liposomal and adenoviral BMP2 gene delivery in a rat mandibular defect, the adenoviral infected BMSCs promoted the formation of excessive and abnormal bone, while the liposome-mediated gene transfer resulted in the desired repaired tissue, more similar to the native bone in thickness and shape (Park et al., 2003) (Fig.2.2.C). This direct comparison between viral and non-viral gene delivery in a critical size bone defect highlights the potential of non-viral gene delivery as a more physiological approach for successful repair.
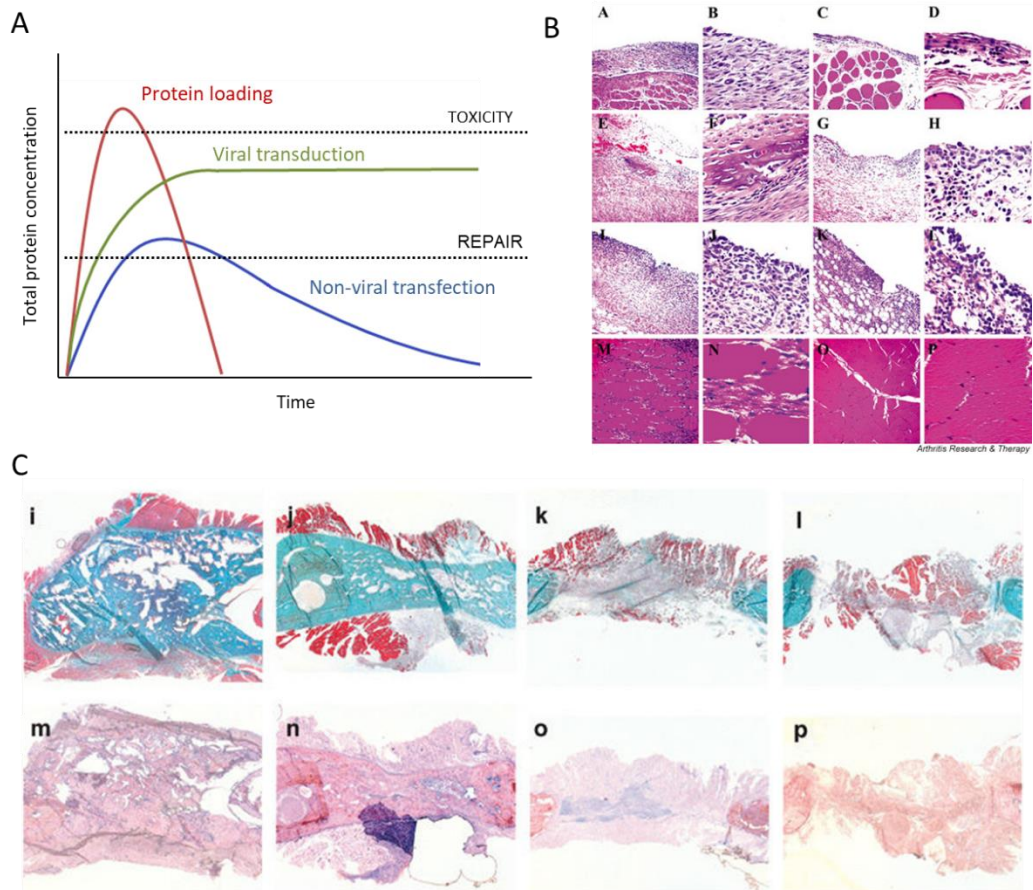
Fig.2.2. (A) Schematic representation of the usual protein levels obtained by loading the protein into 3D matrices, viral gene delivery and non-viral gene delivery over time. Protein release kinetics from 3D constructs is limited by a quick release that occurs during the first few days of loading. Gene delivery offers a more sustained and durable release. The adenoviral delivery of TGF-ß1 through intra-articular administration into arthritic rabbit knee joints resulted in successful transgene overexpression that caused pathological changes in the knee and the surrounding muscle tissue stimulating cartilage degradation, muscle edema and fibrogenesis instead of repair (Mi et al., 2003). Adenoviral infected BMSCs promoted the formation of excessive and abnormal bone, while the liposome-mediated gene transfer resulted in the desired repaired tissue, more similar to the native bone in thickness and shape (Park et al., 2003).

Table 2.1. Characteristics of viral and non-viral gene delivery vectors for their use in combination with 3D matrices.

Characteristics	Types of gene delivery vectors	
	Viral	Non-viral
Transfection efficiency	High	Low/moderate
Transgene expression levels	High	Moderate
Durability of expression	Persistent	Transient
Ease of production	Low	High
Ease of incorporation to 3D matrices	Low	High
Infectivity	Adenoviruses and lentiviruses infect dividing and non-dividing cells, retroviruses only infect dividing cells	Infect dividing and non-dividing cells
Safety	Insertional mutagenesis risk, immunogenicity	Cytotoxicity at high doses, non-infectious
Compatibility with regenerative processes	High expression of growth factors for long time periods can impair tissue healing and aggravate previous tissue pathologies	Low expression for shorter periods of time

2.3. Non-viral gene therapy
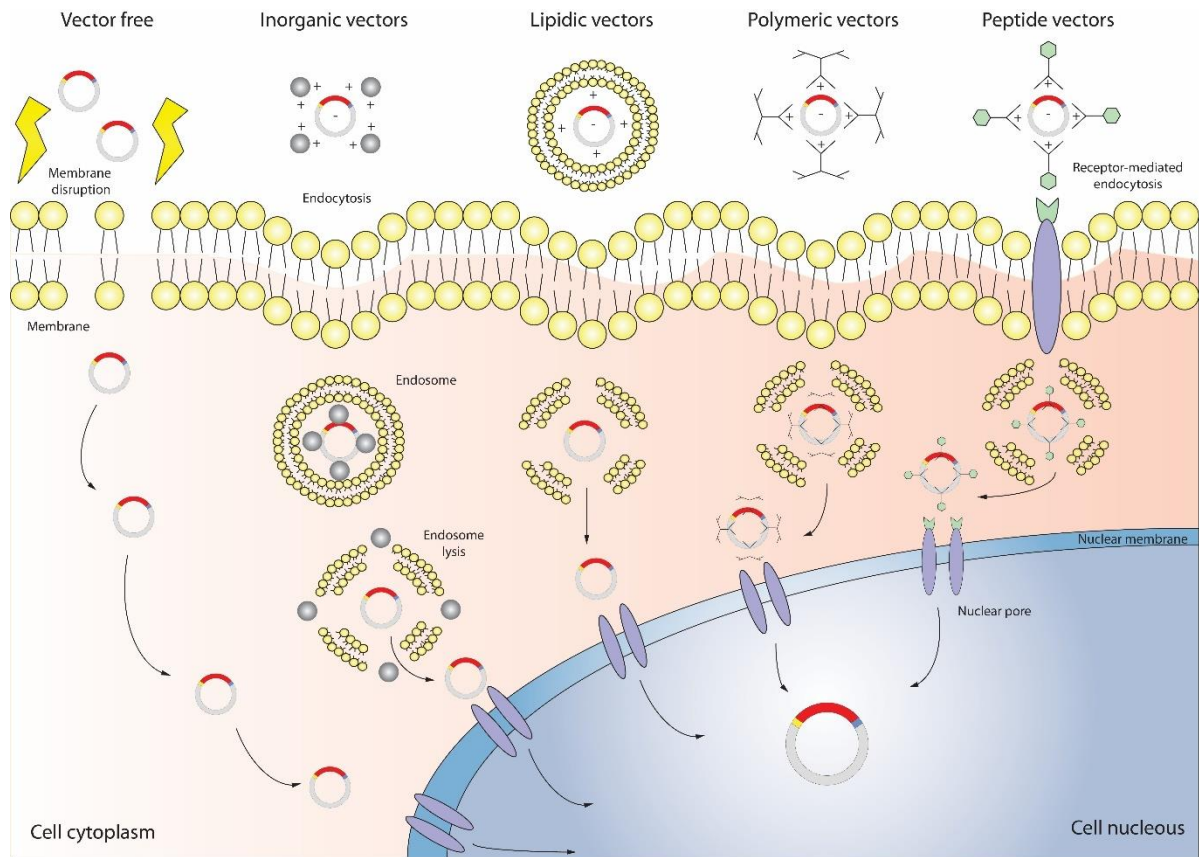
Fig.2.3. Schematic of the different non-viral gene delivery methods.

2.3.1. Vector free

Vector free methods include the techniques based on the physical introduction of the nucleic acid material into the cell in order to overcome the problems of targeting, endocytic processing and immune response (Mellott et al., 2013) (Fig.2.3). These include different types of injection such as microinjection, needle injection and jet injection, pressurised DNA bombardment, high-voltage electrical currents like electroporation, sonoporation through ultrasound-mediated gene transfer, and hydrodynamic gene transfer using hydrostatic pressure.

While some of these techniques such as microinjection, DNA bombardment and hydrodynamic gene transfer show limitations in orthopaedic applications due to the high quantity of nucleic acid needed , lack of specificity, tissue and cell damage, and the need to transfect large cell populations (Mellott et al., 2013), others have shown

51

promise to deliver therapeutic genes to the musculoskeletal system *in vivo* (Bez et al., 2017; DiFranco et al., 2009; Kawai et al., 2005; Mir et al., 1999; Zelenin et al., 1997) and to progenitor cells *in vitro* for their use in *ex vivo* therapies (Im and Kim, 2011; Lee et al., 2011; Rizk and Rabie, 2013; Wang et al., 2005) (Table 2.2). Electroporation has been successfully used for the introduction of therapeutic genes into MSCs to enhance their differentiation into the tenogenic (Wang et al., 2005), osteogenic (Lee et al., 2011) and chondrogenic (Im and Kim, 2011; Rizk and Rabie, 2013) phenotype. Adipose stem cells (ASCs) transfected through electroporation with runt related transcription factor 2 (RUNX2) and osterix genes were able to promote bone formation subcutaneously in a nude mice model after 6 weeks in a PLGA scaffold (Lee et al., 2011). The same approach was used to promote *in vivo* cartilage formation by the electroporation of the SOX trio genes into adipose-derived stem cells (ASCs) (Im and Kim, 2011). Dental pulp stem cells were also electroporated with the TGF-β3 genes showing superior levels of transfection in comparison to chemical vectors and enhanced chondrogenesis (Rizk and Rabie, 2013).

Recently, sonoporation, or the use of ultrasounds for gene delivery, have been shown capable to transfect cells *in vivo* and *in vitro* with pDNA that was previously loaded into a collagen scaffold in a model known as matrix-assisted sonoporation (Bez et al., 2017), allowing for very fine temporal control of the transfection. Two weeks after construct implantation on a mini-pig cranial and tibial defect, the application of ultrasounds allowed for the transfection of 40% of the cells that colonized the construct and the expression of the BMP6 transgene which led to complete fracture healing (Bez et al., 2017; Nomikou et al., 2017). Sonoporation has also been shown effective for *in vivo* transfection of reporter genes inside the rat intervertebral disc and a sustained gene expression up to 24 weeks (Nishida et al., 2006).

2.3.2. Inorganic vectors

Different inorganic materials including CaPs, gold nanoparticles (Au-NPs), silica, magnesium phosphates, carbon nanotubes (CNTs) and magnetic nanomaterials such as iron oxides have been shown to successfully deliver nucleic acids into cells (Dizaj et al.,

2014; Riley et al., 2017; Wagner and Bhaduri, 2012) (Fig.2.3). Inorganic vectors show many advantages such as their ease of production and functionalization, low immunogenicity, high biocompatibility, resistance to microbial attack and stability (Dizaj et al., 2014; Riley et al., 2017; Wagner and Bhaduri, 2012) (Table 2.2). The most popular vector for orthopaedic gene delivery in this category is CaP. Others like Au-NPs, silica, CNTs and magnetic nanoparticles (MNPs) remain relatively unexplored in tissue engineering and regenerative medicine.

CaP have been used extensively for *in vitro* transfection due to the cationic charge of calcium which allows formation of ionic complexes with the anionic DNA molecule (Dizaj et al., 2014), protecting the DNA from the degradative action of nucleases (Brundin et al., 2013; Zuo et al., 2011). CaP offers many advantages as gene delivery vector in orthopaedic bone tissue engineering due to their biocompatibility, biodegradability (Habraken et al., 2016), the predominance of hydroxyapatite in bone composition (Boskey, 2013), and the efficient delivery in both serum and serum-free conditions (Curtin et al., 2012; Fu et al., 2005). The delivery method is based on the internalisation of the complexes through ion channel-mediated endocytosis (Dizaj et al., 2014) and, once inside the cell cytoplasm, on the endosomal scape of the undamaged DNA due to the buffer effect of the CaP on endosomal PH (Nabiev et al., 2007; Wagner and Bhaduri, 2012). Due to the increase of the calcium concentration in the cytoplasm upon delivery, the released DNA is able to migrate into the nucleus through the nuclear pore complex thanks to the blocking of IP3 (Dizaj et al., 2014). Incorporation of CaP nanoparticles into different 3D matrices have been shown to promote successful transfection and bone formation *in vivo* in different animal models (Curtin et al., 2015; Keeney et al., 2010) and the *in vitro* transfection of progenitor cells to enhance their osteogenic differentiation (Castaño et al., 2014; Chernousova et al., 2013; Krebs et al., 2010). Recently, nHA-mediated gene delivery was shown to successfully repair a rat cranial defect through the delivery of the BMP2 and VEGF genes in comparison to the empty defect and the use of PEI as vector, although lower levels of expression were detected when nHA was used as gene carrier in comparison to PEI, suggesting a synergistic effect between the vector and the delivered genes for bone formation (Curtin et al., 2015). The BMP7 and vascular endothelial growth factor (VEGF) genes were also

incorporated into an injectable nano-CaP paste for bone substitution showing succesful transfection of MSCs and expression of the genes of interest, highlighting the potential of this approach for the minimally invasive repair of bone defects (Chernousova et al., 2013). CaP-mediated gene delivery has also been reported to enhance chondrogenic differentiation of stem cells upon gene delivery of TGB-β1 (Cao et al., 2012b).

Gold nanoparticles (Au-NPs) are promising non-viral vector for tissue engineering strategies due to ease of preparation, high surface area and the possibility of surface functionalisation with nucleic acids (Riley et al., 2017; Vial et al., 2017). Although Au-NPs have been previously used for the delivery of different bioactive molecules in 3D such as BMP2 (Kearney et al., 2015) and micro RNA (miRNA) to enhance osteogenic differentiation of MSCs (Yu et al., 2017), their use as gene delivery vectors in orthopaedics remains limited. Importantly, the functionalization of Au-NPs with peptides can enhance their MSC uptake which is critical as MSCs show a restricted cellular uptake (Peng et al., 2014). Au-NPs have also been used to promote differentiation of stem cells towards the osteogenic lineage (Heo et al., 2014; Yi et al., 2010).

Silica nanoparticles, which can be functionalised with amino groups (Dizaj et al., 2014) to bind to DNA molecules, have been reported to efficiently deliver DNA *in vivo* to the mouse brain and could be a powerful delivery strategy for the musculoskeletal system (Bharali et al., 2005). DNA-PEI-silica nanocomposites have also being used for fibroblast transfection in 3D collagen hydrogels (Wang et al., 2015).

Magnetic nanoparticles (MNPs), which include the iron oxide nanoparticles, are attractive for drug and gene delivery in orthopaedics due to their small sizes and magnetic properties allowing directional targeting when a magnetic field is applied (Gao et al., 2015). MNPs have been shown to successfully delivery nucleic acid cargos in a process known as magnetofection in which a magnetic field is used for the MNPs-DNA sedimentation onto target cells (Plank et al., 2011). Another approach for this technique is the combination of MNPs with other transfection agents such as viral particles, liposomes, or cationic polymers and combined with nucleic acids to enhance transfection (Mellott et al., 2013).

2.3.3. Lipid-based vectors

Cationic lipids are positively charged amphiphilic small molecules which structure allows for the formation of self-assembled vesicles and membranes in an aqueous solution (Fig.2.3). This is possible due to their structure, divided into three components: (1) a polar head group that interacts with the DNA and the negatively charged cell membrane for internalisation, (2) a hydrophobic fatty acid tail that will allow the formation of the lipid bilayer, and (3) a glycerol backbone to link the hydrophilic and hydrophobic domains (Bangham et al., 1965; Dizaj et al., 2014; Monteiro et al., 2014a; Yin et al., 2014). Liposomes are lipid bilayers which can encapsulate hydrophobic compounds such as pDNA, forming a cationic complex which is able to interact with the anionic cell membrane allowing entrance into the cell *via* endocytosis. Once inside the cell, the destabilisation of the endosomal membrane allows the release of the nucleic acid into the cytoplasm for its transport into the cell nucleus (Xu and Szoka, 1996). Lipid-based vectors show many advantages such as the versatile structure that can be easily tailored and functionalised for targeted delivery, their wide size range, high DNA loading capacity, and storage stability (Table 2.2). But due to their cytotoxicity due to membrane destabilisation, low stability, low solubility, low half-life, rapid clearance and interaction with serum, their use for orthopaedic applications is limited (Lv et al., 2006) (Table 2.2).

The most used lipid-based vector is the commercially available lipofectamine which has been shown to successfully transfect primary stem cells from diverse origins (Elsler et al., 2012; Guo et al., 2007, 2002; Kayabaşi et al., 2013; Li et al., 2014; Locatelli et al., 2013; Monteiro et al., 2014b; Zheng et al., 2005) with different therapeutic genes of orthopaedic relevance such as VEGF (Locatelli et al., 2013; Michlits et al., 2007), TGF-β1 (Guo et al., 2007, 2002; Li et al., 2014), mothers against DPP homolog 3 (SMAD3) (Zheng et al., 2005), BMP6 (Kayabaşi et al., 2013), BMP2 (Wegman et al., 2011), SOX9 (Yao et al., 2014), RUNX2 (Monteiro et al., 2014b), osterix (Lai et al., 2011), fibromodulin (Delalande et al., 2015) and nerve growth factor (NGF) (Whittlesey and Shea, 2006) between others for cartilage, bone, tendon, nerve and skin repair. Lipofectamine has also been incorporated into different 3D matrices to allow an *in situ* sustained

transfection. The incorporation of liposomes-pDNA complexes into PLG scaffolds for nerve regeneration (Whittlesey and Shea, 2006), electrospun PCL nanofiber constructs (Monteiro et al., 2014b) and porous hydroxyapatite scaffolds (Ono et al., 2004) for osteogenic differentiation are good examples of the promising results of this approach.

2.3.4. Polymeric vectors

Cationic polymeric vectors are, together with lipid-based vectors, one of the most relevant and widely used non-viral gene carriers and they have been considered as the gold standard for non-viral gene transfection (Fortune et al., 2010; Patnaik and Gupta, 2013). They can interact with anionic DNA and RNA molecules thanks to the cationic groups, mainly amines, present in their structure, forming nanoparticulate complexes known as polyplexes (Fig.2.3). Polymeric vectors are chemically diverse and they can be easily functionalised (Yin et al., 2014) and show other advantages for orthopaedic gene delivery such as their small size, protection against enzymatic degradation and ease of incorporation into 3D matrices (Table 2.2). Polymeric vectors can be divided in natural and synthetic polymers depending on their origin. A common limitation of polymeric vectors, especially from synthetic origin, is their cytotoxicity and immunogenicity *in vivo* (Zhao et al., 2017).

One of the most popular synthetic polymeric vector for gene delivery in regenerative medicine is polyethylenimine (PEI). PEI was firstly used by Boussif *et al.* in 1995 (Boussif et al., 1995), and it has been shown successful for localised gene transfection *in vivo* into the skeletal muscle (Hong et al., 2004; Türk et al., 2007), cranial and long bone defects (Cheong et al., 2007; Curtin et al., 2015; Qiao et al., 2013), cartilage defects (Im et al., 2011; Pi et al., 2011) and arthritis anti-inflammatory treatment (Xiang et al., 2012). PEI has been also used *in vitro* for the transfection of adult somatic and progenitor cells (Ahn et al., 2008; Florea et al., 2002; Park et al., 2010, 2017, Wang et al., 2017, 2011) for osteogenic (Cheong et al., 2007; Tierney et al., 2013; Wang et al., 2017), tenogenic (Delalande et al., 2015), adipogenic (Joydeep et al., 2016) and chondrogenic (Im et al., 2011; Park et al., 2012, 2017) applications. Although PEI-

mediated gene delivery for orthopedic applications has been widely reported in literature, PEI has been shown to be cytotoxic due to cell membrane and cytoskeletal alterations (Moghimi et al., 2005). Additionally, the entrance of the PEI-pDNA complexes into the cell nucleus might lead to PEI-chromosomal DNA interactions which could affect the cell viability and differentiation (Akhtar, 2006; Godbey et al., 2001; Larsen et al., 2010). Recently, PEI-mediated gene delivery of pDNA encoding for platelet-derived growth factor-BB (PDF-BB) on a collagen scaffold promoted inflammation and delayed healing when implanted in a rodent periodontal defect model in comparison to the loading of the recombinant protein suggesting the immunogenicity of PEI could impair tissue repair (Plonka et al., 2017). PEI can be also modified to increase its transfection efficiency, decrease cytotoxicity (Thomas and Klibanov, 2002; Thomas et al., 2007), ease PEI-mediated temporal controlled delivery (Türk et al., 2007), and facilitate targeting of a specific cell type or population (Pi et al., 2011). For example, covalently modified PEI with a chondrocyte-affinity peptide to specifically target the knee chondrocytes, demonstrated the feasibility of this approach for the treatment cartilage disorders (Pi et al., 2011).

Other synthetic polymers such as polyethyleneglycol (PEG), poly(L-lysine)-palmitic acid (PLL-PA), activated polyamidoamine dendrimer, copolymer-protean and branched triacrylate/amine polycationic polymers (TAPPs), have also been reported to be promising options for gene delivery for bone repair in comparison to PEI and lipid-based vectors (Chew et al., 2011; Clements et al., 2007; Itaka et al., 2007; Schwabe et al., 2012; Walsh et al., 2017). The use of cationic polysaccharides, such as pullulan-spermine, has also been explored for tissue repair in a cartilage defect (He et al., 2012).

Natural polymers such as Collagen, chitosan and gelatin are also a promising option for gene delivery in regenerative medicine due to their biocompatibility, cytocompatibility and ease of incorporation to 3D scaffolds (Dang and Leong, 2006). Collagen and modified derivatives have been studied for gene delivery. Type I collagen-mediated gene delivery of parathyroid hormone (PTH) in a collagen matrix was shown to promote regeneration in a tibia critical defect *in vivo* canine model (Bonadio et al., 1999), atelocollagen was also promising for the intramuscular administration of the therapeutic genes and their sustained delivery (Sano, 2003). Chitosan is one of the most

relevant natural polymers for non-viral gene delivery due to its biodegradability, biocompatibility and low cytotoxicity (Raftery et al., 2013). The chitosan molecule possesses positively charge amine groups in its backbone that can interact with the anionic DNA molecule to form positively charged nanoparticulate complexes. Chitosan has been successfully reported to transfect stem cells from human (Corsi et al., 2003) and animal (Kayabaşi et al., 2013; Raftery et al., 2015; Wang et al., 2010; Xu et al., 2017) origin, to enhance their chondrogenic and osteogenic differentiation, showing less cytotoxicity and comparable transfection efficiencies to lipofectamine and PEI. Chitosan has also been shown to transfect MSCs loaded into collagen scaffolds in a temporally sustained manner as a promising approach for the use of this vector in tissue engineering applications (Raftery et al., 2015). A cationized chitosan derivative N,N,N-trimethyl chitosan chloride (TMC) has also been used in a gene activated matrix approach for the delivery of the TGF-β1 gene showing successful tissue repair when implanted in a rabbit cartilage defect (Wang et al., 2010). Chitosan-pDNA complexes were also injected *in vivo* into the anterior tibialis muscle showing successful gene delivery in the site of injection in comparison to lipofectamine (Mansouri et al., 2004).

2.3.5. Protein and peptide vectors

Protein-based nanocarriers are naturally-derived polymers characterised for their biodegradability, low toxicity, and high stability and binding capacity. Cationic peptides can have basic aminoacid residues such as lysine or arginine in their structure which allow to bind nucleic acids forming nanoparticulate complexes (Martin and Rice, 2007; McCarthy et al., 2014) (Fig.2.3). The main advantages of the use of these molecules for nucleic acid delivery, apart from the low cytotoxicity and their stability in serum supplemented conditions, are the possibility to use specific peptide sequences to target the membrane receptors of specific cell types, modulate the release of the nucleic acids to the cell cytoplasm by selectively lysing the endosome, and the use of nuclear localisation sequences from viral origin that can facilitate the delivery of the carrier into the cell nucleus (Gupta et al., 2005; Martin and Rice, 2007; McCarthy et al., 2014; Nigg, 1997) (Table 2.2). There are different bio-inspired peptides designed for peptide-guided

58

gene delivery such as the MPG peptide derived from the human immunodeficiency virus (HIV) which facilitates cellular entry, or the nuclear entry sequence of the simian virus 40 (SV40) T antigen which facilitates nuclear delivery (Morris et al., 1997). In order to complex the peptide and the pDNA the presence of cationic aminoacids in their structure such as lysine and arginine is necessary. Synthetic peptides such as the KALA peptide which has multiple lysine residues, and the RALA amphipathic peptide with multiple arginine resiudes in its structure, are examples of this approach (McCarthy et al., 2014; Wyman et al., 1997).

Although cell penetrating peptides have shown better transfection efficiencies and less cytotoxicity than lipofectamine (McCarthy et al., 2014), PEI (McCarthy et al., 2014) and viral vectors (Ho et al., 2001; Wadia and Dowdy, 2002) *in vitro*, and they have been used to deliver proteins (Jo et al., 2014) and calcium phosphates (Sathy et al., 2017) to direct the differentiation of MSCs, their use for gene delivery in orthopaedic tissue engineering remains relatively unexplored. The peptide transduction domain (PTD) in combination with the GAL4 DNA binding domain was used as gene carrier for the delivery of hypoxia inducible factor 1 alpha (HIF-1α) gene into human umbilical vein endothelial cells (HUVECs) to enhance angiogenesis *in vitro* (Jeon et al., 2017). The HIF-1α gene was also delivered by a cysteine-flanked lysine hexamer peptide to promote angiogenesis in a mouse model of dermal wounds *in vivo* (Trentin et al., 2006). PTD in combination with GAG-binding domains have also shown successful transfection of MSCs from human origin at levels comparable to lipofectamine (Dixon et al., 2016).

Table 2.2. Different types of non-viral gene delivery for orthopaedic TE

Types	Advantages	Disadvantages	TE relevant Subtypes	Application for TE *in vivo*	References
Vector free	Simpler, not viral or chemical carriers needed.	Difficult to incorporate to biomaterial-guided approaches. Can cause cell and tissue damage.	Electroporation	Bone and cartilage	(Im and Kim, 2011; Lee et al., 2011)
			Sonoporation	Bone, intervertebral disc	(Bez et al., 2017; Nishida et al., 2006; Nomikou et al., 2017)
Inorganic vectors	High biocompatibility. Possibility of delivery in serum and	Low transfection efficiencies	CaP	Bone	(Chernousova et al., 2013; Curtin et al., 2015; Endo et al., 2006;

	serum free conditions				Keeney et al., 2010; Krebs et al., 2010)
Lipid-based vectors	High DNA loading capacity. Moderate transfection efficiencies.	Cytotoxicity. Low stability Low half-life. Interaction with serum.	Lipofectamine	Bone, cartilage	(Goomer et al., 2001; Guo et al., 2006; Ono et al., 2004; Park et al., 2003, 2007; Wehrhan et al., 2012; Zhang et al., 2015b)
Polymeric vectors	Very diverse (natural and synthetic). Moderate transfection efficiencies. Easy to incorporate into biomaterials.	Cytotoxicity. Immunogenicity.	PEI	Muscle, bone, cartilage	(Cheong et al., 2007; Curtin et al., 2015; D'Mello et al., 2015; Elangovan et al., 2014; Hong et al., 2004; Huang et al., 2005a; Im et al., 2011; Needham et al., 2014; Pi et al., 2011; Plonka et al., 2017; Qiao et al., 2013; Schillinger et al., 2008; Türk et al., 2007)
			PLGA	Cartilage	(Jeon et al., 2012)
			Chitosan	Cartilage	(Wang et al., 2010)
Protein and peptide vectors	Biodegradability. Low toxicity. High stability. Specificity for delivery. Moderate transfection efficiencies.	Unexplored for gene delivery in orthopaedic applications.			

2.4. Incorporation of gene therapy into tissue engineering strategies: Gene activated matrices

TE aims to regenerate damaged tissues by developing biological substitutes to restore, maintain or improve tissue function. This approach is summarized in the tissue engineering triad which includes the combination of cells, scaffolds and bioactive factors in order to engineer a desired tissue type (O'Brien, 2011; Smith and Grande, 2015) (Fig.2.4.A). The combination of gene therapy and tissue engineering can offer a promising alternative for enhancing tissue repair strategies and offering temporal and spatial control of the delivery of genes encoding for relevant therapeutic growth and transcription factors (W. Mark Saltzman, 1999).
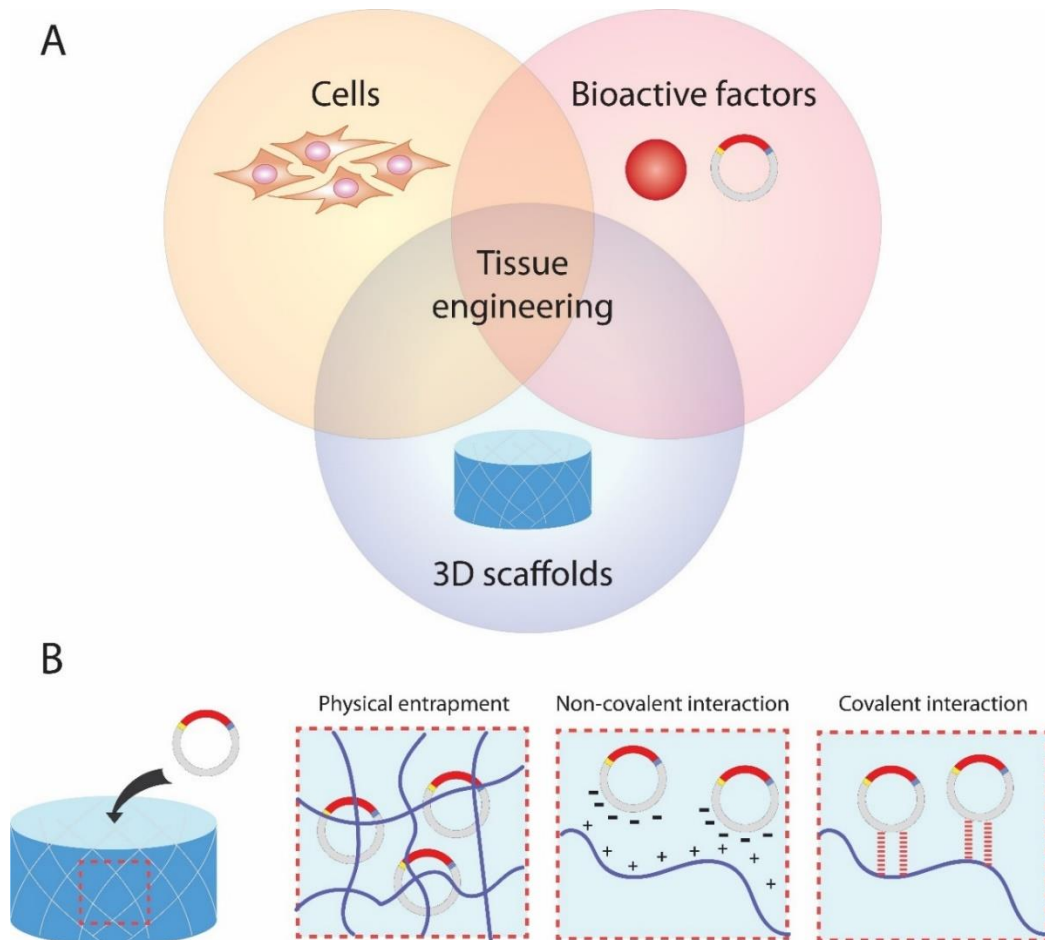
Fig.2.4. (A) TE triad. (B) The incorporation of pDNA into a 3D matrix to form a GAM can be done through physical entrapment, non-covalent interactions and covalent interaction of the pDNA or pDNA-vector complexes and the selected material.

2.4.1. Principles of GAM technology

The importance of the combination of 3D matrices or scaffolds with gene therapy for tissue engineering lies in a more prolonged delivery of the transgene and in a more confined and localized effect of its overexpression, overcoming the limitations of 2D transfection (Dinser et al., 2001; Madry et al., 2003) and direct intra-articular injection which is not appropriate for targeting a specific tissue (Madry and Cucchiarini, 2014). It is also hypothesized to be superior to *ex vivo* approaches in which the therapeutic effect is dependent on the survival of the transfected cells. The sustained cell-mediated production of the desired factors also might be a way to increase their therapeutic potential through increasing the residence time and the bioactivity of the secreted proteins. GAMs are the result of this strategy in which a gene and its delivery vector are contained in a biodegradable scaffold which offers structural support, cell attachment, retention of new tissue formation and confined gene delivery for an *in situ* effect.

GAMs offer a promising platform for localised and sustained gene delivery for the repair of orthopaedic tissues. Initially they were developed by Fang *et al.* and Bonadio *et al.* in the 1990's as an inexpensive off-the shelf alternative to protein and viral gene delivery for the repair of *in vivo* long bone defects (Bonadio et al., 1999; Fang et al., 1996). In these two studies, once implanted in the defect area, the pDNA loaded collagen sponges were colonised by the host cells showing for the first time that repair cells could be transfected *in vivo* (Fang et al., 1996) and continuously express the genes of interest resulting in a faster and reproducible healing of the damaged bone (Bonadio et al., 1999; Fang et al., 1996). Since these early innovative attempts, GAMs have been researched to improve their DNA binding capacities, their capacity to deliver the genes of interest and cell transfection, and their healing outcome.

2.4.2. DNA-GAM interactions

The scaffold requirements for use as a GAM do not differ from the requirements of traditional tissue engineering applications. They should be biocompatible, biodegradable, non-toxic, able to support cell growth and proliferation, and, in addition, they must facilitate and enhance gene transfection. To facilitate gene delivery, the

interaction between the nucleic acid and the matrix is a critical factor. For this purpose, technologies to maximize DNA presentation, release and subsequent transfection have been developed. DNA can be incorporated with scaffolds by three mechanism: (A) physical entrapment, (B) non-covalent interactions and (C) covalent interaction (Fig.2.4.B).

2.4.2.1. Physical entrapment

For the physical entrapment method, the pDNA or vector-pDNA complexes are confined within the 3D matrices during the gelation or crosslinking process (Fig.2.4.B). DNA release depends on the degradation of the matrix (De Laporte and Shea, 2007). Different techniques for the entrapment of pDNA and vector-pDNA complexes have been explored but they are limited to the use of high temperatures, organic solvents and shear stresses that might result in DNA damage (Jang and Shea, 2003). Nucleic acid entrapment in poly(lactade-co-glycolide) (PLG) microspheres through a gas foaming method was shown to sustain temporal pDNA delivery while maintaining the integrity of the DNA molecule during the microsphere fabrication (Mooney et al., 1999). PEI-pDNA complexes were also encapsulated in PLG porous scaffolds using this method, showing long-term *in vivo* transfection (Huang et al., 2005b) and regeneration of a cranial defect model when the BMP4 gene was delivered (Huang et al., 2005a). A different strategy consisting in the *in situ* crosslinking of PEG networks was shown to entrap pDNA encoding for secreted embryonic alkaline phosphatase (pSEAP) which upon intramuscular injection was able to produce high levels of expression in comparison to repeated DNA injections (Roy et al., 2003). One of the most tunable and explored hydrogel materials for cartilage and bone TE is alginate. The biocompatibility of the gelation method and its pore size, which has been reported to be on the order of 5-6 nm, makes alginate also a good candidate for sustained release of vector-pDNA therapeutics (Boontheekul et al., 2005). CaP-pDNA complexes of around 100nm have been encapsulated in alginate showing a slow pDNA release profile due to the degradation of the hydrogels (Krebs et al., 2010). When pDNA encoding for BMP2 encapsulated in this alginate system was injected in the back of mice, the gene activated

hydrogels were able to form bony tissue in two weeks (Krebs et al., 2010). Alginate gene activated hydrogels have also been shown to promote *in vivo* bone formation in a goat iliac crest model (Loozen et al., 2015).

2.4.2.2.   Non-covalent interactions

Nucleic acid adsorption into a material is based on the non-specific interactions of the pDNA or the pDNA-vector complexes with the material substrate due to their affinity (Fig.2.4.B). This method, together with chemical conjugation, allows for the immobilization of the pDNA after the scaffold fabrication process (De Laporte and Shea, 2007), avoiding any DNA damage that can result from the material preparation. The nucleic acid release is determined by the molecular interactions between the vector and the scaffold as a result of their molecular composition and the scaffold degradation. Both, free negatively charged DNA and positively charged DNA-vector complexes, can interact with polymeric scaffolds through hydrophobic, electrostatic and Van der Waals interactions (Segura et al., 2005). Examples of these interactions are the loading of free DNA or DNA complexed to polymeric, lipid-based and inorganic vectors into natural and synthetic polymeric materials such as collagen, ceramics, extracellular matrix (ECM) components, PLG and PCL between others (Jang et al., 2006; Peng et al., 2009; Raftery et al., 2015; Tierney et al., 2012). To promote adsorption, the electrostatic properties of the bulk biomaterial can be tailored. The inclusion of charged moieties or ECM components such as negatively charged sulfated glycosaminoglycans (GAGs) and heparin binding peptides, to promote an optimal electrostatic environment for gene delivery, have shown to increase the amount of retained cationic PEI-DNA complexes and hence increase transfection (Hortensius et al., 2015). The modification of collagen matrices with poly-L-lysine has also been shown to enhance pDNA retention (Cohen-Sacks et al., 2004). Alternatively, the vector-pDNA complexes can be also modified to improve their affinity with the carrier material. Collagen-mimetic peptides have been linked to DNA polyplexes in order to tune the polyplex retention and release in collagen scaffolds (Urello et al., 2014). Also to increase the positive charge of the vector has been

shown to enhance PEI-pDNA polyplexes adsorption into PLG scaffolds allowing for two-fold higher transfection efficiencies than bolus delivery (Jang et al., 2006).

2.4.2.3.   Covalent interaction

The adsorption of the nucleic acid material into a 3D matrix might be limited in TE by the use of conditioned media which might contain serum proteins and other cellular products that could induce release of the adsorbed pDNA through enzymatic reactions or competitive protein adsorption. Chemical immobilization (Fig.2.4.B) could overcome these limitations, help reduce the amount of genetic material needed and also gain fine control of the release kinetics. Incorporation of PEI-pDNA complexes by non-specific adsorption, or using covalent biotin/neutravidin conjugation into hyaluronic acid (HyA) hydrogels, showed increased transfection and overexpression in the biotinylated complexes (Segura et al., 2005). PEI-pDNA complexes covalently attached to deprotected amino groups in poly(ε-CBZ-l-lysine) films was shown to promote gene delivery in comparison to the adsorbed complexes (Zheng et al., 2000). Covalent immobilization of liposome-pDNA complexes into thiol-functionalized PCL nanofiber meshes facilitated the gene delivery of RUNX2 to human MSCs and enhanced their osteogenic potential (Monteiro et al., 2014b).

2.4.3. Biomaterials for GAMs

When applying GAMs to TE we should consider that the matrix should not only be biocompatible and allow for gene transfection, but also to promote and maintain the desired phenotype and guide the formation of new tissue, approaching its native mechanical and biochemical properties. The choice of material for a GAM must be specific for the desired tissue type and be optimized to promote the final goal of orthopedic tissue repair. Based on these cocepts, the ideal characteristics required for a GAM in tissue engineering are:

1. Cell compatible to allow for cell survival, growth and differentiation.

2. Facilitate nucleic acid-matrix interaction, through the mechanisms defined in the previous section, to retain the gene of interest in the site of action and avoiding its uncontrolled diffusion to the surrounding tissues.

3. The material and its production mechanism should be chemically and physically compatible with the nucleic acid and its delivery vector to avoid damage of the genetic material and undesired interactions that might hinder transfection.

4. Adaptability of the material to be easily modified to allow for the desired release/up take kinetics and to be customized for different applications depending on the characteristics of the target tissue and injury type.

Taking these observations into account, different natural and synthetic materials in different conformations have been explored for material-guided gene delivery in orthopaedic tissues.

2.4.3.1. Natural polymers

Polymers of natural origin are a promising biomaterial for TE due to their biocompatibility, biodegradability and their biomimetic signaling that promotes cell migration, proliferation and differentiation. Biopolymers can also be processed in a variety of ways to form different types of scaffolds, from porous solid constructs to hydrogels. Natural materials such as collagen, chitosan, CaP, fibrin, hyaluronic acid (HyA) and alginate between others have been used as GAMs for non-viral gene delivery in the context of bone and cartilage TE. As the major component of ECM, collagen was the initial material used for GAM technology. Collagen has been extensively studied and optimized for gene delivery in cartilage and bone TE. Furthermore, porous collagen scaffolds have been tailored in terms of mechanical properties and chemical composition to direct MSC differentiation towards either the osteogenic or chondrogenic phenotype. While, the incorporation of CaP to a collagen matrix have been shown to increase the material mechanics and osteogenic potential of MSCs, the addition of GAGs to the material has been shown to act as a successful cartilaginous template (O'Brien et al., 2005). Additionally, the gene activation of CaP modified

collagen matrices have shown to be superior for bone regeneration than when collagen-GAG matrices were used (Capito and Spector, 2007). Also, the natural interactions between cells and collagen has been hypothesized to facilitate the cellular uptake of adsorbed pDNA and vector-pDNA complexes (Browne et al., 2012), and collagen natural capacity to bind to cytokines might increase the retention of the overexpressed factors and their therapeutic outcome. These studies highlight the importance of coupling both the matrix material and the gene delivery strategy to leverage the possible synergistic therapeutic effects.

2.4.3.2. Synthetic polymers

Natural polymers face challenges such as batch-to-batch variability, immunogenicity, difficulty of sterilization, low mechanical properties and poor control of the degradation rate and release kinetics (Vo et al., 2012). Synthetic polymers are an alternative to natural materials due to their great versatility which allows for tailoring of their physical, chemical and mechanical properties for different tissue engineering and regenerative medicine (TERM) applications. Additionally, they provide fine control of pore size, geometry and connectivity for tunable controlled release of bioactive factors (Vo et al., 2012). Different synthetic polymers such as PCL, PLG, PEG and PLGA have been explored as substrate for non-viral gene delivery in orthopedic TE (Jeon et al., 2011; Monteiro et al., 2014b; Roy et al., 2003; Whittlesey and Shea, 2006). The major limitation of synthetic polymers is their cellular interaction. Functionalization of these materials with cell adhesion ligands or with ECM-derived materials have been investigated to increase cell interaction, differentiation and specific tissue formation.

2.4.3.3. Material configuration

Not only the choice of material, but its configuration is also important for their use as tissue engineered GAMs. Porous solid GAMs are the main material configuration used as platform for gene delivery. They are preferred due to the ease of pDNA loading and

high cell motility which allows continuous gene uptake. Gene activated hydrogels have also been developed due to their potential delivery *via* minimally invasive administration, high permeability for oxygen and nutrients, homogeneous cell and nucleic acid distribution, and their suitability for the treatment of irregular shaped defects (Madry and Cucchiarini, 2014). In addition, they are suitable for their use as cell and gene carriers in biofabrication techniques such as 3D bioprinting. Two widely used hydrogels for cartilage and bone tissue engineering are agarose (Benya and Shaffer, 1982) and alginate (Goren et al., 2010; Häuselmann et al., 1996; Heiligenstein et al., 2011). Additionally, the incorporation of ECM molecules to different types of hydrogels such as hyaluronic acid or collagen (Benoit et al., 2008) have been studied in order to mimic the biochemical composition of native tissues.

2.5. Non-viral gene therapy for the repair of Bone and Cartilage

The application of non-viral GAMs in orthopaedics is mainly limited to the regeneration of bone and cartilage. Although non-viral gene delivery has been explored for the repair of tendon (Delalande et al., 2015; Gerich et al., 1997; Goomer et al., 2000), skeletal muscle (DiFranco et al., 2009; Hong et al., 2004; Mansouri et al., 2004; Mir et al., 1999; Türk et al., 2007; Zelenin et al., 1997), meniscus (Lee et al., 2014; Zhang et al., 2009), ligament (Gerich et al., 1997) and intervertebral disc (Nishida et al., 2006), to the author's knowledge there are no reports on the use of non-viral biomaterial-guided gene delivery for the repair of the aforementioned tissues.

2.5.1. Bone

The osseous tissue is a supporting connective tissue which comprises specialised cells and a solid matrix formed mainly by mineral salts (HA and calcium carbonate) and collagen type I (Ateshian and Mow, 2005; Martini et al., 2009). Osteocytes are the main cell population in bone tissue, they maintain the protein and mineral content of bone through a constant turnover of its component and also participate in the repair of

damaged bone through its conversion into osteoblasts or osteoprogenitor cells (Martini et al., 2009). In addition to osteocytes, bone also contains other cell types such as mesenchymal stem cells located mainly in the marrow tissue and osteoclast which are in charge of bone resorption (Martini et al., 2009). Bone tissue is also highly vascularised to allow bone growth and maintenance.

To develop a successful gene delivery-based bone regeneration strategy special focus has been performed not only on the matrix and cellular composition of bone but also in the areas of bone developmental and repair processes. Endochondral and intramembranous ossification, bone vascularisation and hormonal factors have been explored to this end (Table 2.3).

Table 2.3. Non-viral gene delivery approaches for bone regeneration *in vivo.*

Strategy	Genes	Transfection approach	Delivery method	Model	Refs
Endochondral / intramembranous ossification	BMP2	*In vivo*, electroporesis	Injection	Rat skeletal muscle injection	(Kawai et al., 2003, 2005)
	BMP2	*Ex vivo*, liposome	Periosteal explants, GAM	Rat mandible defect	(Park et al., 2003)
	BMP2	*In vivo*, CaP	Atelocollagen, GAM	Rat tibia defect	(Endo et al., 2006)
	BMP2	*In vivo*, liposome	Hydroxyapatite, GAM	Rabbit cranial defect	(Ono et al., 2004)
	BMP2	*Ex vivo*, liposome	PEG, scaffold	Porcine cranial defect	(Wehrhan et al., 2012)
	BMP2	*In vivo*, liposome	Injection	Porcine cranial defect	(Park et al., 2007)
	BMP2	*In vivo*, entrapment in alginate hydrogels	Alginate, GAM	Goat iliac crest	(Loozen et al., 2015)
	BMP2	*In vivo*, entrapment in	Alginate, GAM	Subcutaneous, mouse	(Wegman et al., 2013)

		alginate hydrogels			
	BMP2	*In vivo*, CaP	Alginate, GAM	Subcutaneous mouse	(Krebs et al., 2010)
	BMP4	*In vivo*, PEI	PLGA, GAM	Rat cranial defect	(Huang et al., 2005a)
	BMP6	*In vivo*, sonoporation	Collagen, GAM	Porcine tibia defect	(Bez et al., 2017)
	TGF-β3	*In vivo*, entrapment in collagen hydrogel	Collagen, GAM	Rat cranial defect	(Premaraj et al., 2005)
Vascularisation and angiogenesis	VEGF	*Ex vivo*, dendrimer	Gelatin, scaffold	Rabbit tibia defect	(Li et al., 2009)
	VEGF	*In vivo*, pDNA adsorption into collagen scaffold	Collagen, GAM	Rabbit radius defect	(Geiger et al., 2005)
	FGF2	*Ex vivo*, liposome	β-TCP, scaffold	Rabbit radius defect	(Guo et al., 2006)
	PDGF	*In vivo*, PEI	Collagen, GAM	Periodontal rat defect	(Plonka et al., 2017)
	PDGF	*In vivo*, PEI	Collagen, GAM	Rat cranial defect	(Elangovan et al., 2014)
Hormonal process	PTH 1-34	*In vivo*, pDNA adsorption into collagen scaffold	Collagen, GAM	Canine femoral defect	(Bonadio et al., 1999)
Combinatorial gene delivery	PDG VEGF	*In vivo*, PEI	Collagen, GAM	Rat cranial defect	(D'Mello et al., 2015)
	BMP2 BMP7	*In vivo*, sonoporation	Collagen/fibrin, GAM	Mouse intramuscular	(Nomikou et al., 2017)
	BMP2 BMP7	*In vivo*, electroporation	Injection	Rat intramuscular	(Kawai et al., 2005)
	BMP2 VEGF	*In vivo*, nHA/PEI	Collagen, GAM	Rat cranial defect	(Curtin et al., 2015)

2.5.1.1. Bone development strategies

Endochondral ossification is the process by which bones are originated from a cartilage template. The cartilage resident cells, chondrocytes, start increasing in size and become hypertrophic, these hypertrophic chondrocytes calcify the cartilage template and disintegrate leaving cavities in the cartilaginous tissue that allow the penetration of blood vessels and osteoblasts as a result of the fibroblast differentiation (Martini et al., 2009). Following these events, the osteoblasts begin producing spongy bone and creating a primary ossification centre from which bone formation spreads (Yu et al., 2010). The other developmental process of bone formation is called intramembranous ossification which starts with MSCs condensation and alkaline phosphatase mediated mineralisation of the secreted tissue, and differentiation of the MSCs into osteoblasts to form an ossification centre that is subsequently vascularised (Martini et al., 2009). Members of the transforming growth factor-β superfamily are important regulators of these ossification processes.

Of special importance is BMP2 which has shown to initiate the cascade of biological events of endochondral ossification (Kawai et al., 2005; Yu et al., 2010). BMP2 has also been identified as a therapeutic target for intramembranous ossification. Collagen type I scaffolds loaded with recombinant BMP2 have been shown to promote both, intramembranous and endochondral ossification, suggesting that the BMP2-mediated ossification process might be dependent on the BMP2 application method, concentration, tissue environment and *in vivo* model (Kawai et al., 2005; Stoeger et al., 2002). Also, the electroporation of pDNA encoding for BMP2 into the rat musculoskeletal muscle showed the development of both hypertrophic cartilage regions and intramembranous bone formation 10 days post transfection (Kawai et al., 2005). Injection of liposomes-pBMP2 complexes into porcine cranial defects was able to transfect the host cells that were migrating into the tissue and maintaining the gene overexpression for 4 weeks, but not complete osseointegration in the centre of the defect was achieved (Park et al., 2007). Liposome-mediated BMP2 *ex vivo* transfection of BMSCs transplanted into a rat critical size mandible resulted in the differentiation of the BMSCs into osteogenic progenitors and successful repair of the defect by 6 weeks

71

(Park et al., 2003). Collagen scaffolds loaded with CaP complexed to pDNA encoding for BMP2 has also been reported to enhance bone repair and bridge rat tibia defects after 4 weeks of implantation following a GAM approach (Endo et al., 2006). This same GAM approach was explored with liposome-pBMP2 complexes loaded into hydroxyapatite porous scaffolds showing healing of a rabbit cranial defect in 9 weeks (Ono et al., 2004). BMP2 *ex vivo* transfection of human foetal osteoblast using liposomal vectors and posterior seeding in PEG scaffolds and implantation in a porcine cranial defect model enhanced bone formation (Wehrhan et al., 2012). BMP2 gene delivery in MSC-laden alginate hydrogels was shown to promote ossification and mineralisation *in vivo* when implanted subcutaneously (Wegman et al., 2013) and in when implanted in a goat iliac crest model (Loozen et al., 2015). BMP2 gene has also been delivered using a gene-activated injectable alginate gel system capable of promoting bone formatin subcutaneously (Krebs et al., 2010).

Additionally, gene delivery of other factors from the TGF-β superfamily have been explored for bone formation. BMP4 encoding pDNA complexed to PEI and loaded into a PLGA scaffold was tested in a cranial defect resulting in enhanced mineralisation in comparison to the controls (Huang et al., 2005a). BMP6 gene material-guided sonoporation was shown to transfect 40% of the cells that colonized the construct and the overexpression of BMP6 transgene led to complete fracture healing after 6 weeks (Bez et al., 2017). TGF-β3 pDNA was entrapped in a collagen hydrogel and implanted *in vivo* in a rat cranial defect showing successful gene transfection after 14 days, but the potential of this approach for bone regeneration was not reported (Premaraj et al., 2005).

2.5.1.2. Vascularization

Common to both, endochondral and intramembranous ossification, vascularisation is a key process to provide the new bone with enough oxygen and nutrients. Vascular endothelial growth factor (VEGF) has been identified as one of the most potent promoters of vascularisation during endochondral ossification and fracture repair (Street et al., 2002). Non-viral *Ex vivo* transfection of fibroblasts with the VEGF

gene and posterior implantation in a rabbit bone defect was shown to promote blood vessel formation, callus maturation and defect bridging (Li et al., 2009). The delivery of the VEGF gene in a non-viral collagen GAM approach also showed successful bone repair in a rabbit radius model (Geiger et al., 2005). Another target in order to promote angiogenesis for bone repair is fibroblast growth factor 2 (FGF2), which has been shown to promote the regeneration of capillary vasculature (Radomsky et al., 1998). Non-virally FGF2 *ex vivo* transfected BMSCs were seeded on tricalcium phosphate (β-TCP) scaffolds and implanted into rabbit radial defects; increased vascularisation of the constructs and bone formation were observed (Guo et al., 2006). Another target for this approach is the use of platelet derived growth factor (PDGF) which is involved in the stimulation of local angiogenesis and osteoblast migration during bone fracture (Caplan and Correa, 2011). A collagen-based GAM containing PEI-pPDGF complexes was shown to enhance bone production and repair in a rat cranial defect (Elangovan et al., 2014). In a follow up study using the same system, the sustained delivery of PEI-PDGF was shown to prolong inflammation and delayed bone healing in a rat periodontal defect, in comparison to the empty collagen scaffold and the PDGF recombinant protein loading (Plonka et al., 2017), suggesting that optimisation of the system is needed in order to couple gene transfection and physiological repair processes.

2.5.1.3. Hormonal processes

In order to maintain normal bone growth and homeostasis, the hormonal processes are essential for calcium and phosphate absorption, osteoblast activity, matrix production and bone repair. Different repair strategies have been inspired in these processes. Parathyroid hormone 1-34 (PTH 1-34) has been shown to stimulate osteoblasts to produce new bone matrix resulting in an increase of the bone density, mass and mechanical strength (Vahle et al., 2002). Gene delivery of PTH 1-34 in a collagen scaffold was shown to promote fracture repair in a canine critical femoral defect (Bonadio et al., 1999).

2.5.2. Cartilage

Cartilage is a soft connective tissue formed by a highly specialised ECM and chondrocytes, as the single cell type in this tissue (Ateshian and Mow, 2005). Hyaline cartilage, the most common type of cartilage, is present in the articulating surfaces of long bones to lubricate movement and provide protection against friction and wear (Ateshian and Mow, 2005). The main components of cartilage are interstitial water (60-85%), collagen type II (15-22%) and GAGs (4-7%) (Ateshian and Mow, 2005).Due to its avascular nature and the low mitotic activity of chondrocytes, cartilage shows a low capacity for self-repair upon damage.

Cartilage development starts, similarly to the endochondral ossification process, with MSC condensation and differentiation into chondrocytes which secrete the cartilage matrix components such as proteoglycans and collagen type II. Unlike the endochondral ossification process, stable cartilage is characterized by the suppression of chondrocyte hypertrophy, vascularization and calcification of the matrix. This process is highly regulated by different types of growth and transcription factors that have been identified as targets for their use in gene therapy approaches.

Gene therapy strategies for cartilage regeneration are based not only in the developmental processes of cell differentiation and cartilaginous matrix synthesis, but also in the degradative processes experiment by cartilage during pathological processes such as OA. Gene therapy for the treatment of cartilage and osteochondral defects has traditionally focused on the use of anabolic cytokines and transcription factors and co-factors involved in chondrogenic differentiation and cartilage matrix production, the suppression of chondrocyte hypertrophy and endochondral ossification, and the inhibition of catabolic processes that take place during cartilage pathologies.

Table 2.4. Non-viral gene delivery approaches for cartilage regeneration *in vivo.*

Strategy	Genes	Transfection approach	Delivery method	Model	Refs
Cell differentiation / matrix production	TGF-β1	*In vivo*, PLL	PLGA, GAM	Rabbit osteochondral defect	(Li et al., 2013)
	TGF-β1	*In vivo*, chitosan	PLGA, GAM	Rabbit full-thickness cartilage defect	(Wang et al., 2010)
	TGF-β1	*Ex vivo*, pullulan-spermine	Gelatin	Rat full-thickness cartilage defect	(He et al., 2012)
	TGF-β1	*In vivo*, pDNA adsorption into chitosan-gelatin scaffold	chitosan-gelatin, GAM	Rabbit full-thickness cartilage defect	(Diao et al., 2009)
	IGF1	*Ex vivo*, lipoplex	Alginate	Rabbit full-thickness cartilage defect	(Madry et al., 2005)
	FGF2	*Ex vivo*, lipoplex	Alginate	Rabbit osteochondral defect	(Kaul et al., 2006)
	SOX9	*Ex vivo*, PLGA	Injection	Mouse subcutaneous	(Jeon et al., 2012)
	CDMP1	*Ex vivo,* lipoplex	Collagen gel	Rabbit osteochondral defect	(Katayama et al., 2004)
	BMP2	*In vivo*, PEI	Fibrin gel	Rabbit osteochondral defect	(Schillinger et al., 2008)
	IL-10	*In vivo*, electroporesis	Intra-articular injection	Mouse collagen	(Khoury et al., 2006)

				induced arthritis model	
	IL-1RA	*In vivo*, liposome	Intra-articular injection	Rabbit OA model	(Zhang et al., 2015b)
Combinatorial gene delivery	IGF1 FGF2	*Ex vivo*, lipoplex	Alginate	Rabbit osteochondral defect	(Madry et al., 2010; Orth et al., 2011)
	TGF-β1 PTHrP	*Ex vivo*, liposome	PLA	Rabbit full-thickness cartilage defect	(Goomer et al., 2001)
	IL-1RA TGF-β1	*In vivo*, liposome	Intra-articular injection	Rabbit OA model	(Zhang et al., 2015b)
Zonal gene delivery	TGF-β1 (cartilage) / BMP2 (bone)	*In vivo*, pDNA adsorption into the scaffold	Chitosan-gelatin / chitosan-gelatin-hydroxyapatite, GAM	Rabbit osteochondral defect	(Chen et al., 2011)
	SOX trio (cartilage) / RUNX2 (bone)	*In vivo,* PEI-hyaluronic acid	OPF pore-forming hydrogel	Rat osteochondral defect	(Needham et al., 2014)

2.5.2.1. Chondrogenic differentiation and cartilage matrix production strategies

To promote cell differentiation and cartilage matrix production, the anabolic cytokines are a group of genes of major interest for cartilage gene therapy approaches. Over-expression of genes encoding for secreted extracellular growth factors is hypothesized to enhance matrix production in the area defined by the construct, and also on the adjacent tissue facilitating the integration of the newly formed cartilage following *in vivo* implantation (Madry et al., 2012). Between these, the members of the TGF-β superfamily, TGF-β1 and 3, are recognized as two of the most important growth

factors for cartilage tissue engineering (Kock et al., 2012), as they promote chondrocyte proliferation, ECM synthesis (van der Kraan et al., 1992; Morales, 1991; Roman-Blas et al., 2007), and chondrogenic differentiation of MSCs (Almeida et al., 2014; Johnstone et al., 1998; Mackay et al., 1998; Schulz et al., 2008). For these reasons, gene delivery of TGF-β1 and 3 has been widely investigated, offering a promising alternative to growth factor supplementation for cartilage tissue engineering (Elmallah et al., 2015; Hao et al., 2008; Ivkovic et al., 2010; Pagnotto et al., 2007; Zhang et al., 2015a). Moreover, intra-articular injection of genetically modified human chondrocytes overexpressing TGF-β1 has overcome clinical phases I and II providing beneficial effects for OA treatment (Elmallah et al., 2015; Ha et al., 2012). Regarding non-viral gene delivery of these factors *in vivo*, pDNA encoding for TGF-β1 was complexed to a chitosan derivative and loaded into fibrin-PLGA scaffolds which promoted cartilage repair in a rabbit full thickness cartilage defect when BMSCs were included in the GAM system (Wang et al., 2010). In a follow up study, pTGF-β1 complexed to poly(ethylene oxide)-b-poly(L-lysine) (PEO-b-PLL) was loaded into the same PLGA GAM system and implanted in a rabbit osteochondral defect, resulting in cartilage tissue production containing levels of type II collagen and GAGs similar to the native tissue (Li et al., 2013). The adsorption of pTGF-β1 into a chitosan-gelatin scaffold and its implantation in a rabbit full thickness cartilage defect promoted the chondrogenic differentiation of MSCs loaded in the scaffold, the secretion of hyaline cartilage matrix and improved cartilage repair after 10 weeks (Diao et al., 2009). *Ex vivo* approaches have also been studied. Non-viral *ex vivo* transfection of MSCs with TGF-β1 and posterior implantation using a gelatin sponge into a rat full-thickness cartilage defect resulted in the development of a thick repaired cartilage layer but not complete repair of the defect (He et al., 2012). Other targets that remain unexplored for non-viral gene therapy approaches *in vivo* for cartilage regeneration, are TGF-β3 and TGF-β2. Lentiviral gene delivery of TGF-β3 in a PCL scaffold has proven as effective as TGF-β3 medium supplementation for chondrogenic differentiation of human MSCs in terms of ECM formation *in vitro* (Brunger et al., 2014). The application of viral delivery of the TGF-β2 gene in a GAM, has been shown to limit collagen resorption and chondrocyte hypertrophy in an *in vitro* culture of OA patient's explants (Tchetina et al., 2006).

Therapeutic targets from the TGF-β superfamily also include the BMPs and the cartilage-derived morphogenic proteins (CDMP). BMP factors play an important role in MSCs and chondrocyte proliferation and differentiation through the crosstalk with the TGF-β isotypes in the SMAD signaling pathway (Keller et al., 2011; Yoon et al., 2005). For these reasons, different BMPs such as BMP2 (Gelse et al., 2008), BMP4 (Shi et al., 2013), BMP6 (Kayabaşi et al., 2013), and BMP7 (Grande et al., 2003) have been investigated in viral gene delivery approaches to enhance cartilage repair. The delivery of pDNA encoding for BMP2 using gene-activated fibrin glue offered no significant improvement in rabbit osteochondral defects (Schillinger et al., 2008). CDMPs have been shown to promote MSC aggregation and chondrogenic differentiation. Over-expression of CDMP1 in non-virally transfected MSCS and posterior implantation in a collagen gel into a rabbit osteochondral defect, showed better cartilage surface repair and deeper zone remodeling than the controls (Katayama et al., 2004).

Other important anabolic cytokine genes used in GAMs to induce chondrogenesis and cartilage repair are insulin growth factor 1 (IGF1) and FGF2. Chondrocytes non-virally transfected with IGF1 and seeded in alginate hydrogels, showed improved articular cartilage repair and subchondral bone formation in comparison to the reporter gene controls when implanted in a rabbit osteochondral defect (Madry et al., 2005). *Ex vivo* lipid-mediated transfection of chondrocytes with the FGF2 gene was shown to enhance collage type II deposition, and improved cartilage repair in a rabbit osteochondral defect model (Kaul et al., 2006).

The overexpression of transcription factors is another way to induce chondrogenesis and cartilage matrix production. Unlike cytokines, transcription factors are proteins that directly bind to specific DNA sequences promoting or blocking the transcription of a gene (Latchman, 1997). Even though the use of genes encoding for growth factors and other secreted cytokines is preferred to transcription factors when using non-viral gene therapy approaches due to low transfection efficiencies, the delivery of transcription factor genes for tissue engineering is of special interest. Gene delivery of transcription factors also shows a determinant advantage as these factors can't be applied as soluble factors and their localization inside the cell confines their effects to only the transfected cells, preventing any undesired accumulation or side-

effects in a non-targeted tissue. The most common transcription factors used for gene therapy in cartilage tissue engineering are the sex- determining region Y–type high mobility group box (SOX) family, specifically the SOX trio formed by SOX9, SOX5 and SOX6. SOX9 transfection of MSCs using PLGA microspheres and subcutaneous *in vivo* implantation of the genetically modified cells, enhanced their expression of chondrogenic genes such as collagen type II and agreccan and the secretion of a cartilaginous matrix (Jeon et al., 2012). SOX9 has also been shown to be an important factor for the inhibition of endochondral ossification and chondrocyte hypertrophy down-regulating RUNX2 and cartilage vascularization (Chen et al., 2015; Hattori et al., 2010a).

2.5.2.2. Inhibition of endochondral ossification

To suppress endochondral ossification different genes targeting different processes involved in the conversion of cartilage into bone have been studied. The identification of endochondral ossification and chondrocyte hypertrophy inhibitors is also important for the treatment of OA related pathologies which might result in calcification and vascularization of the damaged cartilage. Between these targets, we can highlight the parathyroid hormone receptor protein (PTHrP), antagonist of BMP like gremlin 1 (GREM1), inhibitors of angiogenesis like chondromodulin 1 (CHM1) and endostatins, and histone deacetylases (HDACs) such as HDAC4 which targets the osteogenic gene RUNX2.

PTHrP has been shown to enhance chondrogenic differentiation of MSCs and down-regulate the expression of markers of chondrocyte hypertrophy such as collagen type X, RUNX2 and alkaline phosphatase (ALP) (Chen et al., 2015). Non-viral co-delivery of TGF-β1 and PTHrP was hypothesized to promote cartilage matrix production by chondrocytes and to suppress chondrocyte hypertrophy (Goomer et al., 2001). The therapeutic outcome of this strategy was not tested in an *in vivo* cartilage defect (Goomer et al., 2001).

Antagonists of the BMPs such as GREM1, frizzled related protein (FRZB) and dickkopf 1 homolog (DKK1) have been identified as one of the most upregulated genes

in articular cartilage in comparison to growth plate (Leijten et al., 2012a). GREM1 has been shown to inhibit chondrocyte hypertrophy and matrix mineralization when supplemented into the culture media *in vitro* (Leijten et al., 2012a). Although promising results, the overexpression of these factors remains unexplored for cartilage TE.

Inhibitors of vascularization such as CHM1 and endostatins are a promising option to inhibit endochondral ossification. Furthermore, vascular invasion into the cartilage surface is a hallmark of OA and numerous angiogenic factors such as VEGF have been detected in the OA affected tissues (Suri and Walsh, 2012). Decrease of CHM1 expression in OA degenerated cartilage was shown to correlate with angiogenesis progression (Deng et al., 2017). Viral-mediated transfection of the CHM1 gene into cartilage lesions in miniature pigs stimulated chondrogenic differentiation of the host progenitor cells and inhibited chondrocyte hypertrophy and vascularization (Klinger et al., 2011). Endostatin is a proteolytic fragment of collagen type XVII and it has been shown to inhibit endothelial cell migration and proliferation and angiogenesis (Taddei et al., 1999). Lipoplex-mediated transfection of MSCs in a collagen GAM with the endostatin gene was shown to sustain the expression of the transgene over 14 days (Sun et al., 2009). The therapeutic effects of this approach were not explored *in vivo*.

HDAC4 has been shown to modulate cell fate by modifying the chromatin structure and regulating the expression of transcription factors such as RUNX2 (Chen et al., 2015). Viral-mediated overexpression of HDAC4 has also shown to support chondrogenesis and suppress the expression of collagen type X (Pei et al., 2009). Non-viral gene delivery of HDAC4 for cartilage TE remains unexplored.

2.5.2.3. Inhibition of catabolic processes

Catabolic genes are those that encode for pro-inflammatory cytokines (*e.g.* interleukin 1 alpha (IL-1α), interleukin 1 beta (IL-1β) and tumor necrosis factor alpha (TNF-α)), and extracellular matrix proteases such as matrix metalloproteases (MMPs) and disintegrin and metalloproteinase with thrombospondin motifs (ADAMTs)

(Goldring, 2000). These cytokines and proteases are overexpressed in osteoarthritic cartilage.

Gene therapy featuring anti-inflammatory cytokines has been shown as an effective way to suppress the inflammatory pathology in OA. Retroviral *ex vivo* gene delivery of interleukin 1 receptor antagonist (IL-1Ra) to human arthritic joints has been tested in two clinical trials (Evans et al., 2005; Wehling et al., 2009), while scaffold-mediated lentiviral IL-1Ra gene delivery strategy has been shown to inhibit the negative effects of IL-1 on chondrogenesis of MSCs *in vitro* (Glass et al., 2014). IL-1RA complexed to lipofectamine was also delivered through intra-articular injection in a rabbit OA model showing localised expression and suppressed the formation of bone spurs and improved regeneration (Zhang et al., 2015b). Intra-articular injection of adenoviral vectors containing a tumor necrosis factor antagonist gene (TNFR:Fc) has also been tested as a treatment for rheumatoid arthritis in phase II clinical trials (Mease et al., 2010). Another target explored for reducing the inflammation in arthritis is the gene delivery of the anti-inflammatory cytokine interleukin-10 (IL-10), which non-viral delivery through intra articular injection showed to inhibit the clinical and biological features of arthritis in an arthritic mouse knee (Khoury et al., 2006).

Other catabolic inhibitors of interest are the tissue inhibitors of metalloproteinases (TIMPs) which supress MMP mediated degradation of the cartilaginous ECM (Brew et al., 2000). The retroviral gene transfer of TIMP-1 into chondrocytes has been shown to inhibit the effects of IL-1 and prevent collagen breakdown *in vitro* (Kafienah et al., 2003). The α2-macroglobulin (α2M) protein prevents cartilage degradation through inhibition of MMPs (Tchetverikov et al.) and ADAMTs (Tortorella et al., 2004) but its gene transfer remains to be validated for cartilage tissue engineering applications.

2.6. Future directions

2.6.1. Combinatorial gene therapy in bone and cartilage orthopedic tissue engineering

Bone and cartilage tissue repair and development are dynamic, highly regulated and organized processes that are driven by the action of multiple growth factors, for the modulation of different cellular activities such as cellular recruitment, mitosis, differentiation, and tissue formation. Moreover, the developmental and pathological processes involving bone and cartilage are complex, and the delivery of just one gene might not be enough to develop a successful regenerative strategy. Combinatorial viral and non-viral gene delivery strategies targeting different processes for bone and cartilage regeneration highlight the importance and feasibility of a multigenic approach as an option to secure a more successful and complete repair that can answer current therapeutic challenges.

2.6.1.1. Combinatorial gene therapy for bone TE

The first description of a GAM-based non-viral multiple gene delivery for bone regeneration was based on the potential synergistic effects of the co-delivery of PDGF and VEGF for bone regeneration. The combination of the chemotactic and mitogenic effects of PDGF and the angiogenic potential of VEGF were explored by the PEI-mediated delivery of these two genes *in vivo* using a collagen scaffold as carrier material (D'Mello et al., 2015). Surprisingly, the co-delivery of both factors offered reduced bone repair in comparison to the delivery of PDGF gene alone (D'Mello et al., 2015). The authors hypothesized that a sequential delivery, in order to recapitulate the bone repair processes in which PDGF is secreted first after a fracture and is followed by VEGF expression, could have been beneficial for enhanced bone repair (D'Mello et al., 2015). Another combinatorial gene delivery approach used *in vivo* for bone formation is the co-delivery of the BMP2 and BMP7 genes which co-expression have been reported to synergistically enhance osteogenesis of progenitor cells and ALP activity resulting in

rapid bone formation (De Bari et al., 2006), and ectopic osteogenic differentiation *in vivo* (Nomikou et al., 2017). Another promising strategy for the enhancement of bone formation and vascularization is the co-delivery of osteogenic and angiogenic genes such as BMP2 and VEGF. The co-delivery of both these genes in a collagen-based GAM system resulted in higher bone formation and vessel formation in a rat cranial defect (Curtin et al., 2015).

2.6.1.2.   Combinatorial gene therapy for cartilage and OA

For cartilage TE, instead of the promotion of endochondral ossification, the inhibition of this process is desired. One of the problems of the use of factors from the TGF family is the propensity to undergo chondrocyte hypertrophy and endochondral ossification, characterized for deposition of collagen type X, collagen type I and mineralization of the cartilage templates. For example, in previously mentioned studies, non-viral TGF-β1 delivery in an osteochondral defect showed collagen type II, aggrecan and SOX9 expression levels similar to native cartilage but also high levels of collagen type X and I (Li et al., 2013). The combination of the overexpression of inductors of chondrogenesis such as TGF-β1 and suppressors of hypertrophy has been explored to promote the formation of stable hyaline cartilage. Non-viral delivery of TGF-β1 and parathyroid hormone related protein (PTHrP) was hypothesized to promote cartilage matrix production by chondrocytes and perichondral cells but, at the same time, to suppress collagen type X production and chondrocyte hypertrophy (Goomer et al., 2001), but the therapeutic outcome of this strategy was not tested in an *in vivo* cartilage defect (Goomer et al., 2001). Another strategy explored to promote chondrogenesis of progenitor cells and suppress hypertrophy is the co-delivery of chondrogenic factors such as FGF2 and BMP2 with SOX9 (Cha et al., 2013; Cucchiarini et al., 2009; Liao et al., 2014). Also, the co-delivery of the SOX5, SOX6 and SOX9, also known as the SOX trio, have been hypothesized to enhance chondrogenic differentiation and suppress hypertrophy when delivered together in comparison to the administration of these factors individually. SOX5 and SOX6 have been shown to enhance the transcriptional activity of SOX9 over type II collagen, aggrecan and other chondrogenesis related genes

(Lefebvre et al., 1998). Electroporation of ASCs with the SOX trio genes individually and in combination was shown to enhance chondrogenesis when the three genes were delivered but no significant increase in chondrogenesis was observed when the genes were administered individually (Im and Kim, 2011). The PLGA-mediated transfection of a multicistronic pDNA encoding for these 3 genes was also proven superior for chondrogenic differentiation of MSCs than the transfection of each single gene (Park et al., 2017).

IGF1 and FGF non-viral co-delivery has also been hypothesized to synergistically enhance chondrogenesis and cartilage repair though the induction of chondrogenesis and chondrocyte proliferation due to FGF2 overexpression and the promotion of cartilage matrix production and phenotype stabilization due to IGF1 delivery. NIH 3T3 cells and chondrocytes transfected with lipoplexes complexed to both FGF2 and IGF1 showed to promote articular cartilage repair, subchondral bone formation and a protective effect in the neighboring cartilage in a rabbit osteochondral defect (Madry et al., 2010; Orth et al., 2011).

Another promising strategy for the treatment of OA in which both, cartilage matrix production and decrease of inflammation are needed, could be the combination of induction of chondrogenesis through the delivery of factors from the TGF-β family and inflammation inhibitors such as IL-10 and IL-1RA. The intra-articular injection of IL-1RA and TGF-β1 genes complexed to lipofectamine into a rabbit OA model showed better repair outcomes than the injection of the single genes, and surprisingly offered a synergistic effect as the TGF-β1 overexpression increased the endogenous expression of IL-1RA (Zhang et al., 2015b). A GAM based strategy combining both, regenerative and anti-inflammatory gene overexpression could also be successful for the treatment of cartilage defects.

2.6.2. Spatially controlled biomaterial-guided gene delivery

Traditionally, tissue engineering strategies have focused on the development of homogenous implants of uniform composition, but in orthopaedic tissues cell types, ECM components and bioactive cues are spatially organised. For example, bone is a complex organ which comprises mineralised osseous tissue, marrow, endosteum and periosteum nerves and blood vessels which are organised according to the different areas of the bone anatomy (Martini et al., 2009). Cartilage tissue also shows a heterogenous composition formed by a superficial layer of hyaline cartilage, a middle zone and a deep zone of calcified cartilage (Martini et al., 2009) (Fig.2.5.A). Successful tissue engineering strategies must recapitulate this heterogeneous architecture to produce biologically functional devices that once implanted will perform similarly to native tissues. The engineering of scaffolds with a gradient in composition, structure, mechanical and chemical properties that can modulate cellular behaviour in a graded way are a promising alternative to support the growth of heterogeneous tissues. This same reasoning can be applied to biomaterial-guided gene delivery, but the spatial presentation of nucleic acids faces many challenges and novel strategies are needed.

For this purpose, the biomaterial-nucleic acid interaction is a critical factor, and it must be finely tuned for the effective micropatterning of different genes and gene carriers. While the spatial distribution of nucleic acid adsorbed into 3D porous materials faces multiple challenges due mainly to diffusion of the loaded genetic material and the unspecific interactions between the DNA and the substrate, DNA entrapment into hydrogels and chemical immobilisation might be more suitable approaches for the spatial incorporation of genetic cues. Lipoplex-pDNA complexes were chemically immobilised in a polydimethylsiloxane (PDMS) substrate to create 100-1000 μm wide patterns of transgene expression of nerve growth factor (NGF) in order to engineer *in vitro* graded neural tissue (Houchin-Ray et al., 2007). The engineering of pDNA gradients based on the production of HA gradients in a electrospun fibrous scaffold, also resulted in zonal reporter gene overexpression (Zou et al., 2012). Entrapment of lipofectamine-pDNA complexes in fibrin hydrogels during the polymerisation process was shown to provide confined gene transfer suitable for the development of cell transfection microarrays that could be also used for graded TE (Lei et al., 2009).

Also, different materials loaded with different nucleic acids can be organised following the architecture of the desired tissue in a multilayer approach. The spatial organisation of materials with different biological properties could also act synergistically with the delivered genes to promote graded cell differentiation and organised new tissue deposition. For example, a pTGF-β1 loaded chitosan-gelatin scaffold and a pBMP2 loaded HA/chitosan-gelatin scaffold were combined through fibrin glue fixation for osteochondral tissue engineering (Chen et al., 2011). A major limitation of this approach might be the delamination of the multiple layers when implanted *in vivo* (Nooeaid et al., 2012).

2.6.2.1. Spatial gene delivery at the tissue interface: the osteochondral unit

As introduced previously, articular cartilage is a highly organised tissue. It is structured in three different zones which show different composition and mechanical properties (Fig.2.5.A). These three zones are: superficial zone, middle zone, and deep zone. The superficial zone contains high levels of collagen type II and lower levels of GAG, the middle zone contains the highest GAG concentration and the lowest levels of collagen type II, and the deep zone is characterised for the presence of high levels of collagen type X and calcification which integrates into the subchondral bone (Nguyen et al., 2011) (Fig.2.5.A). Due to this different ECM distribution and organisation, the mechanical properties of the tissue also vary throughout the different layers. The compressive modulus increases significantly from the superficial zone to the deep zone (Nguyen et al., 2011). Since the functionality of cartilage depends on the described spatial architecture, it is important that tissue engineering strategies reproduce this native structure.
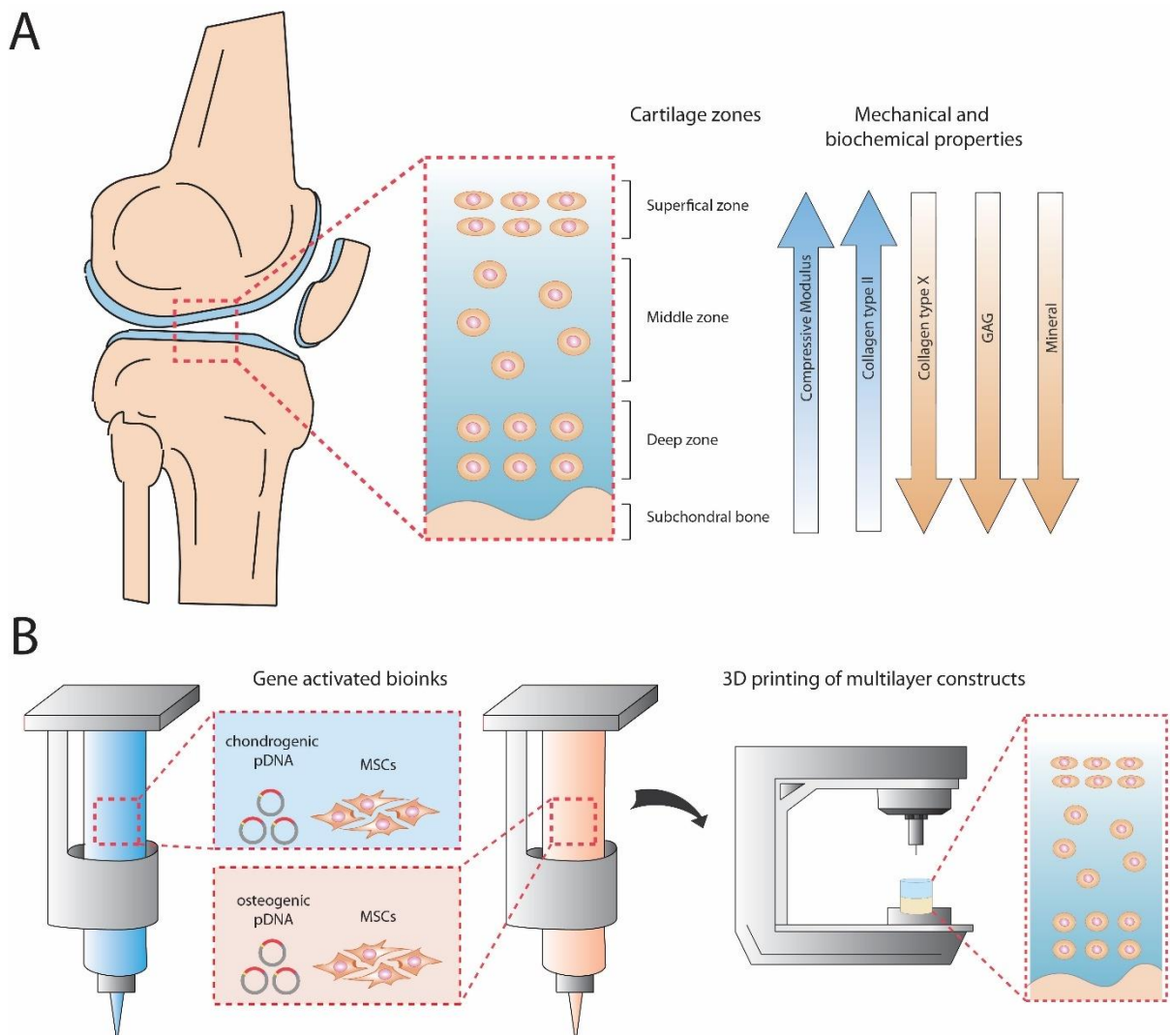
Fig.2.5. (A) Structure of articular cartilage and its different mechanical and biochemical properties. (B) The incorporation of chondrogenic and osteogenic genes into bioinks to form GABs could be used for the 3D printing of gene activated constructs to recapitulate cartilage native structure.

Different biomaterial, cell and protein-based strategies have been explored to this end but challenges remain. For example, previously in our research group, the differential distribution of chondrocytes and stem cells in agarose hydrogels developed zonal chondrogenesis and endochondral ossification *in vitro* and *in vivo* when implanted subcutaneously (Sheehy et al., 2013). Due to the limitations associated with the use of autologous chondrocytes for TE (Brittberg et al., 1994), progenitor stem cells have been hypothesized as a promising alternative. For the spatial differentiation of progenitor cell types, the use of the zonal presentation of material stiffness and growth factors has also been studied. The engineering of stem cell laden constructs composed of a soft

chondrogenic layer and a stiffer bone layer was not enough to spatially guide MSC differentiation (Steinmetz et al., 2015). Multilayer MSC seeded bilayered PLG scaffolds containing a zonal gradient of the growth factors TGF-β3 and BMP4 in the cartilage and bone layer respectively, resulted in the spatial differentiation of the stem cells, but collagen type X was found in both layers suggesting the development of a hypertrophic phenotype in the cartilage layer and the need of the local inhibition of this process for the generation of stable hyaline cartilage.

Similar approaches have been explored for gene delivery. As previously mentioned, MSC-laden pTGF-β1 loaded chitosan-gelatin and pBMP2 loaded HA/chitosan-gelatin scaffolds were combined through fibrin glue fixation to create a bilayered osteochondral construct which provided simultaneous formation of articular cartilage and subchondral bone when implanted *in vivo* in an osteochondral defect model (Chen et al., 2011). Gene delivery also offers the possibility of the overexpression of transcription factors whose effect is much more localised in comparison to the delivery of growth factors that can diffuse through the construct. Polymeric delivery of pDNA encoding for the SOX trio genes in the cartilage layer and RUNX2 in the bone layer was explored to spatially control MSC differentiation in a oligo[poly(ethylene glycol) fumarate] (OPF) hydrogel (Needham et al., 2014). When these constructs were implanted in a rat osteochondral defect the bilayered scaffolds showed improved healing in comparison to empty controls and the application of only one gene (Needham et al., 2014). The main limitations of this study was the possible interaction between the SOX trio and RUNX2 overexpression which could counteract each other's action and the coupling of the processes of gene transfection and scaffold degradation for the regeneration of higher quality tissue (Needham et al., 2014).

2.6.2.2. Biofabrication and gene delivery

Recently biofabrication methods have started to gain importance as they allow the production of multiphasic scaffolds that can potentially reproduce the structural and biological cues of intricate tissues (Lopa and Madry, 2014; Shimomura et al., 2014; Visser et al., 2015). The combination of biofabrication techniques with gene therapy is an interesting option for achieving a zonal distribution of genes encoding for different molecules that can help mimic the zonal genetic gradients found in non-homogenous tissues such as articular cartilage (Fig.2.5.B). 3D printing of gene activated alginate hydrogels has been considered as a promising approach for bone tissue engineering (Loozen et al., 2013), and thermal inkjet printing has been reported to generate transient pores in the membrane of cells that can be used for plasmid DNA delivery with a 30% transfection efficiency (Cui et al., 2010). Furthermore, the co-printing of gene activated materials and mechanically robust polymers such as PCL could be a promising alternative for the generation of mechanically robust constructs in which multiple layers are mechanically integrated to avoid delamination. Bioprinting might solve the limitations of traditional tissue engineering associated with poor layer integration, the scalability of the approach and the tissue organization present in the repair tissue. In addition, more sophisticated patterns of genetic material could be achieved using bioprinting technology to recapitulate the body's natural developmental and regenerative pathways.

2.6.3. Temporally controlled biomaterial-guided gene delivery

The presentation of microenvironmental signals during tissue development and healing is highly regulated, not only spatially but also temporally. The temporal regulation of bioactive factor delivery has been explored to prolong its action during the required time to promote a cellular response, and to recapitulate the timing of its presentation to match with the natural processes that are necessary for tissue development and healing (Samorezov and Alsberg, 2015).

In the context of gene delivery, temporal regulation of gene expression has multiple advantages over constitutive gene expression since the overexpression of a determined transgene is usually only required during a determined phase of repair, and its continuous expression can result in abnormal regulation of cell growth and differentiation with non-expected side-effects (Crystal, 1995). For example, for cartilage tissue repair, when using gene therapy to enhance chondrogenesis by the overexpression of differentiating factors, the termination of gene expression might be required in order to maintain the differentiated state and avoid further differentiation into the hypertrophic or fibroblastic phenotype (Glass et al., 2014), or to avoid undesired accumulation of growth factors that can result in abnormal tissue formation and inflammation (Zara et al., 2011). Furthermore, when applying anti-inflammatory gene therapy for the treatment of inflammatory disorders such as OA, we have to take into account that some inflammatory cytokines such as IL-1 are required for early stages of tissue repair (Gerstenfeld et al., 2003).

Temporal control of gene overexpression is also of great importance when a combinatorial gene delivery approach is chosen. For example, the process of osteochondral ossification is based on the development of a cartilage template that becomes vascularized and remodeled. The presentation of chondrogenic and angiogenic signals at the same time to reproduce this process might not be ideal as low oxygen levels play an important role in MSC chondrogenesis. Similarly, when trying to engineer articular cartilage in a multilayer approach, the overexpression of potent inhibitors of chondrocyte hypertrophy in the cartilage layer might also affect the promotion of endochondral ossification needed for the integration with the subchondral bone required in an osteochondral defect model.

The promotion of temporal control in non-viral GAM-based gene delivery provides a significant challenge. Recently, the use of ultrasound pulses and pDNA loaded porous constructs has been explored for gaining temporal control over the transfection of cells recruited to a bone fracture site (Bez et al., 2017; Shapiro et al., 2014). Also, the use of ultrasound to open up pores in a pDNA loaded alginate hydrogel was shown to offer temporal transfection of cells encapsulated in the matrix (Huebsch et al., 2014). Although this technique allows for on-demand control of gene delivery in the site of

injury, it is still unclear how this approach could be applied for the sequential delivery of multiple genes.

Another option to temporally control the overexpression of multiple genes is the use of inducible expression systems such as tetracycline-inducible promoters, also called tetracycline-on (Tet-On). This system is controlled by the administration of tetracycline or doxycycline for induction of transgene expression, meaning that the gene of interest will only be expressed in the presence of a specific drug (Gossen and Bujard, 1992). The on-toxicity, high specificity and reversibility, are the main advantages of this approach (Gossen and Bujard, 1992; Lamartina et al., 2003). In cartilage tissue engineering the Tet-On system has been established for *in vivo* and *in vitro* induction of gene expression (Ueblacker et al., 2004), and modulation of the expression of growth factors such as BMP2 (Wübbenhorst et al., 2010) and anti-inflammatory cytokines (Glass et al., 2014). The use of inducible promoters to control the expression of delivered genes might be a promising strategy to temporally recapitulate the processes of tissue formation and healing.

2.7. Towards commercialization: From bench to bedside

The application of gene therapy in orthopedics has the potential to broaden the field of gene therapy from the treatment of rare genetic diseases to its presence in the daily life of millions of people suffering from degenerative diseases such as OA. Still numerous hurdles exist for the translation of orthopedic gene therapy strategies from bench to bedside. The primary limitations are financial, safety, regulatory and sociological (C.H. Evans, S.C. Ghivizzani, 2012).

Two significant challenges that the application of gene therapy must address for musculoskeletal tissue engineering are: to offer a cost-effective treatment that can provide stable long-term repair of the tissue and its functionality, and the safety of the gene transfer methods. Despite over 1800 clinical trials worldwide (C.H. Evans, S.C. Ghivizzani, 2012; Ledley et al., 2014) that demonstrate gene therapy can be used as a safe and effective treatment, this technology has been traditionally viewed as an unsafe

treatment that will struggle to meet the constraints of the regulatory bodies. This vision prevents orthopedic gene therapy from being an attractive candidate for funding by the large pharmaceutical companies, leaving gene therapy in the hands of start-up companies dependent on venture capital and unable to assume the expenses of performing late-stage clinical trials needed for commercialization of gene therapy products (Ledley et al., 2014; Michael, 1996).

In addition to the economic and safety issues, the regulatory constraints that gene therapy must overcome have increased exponentially, resulting in an expensive and time-consuming process. This reduces the attractiveness of gene therapy for the pharmaceutical industry.

Gene therapy faces a difficult translational environment that must be overcome to convert the recent favorable clinical results into effective market products available for the treatment of common musculoskeletal disorders. To change this scenario, closer cooperation between scientists, clinicians, regulatory bodies and the pharmaceutical industry is needed.

2.8. Conclusion

Direct protein delivery for orthopedic tissue engineering is limited by low stability and challenges associated with controlled, localized release over therapeutically relevant windows; however, non-viral gene therapy can potentially overcome these limitations and offer a more physiological option which can be spatiotemporally regulated for a durable therapeutic effect. Tissue engineering strategies that combine these characteristics of non-viral gene therapy with the mechanical and biological support of 3D scaffolds and hydrogels are especially suited for regenerative therapies targeting orthopedic tissues such as bone and cartilage.

In this review the current concepts and strategies for the use of non-viral gene therapy in combination with 3D matrices for the repair of orthopedic tissues were described to analyze the current successes and future challenges for their establishment as a viable clinical option. The combination of 3D matrices and gene therapy depends

on a multifactorial design in which the gene delivery vector, the carrier material, and the target tissue play a fundamental role for the ultimate success of this approach for the treatment of traumatic injuries and degenerative diseases such as arthritis and OA. To this end, challenges that remain to be addressed include the determination of which transgene combination is optimal for specific aspects of tissue repair, and the engineering of novel systems for the spatiotemporal control of gene delivery to recapitulate the architecture of native tissues and also the signaling cascades of developmental and repair processes.

The current thesis explores these scientific questions, focusing on the engineering of non-viral biomaterial-guided gene delivery for osteochondral TE as a model of complex orthopedic tissues. The type of gene carrier, gene combination and supporting material will be systematically analysed to gain spatiotemporal control of gene transfection of primary stem cells and subsequent protein production and differentiation, in order to spatially differentiate a single progenitor differentiation into either articular cartilage or subchondral bone within a 3D printed clinically relevant gene activated construct.

CHAPTER 3

Gene Delivery of TGF-β3 and BMP2 in a MSC-Laden Alginate Hydrogel for Articular Cartilage and Endochondral Bone Tissue Engineering

Abstract

Incorporating therapeutic genes into 3D biomaterials is a promising strategy for enhancing tissue regeneration. Alginate hydrogels have been extensively investigated for cartilage and bone tissue engineering, including as carriers of transfected cells to sites of injury, making them an ideal gene delivery platform for cartilage and osteochondral tissue engineering. The objective of this study was to develop gene-activated alginate hydrogels capable of supporting nanohydroxyapatite (nHA)-mediated non-viral gene transfer to control the phenotype of mesenchymal stem cells (MSCs) for either cartilage or endochondral bone tissue engineering. To produce these gene-activated constructs, MSCs and nHA complexed with plasmid DNA (pDNA) encoding for TGF-β3 (pTGF-β3), BMP2 (pBMP2), or a combination of both (pTGF-β3/pBMP2), were encapsulated into alginate hydrogels. Initial analysis using reporter genes showed effective gene delivery and sustained overexpression of the transgenes was achieved. Confocal microscopy demonstrated that complexing the plasmid with nHA prior to hydrogel encapsulation led to transport of the plasmid into the nucleus of MSCs, which did not occur with naked pDNA. Gene delivery of TGF-β3 and BMP2 and subsequent cell-mediated expression of these therapeutic genes resulted in a significant increase in sGAG and collagen production, particularly in the pTGF-β3/pBMP2 co-delivery group in comparison to the delivery of either pTGF-β3 or pBMP2 in isolation. In addition, stronger staining for collagen type II deposition was observed in the pTGF-β3/pBMP2 co-delivery group. In contrast, greater levels of calcium deposition were observed in the pTGF-β3 and pBMP2 only groups compared to co-delivery, with strong staining for collagen type X deposition, suggesting these constructs were supporting MSC hypertrophy and progression along an endochondral pathway. Together these results suggest that the developed gene-activated alginate hydrogels were able to support transfection of

encapsulated MSCs and directed their phenotype towards either a chondrogenic or osteogenic phenotype depending on whether TGF-β3 and BMP2 were delivered in combination or in isolation.

3.1. Introduction

In this chapter we aimed to investigate nHA as non-viral gene carrier vector for the delivery of therapeutic genes to MSCs to develop gene activated hydrogels capable of sustaining both, nHA-pDNA complex uptake and differentiation of MSCs. Thus, we addressed the first objective of this thesis of exploring the capacity of nHA to transfect MSCs encapsulated in alginate hydrogels for bone and cartilage TE.

Adult mesenchymal stem cells (MSCs) are a promising cell source for cell-based cartilage tissue engineering strategies due to their capacity to differentiate into cells of the chondrogenic lineage (Tuan et al., 2003). In comparison to chondrocytes, MSCs can be obtained in high numbers from a variety of adult tissues *via* minimally invasive procedures (Steinert et al., 2007; Tuan et al., 2003) and can be expanded in culture without losing their chondrogenic differentiation potential, even when isolated from elderly or diseased donors (Dudics et al., 2009; Scharstuhl et al., 2007). A major concern with the use of MSCs for articular cartilage regeneration is their inherent tendency to progress towards hypertrophy and endochondral ossification or to undergo fibrous dedifferentiation (Steinert et al., 2007; Vinardell et al., 2012). However, this inherent potential of chondrogenically primed MSCs to become hypertrophic can be leveraged for endochondral bone tissue engineering, which aims to recapitulate embryonic skeletal development in order to engineer fully functional bone tissue (Cunniffe et al., 2015a; Farrell et al., 2011; Scotti et al., 2013; Sheehy et al., 2013; Thompson et al., 2014). Ultimately, it is important to be able to control the MSC phenotype towards a particular target application (e.g. stable articular cartilage or bone). One way to achieve this is through the use of gene or growth factor delivery in combination with biomaterials for tissue repair.

Recombinant growth factor administration has been widely investigated for tissue engineering, however the delivery of such factors *in vivo* for therapeutic effect is hampered by issues such as their short half-life, transient action, and side effects

associated with the need for delivery of high concentrations of protein to elicit a therapeutic outcome (Zara et al., 2011). Non-viral gene therapy may provide a more physiological, durable and cost-effective alternative (Meinel et al., 2006; Saraf and Mikos, 2006). Expression of the gene product also guarantees authentic post-translational modifications reducing possible immunogenicity and increasing biological activity in comparison to pre-synthesised recombinant proteins (Evans, 2014). Additionally, gene therapy allows for a simpler way of simultaneous and sequential delivery of cell-mediated growth and transcription factors that could enhance the multifactorial process of articular cartilage regeneration. In tissue engineering applications, gene therapeutics can be combined with biomaterials for a prolonged, sustained and localized *in situ* delivery of a protein of interest. This approach may overcome the limitations associated with 2D transfection (Dinser et al., 2001; Madry et al., 2003) and direct injection which are not ideal for targeting a specific tissue or cell type (Madry and Cucchiarini, 2014). Hydrogels are extensively used in tissue engineering to provide cells with a three-dimensional (3D) environment similar to native extracellular matrix (ECM). Hydrogels offer many advantages over pre-fabricated porous scaffolds; they are typically more compatible with minimally invasive delivery strategies, permit efficient oxygen and nutrient transport, facilitate homogeneous cell distribution, and can be used in the treatment of irregular shaped defects. However, to date, only a limited number of studies have explored the use hydrogels as gene delivery platforms or gene activated matrices (GAMs) for articular cartilage tissue engineering (Kaul et al., 2006; Madry et al., 2005).

Alginate is a naturally occurring anionic polymer that is ideally suited to cartilage and bone tissue engineering due to its biocompatibility, tailorable degradation kinetics and low toxicity (Lee and Mooney, 2012). Encapsulation of MSCs in alginate hydrogels has demonstrated potential for both cartilage and bone regeneration *in vitro* and *in vivo* (Igarashi et al., 2010; Ma et al., 2003; Sheehy et al., 2014a; Simmons et al., 2004; de Vries-van Melle et al., 2014). Alginate hydrogels have also been used as a 3D gene delivery platform for bone tissue engineering applications (Krebs et al., 2010; Loozen et al., 2013; Wegman et al., 2011, 2014), and to support transfected chondrocytes for articular cartilage regeneration (Kaul et al., 2006; Madry et al., 2005; Orth et al., 2011).

This hydrogel therefore has broad potential applications in orthopedic medicine if appropriate strategies can be developed to control therapeutic gene delivery and hence cell fate within such constructs. The overall objective of this study was thus to develop and characterise a novel nanohydroxyapatite (nHA)-mediated non-viral gene-activated alginate hydrogel capable of directing MSC fate by delivering the therapeutic genes TGF-β3 and/or BMP2. It was hypothesized that chondrogenesis and the progression towards hypertrophy and endochondral ossification within such an alginate construct can be either suppressed or enhanced by the delivery of specific genes to encapsulated MSCs.

3.2. Materials and methods

3.2.1. Experimental design

In order to achieve the objectives of this study, a series of different experiments were performed. Firstly, nHA transfection efficiency and its effects on cell viability were assessed in 2D using PEI as a control. Secondly, nHA-gene-activated alginate hydrogels were produced and reporter genes encoding for green fluorescent protein (pGFP) and luciferase (pLuc) were used to determine the capacity of these gels to transfect MSCs over time and to explore their potential cytotoxicity. Additionally, tracking of nHA-pGFP complex uptake in the gene-activated alginate hydrogels was performed through pDNA labelling and cell fluorescent staining using confocal microscopy. Thirdly, the effects of the delivery of the therapeutic genes TGF-β3 and BMP2 in isolation or in combination on MSCs encapsulated within these hydrogels were assessed. Specific protein expression was confirmed using ELISA and differentiation of the MSCs was assessed through biochemical, histological and immunohistochemical analysis of the secreted extracellular matrix components. Mechanical testing of the gene activated hydrogels was also conducted.

3.2.2. Isolation and expansion of bone marrow-derived MSCs

Bone marrow-derived stem cells (BMSCs) were isolated from the femora of porcine donors (3-4 months, >50 kg) within 3 hours of sacrifice according to a modified method developed for human MSCs (Lennon and Caplan, 2006). Mononuclear cells were

plated at a seeding density of 5×10^3 cells/cm² in standard culture media containing high-glucose Dulbecco's modified eagles medium (4.5 mg/mL D-Glucose, 200 mM L-Glutamine; hgDMEM) supplemented with 10% fetal bovine serum (FBS), penicillin (100 U/mL)–streptomycin (100 g/mL) (all GIBCO, Biosciences, Dublin, Ireland), and expanded to passage two in a humidified atmosphere at 37 °C, 5% CO_2 and 20% pO_2.

3.2.3. Plasmid propagation

Four different plasmids were used in the current study, two plasmids encoding for the reporter genes luciferase (pGaussia- Luciferase, New England Biolabs, Massachusetts, USA) and green fluorescent protein (pGFP) (Amaxa, Lonza, Cologne AG, Germany), and another two encoding for the therapeutic genes bone morphogenic protein 2 (BMP2) (the BMP2 plasmid was a kind donation from Prof. Kazihusa Bessho, Kyoto University, Japan) and transforming growth factor beta 3 (TGF-β3) (InvivoGen, California, USA). Plasmid amplification was performed by transforming One Shot® TOP10 Chemically Competent E. coli bacterial cells (Biosciences, Ireland) according to the manufacturer's protocol. The transformed cells were cultured on LB plates with 50 mg/L kanamycin (Sigma-Aldrich, Ireland) as the selective antibiotic for pGFP, and 100 mg/L of ampicillin (Sigma-Aldrich, Ireland) as the selective antibiotic for pLuc, pTGF-β3 and pBMP2 competent bacteria. Bacterial colonies were harvested and inoculated in LB broth (Sigma-Aldrich, Ireland) overnight for further amplification. The harvested bacterial cells were then lysed and the respective pDNA samples were collected using a MaxiPrep kit (Qiagen, Ireland). Nucleic acid content was analysed using NanoDrop 1000 spectroscopy, taking the 260/280 ratio and 230 nm measurement to determine the ng/µl measurement. Plasmids in this study were used at a concentration of 0.5 µg of plasmid in 1 µl of Tris-EDTA (TE) buffer.

3.2.4. Nanohydroxyapatite (nHA)–plasmid DNA (pDNA) complex formation and monolayer transfection

The synthesis of the nHA nanoparticles was performed as previously described (Cunniffe et al., 2010). Briefly, a solution of 12 mM sodium phosphate, containing 0.017% Darvan 821A (RT Vandervilt, Norwalk, CT), was added to an equal volume of a

20 mM calcium chloride solution and filtered through a 0.2 μm filter. The nHA-pDNA transfection mix consisted of 150 μl (monolayer transfections) or 50 μl (gene-activated alginate hydrogels) of the nHA solution added to the pDNA (specific amounts detailed below) combined with 0.25 M of CaCl$_2$. Monolayer nHA-pGFP and nHA-pLuc transfections were performed adding the 2 μg of nHA-pGFP or nHA-pLuc complexes suspended in 500 μl standard culture media to BMSCs seeded in 6 well plates at a cell density of 5 x 10^4 cells/well. Residual complexes were removed after 4 hours of incubation and replaced with fresh culture media.

3.2.5. Polyethylenimine (PEI)-pDNA complex formation and monolayer transfection

PEI was used as a positive control for the determination of the transfection efficiency of the MSCs in monolayer. Branched 25kDa PEI (Sigma-Aldrich, Ireland) was condensed with pDNA encoding for GFP in an N/P ratio = 7. PEI-pGFP monolayer transfections were performed adding 2 μg of the PEI-pGFP complexes suspended in 500 μl of Opti-MEM Reduced Serum Media (Life Technologies, Dun Laoghaire, Ireland) to BMSCs seeded in 6 well plates at a cell density of 5 x 10^4 cells/well. PEI-pGFP complexes were removed after 4 hours of incubation and new standard culture media was added.

3.2.6. Assessment of MSC monolayer transfection efficiency

Analysis of monolayer transfection efficiency was conducted by determining the percentage of green fluorescent cells at 3 and 7 days post-transfection in relation to the whole population through cell sorting using a BD Accuri™ C6 flow cytometer.

3.2.7. Assessment of metabolic activity and cell viability

Cell metabolic activity was evaluated using AlamarBlue^{TM} (BioSciences, Dun Laoghaire, Ireland), a non-endpoint, non-toxic assay, after 3 and 7 days of nHA and PEI-mediated gene delivery in monolayer, and after 1 and 7 days in the 3D gene-activated alginate hydrogel system. 10% AlamarBlue^{TM} in 1 ml of standard culture media was used for the assay. All samples were incubated for 4 hours at 37 °C. After the incubation time,

200 µl of the supernatant was plated in triplicate into a 96-well plate, absorbance was read at 570 nm and 600 nm and its reduction was translated to cell activity relative to the non-transfected control.

For nHA-pLuc transfected groups, cell viability was assessed using LIVE/DEAD® Viability/Cytotoxicity Assay Kit (Invitrogen, Bio-science, Ireland). Images were taking by confocal microscopy using an Olympus FV-1000 Point-Scanning Confocal Microscope (South-on-Sea, UK) at 488 and 543 nm channels and analysed using FV10-ASW 2.0 Viewer software, and cell viability was calculated using ImageJ software.

DNA analysis was performed by digesting the samples with papain (125 µg/ml, pH = 6.5) in 0.1 M sodium acetate, 5 nM L-cysteine HCl, and 0.05 M EDTA (Sigma-Aldrich, Ireland) at 60 °C under constant rotation for 18 hours. DNA content was quantified using the Hoescht 33258 dye-based DNA QF kit and standard curve (Sigma-Aldrich, Ireland).

3.2.8. Production of the control and gene-activated alginate hydrogels

Expanded BMSCs were trypsinised and counted using trypan blue exclusion staining. For the non-transfected control groups they were encapsulated in 2% alginate yielding a final concentration of 1×10^7 cells/ml of alginate (5×10^5 cells per hydrogel). For the gene-activated alginate hydrogels, the trypsinised BMSCs were incubated with different concentrations of pDNA complexed to nHA nanoparticles for 60 minutes prior to alginate encapsulation. In the case of pGFP-gene-activated hydrogels, 2 µg of pDNA per hydrogel were used. For pLUC-gene activated hydrogels, 2 µg, 5 µg or 10 µg per hydrogel were used. For therapeutic gene delivery, 2 µg of pBMP2 (pBMP2 group), 2 µg of pTGF-β3 (pTGF-β3 group) and a combination of 2 µg of pBMP2 and 2 µg of pTGF-β3 (pTGF-β3/pBMP2 group) per hydrogel were used. After incubation, the BMSCs and the pDNA-nHA complexes were encapsulated in 2% alginate for a final concentration of 1×10^7 cells/ml of alginate.

Alginate/cell suspensions were pipetted into 3% agarose/100 mM $CaCl_2$ cylindrical moulds and the gels were allowed to ionically crosslink within these moulds at room temperature for 15 minutes to form cylindrical constructs (Ø5 x H3 mm).

3.2.9. Characterization of nHA-pDNA complex uptake and internalization in the gene-activated alginate hydrogels

Cellular uptake and internalization of labelled pDNA on its own and complexed to nHA nanoparticles were assessed through confocal microscopy using an Olympus FV-1000 Point-Scanning Confocal Microscope (South-on-Sea, UK). Actin cellular cytoskeleton staining with Alexa488 Phalloidin (Invitrogen, Ireland) and nuclear staining with diamidino-2-phenylindole (DAPI, Invitrogen, Ireland) and cyanine 3 (Cy3, LifeTechnologies, Ireland) labelling of pDNA encoding for luciferase were performed. Constructs were fixed in 4% paraformaldehyde at 4, 24 and 72 hours post-transfection and were subsequently imaged using confocal microscopy.

3.2.10. Hydrogel culture

For assessment of reporter gene expression, alginate hydrogels were cultured in standard culture medium in 24 well plates with 1 gel per well in a humidified atmosphere at 37 $^{\circ}$C, 5% CO_2 and 20% O_2. Each construct was maintained in 1.5 mL of medium with complete media changes performed twice weekly.

For differentiation of MSCs, after 1 day in standard culture media, the alginate hydrogels were cultured in a chemically defined medium (CDM) consisting of DMEM GlutaMAXTM supplemented with penicillin (100 U/ml)-streptomycin (100 µg/ml) (both Gibco, Biosciences, Ireland), 100 µg/ml sodium pyruvate, 40 µg/ml L-proline, 50 µg/ml L-ascorbic acid-2-phosphate, 1.5 mg/ml bovine serum albumin (BSA), 1 × insulin–transferrin–selenium (ITS), 100 nM dexamethasone (all from Sigma-Aldrich, Ireland), in 24 well plates with 1 gel per well in a humidified atmosphere at 37 $^{\circ}$C, and hypoxic conditions of 5% O_2 and 5% CO_2 for 28 days. Each construct was maintained in 1.5 mL of medium with complete medium changes performed twice weekly.

3.2.11. Enzyme-linked Immunosorbent Assay (ELISA) for BMP2 and TGF-β3 quantification post-transfection

The levels of BMP2 and TGF-β3 in the culture medium expressed by transfected MSCs encapsulated in the gene-activated alginate hydrogels (n=4) were quantified using ELISAs (Koma Biotech, Korea). The cell culture supernatant was collected and analysed at the following time-points: day 1, day 3, day 7, day 10 and day 14. Assays were carried out according to the manufacturer's instructions and the absorbance of each sample was read at 450 nm using a plate reader whereby the quantity of either BMP2 or TGF-β3 protein present was deduced by calculating against a standard curve.

3.2.12. Quantitative biochemical analysis

Samples were digested with papain (125 μg/ml, pH = 6.5) in 0.1 M sodium acetate, 5 nM L-cysteine HCl, and 0.05 M EDTA (Sigma-Aldrich, Ireland) at 60 $^{\circ}$C under constant rotation for 18 hours. DNA content was quantified using the Hoescht 33258 dye-based DNA QF kit (Sigma-Aldrich, Ireland). Proteoglycan content was estimated by quantifying the amount of sulphated glycosaminoglycan (sGAG) in the gels using the dimethylmethylene blue (DMMB) dye-binding assay (Blyscan, Biocolor Ltd, Northern Ireland), with a chondroitin sulphate standard. Total collagen content was determined by measuring the hydroxyproline content. Samples were hydrolysed at 110 $^{\circ}$C for 18 hours in concentrated hydrochloric acid (HCl) 38%, allowed to dry and analysed using a chloramine-T assay (Hollander and Hatton, 2003) using a hydroxyproline-to-collagen ratio of 1 : 7.69 (Ignat'eva et al., 2007). Calcium content was determined using a Sentinel Calcium Kit (Alpha Laboratories Ltd, UK) after digestion in 1 M HCl at 110 $^{\circ}$C for 36 hours. Four constructs per group were analysed for each biochemical assay.

3.2.13. Histological and immunohistochemical analysis

Constructs were fixed in 4% paraformaldehyde, dehydrated in a graded series of ethanol baths, embedded in paraffin wax, sectioned at 8 μm and affixed to microscope slides. The sections were stained with 1% alizarin red to assess calcium accumulation, aldehyde fuschin/alcian blue to assess sGAG content, and picrosirius red (all Sigma-

Aldrich, Ireland) to assess collagen production after 28 days of *in vitro* culture. Collagen types II and X were evaluated using a standard immunohistochemical technique as described previously (Sheehy et al., 2013). Negative and positive controls of porcine ligament, cartilage and growth plate were included for each immunohistochemical analysis.

3.2.14. Mechanical Testing

Constructs were mechanically tested (n=3) in unconfined compression using a standard material testing machine with a 5 N load cell (Zwick Roell Z005, Herefordshire, UK). Briefly, constructs were kept hydrated through immersion in Dulbecco's modified eagles medium (GIBCO, Biosciences, Dublin, Ireland) bath maintained at room temperature. A pre-load of 0.01 N was applied to ensure that the construct surface was in direct contact with the impermeable loading platens. Stress relaxation tests were performed consisting of a ramp displacement of 1 m/s up to 10% strain, which was maintained until equilibrium was reached (~30 min).

3.2.15. Statistical analysis

Statistical analyses were performed using GraphPad Prism (version 5) software with 3-4 samples analysed for each experimental group. Pairwise comparisons between means of different groups were performed using a Student t-test. Two-way ANOVA was used for analysis of variance with Tukey's post-hoc test to compare between groups. Numerical and graphical results are displayed as mean ± standard deviation. Significance was accepted at a level of $p < 0.05$.

3.3. Results

3.3.1. nHA can be used to effectively transfect MSCs

PEI and nHA demonstrated a comparable capacity to transfect bone marrow-derived MSCs (BMSCs) in monolayer culture, with approximately 20% of cells GFP positive at day 3 in both groups. At day 7 the percentage of GFP positive cells significantly decreased in the nHA-pGFP group, but stayed constant in the PEI group (Fig.3.1.A). Assessment of cell viability using alamar blue showed significantly higher cell metabolic activity in the non-transfected control and the nHA-pGFP group in comparison to the PEI transfected cells at day 3 (Fig.3.1.B), suggesting that PEI has a negative effect on the metabolic activity of MSCs. Increased metabolic activity was observed in the nHA-pGFP group showed at day 7 compared to the control and PEI-pGFP constructs (Fig.3.1.B).
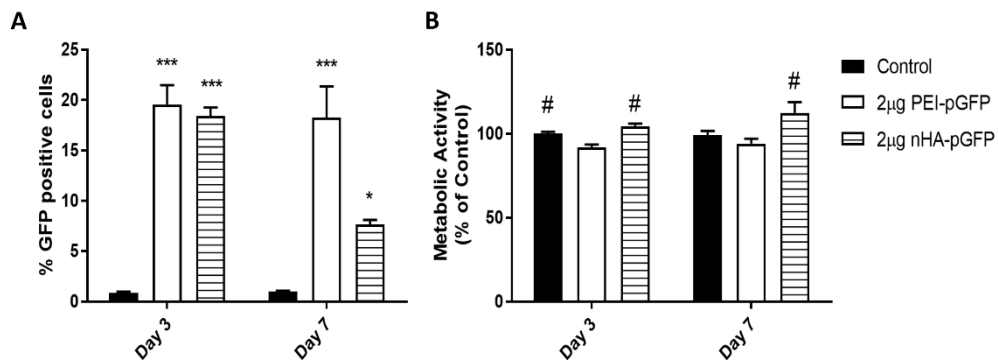
Fig.3.1. (A) Percentage of GFP positive MSCs at day 3 and 7 post-transfection with nHA nanoparticles (nHA-pGFP) and PEI (PEI-pGFP) in comparison to the non-transfected control.(B) Cell metabolic activity (% of non-transfected control) after 3 and 7 days of transfection with nHA nanoparticles or PEI complexed to pGFP. (***) Denotes significance (n=4, p<0.001) in comparison to the non-transfected control group, (*) denotes significant (n=4, p<0.05) in comparison to the non-transfected control group; (#) denotes significance (n=4, p<0.05) in comparison to the PEI-pGFP at the same time point.

3.3.2. Alginate hydrogels are able to support nHA-mediated gene delivery and sustained expression of the transgene over time without negatively impacting cell viability

Quantification of luciferase expression confirmed effective gene delivery to MSCs in the gene-activated alginate hydrogels containing nHA complexed with different concentrations of pLuc, with sustained expression of the transgene over 14 days (Fig.3.2.A). The luciferase expression peaked at day 7 in all gene-activated groups (Fig.3.2.A), in comparison to 2D transfection in which the luciferase expression peaked at day 3, and was not significantly different to the non-transfected control by day 7 (Fig.A.1). The use of 2 µg of pLuc per gel appeared to be the optimal concentration of pDNA, as evidenced by significantly higher levels of luciferase expression in comparison to 5 ug and 10 ug of pLuc at specific time points (Fig.3.2.A). Importantly, luciferase expression was also sustained over 14 days within the 2 µg of pLuc per hydrogel group.
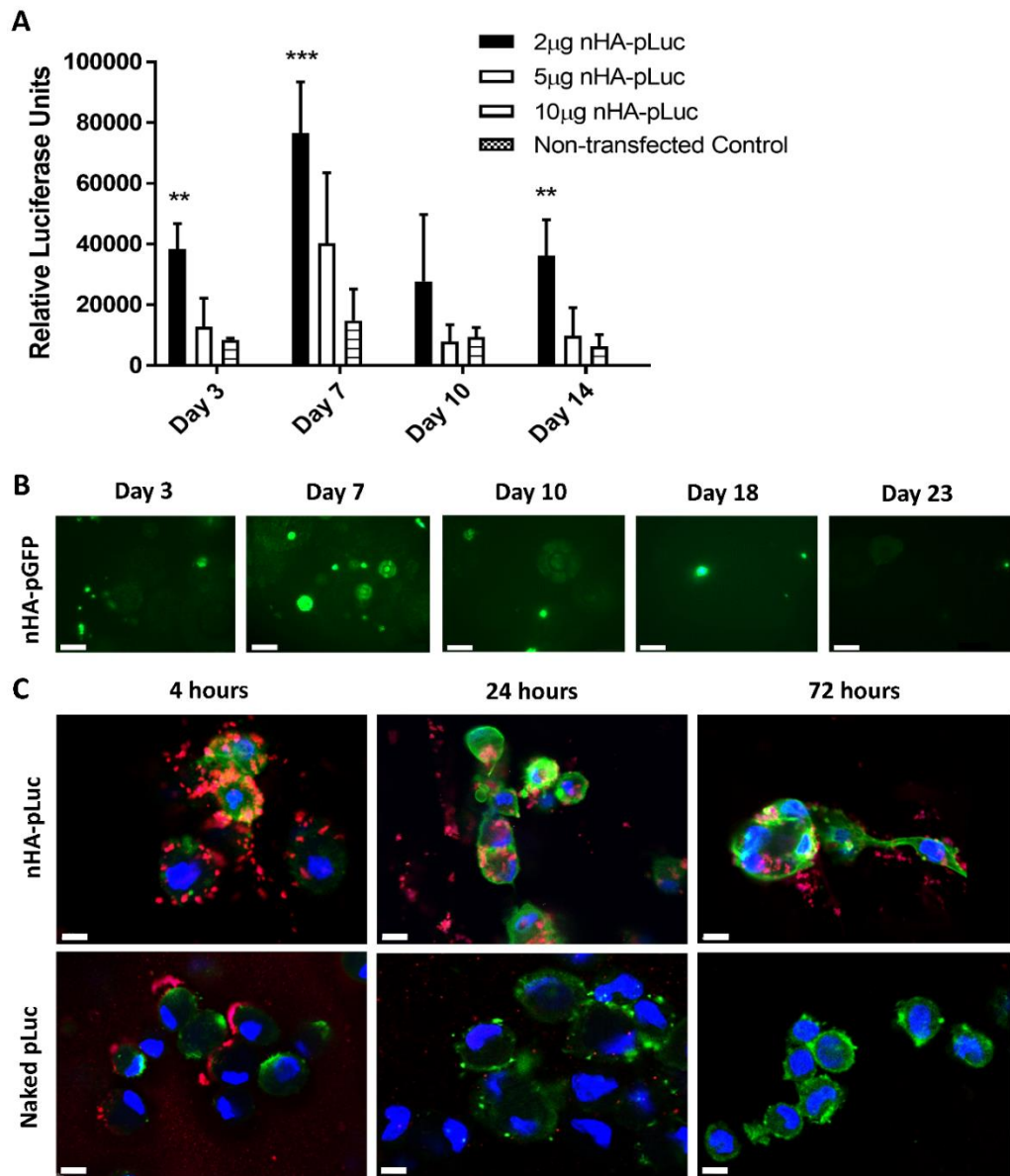
Fig.3.2. (A) Luciferase expression profile of the MSCs in the gene activated hydrogels containing nHA nanoparticles complexed to different concentrations of pLuc (2 ug, 5 ug and 10 ug) over 14 days; (**) denotes significance (n=4, p<0.01) in comparison to the 5 μg nHA-pLuc and the 10μg nHA-pLuc groups; (***) denotes significance (n=4, p<0.001) in comparison to the 5 μg nHA-pLuc, 10 μg nHA-pLuc and non-transfected control groups. (B) Fluorescent inverted microscope images of the gene-activated alginate hydrogels containing MSCs and nHA-pGFP complexes over 23 days; Scale bars: 100 μm. (C) Confocal microscopy analysis of the cellular uptake and internalization of pDNA encoding for Luciferase (naked pLuc) and complexed to the nHA nanoparticles (nHA-pLuc) by MSCs encapsulated in alginate hydrogels, at 4, 24 and 72 hours post transfection and alginate encapsulation. Cellular actin cytoskeleton was stained in green, the nucleus in blue and the pDNA in red; Scale bars = 10 μm.

Fluorescent inverted microscope images of the gene-activated alginate hydrogels containing MSCs and nHA-pGFP complexes revealed the presence of green fluorescent cells inside the hydrogels, indicating effective transfection and GFP production over 23 days (Fig.3.2.B). Fluorescent staining of the cellular actin cytoskeleton and the nucleus of the encapsulated MSCs, and pDNA encoding for luciferase, showed naked pLuc and nHA-pLuc uptake over 72 hours (Fig.3.2.C). pDNA could be observed inside the cell cytoplasm and nucleus of the MSCs in the nHA-pLuc group at 4, 24 and 72 hours after encapsulation in alginate. In contrast, the pDNA was completely degraded after 72 hours in the naked pLuc group and it could not be observed inside the cellular compartment or around the cell membrane (Fig.3.2.C). Additionally, imaging of the nHA-pLuc group suggested the presence of stable nHA-pDNA complexes inside and outside the cell over 72 hours post transfection (Fig.3.2.C).

No significant differences were observed between the DNA content and the cell metabolic activity of the nHA-pLuc gene-activated hydrogels and the non-transfected controls at day 1 and 7 (Fig.3.3.A and B), suggesting that cell viability was unaffected by the incorporation of the complex into the alginate hydrogels. Confocal imaging of live and dead cells revealed a homogeneous distribution of the cells throughout each gel, with no obvious differences in cell viability between the groups (Fig.3.3.C and D).
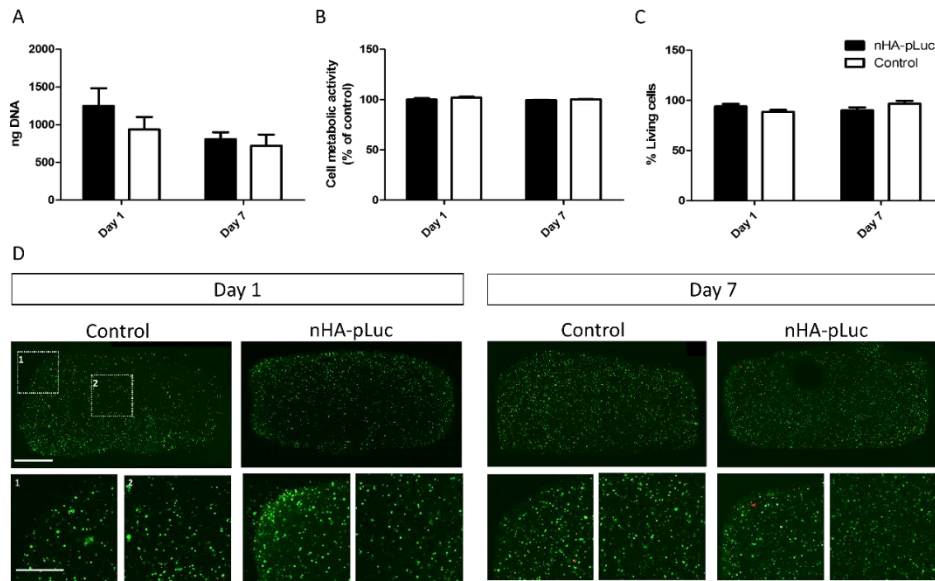
Fig.3.3. (A) DNA quantification of the nHA-pLuc gels and the non-transfected control at day 1 and 7 after encapsulation. (B) Cell metabolic activity (% of non-transfected control) of the nHA-pLuc gene-activated gels (nHA-pLuc) and the non-transfected control (control) at day 1 and 7 after alginate encapsulation (C) Percentage of living cells in the nHA-pLuc gene-activated gels (nHA-pLuc) and the non-transfected control (control) at day 1 and 7 after alginate encapsulation. (D) Cell viability at day 1 and 7; green fluorescence indicate viable cells (calcein) and red indicates dead cells (ethidium homodimer-1). 1 refers to image in the edge of the gel and 2 to the center of the gels. Scale bars = 1 mm and 0.5 mm.

3.3.3. Addition of therapeutic genes into 3D alginate hydrogels results in effective delivery and sustained expression of the transgene

Successful expression of therapeutic proteins was achieved using nHA-mediated transfection of MSCs within the alginate hydrogels. This resulted in increased levels of TGF-β3 (Fig.3.4.A) and BMP2 (Fig.3.4.B) in the culture media of the pTGF-β3, pBMP2 and pTGF-β3/pBMP2 co-delivery groups (Fig.3.4). The peak of expression was observed at day 7 for TGF-β3 and at day 3 for BMP2, high reduction in the expression of the gene products was observed at day 14. These results verify effective MSC transfection with pTGF-β3 and pBMP2 within the gene-activated hydrogels and demonstrate sustained expression of the genes of interest. A similar trend and level of expression was observed for each protein, independent of whether the pDNA had been delivered in isolation or in combination with another pDNA, implying that co-delivery of two plasmids did not hinder the expression of either gene.
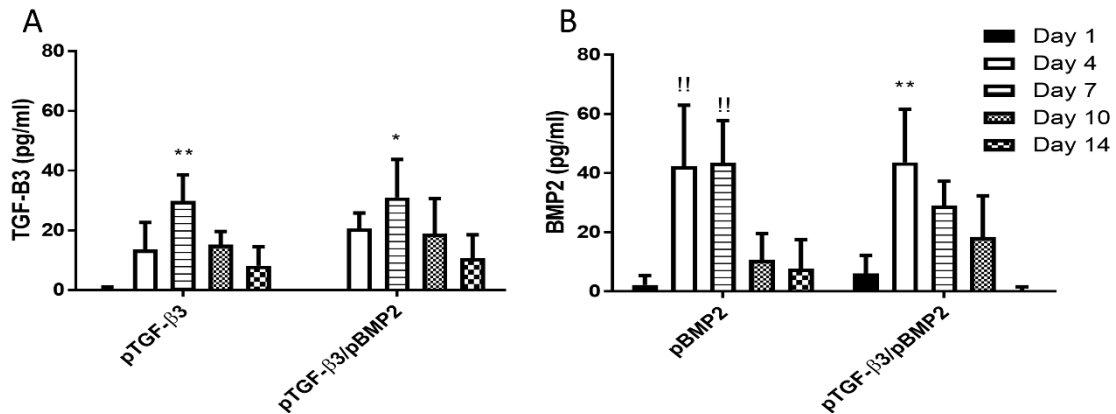
Fig.3.4. (A) pTGF-ß3 and BMP2 (B) protein expression in the pTGF-ß3 and the pTGF-ß3/pBMP2 gene-activated hydrogels over 14 days. (*) Denotes significance (n=4, p<0.05) in comparison to day 1 and day 14; (**) denotes significance (n=4, p<0.01) in comparison to day 1 and day 14; (!!) denotes significance (n=4, P<0.01) in comparison to day 1, 10 and 14.

3.3.4. Co-delivery of TGF-β3 and BMP2 genes enhances chondrogenesis and suppresses hypertrophy and calcification compared to delivery of either gene in isolation

pTGF-β3/pBMP2 co-delivery led to significantly higher levels of sGAG and collagen accumulation compared to all other groups after 28 days of culture (Fig.3.5.A and C). Collagen accumulation in the pTGF-β3 group was significantly higher than in pBMP2 and nHA-alone groups (Fig.3.5.C). Similar trends were found when the sGAG and collagen content were normalized to the DNA levels (Fig.3.5.B and D). In contrast, significantly higher levels of calcium deposition were observed in both the pTGF-β3 and pBMP2 only groups in comparison to the co-delivery of both genes (Fig.3.5.E and F). At the levels of nHA used within this study, no evidence of osteoinductivity or calcification was observed in a nHA alone control group (Fig.3.5.E and F).

The equilibrium modulus (Fig.3.5.H) of the pTGF-β3/pBMP2 co-delivery group was significantly higher than the nHA-only control after 28 days of *in vitro* culture, with a similar trend observed for the Young's modulus (Fig.3.5.G).
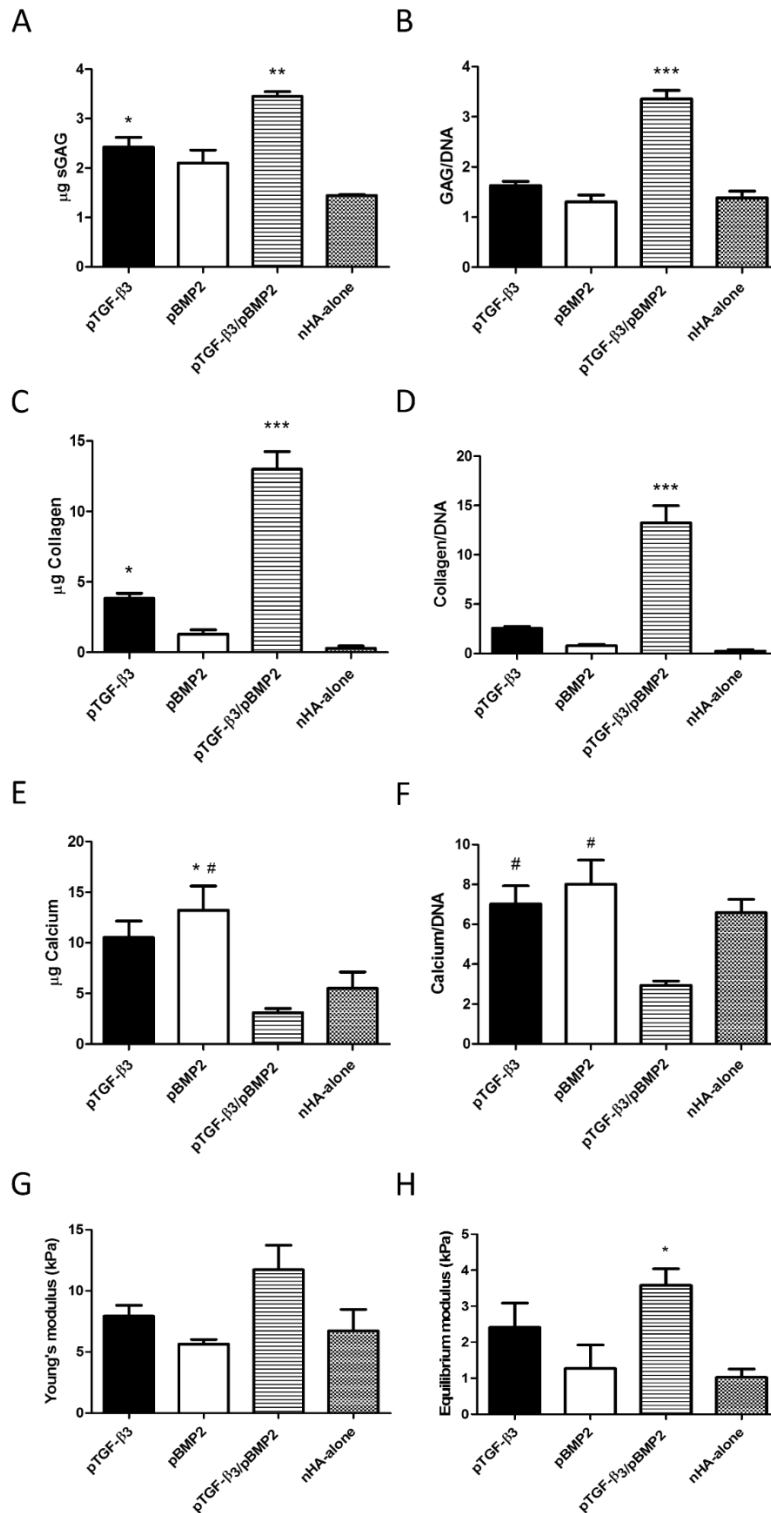
Fig.3.5. Biochemical and mechanical analysis of the constructs after 28 days of in vitro culture. (A) sGAG content. (B) sGAG content normalized to DNA. (C) Collagen content. (D) Collagen content normalized to DNA. (E) Calcium content. (F) Calcium content normalized to DNA. (G) Young modulus and (H) equilibrium modulus. (**) (n=4, p<0.01) and (***) (n=4, p<0.001) denotes significance in comparison to the rest of the groups, (*) (n=4, p<0.05) denotes significance in comparison to the nHA-alone group, (#) (n=4, p<0.05) denotes significance in comparison to the pTGF-ß3/pBMP2 co-delivery group.

Histological evaluation of the hydrogels after 28 days in culture demonstrated higher pericellular sGAG and type II collagen deposition in the pTGF-β3/pBMP2 co-delivery constructs compared to all other groups (Fig.3.6). Greater calcification (Fig.3.6.G and H) was observed in the pBMP2 and pTGF-β3 delivery only groups. Aldehyde fuschin/alcian blue and picrosirius red staining revealed higher sGAG (Fig.3.6.A, B and C) and collagen (Fig.3.6.D, E and F) accumulation in the pTGF-β3/pBMP2 co-delivery group, confirming the results of the biochemical analysis. Minimal immunostaining for collagen type X, a marker of hypertrophy, was seen in the pTGF-β3/pBMP2 co-delivery group compared to the pTGF-β3 and pBMP2 only constructs (Fig.3.6.M, N and O), with the most intense staining in the pBMP2 group. These results suggest enhancement of chondrogenesis in the co-delivery group, and the promotion of hypertrophy and calcification when TGF-β3 and BMP2 genes are delivered in isolation using nHA as a delivery vector. Confocal imaging of live and dead cells confirmed the presence of living cells in all the groups after 28 days of *in vitro* culture (Fig.3.6.P, Q and R).
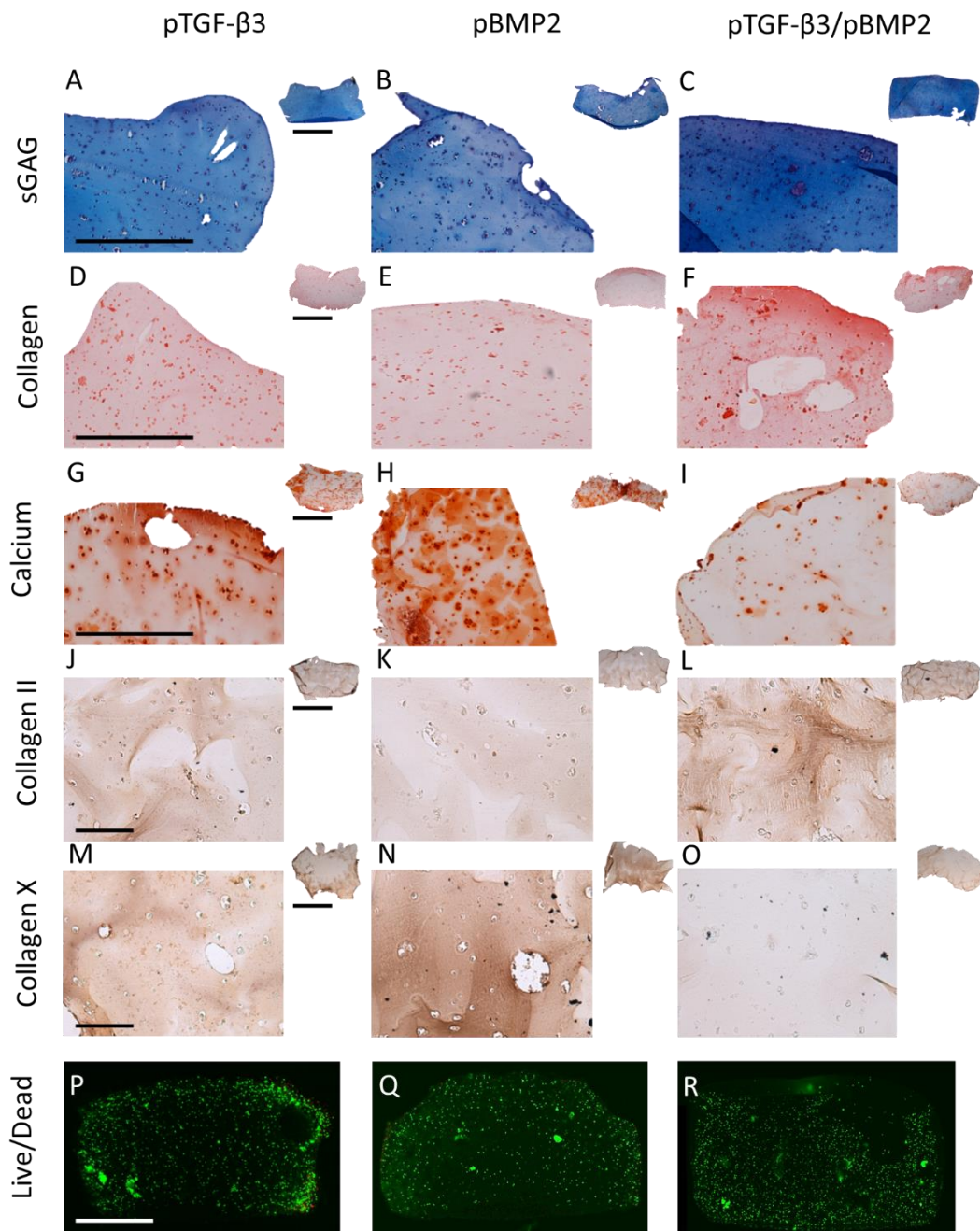
Fig.3.6. Histological examination of the gene-activated hydrogels and the controls after 28 days of in vitro culture. (A, B and C) sGAG histological examination through aldehyde fuschin / alcian blue staining at day 28. Scale bars = 0.5 mm and 1 mm. (D, E and F) Collagen histological examination through picrosirius red staining at day 28. Scale bars = 0.5mm and 1 mm. (G, H and I) Calcium deposition histological examination through alizarin red. Scale bars = 0.5 mm and 1 mm. Collagen type II (J, K and L) and Collagen type X (M, N and O) immunostaining at day 28. Scale bars = 0.1 mm and 1 mm. (P, Q and R) Cell viability at day 28; green fluorescence indicates viable cells, red fluorescence indicates dead cells. Scale bar = 1mm.

3.4. Discussion

The overall goal of the present study was to develop a novel nHA-mediated gene-activated alginate hydrogel capable of supporting sustained delivery of pDNA encoding for therapeutically relevant factors to MSCs in order to control their differentiation for either articular cartilage or endochondral bone tissue engineering. Luciferase expression analysis, fluorescent imaging and cell viability assessment confirmed effective gene delivery to MSCs encapsulated within the gene-activated hydrogels without any toxic effects. Therapeutic gene delivery of TGF-β3 and BMP2 and subsequent expression of the transgenes promoted sGAG and collagen type II production when the two genes were delivered in combination, or calcification and collagen type X deposition when these genes were delivered in isolation. Taken together, these results indicate that the nHA-gene-activated hydrogels are able to efficiently sustain non-viral transfection and expression of the genes of interest over a temporary timeframe, providing relevant concentrations of proteins which modulated the phenotype of MSCs towards either cartilage or down an osteogenic/endochondral pathway depending on whether TGF-β3 and BMP2 were delivered in combination or in isolation.

In-house synthesized hydroxyapatite (HA) nanoparticles showed transfection efficiencies similar to PEI, but without the cytotoxicity associated with this cationic polymer. HA nanoparticles have been investigated as delivery vectors for diverse biomedical applications including growth factors (Gorbunoff, 1984), anticancer drugs (Dorozhkin and Epple, 2002), enzymes and antibodies (Matsumoto et al., 2004), and nucleic acids such as plasmid DNA (Curtin et al., 2012; Welzel et al., 2004) and small interfering RNA (siRNA) (Castaño et al., 2014). In terms of gene delivery, HA nanoparticles have a high binding affinity for pDNA due to the interactions between the calcium ions in the apatite and the negatively charged phosphate groups of DNA (Okazaki et al., 2001). Previous studies have reported MSC transfection efficiency to be higher using nHA than commercial calcium phosphate (CaP) kits, and to offer better cell viability than Lipofectamine 2000 (Curtin et al., 2012), the most referenced transfection reagent. Additionally, nHA-mediated gene delivery within collagen scaffolds have shown greater therapeutic benefits for bone regeneration *in vivo* in comparison to

polyethylenimine (PEI), which is often considered the gold standard for cationic gene delivery (Curtin et al., 2015). Although relatively low levels of nHA-mediated transfection efficiency were reported in this study in comparison to viral vectors such as recombinant adeno-associated viruses (rAAV) (Cucchiarini et al., 2007; Weimer et al., 2012) or physical cell stimulation methods such as electroporation (Haleem-Smith et al., 2005), the use of non-viral particles for gene delivery is a promising option for their application in tissue engineering approaches due to their low immunogenicity, transient effect and the ease of incorporation to 3D matrices for a sustained and localised delivery of the gene of interest.

In this study, these nHA nanoparticles were incorporated into alginate hydrogels in order to facilitate and sustain gene delivery to MSCs over time. This resulted in effective transfection with pDNA encoding for Luc and GFP, and subsequent expression of the transgenes over 23 days as confirmed by fluorescent imaging and Luc analysis. Luc expression peaked at day 7 in the gene-activated hydrogels, suggesting a sustained uptake of the nHA-pLuc complexes over time, in comparison to the transfection with pLuc or pGFP in 2D monolayer culture, where expression peaked at day 3 and showed a significant reduction by day 7. Different pLuc concentrations (2 µg, 5 µg and 10 µg/gel) were also assessed. 2 µg/gel was found to be the optimal in terms of gene expression, with significantly higher Luc expression at every time point, which may be due to the formation of larger complexes with increasing concentrations of pDNA preventing cellular uptake (Gratton et al., 2008). Cytotoxicity analysis of the system showed similar levels of DNA content, metabolic activity and percentage of living cells across the gene-activated groups and the non-transfected controls, confirming the monolayer results and previous studies that highlighted the non-toxic effects of these nanoparticles (Curtin et al., 2012), making them ideal for many tissue engineering applications.

In order to track the pDNA uptake in the gene-activated hydrogels and to better understand the efficacy of the nHA nanoparticles in the system, the internalization of pDNA was monitored through fluorescent staining at 4, 24 and 72 hours after alginate encapsulation of the nHA-pDNA complexes and MSCs. Confocal imaging of the fluorescent labelled pDNA, cellular cytoskeleton and cellular nucleus showed that the combination of nHA nanoparticles and pDNA resulted in formation of pDNA complexes,

sustained cellular internalization, and protection of the internalized pDNA overtime inside the alginate hydrogels. In contrast, in the absence of the nHA nanoparticles, the naked pDNA was not able to be internalized by the MSCs and it was not observed in the cells or their periphery after 72 hours, suggesting degradation of the plasmid. Hydroxyapatite particles have previously been reported to protect pDNA from degradation driven by serum and nucleases such as DNase I (Brundin et al., 2013; Zuo et al., 2011), these results further demonstrate this protective action. The presence of nHA also resulted in effective gene transfection, confirming that these nanoparticles acted as a successful gene delivery vector in the developed system.

nHA nanoparticles were able to effectively deliver pDNA encoding for TGF-β3 or BMP2 in the 3D alginate hydrogels and sustain their expression over 14 days. Media supplementation with growth factors from the transforming growth factor (TGF) family such as transforming growth factor-beta 1 (TGF-β1) and 3 (TGF-β3), or bone morphogenic protein 2 (BMP2), have previously been used to direct differentiation of MSCs encapsulated in alginate hydrogels towards either a chondrogenic or an osteogenic phenotype (Gründer et al., 2004; Sheehy et al., 2013; Shen et al., 2009). Although relatively low levels of the transgene expression were quantified in the media (compared to studies that directly supplement the media with the gene product), it is likely that a significant proportion of the TGF-β3 and BMP2 proteins being produced are retained within the alginate construct, particularly within the pericellular matrix (PCM) deposited by the encapsulated cells. Such matrix components have previously been shown to bind strongly with such growth factors (Macri et al., 2007). In comparison to recombinant growth factor media supplementation, this approach offers a continuous production of proteins of interest which overcomes the limitations related to the short half-life and quick degradation of proteins *in vivo* and the adverse effects associated with the administration of supraphysiological amounts of growth factors (Zara et al., 2011).

Gene delivery of either TGF-β3 or BMP2 in isolation showed only moderate sGAG and collagen synthesis and significantly increased calcification in comparison to the pTGF-β3/BMP2 co-delivery group. Furthermore, the delivery of these genes in isolation enhanced the production of collagen type X, a marker for chondrocyte hypertrophy and

endochondral ossification. While it is perhaps unsurprising that the delivery of BMP2 appeared to support a more osteogenic phenotype (Krebs et al., 2010; Wegman et al., 2013), the finding that pTGF-β3 delivery supported a similar phenotype was less expected. It is likely that the combination of the osteogenic stimulus provided by the nHA, with the overexpression of pTGF-β3 led to promotion of hypertrophic/osteogenic differentiation in the MSCs (Cals et al., 2012). In contrast, nHA-mediated co-delivery of pTGF-β3 and pBMP2 resulted in suppressed calcification and collagen type X deposition, and promoted a more stable chondrogenic phenotype characterized by increased GAG and collagen type II production. Combined medium supplementation of either TGF-β3 or TGF-β1 with BMP2 has been shown previously to synergistically enhance chondrogenic differentiation of MSCs encapsulated in alginate beads (Mehlhorn et al., 2007; Shen et al., 2009). This synergistic effect on MSC chondrogenesis may be produced through modulation of the mothers against DPP homolog (SMAD) and mitogen-activated protein kinase (MAPK) signalling pathways (Keller et al., 2011; Shanmugarajan et al., 2011) and suppression of RUNX2 expression (Lee et al., 2003) resulting in the promotion of collagen type II, cartilage oligomeric matrix protein (COMP) and aggrecan (ACAN) gene expression, sGAG synthesis, and, at the same time, decreasing the expression of bone-specific alkaline phosphatase (Mehlhorn et al., 2007; Shen et al., 2009). While the present study shows that the co-delivery of TGF-β3 and BMP2 produced more stable chondrogenesis and suppressed hypertrophy, Simmons *et al.* showed that the combination of TGF-β3 and BMP2 growth factors in peptide modified alginate laden with MSCs led to higher bone formation compared to when either growth factor was delivered in isolation (Simmons et al., 2004). This could be due to the presence of peptide modification and/or the reduced molecular weight of the alginate used in that study (Alsberg et al., 2001). Other factors to be considered are the relatively low concentrations of TGF-β3 and BMP2 produced by the MSCs in the gene-activated hydrogels, and the hypoxic conditions of the *in vitro* culture which have previously shown to suppress the hypertrophic phenotype of MSCs (Ronzière et al., 2010; Sheehy et al., 2012). The exact molecular mechanism by which combined delivery of TGF-β3 and BMP2 suppressed calcification *in vitro* and promoted chondrogenesis remains unclear. Its elucidation could help to understand and modulate hypertrophy and endochondral ossification of MSCs and should be addressed in future studies.

3.5. Conclusion

In conclusion, the nHA-gene-activated alginate hydrogels developed in this study were capable of sustaining gene transfection of MSCs, leading to transgene expression over at least 14 days of culture. The expression of the transgenes was capable of modulating stem cell fate towards either a chondrogenic or osteogenic/endochondral phenotype, depending on whether pTGF-β3 and pBMP2 were delivered in isolation or in combination. This is the first study to show that nHA-mediated gene delivery is capable of inducing chondrogenic differentiation of MSCs, and that alginate hydrogels can be used as gene delivery platform for both cartilage and endochondral bone tissue engineering. Altogether, these results may be of clinical importance for the treatment of osteochondral defects as this system offers control of MSC fate towards either a chondrogenic or endochondral phenotype, while avoiding the risks and drawbacks associated with recombinant protein administration.

The results of this chapter, therefore, identified alginate as a promising platform for non-viral gene delivery to encapsulated MSCs, and nHA as gene carrier to deliver pDNA encoding for reporter and therapeutic genes. This 3D printable material will be explored in following chapters as versatile gene activated bioink for the engineering of cartilage and bone tissues. Although, nHA was shown to promote chondrogenesis of MSCs in the gene activated gels, due to its inherent osteogenic potential, it will be further investigated for bone tissue engineering, whereas, in the next chapter, other non-viral gene delivery vectors will be assessed for stable chondrogenesis of MSCs.

CHAPTER 4

Mesenchymal Stem Cell Fate Following Non-viral Gene Transfection Strongly Depends on the Choice of Delivery Vector

Abstract

Controlling the phenotype of mesenchymal stem cells (MSCs) through the delivery of regulatory genes is a promising strategy in tissue engineering (TE). Essential to effective gene delivery is the choice of gene carrier. Non-viral delivery vectors have been extensively used in TE, however their intrinsic effects on MSC differentiation remain poorly understood. The objective of this study was to investigate the influence of three different classes of non-viral gene delivery vectors: (1) cationic polymers (polyethylenimine, PEI), (2) inorganic nanoparticles (nanohydroxyapatite, nHA) and (3) amphipathic peptides (RALA peptide) on modulating stem cell fate after reporter and therapeutic gene delivery. Despite facilitating similar reporter gene transfection efficiencies, these nanoparticle-based vectors had dramatically different effects on MSC viability, cytoskeletal morphology and differentiation. After reporter gene delivery (pGFP or pLUC), the nHA and RALA vectors supported an elongated MSC morphology, actin stress fibre formation and the development of mature focal adhesions, while cells appeared rounded and less tense following PEI transfection. These changes in MSC morphology correlated with enhanced osteogenesis following nHA and RALA transfection and adipogenesis following PEI transfection. When therapeutic genes encoding for transforming growth factor beta 3 (TGF-β3) and/or bone morphogenic protein 2 (BMP2) were delivered to MSCs, nHA promoted osteogenesis in 2D culture and the development of an endochondral phenotype in 3D culture, while RALA was less osteogenic and appeared to promote a more stable hyaline cartilage-like phenotype. In contrast, PEI failed to induce robust osteogenesis or chondrogenesis of MSCs, despite effective therapeutic protein production. Taken together, these results demonstrate that the differentiation of MSCs through the application of non-viral gene delivery strategies depends not only on the gene delivered, but also on the gene carrier itself.
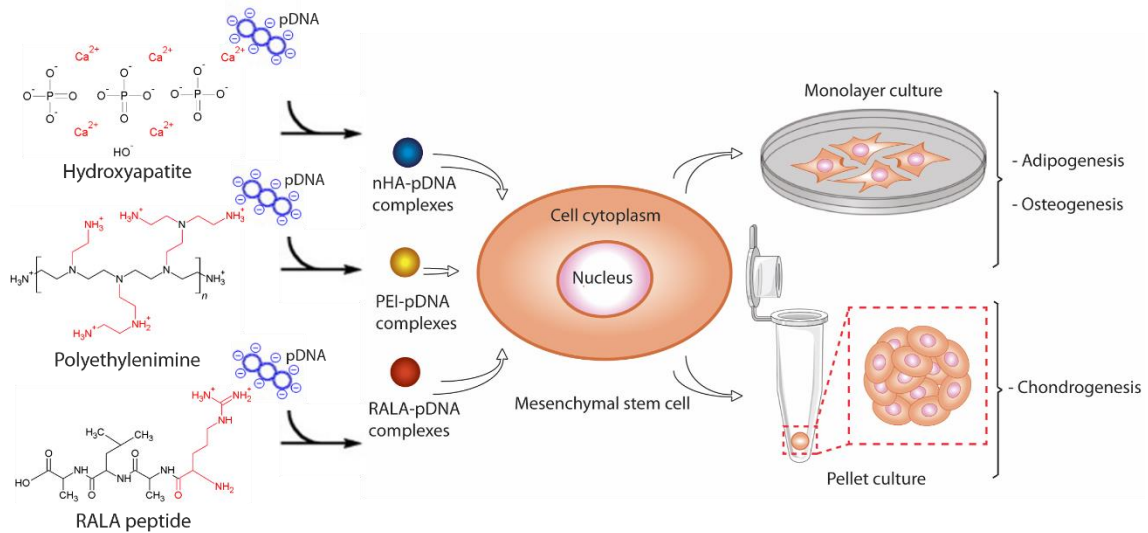
Fig.4.1. Graphical abstract (experimental design): MSCs were transfected using either ceramic (nHA), cationic polymer (PEI) or amphipathic peptide (RALA) non-viral gene delivery vectors, complexed to plasmid DNA (pDNA) encoding for either reporter or therapeutic genes. After transfection, the adipogenic, osteogenic and chondrogenic potential of the treated MSCs were assessed in 2D (monolayer culture in bi-potent media) and 3D (pellet culture) in order to elucidate the effects of the gene transfer nanomaterial on MSC fate.

4.1. Introduction

In this experimental chapter we aimed to address the second thesis objective of comparing novel and stablished non-viral vectors for chondrogenic and osteogenic differentiation of MSCs.

Adult mesenchymal stem cells (MSCs) are a promising cell source for regenerative medicine due to their multipotent differentiation capacity (Tuan et al., 2003) and immunomodulatory properties (Uccelli et al., 2008). Controlling the phenotype of MSCs is a central challenge in tissue engineering and regenerative medicine. The fate of progenitor cells can potentially be modulated through the introduction of exogenous genes for the cell-mediated synthesis of specific proteins. This approach may be preferable over the delivery of recombinant cytokines and growth factors which involves the administration of non-physiological concentrations, due to the short half-life and fast body clearance and a lower therapeutic effect in comparison to natural proteins (Evans, 2014; Heyde et al., 2007; Santos et al., 2011). A variety of

genes have been explored to this end, including members of the transforming growth factor-beta (TGF-β) superfamily of proteins such as bone morphogenic protein 2 (BMP2) and transforming growth factor-beta 3 (TGF-β3), whose overexpression has been previously reported to enhance bone and cartilage regeneration *in vivo* (Curtin et al., 2015; Lin et al., 2013; Venkatesan et al., 2013). But the success of gene therapy ultimately depends on the gene delivery mechanism to maximise nucleic acid uptake and, consequently, downstream protein production (Bessis et al., 2004; Heyde et al., 2007; Kay, 2011; Li and Huang, 2007; Santos et al., 2011).

Traditionally, viral vectors such as retrovirus, lentivirus and adenovirus, have been used for the delivery of genes into cells *via* a process known as transduction (Kay, 2011; Mastrobattista et al., 2005; Yin et al., 2014). Although they offer high transduction efficiencies and stable gene expression, many limitations remain associated with viral vectors (Raisin et al., 2016; Somia and Verma, 2000; Thomas et al., 2003) such as insertional mutagenesis (Baum et al., 2006), immunogenicity (Bessis et al., 2004), limited DNA packaging capacity (Waehler et al., 2007) and cumbersome large-scale production (Bouard et al., 2009). Non-viral gene carriers are promising alternatives for gene delivery and have the potential to address these limitations (Li and Huang, 2007). Moreover, the transient expression associated with these systems can be more compatible with the natural wound healing processes (Bonadio et al., 1999). Several non-viral vectors are commonly used for gene delivery, including lipids, polymers, cell penetrating peptides (CPPs) and inorganic nanoparticles (Yin et al., 2014). While such systems can be used to efficiently transfect cells with specific genes, the effects that these non-viral vectors have on stem cell fate remains relatively unknown (Ballarín-González and Howard, 2012; Yang et al., 2014).

Cationic lipid-based and polymeric DNA vectors such as lipofectamine and polyethylenimine (PEI) are amongst the most widely used non-viral gene delivery methods (Wang et al., 2013; Yang et al., 2014; Yin et al., 2014), and are often used as a gold standard for non-viral gene transfection (Santos et al., 2011). However their potential cytotoxicity (Lv et al., 2006; Yin et al., 2014) and sensitivity to media supplementation with serum and antibiotics (Baker et al., 1997) limits their use in tissue engineering applications. Among alternative options, inorganic nanoparticles made of

calcium phosphate, gold or silica, have been drawing attention for their use in tissue engineering due to their biocompatibility, wider availability, long-term stability, ease of preparation and low toxicity (Castaño et al., 2014; Curtin et al., 2012; Santos et al., 2011; Xu et al., 2006). More recently, different classes of peptides (McCarthy et al., 2014; Suh et al., 2014), such as the RALA amphipathic peptide (RALA) comprised of repeating arginine/alanine/leucine/alanine units (McCarthy et al., 2014), have been developed as novel nucleic acid carriers (Kaitsuka and Tomizawa, 2015; Suh et al., 2013), showing excellent cytocompatibility and moderate transfection efficiencies *in vivo* and *in vitro* (McCaffrey et al., 2016; McCarthy et al., 2014). These non-viral delivery vehicles are promising in terms of compatibility and transfection efficiency, however the suitability of a gene delivery vector for stem cell-mediated tissue engineering is not only determined by its transfection efficiency, cytocompatibility and levels of expression of the gene product, but also by its chemical composition and how the intracellular delivery of such nanomaterials may influence stem cell fate (Yang et al., 2014).

Therefore, the objective of this study was to first compare the capacity of three different classes of non-viral gene delivery vectors (PEI, nanohydroxyapatite (nHA) and RALA) to transfect bone marrow-derived MSCs. The impact of intracellular delivery of such nanomaterials on the viability, cytoskeletal structure and multi-lineage differentiation potential of MSCs was assessed. We then used these vectors to deliver BMP2 and TGF-β3 genes to MSCs as a means to promote either osteogenesis or chondrogenesis in a 2D or 3D environment, and investigated the influence of different gene carriers on MSC lineage commitment. Collectively the results of this study demonstrate that gene vectors with comparable capacities to transfect MSCs with reporter and therapeutic genes can have dramatically different effects on MSC differentiation.

4.2. Materials and methods

4.2.1. Plasmid propagation

Four different plasmids were used in the current study: two plasmids encoding for the reporter genes green fluorescent protein (pGFP, Amaxa, Lonza Cologne AG, Germany) and luciferase (pLUC, pGaussia Luciferase; New England Biolabs, Massachusetts, USA), and another two encoding for the therapeutic genes BMP2 (donation from Prof. Kazihusa Bessho, Kyoto University, Japan) and TGF-β3 (InvivoGen, Ireland). Plasmid amplification was performed by transforming chemically competent *Escherichia coli* bacterial cells (One Shot TOP10; Biosciences, Ireland) according to the manufacturer's protocol. The transformed bacteria were cultured on LB plates with 50 mg/L kanamycin (Sigma-Aldrich, Ireland) as the selective antibiotic for pGFP and 100 mg/L ampicillin (Sigma-Aldrich, ireland) as the selective antibiotic for pLUC, pTGF-β3, and pBMP2. Bacterial colonies were harvested and inoculated in LB broth (Sigma-Aldrich, Ireland) and incubated overnight for further amplification. The harvested bacterial cells were then lysed, and the respective pDNA samples were purified using qiagen plasmid kit (MaxiPrep Kit; Qiagen, Ireland). Nucleic acid concentration (ng/μL) was determined by analyzing the 260:280 ratio and 230 nm measurement using NanoDrop spectrophotometer (Labtech International, Uckfield, UK). Plasmids in this study were used at a concentration of 0.5 μg plasmid in 1 μL Tris–EDTA (TE) buffer.

4.2.2. Preparation of delivery vectors and vector-pDNA complexes

The synthesis of the nHA particles was performed as previously described (Cunniffe et al., 2010). Briefly, a solution of 12 mM sodium phosphate (Sigma-Aldrich, Ireland), containing 0.017% DARVAN821A (RTVanderbilt, Norwalk, USA) was added to an equal volume of a 20 mM calcium chloride solution (Sigma-Aldrich, Ireland) and filtered through a 0.2 mm filter (Fisher, Ireland). nHA-pDNA complexes were prepared by adding 150 μL of the nHA solution to 2 μg of pDNA pretreated with 0.25 M $CaCl_2$ (Sigma-Aldrich, Ireland) as previously optimized (Castaño et al., 2014; Curtin et al., 2012). The nHA-pDNA solutions were not incubated prior to transfection in order to

avoid particle aggregation that could impair cellular uptake as previously optimized (Curtin et al., 2012).

PEI-pDNA complexes were prepared using branched PEI with a molecular weight of 25 kDA (Sigma-Aldrich, Ireland). PEI was condensed with pDNA in an N:P ratio (the molar ratio of positively charged nitrogen atoms in the PEI to negatively charged phosphates in the pDNA backbone) of 7, a ratio previously optimized for MSC transfection (Tierney et al., 2012). The PEI-pDNA solution was then incubated for 30 minutes for complex formation.

The RALA peptide was synthesised as previously described (McCarthy et al., 2014). Briefly, the peptide was produced by 9-fluorenylmethyloxycarbonyl (Fmoc) solid-state peptide synthesis (Biomatik, USA) and supplied as a desalted, lyophilised powder. The product was purified and validated by reversed-phase high-performance liquid chromatography (RPHPLC); molecular mass was confirmed as 3327.98. The RALA-pDNA complexes were prepared at N:P ratio of 6, previously optimized to achieve low cytotoxicity and high transfection efficiency (McCaffrey et al., 2016; McCarthy et al., 2014). The RALA-pDNA solution was then incubated for 30 minutes for complex formation.

4.2.3. Determination of size and zeta potential of the nanoparticles-pDNA complexes

The morphology of the nHA-pDNA, PEI-pDNA and RALA-pDNA complexes were characterized using transmission electron microscopy (TEM). The nHA-pDNA sample was prepared by placing 5 µL droplet onto a Formvar/SiO TEM Cu grid (Agar Scientific, UK) and allowed to air dry overnight. Similarly, the PEI-pDNA and RALA-pDNA were prepared on holey-carbon film Cu TEM grids and post-stained with 5% uranyl acetate as previously described (McCarthy et al., 2014). nHA-pDNA and PEI-pDNA vectors were characterized using an FEI Titan TEM (FEI, USA) operating at 300 kV. RALA-pDNA was characterized using a JEOL CXII TEM (JEOL, USA) operating at 80 kV. The size and zeta potential of the complexes were assessed using a Nano ZS Zetasizer and DTS software (Malvern Instruments, UK).

4.2.4. Isolation and expansion of bone marrow-derived MSCs

Bone marrow-derived MSCs were isolated from the femora of porcine donors (3-4 months, >50 Kg) within 3 h of sacrifice according to a modified method developed for human MSCs(Lennon and Caplan, 2006). Mononuclear cells were plated at a seeding density of 5 x 10^3 cells/cm^2 in standard culture media, high glucose Dulbecco's modified Eagle's medium (4.5 mg/mL d-glucose and 200 mM L-glutamine; hgDMEM) supplemented with 10% fetal bovine serum (FBS) and penicillin (100 U/mL)– streptomycin (100 g/mL) (all from Gibco, Biosciences, Ireland), and expanded in a humidified atmosphere at 37 °C, 5% CO_2, and 20% pO_2. MSCs at passage 2 were used for all experiments.

4.2.5. MSC transfection

Expanded MSCs were plated at a seeding density of 5 x 10^4 cells/cm^2 in 6 well plates and cultured for 24 hours in standard culture media prior to transfection. pDNA-vector complexes were prepared immediately before transfection. For the RALA-pDNA and PEI-pDNA transfections (McCarthy et al., 2014; Tierney et al., 2012), the plated cells were washed with PBS and incubated in 1-2 ml of Opti-MEM (Life Technologies, Ireland) for 2 h. After the incubation time, complexes were suspended in 500 μL of Opti-MEM and added to MSCs to a density of 0.2 μg of DNA/cm^2. Following incubation for 5 h, the media was removed and replaced with standard culture media. For the nHA-pDNA transfections (Curtin et al., 2012), complexes were suspended in 500 μL of standard media and added to MSCs to a density of 0.2 μg of DNA/cm^2, residual complexes were removed after 4 h of incubation and replaced with standard culture media.

4.2.6. Assessment of transfection efficiency

In order to evaluate the transfection efficiency, pDNA encoding the GFP gene was prepared, complexed with each of the three vectors (section 4.2.2) and MSCs were transfected as described above. Transfection efficiency was determined by quantifying the percentage of green fluorescent cells at days 3 and 7 post transfection using flow cytometry (BD FACSCALIBUR system, BD Biosciences, UK).

4.2.7. Assessment of cell viability and metabolic activity

After 1 and 3 days of nHA-, PEI- or RALA-mediated gene delivery, metabolic activity of treated cells was evaluated using standard Alamar Blue (Biosciences, Ireland) assay. For the assay, cell culture media from the wells was replaced, at specific time points, with 10% Alamar Blue containing standard culture media (1 mL/well) and were incubated for 4 h at 37 °C. After the incubation time, 200 μL of the supernatant was plated in triplicate into a 96-well plate; absorbance was read at 570 and 600 nm using a plate reader (Bioteck, Instruments Inc, UK). Optical density of the media was translated to cell metabolic activity relative to the non-transfected control as previously described (Hamid et al., 2004).

4.2.8. Fluorescent imaging and cell morphology analysis

Qualitative and semi-quantitative analysis of cell morphology was performed on nHA-pGFP, PEI-pGFP and RALA-pGFP transfected cells. Cells were imaged at day 1 and 3 after transfection using an inverted epifluorescent microscope (Olympus IX83, Germany). Cell morphology was assessed semi-quantitatively through the calculation of the cell surface area, aspect ratio and circularity using ImageJ software, n=4 and 6 pictures per sample.

Analysis of actin cytoskeleton and focal adhesion points on vector-pLUC transfected cells were performed by actin and vinculin immunofluorescent staining. At day 1 and 3 after transfection, MSCs previously seeded on μ-slide 4 well IBItreat chambers (IBIDI, Germany), were fixed in 4% paraformaldehyde (PFA) (Sigma-Aldrich, Ireland) for 15 min at room temperature (RT). Samples were first blocked with 5% bovine serum albumin (BSA) and incubated overnight with vinculin primary antibody (AB) (1:500 α mouse monoclonal anti-vinculin) (Abcam, ab18058, Ireland) at 4°C. After incubation, samples were permeabilised with 0.5% Triton X-100 (Sigma-Aldrich, Ireland) and incubated with secondary AB (1:250 α mouse Alexa Fluor 488 IgG) (Biosciences, Ireland) and stained with rhodamine phalloidin (VWR, Ireland) for 1 h at RT. Cell nuclei were stained with DAPI (VWR, Ireland) for 10 min at RT, washed in PBS and were imaged using confocal microscopy (Leica SP8, Ireland).

4.2.9. Osteo-adipo and chondrogenic differentiation of MSCs

For evaluating osteo-adipo lineage differentiation of MSCs, transfected MSCs and the non-treated controls were maintained in standard culture media for a period of 24 h followed by 14 days in osteo-adipo bi-potent media at 20% O_2 and 37° C. Osteo-adipo bi-potent media(Kilian et al., 2010) was prepared by mixing osteogenic media (standard culture media containing β-glycerolphosphate (10 mM), dexamethasone (100 nM) and L-ascorbic acid-2-phosphate (0.05 mM) with adipogenic media (standard culture media containing dexamethasone (100 mM), isobutyl-1-methyl xanthine (IBMX) (0.5 mM) and indomethacin (50 μM) (all from Sigma-Aldrich, Ireland) at 1:1 ratio. Culture media was replaced twice weekly. Negative controls (non-transfected and transfected cells in standard culture media) were also maintained in parallel.

For evaluating chondrogenic differentiation of MSCs, transfected MSCs and the non-treated controls maintained in standard culture media for a period of 24 h were pelletized by centrifugation at 2000 rpm at a cell density of 250 x 10^3 cells/pellet. Pellets were maintained in a chemically defined medium consisting of DMEM GlutaMAX supplemented with penicillin (100 U/mL)–streptomycin (100 mg/mL), 100 mg/mL sodium pyruvate, 40 mg/mL l-proline, 50 mg/mL l-ascorbic acid-2-phosphate, 1.5mg/mL BSA, 1 x insulin–transferrin–selenium, and 100 nM dexamethasone (all from Sigma-Aldrich, Ireland) at 20% pO_2 and 37 °C for a period of 21 days. Half media changes (only half the media was changed) were performed twice weekly in an attempt to avoid complete removal of the overexpressed factors. No exogenous recombinant growth factors were added to the culture media.

4.2.10. Gene expression analysis

Transfected and control cells after 7 days of *in vitro* culture were lysed using R lysis buffer (Qiagen, UK) supplemented with 10 μL mL^{-1} β-mercaptoethanol (Sigma-Aldrich, Ireland) and stored at −80°C. Lysates were thawed and homogenized using a QIAshredder column (Qiagen, UK) and total RNA was isolated and purified using the RNeasy mini kit (Qiagen, UK) using the manufacturer suggested protocol. Purity and yield of RNA was quantified using the NanoDrop Spectrophotometer (Labtech

International, Uckfield, UK). For cDNA preparation, 50 ng total RNA of each sample was reverse transcribed into cDNA per 20 µL of reaction volumes using the high capacity reverse transcription cDNA kit (Applied Biosystems, Paisley, UK) as per manufacturer's instructions. Quantitative PCR was performed using an ABI 7500 sequence detection system (Applied Biosystems, Paisley, UK) and SYBR select master mix (Applied Biosystems, Paisley, UK) for evaluating the expression SRY-box-9 (SOX9), Runt related transcription factor 2 (RUNX2), Aggrecan (ACAN), and Glyceraldehyde-3-phosphate dehydrogenase (GAPDH) genes. Primer sequences that were used for amplification of these genes are listed in Table 4.1. Comparative Threshold (cT) data were analysed using the ΔΔCT method as described previously (Livak and Schmittgen, 2001) with GAPDH as the endogenous control. Relative expression of the genes is presented as fold changes relative to the control group.

Table 4.1. Primer sequences used for real-time PCR

Gene	Forward primer	Reverse primer
RUNX2	CCAACAGAGGCATTTAAGG	CCAAAAGAAGTTTTGCTGAC
SOX9	CAGACCTTGAGGAGACTTAG	GTTCGAGTTGCCTTTAGTG
ACAN	GACCACTTTACTCTTGGTG	TCAGGCTCAGAAACTTCTAC
GAPDH	TTTAACTCTGGCAAAGTGG	GAACATGTAGACCATGTAGTG

4.2.11. BMP2 and TGF-β3 protein expression quantification

The levels of BMP2 and TGF-β3 in the culture medium expressed by nHA, PEI and RALA transfected MSCs were quantified using ELISAs (R&D Systems). The cell culture supernatant was collected and analyzed at day 3 and 7. Assays were carried out according to the manufacturer's instructions, and the absorbance of each sample was read at 450 nm using a plate reader, whereby the quantity of either BMP2 or TGF-β3 protein present was deduced by calculating against a standard curve.

4.2.12. Quantitative biochemical analysis

Monolayers were lysed using Cell Lytic (Sigma-Aldrich, Ireland) and pellets were digested with papain (125 mg/mL, pH 6.5) in 0.1 M sodium acetate, 5 nM L-cysteine HCl, and 0.05 M EDTA (all Sigma-Aldrich, Ireland) at 60 °C under constant rotation for 18 h. Calcium content was determined using a Sentinel Calcium Kit (Alpha Laboratories Ltd, UK) after digestion in 1M HCl at 110 °C for 48 h. Proteoglycan content was estimated by quantifying the amount of sulfated glycosaminoglycan (sGAG) in the pellets using the dimethylmethylene blue (DMMB) dye-binding assay (Blyscan, Biocolor Ltd. Northern Ireland), with a chondroitin sulfate standard. Total collagen content was determined by measuring the hydroxyproline content. Samples were hydrolyzed at 110 °C for 18 h in concentrated HCl 38%, allowed to dry, and analyzed using a chloramine-T assay (Hollander and Hatton, 2003) with a hydroxyproline-to-collagen ratio of 1:7.69 (Ignat'eva et al., 2007). Four samples per group were analyzed for each biochemical assay.

4.2.13. Histological and immunohistochemical analysis

To evaluate mineral deposition, cells in monolayer culture at day 14 were fixed in 100% ethanol and stained with 1% alizarin red (AR) (Sigma-Aldrich, Ireland). Stained samples were air dried and images were captured using phase transmission microscope (Olympus, UK). Semi-quantitative analysis of AR staining was done through extraction of the dye using 10% cetylpyridinium chloride (Sigma-Aldrich, Ireland) and measuring the absorbance at 540 nm (Cunniffe et al., 2016a).

For evaluating oil droplets, cells were fixed in 4% PFA and stained with Oil-Red-O (ORO) at day 14. Semi-quantitative analysis of ORO staining was done through extraction of the dye using 100% isopropanol (Sigma-Aldrich, Ireland) and measuring the absorbance at 490 nm.

For evaluating sGAG, calcium and collagen deposition, cell pellets were fixed with 4% PFA after 21 days *in vitro*, wax embedded, sliced (8 μm) and mounted on microscopic slides. The sections were stained with 1% AR to assess calcium accumulation and Alcian blue (Sigma-Aldrich, Ireland) to assess sGAG content. Collagen types I, II and X were

evaluated using a standard immunohistochemical technique as described previously (Sheehy et al., 2013). Negative (porcine cartilage and ligament for collagen type X, and growth plate for collagen type I and II) and positive controls (cartilage for collagen type II, ligament for collagen type I and growth plate for collagen type X) were included for each immunohistochemical analysis.

4.2.14. Statistical analysis

Statistical analyses were performed using GraphPad Prism (version 5) software. One-way ANOVA was used for analysis of variance with Tukey's post hoc test to compare between groups. Numerical and graphical results are displayed as mean ± standard deviation. Significance was accepted at a level of $p < 0.05$.

4.3. Results

4.3.1. Particle size and Zeta potential of the nHA-pGFP, PEI-pGFP and RALA-pGFP complexes

Following conjugation with pGFP, the nHA, PEI and RALA complexes were found to be of different size (Fig.4.1.A), charge (Fig.4.2.B) and shape (Fig.4.2.C, D and E). nHA-pGFP complexes were on average larger in size (~300 nm) and had a negative zeta potential. In contrast, the PEI-pGFP and RALA-pGFP complexes were smaller (<150 nm) and had a positive charge. TEM analysis showed aggregation of the nHA-pGFP complexes (Fig.4.2.D), while PEI-pGFP (Fig.4.2.C) and RALA-pGFP (Fig.4.2.E) complexes exhibited a uniform shape and distribution with less aggregation.
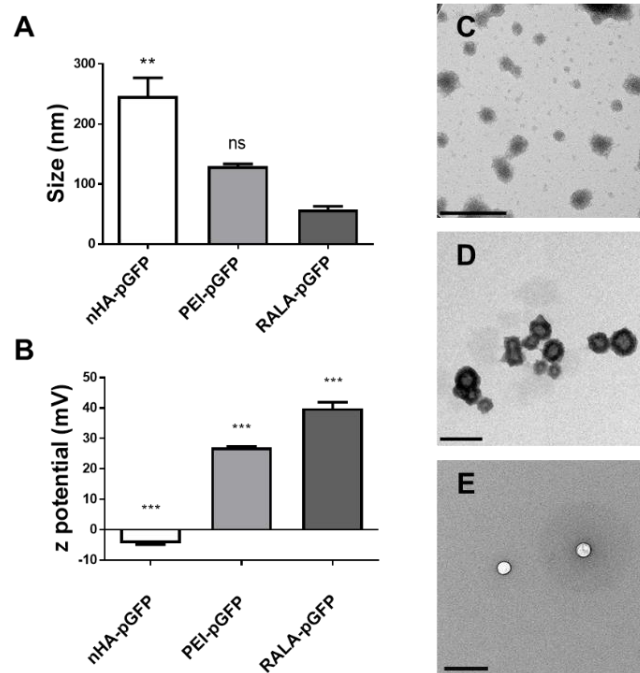
Fig.4.2. Size (A) and charge (B) of the nHA-pGFP, PEI-pGFP and RALA-pGFP complexes. (**) denotes significance (n=3, p<0.01) in comparison to all other groups, (***) denotes significance (n=3, p<0.001) in comparison to all other groups; (ns) denotes no significance (n=3, p>0.05) in comparison to the RALA-pGFP group. TEM images of the nHA-pGFP (D), PEI-pGFP (C) and RALA-pDNA (E) complexes. Scale bar = 200 nm.

4.3.2. nHA, PEI and RALA possess similar capacities to transfect MSCs but have unique effects on metabolic activity and cellular morphology

All 3 gene delivery vectors demonstrated similar transfection efficiencies of approximately 15-20% at day 3 (Fig.4.3.A). However, 7 days after treatment, the percentage of GFP positive cells decreased in the nHA and RALA transfected groups while it stayed constant in the PEI group (Fig.4.3.A). The metabolic activity of treated cells significantly decreased in the PEI group at day 1 in comparison to the RALA and nHA groups (Fig.4.3.B). GFP positive cells were imaged at day 1 and 3 after transfection (Fig.4.3.C) and the cell surface area (Fig.4.3.D), circularity (Fig.4.3.E) and cell aspect ratio (Fig.4.3.F) of the transfected cells were assessed at the two different time points. GFP positive MSCs transfected by nHA-pGFP or RALA-pGFP complexes displayed an elongated and spread morphology, while MSCs transfected by PEI-pGFP complexes appeared more rounded (Fig.4.3.C). Quantitative analysis of the images confirmed a significantly higher

cell surface area (Fig.4.3.D) and cell aspect ratio (Fig.4.3.F) in MSCs transfected by nHA-pGFP or RALA-pGFP complexes and significantly higher circularity in MSCs transfected by PEI-pGFP complexes (Fig.4.2.C).
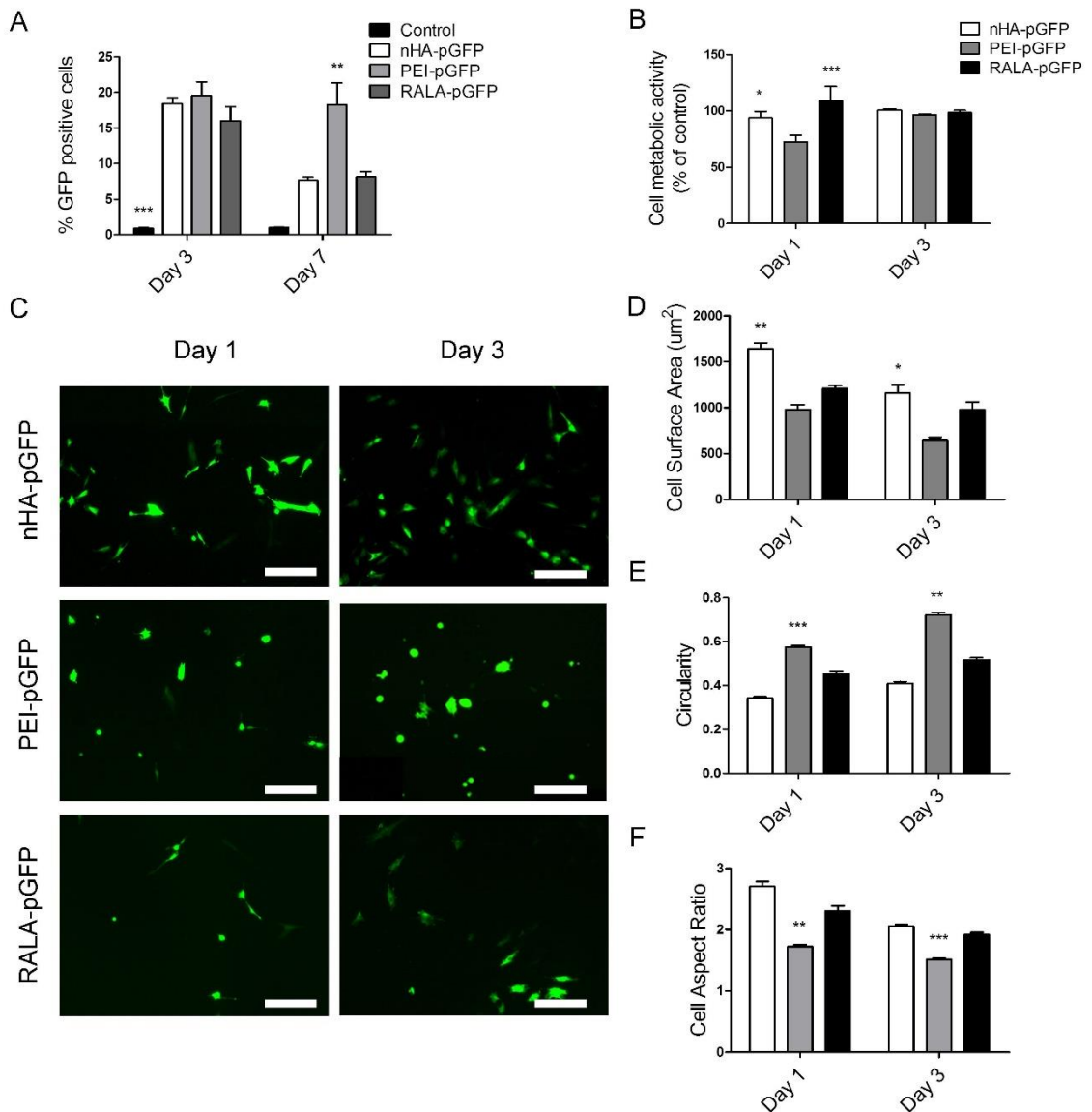
Fig.4.3. (A) Percentage of GFP positive cells at days 3 and 7 post transfection with nHA-pGFP, PEI-pGFP and RALA-pGFP complexes. (B) Cell metabolic activity (% of non-transfected control) at days 1 and 3 post transfection. (C) Fluorescent inverted microscopy images of the transfected MSCs and day 1 and 3 after transfection. Scale bar = 200 μm. (D) Cell surface area, (E) circularity and (F) cell aspect ratio of the transfected cells at days 1 and 3 post transfection. (*) denotes significance (n=4 for A and B, n=6 for D, E and F, p<0.05) in comparison to all groups in the same time point; (**) denotes significance (n=4 for A and B, n=6 for D, E and F, p<0.01) in comparison to all groups at the same time point; (***) denotes significance (n=4 for A and B, n=6 for D, E and F, p<0.001) in comparison to all groups at the same time point.

Immunofluorescent imaging of cells treated with either nHA, PEI or RALA, complexed to pDNA encoding for luciferase (pLUC) and stained for vinculin (green), F-actin (red) and nuclei (blue), revealed the presence of more well developed and intensely stained actin stress fibers and a higher number of mature focal adhesions in the nHA (Fig.4.4.B and F) and RALA (Fig.4.4.D and H) in comparison to PEI transfected MSCs (Fig.4.4.C and G). It also confirmed the effects of PEI on cell morphology, where MSCs appeared smaller with minimal spreading in comparison to the elongated MSCs when nHA and RALA were used as gene delivery vectors (Fig.4.4).
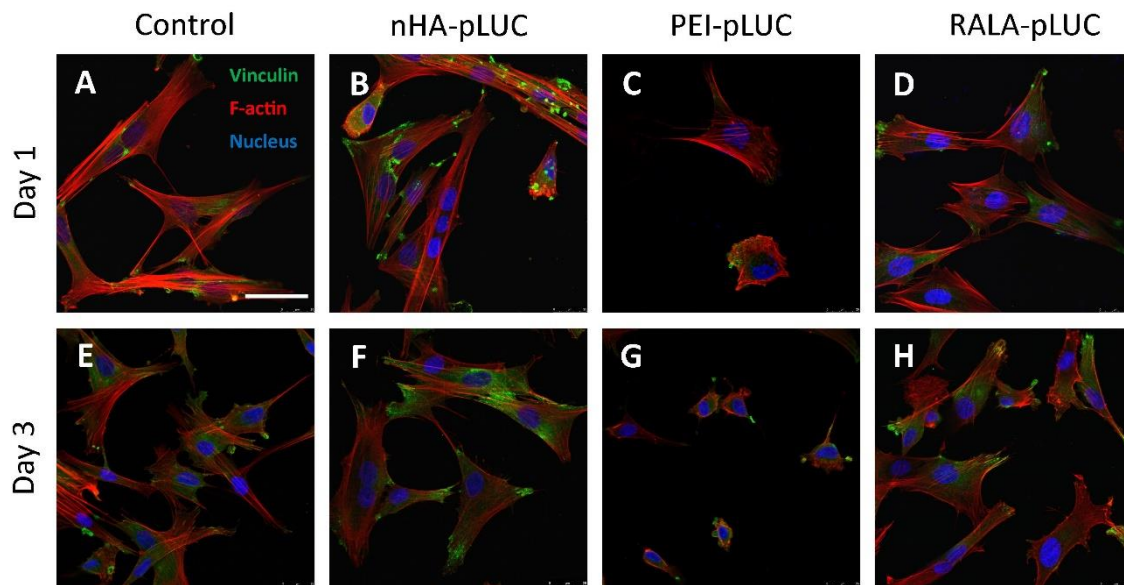
Fig.4.4. Immunofluorescent images of cells stained for vinculin (green), F-actin (red) and nuclei (blue) at day 1 (A-D) and 3 (E-H) after transfection with nHA-pLUC (B,F), PEI-pLUC (C,G) and RALA-pLUC (D,H) complexes and the untreated control (A,E). Scale bar = 50 μm.

4.3.3. The choice of gene delivery vector influences osteo-adipo lineage specification in MSCs

Delivery of plasmid DNA encoding for the reporter gene GFP (pGFP) to MSCs in 2D culture resulted in significantly enhanced calcification (Fig.4.5.A and D) when nHA and RALA were used as transfection vectors in comparison to the PEI transfected group and non-transfected controls after 14 days maintained in mixed osteo-adipo media. In both the nHA and RALA transfected groups, GFP positive cells formed aggregates at day 14 (Fig.4.5.C) confirming the presence of transfected cells in the mineralized nodules

observed after calcium staining (Fig.4.5.A). In contrast, the PEI transfected cells tended to undergo adipogenesis, as demonstrated by a higher presence of lipid granules in comparison to the control and the nHA and RALA groups (Fig.4.5.B and E). No mineralized nodules were observed in PEI transfected cells (Fig.4.5.A and C).
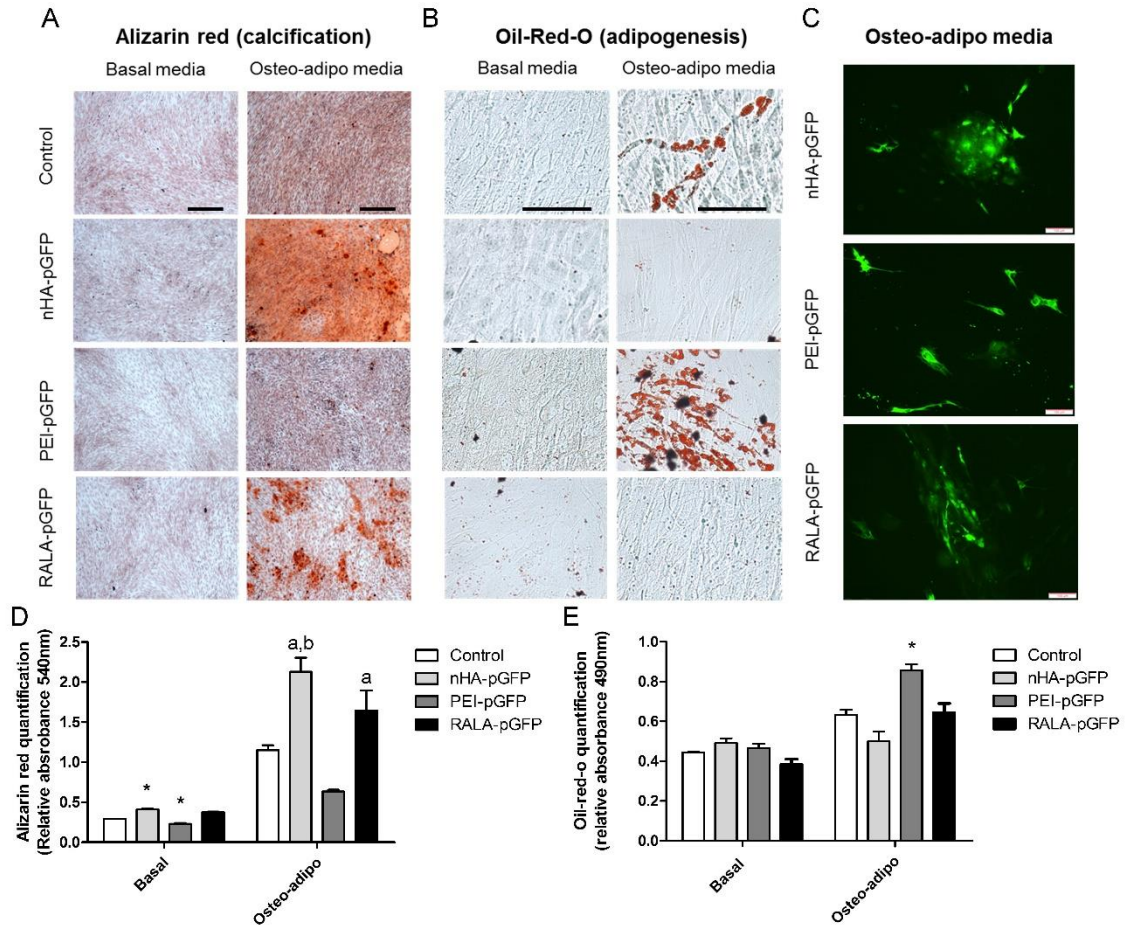
Fig.4.5. Assessment of the osteogenic and adipogenic potential of MSCs transfected with pGFP complexed to either nHA, PEI and RALA after 14 days of in vitro 2D culture in basal and osteo-adipo media. (A) Alizarin red staining. Scale bar = 500µm (B) Oil-Red-O (ORO) staining. Scale bar = 200 µm (C) Fluorescent microscope images of the GFP expressing MSCs after 14 days of in vitro 2D culture. Scale bar = 100 µm. (D) Quantification of alizarin red (AR) staining of the transfected monolayers. (E) Quantification of oil-red-o (ORO) staining of the transfected monolayers. (*) Denotes significance (n=3, p<0.05) in comparison to all groups in the same culture condition; (a) denotes significance (n=3, p<0.05) in comparison to PEI-pGFP in the same culture condition; (b) denotes significance (n=3, p<0.05) in comparison to the control group in the same culture condition.

4.3.4. Osteogenesis of MSCs after therapeutic gene delivery is highly dependent on the choice of gene delivery vector and does not correlate with therapeutic protein production

Therapeutic gene delivery of pDNA encoding for either TGF-β3 or BMP2 in combination or isolation to MSCs in 2D culture resulted in effective protein production using the three vectors (Fig.4.6.A and B). At day 3, the highest levels of protein were produced using RALA and PEI as the delivery vector, while at day 7 the highest levels were observed with PEI with low levels of protein production measured using nHA or RALA as the delivery vector (Fig.4.6.A and B). Although nHA-mediated transfection led to significantly lower overall levels of TGF-β3 (Fig.4.6.A) and BMP2 protein production (Fig.4.6.B), it resulted in the highest levels of mineral deposition after 14 days of 2D *in vitro* culture under basal media conditions in comparison to the RALA and PEI groups and the nHA-pGFP control (Fig.4.6.C and D).
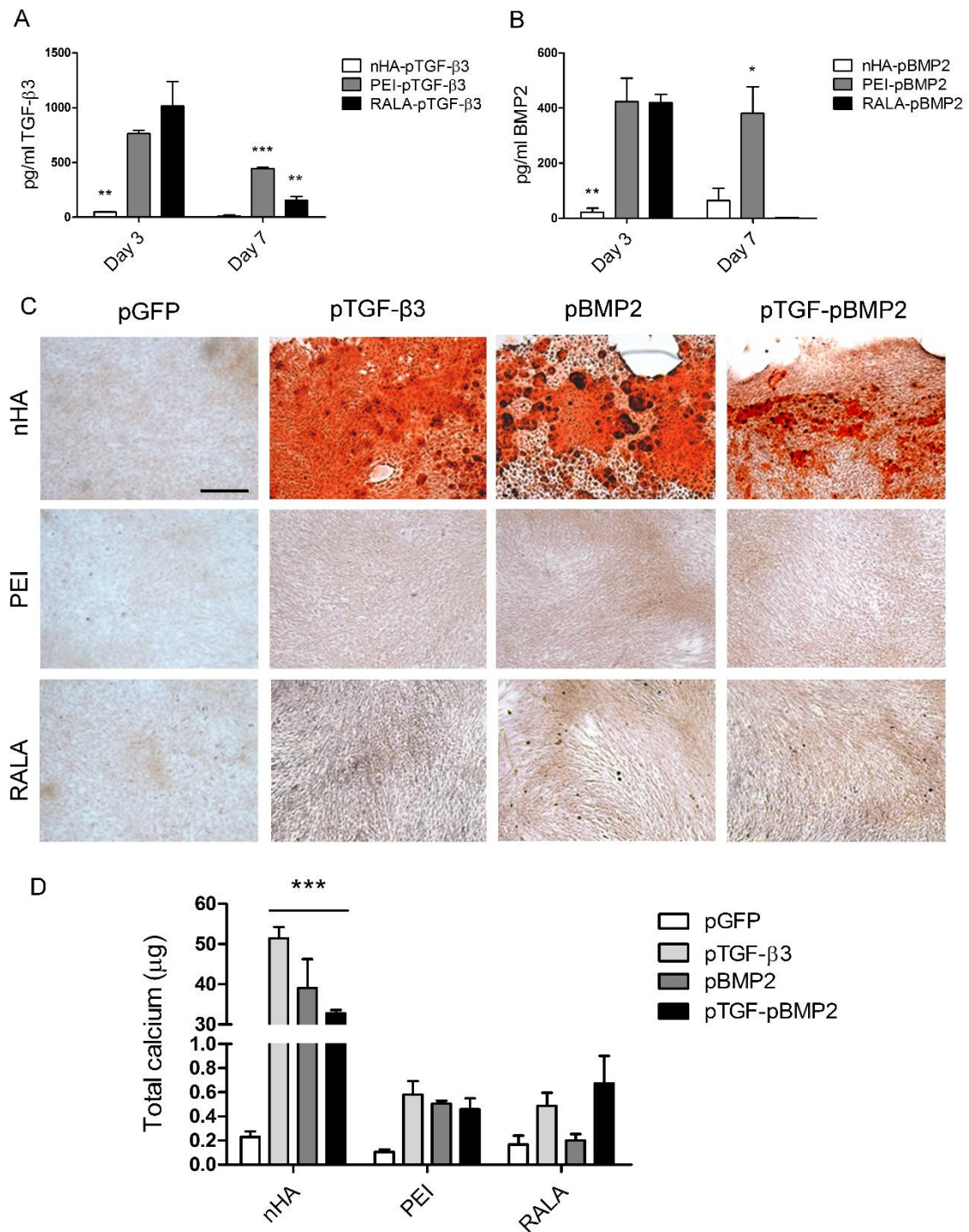
Fig.4.6. (A) TGF-β3 and (B) BMP2 protein expression after 3 and 7 days of MSC in vitro 2D transfection using nHA, PEI and RALA as gene delivery vectors. (C) Alizarin red staining. Scale bar = 500 µm. (D) Total calcium content of the transfected monolayers after 14 days of in vitro culture. (*) denotes significance (n=3, p<0.01) in comparison to all the groups in the same time point. (**) denotes significance (n=3, p<0.01) in comparison to all the groups in the same time point. (***) denotes significance (n=3, p<0.001) in comparison to all the groups in the same time point.

4.3.5. Chondrogenesis of MSCs after delivery of TGF-β3 and BMP2 plasmid DNA is highly dependent on the choice of gene delivery vector

MSCs transfected using the previously described non-viral gene delivery vectors complexed to pDNA encoding for the therapeutic genes TGF-β3 or BMP2 in combination or isolation were used to produce pellets and cultured within basal, chemically defined media conditions for 21 days. PCR analysis of gene expression at day 7 showed increased expression of the early chondrogenic differentiation marker SOX9 (Akiyama, 2008; Loebel et al., 2015) in the nHA and RALA pTGF-β3–pBMP2 co-delivery group and in the RALA-BMP2 group in comparison to the PEI treated MSCs (Fig.4.7.A). The MSCs transfected with RALA-pBMP2 and RALA-pTGF-β3-pBMP2 expressed increased levels of ACAN (a protein that forms an integral part of the extracellular matrix in cartilaginous tissue) compared to the other groups (Fig.4.7.B). RUNX2, a marker of endochondral ossification, was expressed at higher levels in the RALA-TGF-β3 and nHA-TGF-β3 groups compared to when pBMP2 and pTGF-β3 were co-delivered using these vectors (Fig.4.7.C). The SOX9:RUNX2 ratio (a predictor of the osteogenic potential of MSCs where a higher value suggests a more stable chondrogenic phenotype (Loebel et al., 2015; Mhanna et al., 2014)) was also higher in the nHA and RALA co-delivery groups than the other groups (Fig.4.7.D), suggesting an increased chondrogenic potential of these vectors and pDNA combinations.

The biochemical analysis of the pellets at 21 days of culture showed significantly higher levels of GAG (Fig.4.7.E) and collagen (Fig.4.7.F) accumulation following RALA and nHA-mediated delivery of pBMP2 and co-delivery of pTGF-β3–pBMP2 in comparison to PEI-mediated delivery of the same genes.
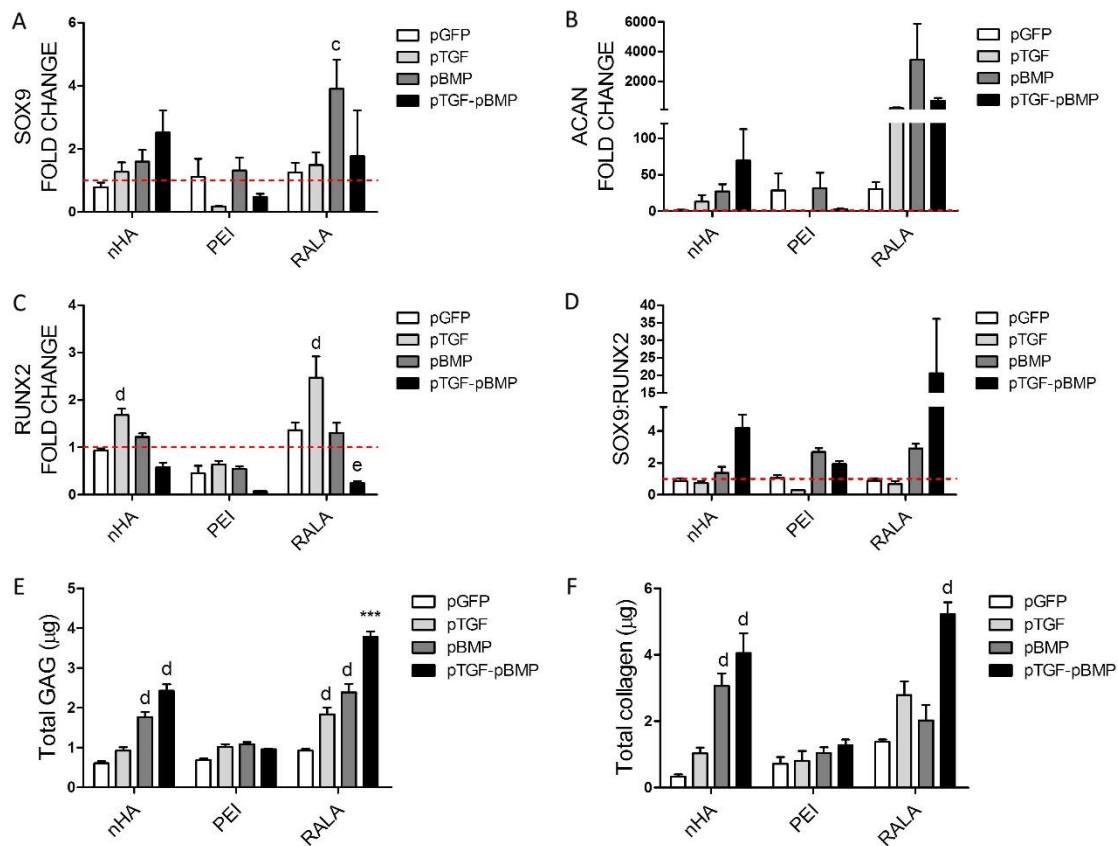
Fig.4.7. Relative expression levels of SOX9 (A), ACAN (B) and RUNX2 (C) in the nHA, PEI and RALA transfected pellets with either pGFP, pTGF-β3 (pTGF), pBMP2 (pBMP) or a combination of both (pTGF-pBMP) after 7 days of in vitro culture. (D) SOX9:RUNX2 relative expression levels ratio. Total GAG (E) and collagen (F) content in the nHA, PEI and RALA transfected pellets after 21 days of in vitro culture. (c) Denotes significance (n=4, p<0.05) in comparison to the PEI-pTGF and PEI-pTGF-pBMP groups. (d) Denotes significance (n=4, p<0.05) in comparison to all PEI transfected groups. (e) Denotes significance (n=4, p<0.05) in comparison to all the rest RALA-transfected groups. (***) denotes significance (n=4, p<0.001) in comparison to all the groups. The dotted line indicates the non-transfected control (fold change = 1).

Histological examination of the pellets after 21 days of *in vitro* culture demonstrated higher accumulation of GAG and collagen type II deposition, as markers of chondrogenesis, in the nHA-pBMP2, nHA-pTGF-pBMP, RALA-pBMP2 and RALA-pTGF-pBMP groups (Fig.4.8.B and D). Within nHA and RALA transfected MSCs, staining for these cartilage specific markers was most intense following the co-delivery of TGF-β3 and BMP2. Small nodules of mineral were observed in the pellets generated using nHA transfected MSCs (Fig.4.8.B), except in the nHA-pTGF-pBMP2 group despite the fact that this tissue stained intensely for collagen type X, a marker of chondrocyte hypertrophy

(Iyama et al., 1991) (Fig.4.8.B). Staining for collagen type X was also detected in the nHA-pBMP2 and RALA-pBMP2 groups (Fig.4.8.B and D). The PEI treated groups did not stain positively for GAG, calcium, collagen type II or collagen type X deposition (Fig.4.8.C). Collagen type I staining was also more intense in the pellets generated using nHA-BMP2 and nHA-TGF-BMP transfected MSCs (Fig.4.8.B), but it was also present in the RALA-BMP2, RALA-TGF-BMP (Fig.4.8.D) and PEI-pBMP2 groups (Fig.4.8.C).
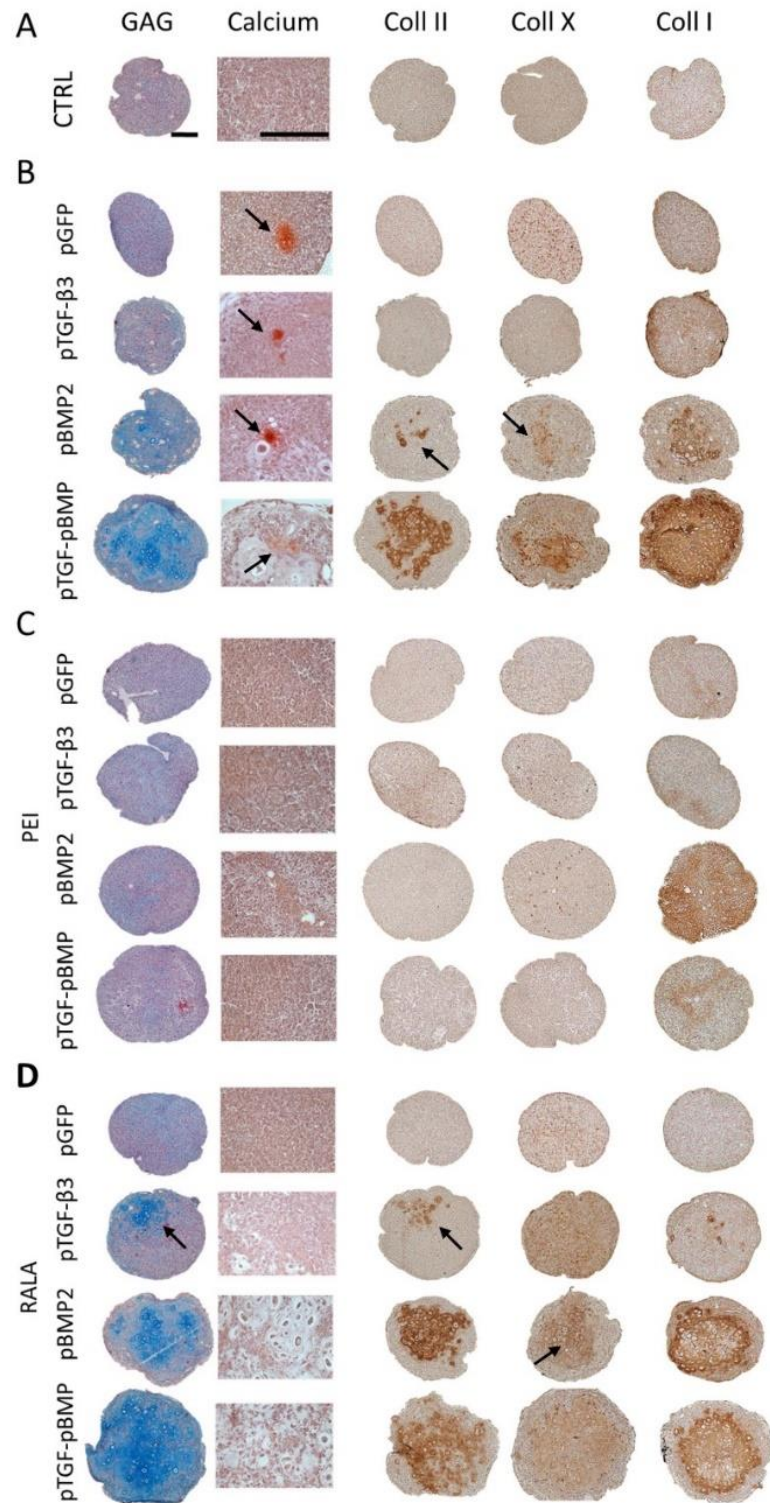
Fig.4.8. Histological examination of the non-transfected MSC pellets (A) and transfected MSC pellets with either (B) nHA, (C) PEI or (D) RALA, complexed to pDNA encoding for either GFP, TGF-ß3, BMP2 or a combination of both, after 21 days of in vitro culture. sGAG histological examination through Alcian blue staining; calcium deposition histological examination through alizarin red; collagen type II, collagen type I and collagen type X immunostaining. Scale bar = 200 µm. Black arrows indicate details of localised specific matrix deposition.

4.4. Discussion

The overall aim of this study was to investigate the influence of different types of non-viral gene delivery vectors on modulating stem cell fate after the delivery of pDNA encoding for specific genes of interest. Three delivery vectors, PEI, nHA and the RALA amphipathic peptide were selected based on their chemistry and mode of action and complexed with either reporter or therapeutic genes. Systematic *in vitro* analysis were performed to evaluate the influence of the vectors and gene combinations on MSC fate. Even though the transfection efficiencies of these three vectors were comparable, they exerted unique effects on the metabolic activity, cellular morphology and the phenotype of MSCs. When maintained in mixed osteo-adipo media, MSCs underwent osteogenesis following transfection with nHA and RALA delivery vectors (complexed to reporter genes), and adipogenesis when transfected with PEI. In order to understand the influence of the delivery vector when complexed with therapeutic genes, we next evaluated the delivery of pDNA encoding for the growth factors TGF-β3 and BMP2, in combination or in isolation, on MSC differentiation. nHA, despite promoting significantly lower transgene expression than the other vectors, induced more robust osteogenesis in 2D and accelerated MSC hypertrophy and endochondral ossification in 3D pellet culture. On the contrary, RALA-mediated gene delivery appeared less osteogenic in both 2D and 3D culture, promoting significantly higher expression of chondrogenic markers and a more stable hyaline cartilage-like phenotype in pellet culture. The PEI treated MSCs failed to undergo either osteogenesis or chondrogenesis in 2D and 3D pellet culture despite high levels of therapeutic protein production.

Size, shape and surface charge have been shown to be crucial for internalization and intracellular trafficking of nanoparticle-based drug delivery systems (Euliss et al., 2006; Gratton et al., 2008). Cationic nanoparticles of a size in the 10-200 nm range have been identified as the ideal to efficiently overcome physiological and cellular barriers (Adair et al., 2010; Bose and Tarafder, 2012). But successful delivery of nucleic acids using PEI and chitosan complexes bigger than 500 nm and negatively charged lipoplexes and ceramic nanoparticles have also been previously reported (Castaño et al., 2014; Curtin et al., 2012; Kapoor and Burgess, 2012; McKiernan et al., 2013). In this study, three different vectors with different size, surface charge and chemistry were used

(Fig.4.2). PEI and RALA were shown to have a positive Z potential (Fig.4.2.B) due to the cationic amino groups in PEI and the guanidinium groups present in the peptide's arginine amino acids, which allow them to react with the negatively charged phosphate groups in pDNA (Boussif et al., 1995; McCarthy et al., 2014; Oba et al., 2015) (Fig.4.2) to form a vector-pDNA complex with a size lower than 150 nm (Fig.4.2.A, C and E). nHA nanoparticles possessed a negative zeta potential (Fig.4.2.B) and a size of approximately 200-300 nm (Fig.4.2.A and D) after complexing with pDNA due to particle aggregation caused by the interactions between the calcium ions in the apatite and the anionic phosphate groups in the pDNA (Curtin et al., 2012; Okazaki et al., 2001) (Fig.4.1). The charge and size of the nHA nanoparticles and nHA-pDNA complexes were consistent with previous reports (Castaño et al., 2014; Curtin et al., 2012).

Even though the RALA, nHA and PEI complexes showed different chemical and physical characteristics, similar transfection efficiencies were observed after 3 days of treatment (Fig.4.3.A). PEI associated cytotoxicity has been previously described due to membrane and cellular organelles destabilization (Larsen et al., 2010), actin cytoskeleton disruption (Grosse et al., 2007; Larsen et al., 2010; Wong et al., 2000) and an altered gene transcription (Akhtar, 2006; Godbey et al., 2001; Larsen et al., 2010). In this study, a significant decrease in cell metabolic activity was observed in the PEI-pGFP treated group one day after transfection due to polymer-induced cytotoxicity, but this was temporary as metabolic activity recovered by day 3 (Fig.4.3.B), as seen in previous reports (Tierney et al., 2012; Yang et al., 2014). The hypothesized PEI-induced cytoskeleton and membrane alterations may affect the transfected MSCs, promoting a more rounded cell morphology with a less tense and organized actin cytoskeleton that is more conducive to adipogenesis (Feng et al., 2010; Godbey et al., 2001; Margadant et al., 2013; McBeath et al., 2004). These observations are consistent with previous reports by Godbey *et al.* (Godbey et al., 2001) who observed that cells exposed to PEI-pDNA complexes showed a rounded phenotype 8 h post-transfection. On the contrary, nHA transfected cells showed a more spread morphology (Fig.4.3.F) with well-developed stress fibres (Fig.4.4.B and F). This may be due to the anionic Z potential of the nHA-pDNA complexes, which have been shown to induce actin polymerization (Ng et al., 2009) and an increased concentration of intracellular calcium which plays an important

role in cell spreading and cytoskeletal events (Kruskal et al., 1986). Although the cell aspect ratio and surface area of the RALA-pGFP transfected cells was significantly lower than the nHA-pGFP group at day 1 and 3, these parameters were higher in comparison to the PEI-transfected cells in both time points (Fig.4.3.D and F). CPPs have been previously shown to induce actin remodeling and a selective activation of Rho GTPases (Foerg et al., 2007; Heitz et al., 2009) contributing to focal adhesion and stress fiber formation (Burridge and Wennerberg, 2004; Foerg et al., 2007), which play an important role in shape-dependent control of MSC lineage commitment (McBeath et al., 2004).

It is well established that morphology, cytoskeletal tension and focal adhesions have a determinant influence on stem cell differentiation towards the osteogenic, adipogenic and chondrogenic pathways (Mathieu and Loboa, 2012; McBeath et al., 2004). While a spread phenotype is related to an increase in cytoskeletal organization, focal adhesions and osteogenesis of MSCs, a more rounded morphology can be an indication of cytoskeletal disruption and dispersed actin, which can lead to a switch towards the adipogenic pathway (Feng et al., 2010; Kilian et al., 2010; Rodríguez et al., 2004; Sonowal et al., 2013). To investigate the role of the observed transfection-induced morphological and cytoskeletal tension changes, the treated MSCs were cultured under osteo-adipo conditions (McBeath et al., 2004) and their commitment towards the osteogenic or adipogenic lineage was analysed. As might be expected for MSCs adopting a more spread morphology with a tenser cytoskeleton, RALA-pGFP and nHA-pGFP treated cells showed increased mineralization and mineralized nodule formation in comparison to the non-transfected control group and the PEI treated group, in which calcification was suppressed (Fig.4.5.A, C and D). On the other hand, adipogenesis was significantly higher in the PEI-pGFP transfected MSCs where the cells adopted a more rounded morphology (Fig.4.5.B and E). Previous studies have also shown that PEI-mediated transfection can suppress mineralization and enhance adipogeneis of stem cells (King et al., 2012; Zhao et al., 2013).

The ultimate goal of gene delivery in stem cell-based tissue engineering approaches is to direct stem or progenitor cells to differentiate into clinically relevant cell types. In order to achieve this objective, TGF-β3 and BMP2 have been extensively used in gene and protein-mediated strategies for the repair of musculoskeletal tissues

(Brunger et al., 2014; Diao et al., 2009; Hao et al., 2008). In this study the delivery of pDNAs encoding for either or both of these factors was used to assess vector-associated effects over stem cell fate. In 2D culture, in the absence of osteogenic supplements, nHA was the only vector capable of inducing mineralization of MSCs when pDNA encoding for either TGF-β3 or BMP2 were delivered in isolation or combination (Fig.4.6.C and D). Interestingly, this occurs despite the fact that nHA-mediated transfection resulted in the lowest levels of therapeutic growth factor production (Fig.4.6.A and B), suggesting a synergistic effect between the osteogenic stimulus provided by nHA and the overexpressed proteins (Curtin et al., 2012). Of relevance to this study, Curtin *et al*. evaluated PEI and nHA as gene carriers for bone formation and observed that even though PEI-mediated transfection of pBMP2 and pVEGF led to higher levels of protein expression, a better healing profile was observed *in vivo* when nHA was used (Curtin et al., 2015). These results suggest that high levels of expression may not directly translate into an increased osteogenic effect and that the choice of delivery vector influences the bioactivity of the gene product (Raisin et al., 2016).

Chondrogenic differentiation of transfected MSCs was also analysed. RALA-mediated delivery of pBMP2 and co-delivery of pTGF-β3 and pBMP2 resulted in the promotion of a stable hyaline cartilage-like phenotype in pellet culture, with strong staining for GAG and collagen type II deposition (Fig.4.8.D), and significantly higher expression of the chondrogenic markers ACAN and SOX9 (Fig.4.7.A and B). MSCs treated with nHA complexed to pTGF-β3 and pBMP2 in isolation or combination also expressed high levels of SOX9 and ACAN (Fig.4.7.A and B) and stained strongly for collagen type II, but high levels of collagen type X and calcium deposition suggest chondrocyte hypertrophy and progression along an endochondral pathway (Fig.4.8.B) (Iyama et al., 1991). This is likely due, at least in part, to the osteo-inductive nature of the nHA. The lower levels of TGF-β3 protein production following nHA-mediated gene delivery may also play a role in promoting a more endochondral phenotype, as extended growth factor presentation has been associated with a more stable cartilage phenotype (Liu et al., 2008). In contrast to the nHA and RALA-transfected cells, the PEI-transfected MSCs promoted low levels of GAG and collagen synthesis (Fig.4.7.E and F) and failed to induce collagen type II deposition (Fig.4.8.C), despite high levels of TGF-β3 and BMP2

expression. The observation of a more rounded phenotype of the cells treated with PEI in 2D (Fig.4.3.E) might suggest a propensity towards chondrogenic differentiation (Gao et al., 2010), but in this study PEI-mediated transfection failed to promote robust chondrogenesis of MSCs in pellet culture. This might be due to an altered gene transcription produced by the interaction of polycationic polymers with the host DNA upon nuclear entry (Akhtar, 2006; Godbey et al., 2001). The co-delivery of pTGF-β3 and pBMP2 by either RALA or nHA promoted the highest levels of chondrogenesis. Furthermore, it was observed that a suppression of calcification and a decrease in RUNX2 expression when both genes were delivered in combination in comparison to the delivery of pTGF-β3 and pBMP2 in isolation (Fig.4.7.C). This is consistent with previous studies that show a synergistic effect of delivering both growth factors on chondrogenesis of MSCs (Diao et al., 2009) and previous chapter 3.

4.5. Conclusion

This study demonstrates that different classes of commonly used non-viral vectors are not inert and that the chemical and physical characteristics of these nanomaterials have a strong effect on cell morphology, stress fiber formation and gene transcription in MSCs which modulates their capacity to differentiate along the osteogenic, adipogenic and chondrogenic lineages. Furthermore, the inherent effects associated with the intracellular delivery of these nanoparticle complexes was in many cases more potent than that associated with the overexpressed therapeutic genes, emphasizing the importance of understanding the cellular events upon nanoparticle entry before these approaches are used in tissue engineering and regenerative medicine strategies. The results of this study point to the need for careful and tissue-specific selection of non-viral delivery vectors to prevent undesired phenotypic changes and off-target effects when delivering therapeutic genes to damaged or diseased tissues.

In this chapter, the RALA peptide was identified as a promising non-viral gene carrier for the stable chondrogenic differentiation of MSCs, in comparison to nHA. Therapeutic gene delivery using nHA as gene carrier, was confirmed as a potent inducer of MSC mineralization and endochondral ossification. Although MSCs transfected with RALA complexed with pDNA encoding for BMP2 and TGF-β3, developed robust

chondrogenesis, the overexpression of these growth factors could enhance MSC hypertrophy and terminal endochondral differentiation. In the following chapters, RALA-mediated combinatorial gene delivery will be explored to promote stable MSC chondrogenesis and suppress MSC hypertrophy, while nHA will be used as a gene carrier to promote *in vivo* bone formation.

CHAPTER 5

Combinatorial Non-viral Gene Delivery for Stable Chondrogenesis of MSCs

Abstract

Bone marrow-derived mesenchymal stem cells (BMSCs) are a promising cell source for musculoskeletal tissue engineering, but their clinical utility for the treatment of cartilage injuries is limited due to their potential to undergo endochondral ossification and form bone tissue. Non-viral gene delivery can be used to direct MSC fate, but the delivery of just a single gene might not be sufficient to promote stable chondrogenic differentiation of BMSCs. In this study, combinatorial non-viral gene delivery of chondrogenic growth (TGF-β3, BMP2 and BMP7) and regulatory (CHM1, GREM1, HDAC4 and SOX9) factors was explored to promote chondrogenesis of MSCs and to suppress hypertrophy and endochondral ossification. Firstly, RALA peptide mediated non-viral gene delivery was optimized to obtain maximal transfection efficiency of BMSCs with minimal cell dead. Having identified appropriate conditions for robust transfection, the delivery of chondrogenic growth and regulatory factors was explored in both normoxic and hypoxic culture conditions. Whereas the overexpression of growth factors successfully initiated chondrogenesis of BMSCs in hypoxia, they promoted a more hypertrophic or osteogenic phenotype in normoxia, as evidenced by more robust collagen type X deposition and tissue mineralisation. To suppress hypertrophy, pDNA encoding for CHM1, GREM1, HDAC4 and SOX9 were delivered to MSCs, but their overexpression alone failed to induce chondrogenesis of BMSCs. In contrast, their co-delivery with TGF-β3 and BMP2 genes was able to induce chondrogenesis of MSCs and to suppress endochondral progression, as evident by reduced mineralisation and collagen type X deposition. This study highlights the potential of non-viral combinatorial gene therapy for the modulation of MSC phenotype in bone and cartilage tissue engineering.

5.1. Introduction

In this chapter, objective three was addressed. RALA-mediated combinatorial gene delivery was explored to determine the best gene combination (chondrogenic and antihypertrophic factors) and culture conditions (hypoxia and normoxia) for the promotion of a stable hyaline cartilage phenotype.

Articular cartilage defects, caused by acute traumatic events or repetitive micro trauma, show poor self-healing capacity due to the avascular nature of cartilage and the low mitotic activity of chondrocytes (Bedi et al., 2010; Brittberg et al., 1994). Cartilage injuries have been reported to disrupt the cartilage macromolecular structure, promote sulphated glycosaminoglycans (sGAG) loss and, ultimately, increase its permeability and reduce its mechanical properties, which, if not treated, may result in further joint degeneration and disabling osteoarthritis (OA) (Bedi et al., 2010; Charalambous, 2014). Current surgical treatments such as microfracture, osteochondral autografts, and autologous chondrocyte implantation (ACI) are limited by the generation of lower quality fibrocartilage, poor integration with the surrounding hyaline cartilage, hypertrophy and calcification of the grafts, and donor site-morbidity (Bedi et al., 2010; Hjelle et al., 2002).

Autologous and allogenic mesenchymal stem cells (MSCs) from different tissue origins have been clinically investigated for cartilage repair (Emadedin et al., 2015; Vangsness et al., 2014; Vega et al., 2015; Veronesi et al., 2013). Due to their multipotent differentiation capacity and their ability to proliferate *in vitro* without losing their differentiation capacity, MSCs have been considered as a promising candidate for cartilage regeneration (De Bari et al., 2006). Furthermore, MSCs have been shown to possess immunomodulatory properties (Atoui and Chiu, 2012; Gao et al., 2016; Nauta and Fibbe, 2007) and are capable of inhibiting certain inflammatory responses in experimental models of arthritis (Gonzalez et al., 2009; Yan et al., 2017). Bone marrow-derived MSCs (BMSCs) are the most common type of MSC used for musculoskeletal tissue engineering applications(Goldberg et al., 2017). Although BMSCs are able to differentiate *in vitro* into chondrocytes, characterised by SOX9 and collagen type II expression, they typically terminally differentiate along an endochondral route

expressing collagen type X, alkaline phosphatase (ALP) and matrix metalloprotease 13 (MMP13) (Hellingman et al., 2011; Mueller and Tuan, 2008; Pelttari et al., 2006; Vinardell et al., 2012). This endochondral programming in BMSCs has been leveraged for bone tissue engineering applications (Cunniffe et al., 2015a; Daly et al., 2016b; Sheehy et al., 2014b), but presents a significant challenge for the engineering of stable articular cartilage.

To induce chondrogenesis of MSCs, gene delivery is a promising alternative to recombinant protein administration, which poses many limitations *in vivo* such as the use of supra-physiological concentrations which might impair tissue repair and induce off-target effects (Baldo, 2014; Carragee et al., 2011; Zara et al., 2011). Moreover, unlike protein delivery, gene therapy allows for the overexpression of transcription factors and receptor proteins which are localised in specific cellular compartments (Evans and Huard, 2015). Viral gene delivery to BMSCs of chondrogenic growth factors such as transforming growth factor beta (TGF-β) superfamily members like TGF-β1 (Frisch et al., 2016; Ivkovic et al., 2010; Pagnotto et al., 2007), TGF-β3 (Brunger et al., 2014; Hao et al., 2008), bone morphogenic protein 2 (BMP2) (Palmer et al., 2005; Zachos et al., 2007) and BMP7 (Grande et al., 2003; Mason et al., 1998) have been extensively explored for cartilage tissue engineering. But the risk of hypertrophy and endochondral ossification still persists when using gene delivery of these growth factors (Frisch et al., 2016). Gene delivery of chondrogenic regulators such as gremlin 1 (GREM1) (Leijten et al., 2012a), chondromodulin 1 (CHM1) (Chen et al., 2016), sex-determining region Y-type mobility group (SOX) 5, 6 and 9 (Cao et al., 2011; Cucchiarini et al., 2007; Frisch et al., 2016; Ikeda et al., 2004), and histone deacetylase 4 (HADC4) (Pei et al., 2009), among others, have been proposed for the suppression of endochondral ossification and the stable chondrogenic differentiation of MSCs. It remains unclear, however, whether these regulatory factors alone will be sufficient to promote robust and stable chondrogenesis of MSCs.

Viral gene delivery to MSCs and chondrocytes has shown promising results for the *in vivo* treatment of cartilage defects (Hidaka et al., 2003; Ivkovic et al., 2010; Madry et al., 2010, 2012). But their therapeutic translation is limited by safety concerns, immunogenicity, and costly and time consuming production (Gresch et al., 2004; Li and

Huang, 2007). In addition, the small DNA packaging capacity of viral vectors might limit the delivery of larger genes and the simultaneous delivery of more than one gene (Yin et al., 2014). Moreover, continuous high levels of protein production offered by viral transduction at the site of implantation could impair tissue repair and cause off-target side-effects in the long-term, similar to those reported by the delivery of high concentrations of recombinant proteins (Mi et al., 2003; Park et al., 2003; Zara et al., 2011). Therefore, a more controlled overexpression, such as that offered by non-viral transfection, might be more desirable for enhanced matrix formation and cell differentiation. Nanoparticle-based non-viral gene delivery is a promising alternative in orthopaedics due to their transient expression, low immunogenicity, enhanced DNA packaging capacity, ease of large-scale production and potential incorporation into 3D matrices for localised delivery (Li and Huang, 2007; Santos et al., 2011; Yin et al., 2014). Recently, the development of peptides for targeted gene delivery, such as the RALA amphipathic peptide (RALA) comprising repeating units of arginine/alanine/leucine/alanine (McCarthy et al., 2014), represents a promising route for non-viral gene delivery to MSCs due to their cytocompatibility and high transfection efficiencies. RALA is particularly promising for cartilage tissue engineering applications as it is less inherently osteogenic than other vectors used for non-viral gene delivery as discussed in the fourth chapter of this thesis.

The overall objective of this study was to assess the optimal combination of growth and regulatory factors to induce stable chondrogenesis of MSCs through non-viral mediated gene delivery. To this end, RALA-mediated transfection of BMSCs was first optimised to identify the best parameters for optimal transfection efficiency and maintenance of cell viability (Fig.5.1.A). Once these parameters were defined, combinatorial gene delivery of the growth factors TGF-β3, BMP2 and BMP7 was assessed for their capacity to promote chondrogenesis of BMSCs (Fig.5.1.B). As chondrogenically primed BMSCs possess an inherent tendency to progress along an endochondral pathway and form bone (Hellingman et al., 2011; Mueller and Tuan, 2008; Pelttari et al., 2006; Vinardell et al., 2012), we next assessed if gene delivery of the regulatory factors SOX9, CHM1, GREM1 and HDAC4 could be used to promote a stable chondrogenic phenotype in BMSCs (Fig.5.1.C). Finally, co-delivery of these chondrogenic

regulators and inducers was explored as a strategy to drive robust chondrogenesis of BMSCs and to suppress their tendency to progress along an endochondral pathway (Fig.5.1.D).
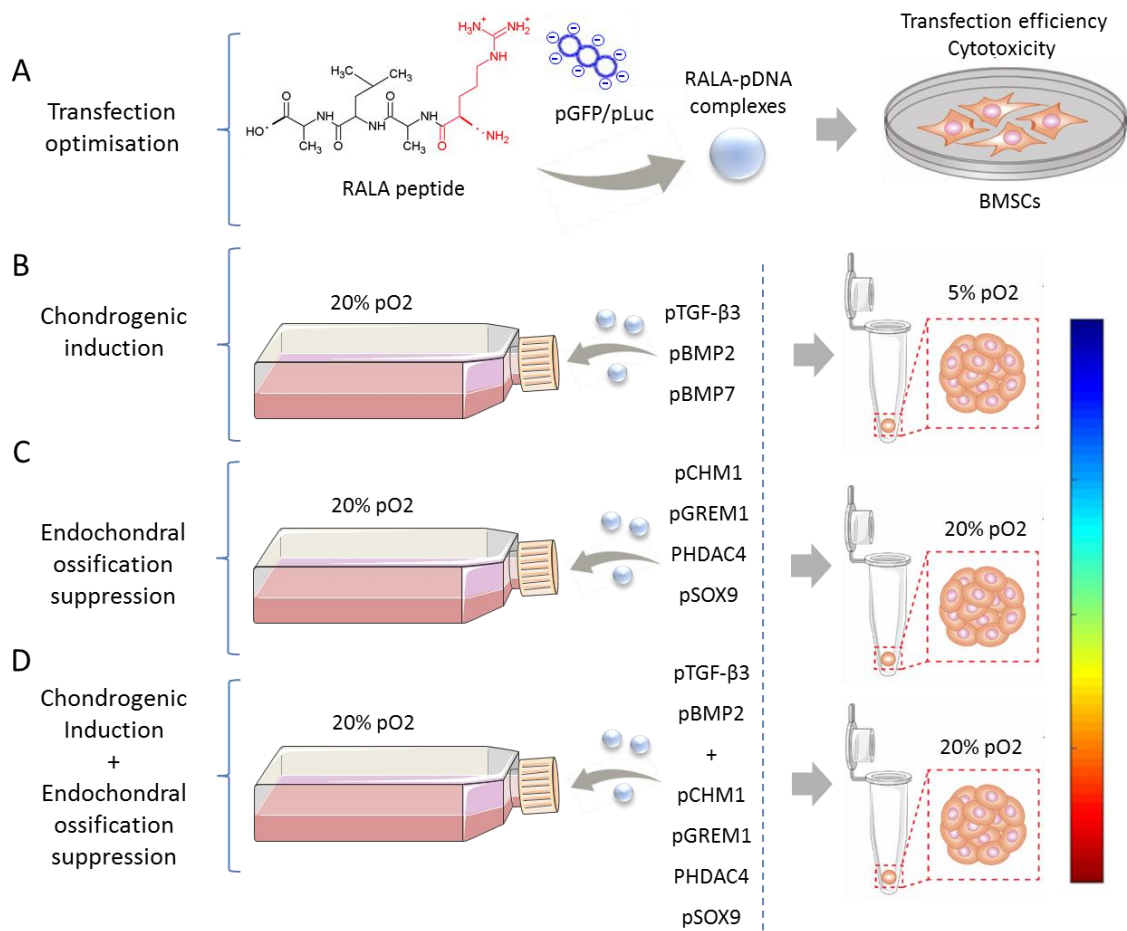
Fig.5.1. Graphical abstract. (A) Optimisation of RALA-mediated delivery of reporter genes (pGFP and pLUC) to BMSCs. (B) Combinatorial gene delivery of pDNA encoding for the growth factors TGF-β3, BMP2 and BMP7 to induce BMSCs chondrogenesis at 5% pO2. (C) Gene delivery of the chondrogenesis regulatory factors CHM1, GREM1, HDAC4 and SOX9 to suppress endochondral ossification of BMSCs at 20% pO2. (D) Combinatorial gene delivery of the growth factors TGFβ3 and BMP2, and the regulatory factors CHM1, GREM1, HDAC4 and SOX9 to promote chondrogenesis of BMSCs and suppression of endochondral ossification at 20% pO2.

5.2. Materials and methods

5.2.1. Plasmid propagation

Nine different plasmids were used in the current study: two plasmids encoding for the reporter genes green fluorescent protein (pGFP, Amaxa, Lonza Cologne AG, Germany) and luciferase (pLUC, pGaussia Luciferase; New England Biolabs, Massachusetts, USA), and seven encoding for the therapeutic human gene sequences of BMP2 (kind donation from Prof. Kazihusa Bessho, Kyoto University, Japan), BMP7 (donation from Dr. Georg Feichtinger, University of Leeds, UK), pTGF-β3 (InvivoGen, Ireland), CHM1 (BioCat, Germany), GREM1 (kind donation from Prof. Derek Brazil, Queen's University Belfast, UK), HDAC4 (kind donation from Dr. Tso-Pang Yao from Duke University, NC, USA, through Addgene), and SOX9 (kind donation from Prof. Gun-Il Im from Dongguk University, South Korea). Plasmid amplification was performed by transforming chemically competent *Escherichia coli* bacterial cells (One Shot TOP10; Biosciences, Ireland) according to the manufacturer's protocol. The transformed bacteria were cultured on LB plates with 50 mg/L kanamycin (Sigma-Aldrich, Ireland) as the selective antibiotic for pGFP, pSOX9 and BMP7, and 100 mg/L ampicillin (Sigma-Aldrich, ireland) as the selective antibiotic for pLUC, pTGF-β3, pBMP2, pCHM1, pGREM1 and pHDAC4. Bacterial colonies were harvested and inoculated in LB broth (Sigma-Aldrich, Ireland) and incubated overnight for further amplification. The harvested bacterial cells were then lysed, and the respective pDNA samples were purified using qiagen plasmid kit (MaxiPrep Kit; Qiagen, Ireland) and kept in Tris–EDTA (TE) buffer (Qiagen, Ireland). Nucleic acid concentration (ng/μL) was determined by analyzing the 260:280 ratio and 230 nm measurement using NanoDrop spectrophotometer (Labtech International, Uckfield, UK).

5.2.2. Preparation of RALA-pDNA complexes

The RALA peptide was synthesized as previously described (McCarthy et al., 2014). Briefly, the peptide was produced by 9-fluorenylmethyloxycarbonyl (Fmoc) solid-state peptide synthesis (Biomatik, USA) and supplied as a desalted, lyophilised powder. The product was purified and validated by reversed-phase high-performance liquid

chromatography (RPHPLC); molecular mass was confirmed as 3327.98. The RALA-pDNA complexes were prepared at different n:p ratios (4, 6, 8 and 10). The RALA-pDNA solution was then incubated for 30 minutes for complex formation.

5.2.3. Isolation and expansion of BMSCs

BMSCs were isolated from the femora of porcine donors (3-4 months, >50 Kg) within 3 h of sacrifice according to a modified method developed for human MSCs (Lennon and Caplan, 2006). Mononuclear cells were plated at a seeding density of 5×10^3 cells/cm^2 in standard culture media, high glucose Dulbecco's modified Eagle's medium (4.5 mg/mL d-glucose and 200 mM L-glutamine; hgDMEM) supplemented with 10% fetal bovine serum (FBS) and penicillin (100 U/mL)–streptomycin (100 g/mL) (all from Gibco, Biosciences, Ireland), and expanded in a humidified atmosphere at 37 °C and 20% pO$_2$. MSCs at passage 2 were used for all experiments.

5.2.4. BMSC transfection and *in vitro* culture

For RALA-pDNA transfection, expanded BMSCs were plated at a seeding density of 5×10^3 cells/cm^2 in 6 well plates for reporter gene optimization or in T175 flasks for therapeutic gene transfection, and cultured for either 24 h (reporter gene optimization) or 72 h (therapeutic gene transfection) in standard culture media prior to transfection. RALA-pDNA complexes were prepared immediately before transfection. Before transfection, cells were washed twice with PBS and incubated in Opti-MEM (Life Technologies, Ireland) for 2 h. After the incubation time, complexes were suspended in either 500 µL (reporter gene optimization) or 5 mL (therapeutic gene transfection) of Opti-MEM and added to MSCS to a density of 0.2 (low), 0.5 (medium) or 1 (high) µg of pDNA/cm^2 for the optimization with reporter genes, or at 0.2 µg of pDNA/cm^2 for therapeutic gene transfection. Following incubation for 4-6 h, the Opti-MEM was removed, cell monolayers washed twice with PBS and standard culture media was added.

For combinatorial therapeutic gene delivery, a total of 0.2 µg of pDNA/cm^2 were used for transfection, meaning that when two genes were co-delivered 0.1 µg of

pDNA/cm^2 of each gene was used, and when three genes were co-delivered 0.067 μg of pDNA/cm^2 of each was used.

5.2.5. Chondrogenic differentiation of MSCs

For evaluating chondrogenic differentiation of MSCs, transfected MSCs and the non-treated controls maintained in standard culture media were pelletized 24 h after transfection by centrifugation at 2000 rpm at a cell density of 250 x 10^3 cells/pellet. Negative controls and transfected pellets were maintained in a chemically defined medium consisting of DMEM GlutaMAX supplemented with penicillin (100 U/mL)– streptomycin (100 mg/mL), 100 mg/mL sodium pyruvate, 40 mg/mL l-proline, 50 mg/mL l-ascorbic acid-2-phosphate, 1.5mg/mL bovine serum albumin, 1 x insulin–transferrin–selenium, and 100 nM dexamethasone (all from Sigma-Aldrich, Ireland) at 5% or 20% pO$_2$ and 37 °C for a period of 28 days. Positive controls were maintained in a chemical defined medium as previously defined supplemented with 10 ng/mL human TGF-β3 (PrepoTech, UK) for 7 days after which the media was replaced with chemically defined medium without recombinant TGF-β3. Half media changes were performed twice weekly. No exogenous recombinant growth factors were added to the culture media.

5.2.6. Assessment of transfection efficiency and cell metabolic activity

In order to evaluate the transfection efficiency, pDNA encoding the gene for green fluorescent protein (GFP) was complexed to RALA at different n:p ratios (section 5.2.2) and MSCs were transfected as described above. To confirm pGFP expression in the transfected monolayers, cells were image using a fluorescent microscope (Olympus IX83 epifluorescence microscope). To confirm GFP positive cells in pellet culture, pellets were imaged using a Leica SP8 scanning confocal microscope (Leica Microsystems, Ireland). Transfection efficiency was determined by quantifying the percentage of green fluorescent cells at day 1, 3 and 7 post transfection using flow cytometry (BD Accuri C6, BD Biosciences, USA). Luciferase expression in the culture media was also quantified using a Pierce Gaussia Luciferase Flash Assay Kit (ThermoFisher, Ireland) at day 1, 3 and 7.

After 1, 3 and 7 of RALA-mediated gene delivery, metabolic activity of treated cells was evaluated using standard Alamar Blue (Biosciences, Ireland) assay. For the assay, cell culture media from the wells was replaced, with 10% Alamar Blue containing standard culture media (1 mL/well) and were incubated for 4 h at 37 °C and 20% pO$_2$. After the incubation time, 200 mL of the supernatant was plated in triplicate into a 96-well plate; absorbance was read at 570 and 600 nm using a plate reader (Bioteck, Instruments Inc, UK). Optical density of the media was translated to cell metabolic activity relative to the non-transfected control as previously described (Hamid et al., 2004).

5.2.7. Gene expression analysis

At day 3 after transfection, transfected and control cells were lysed using RLT lysis buffer (Qiagen, UK) supplemented with 10 µL mL^{-1} β-mercaptoethanol (Sigma-Aldrich, Ireland) and stored at –80°C. Lysates were thawed and homogenized using a QIAshredder column (Qiagen, UK) and total RNA was isolated and purified using the RNeasy mini kit (Qiagen, UK) using the manufacturer's protocol. Purity and yield of RNA was quantified using the NanoDrop Spectrophotometer (Labtech International, Uckfield, UK). For cDNA preparation, 100 ng total RNA of each sample was reverse transcribed into cDNA per 20 µL of reaction volumes using the high capacity reverse transcription cDNA kit (Applied Biosystems, Paisley, UK) as per manufacturer's instructions. Quantitative PCR was performed using an ABI 7500 sequence detection system (Applied Biosystems, Paisley, UK) and SYBR select master mix (Applied Biosystems, Paisley, UK) for evaluating the expression of GAPDH (porcine sequence), TGF-β3, BMP2, BMP7, CHM1, GREM1, HDAC4 and SOX9 (human sequences). Primer sequences that were used for amplification of these genes are listed in Table 5.1. Comparative Threshold (cT) data were analysed using the ΔΔCT method as described previously (Livak and Schmittgen, 2001) with GAPDH as the endogenous control. Relative expression of the genes is presented as fold changes relative to the non-transfected control group.

Table. 5.1. Primer sequences used for qPCR

Gene	Forward primer	Reverse primer
TGF-β3	TGTTGAGAAGAGAGTCCAAC	ATCACCTCGTGAATGTTTTC
BMP2	TCCACCATGAAGAATCTTTG	TAATTCGGTGATGGAAACTG
BMP7	TGGTCCACTTCATCAACC	TTCTGTATTTCTTCAGGATGAC
CHM1	GAAATCCAGAGGGAAAGAAG	GGTCTGGTTTCATTATTCAGTC
GREM1	AATGAGATTGCCAGAAAGTG	GAGGAGTTGGTTTGGTTTAG
HDAC4	AAAAGAGACCAGATGAGGAG	AGACAGACAGACAAGAGAAC
SOX9	CTCTGGAGACTTCTGAACG	AGATGTGCGTCTGCTC
GAPDH	TTTAACTCTGGCAAAGTGG	GAACATGTAGACCATGTAGTG

5.2.8. Quantitative biochemical analysis

Pellets and monolayers were digested with papain (125 mg/mL, pH 6.5) in 0.1 M sodium acetate, 5 nM L-cysteine HCl, and 0.05 M EDTA (all Sigma-Aldrich, Ireland) at 60 °C under constant rotation for 18 h. Calcium content was determined using a Sentinel Calcium Kit (Alpha Laboratories Ltd, UK) after digestion in 1M HCl at 110 °C for 48 h. Proteoglycan content was estimated by quantifying the amount of sulfated glycosaminoglycan (sGAG) in the pellets using the dimethylmethylene blue (DMMB) dye-binding assay (Blyscan, Biocolor Ltd. Northern Ireland), with a chondroitin sulfate standard. Total collagen content was determined by measuring the hydroxyproline content. Samples were hydrolyzed at 110 °C for 18 h in concentrated HCl 38%, allowed to dry, and analyzed using a chloramine-T assay (Hollander and Hatton, 2003) with a hydroxyproline-to-collagen ratio of 1:7.69 (Ignat'eva et al., 2007).

5.2.9. Histological and immunohistochemical analysis

For evaluating sGAG, calcium and collagen deposition, cell pellets were fixed with 4% PFA after 21 days *in vitro*, wax embedded, sliced (8 μm) and mounted on microscopic

slides. The sections were stained with alizarin red (Sigma-Aldrich, Ireland) to assess calcium accumulation, Alcian blue (Sigma-Aldrich, Ireland) to assess sGAG content and picrosirius red (Sigma-Aldrich, Ireland) to assess collagen content. Collagen types I, II and X were evaluated using a standard immunohistochemical technique as described previously (Sheehy et al., 2013). Negative and positive controls of porcine ligament, cartilage, and growth plate were included for each immunohistochemical analysis.

5.2.10. Statistical analysis

Statistical analyses were performed using GraphPad Prism (version 5) software. Statistical differences were determined by analysis of variance (ANOVA) followed by Tukey's multiple comparison test or Student's t-test where appropriate. Numerical and graphical results are displayed as mean ± standard deviation. Significance was accepted at a level of $p < 0.05$. Sample size (n) is indicated within the corresponding figure legends.

5.3. Results

5.3.1. Optimisation of 2D RALA-pDNA transfection

To optimise the transfection of MSCs using RALA-mediated pDNA delivery, the effect of the ratio of moles of the amine groups present in the RALA molecule to those of the phosphate in the DNA molecule (Zhao et al., 2009), also known as the n:p ratio, was assessed. Four different ratios of RALA to either pGFP or pLUC were tested (n:p = 4, 6, 8 and 10). Successful transfection of BMSCs with RALA-pGFP complexes was observed for all four ratios. BMSCs transfected using an n:p ratio of 10 showed the highest transfection efficiency of around 40% at day 1 and 3 after transfection (Fig.5.2.A). Similar results were observed when pLUC was delivered, with significantly higher luciferase expression observed at an n:p of 10 (Fig.5.2.B). The amount of GFP positive cells and of levels of luciferase expression were observed to decrease over 7 days of *in vitro* culture (Fig.5.2.A and B). BMSC viability was also assessed, with no negative effects on DNA content (as a measure of cell number) or cell metabolic activity observed in the transfected groups in comparison to the non-transfected control (Fig.5.2.C and D). Moreover, an increase in DNA content was observed in the transfected groups suggesting a proliferative effect.
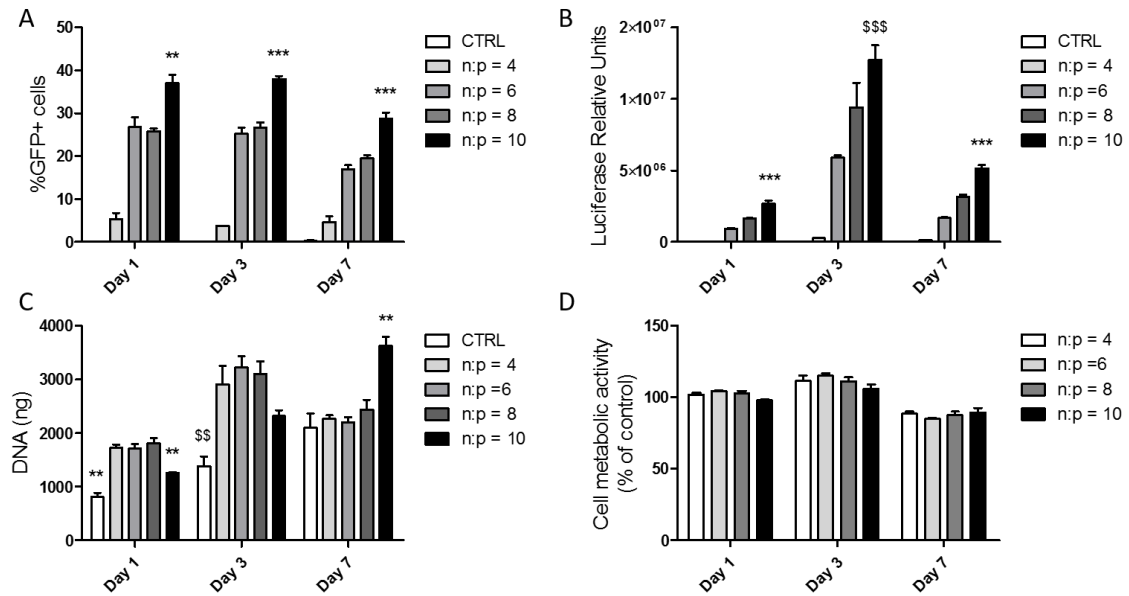
Fig.5.2. Optimisation of the RALA:pDNA n:p ratio for BMSC transfection. (A) % of GFP positive cells at day 1, 3 and 4 after transfection with RALA-pDNA complexes at n:p ratio of 4, 6, 8 and 10. (B) Quantification of luciferase expression in culture media at day 1, 3 and 7 after transfection. (C) Quantification of DNA (ng) of the control and transfected cells at day 1, 3 and 7 after transfection. (D) Cell metabolic activity as a % of the control at day 1, 3 and 7 after transfection. (**) Denotes significance (n=4, p<0.01) to all the groups at the same time point; (***) denotes significance (n=4, p<0.001) to all the groups at the same time point; ($$) denotes significance (n=4, p<0.01) to all the transfected groups at the same time point. ($$$) denotes significance (n=4, p<0.001) in comparison to the CTRL, n:p = 4 and n:p = 6 groups at the same time point.

The effect of pDNA concentration at two different n:p ratios (6 and 10) on BMSC transfection was also assessed. Three different pDNA concentrations were tested: 0.2 $\mu g/cm^2$ (low), 0.5 $\mu g/cm^2$ (medium) and 1 $\mu g/cm^2$ (high). When RALA-pDNA complexes were delivered to BMSCs, the low concentration n:p ratio of 10 resulted in significantly higher luciferase expression in comparison to the rest of the groups at day 3 and 7 (Fig.5.3.A). In terms of cell viability, even though no differences between groups were observed one day after transfection, the high concentration of RALA and pLUC complexed at both n:p ratios was shown to significantly reduce DNA levels and cell metabolic activity in comparison to the other groups (Fig.5.3.B and C).

In summary, the delivery of the low concentration RALA-pDNA complexes at an n:p of 10 resulted in the highest transfection efficiency and transgene expression, with no negative effects on cell number or metabolic activity observed.

In order to assess chondrogenesis of BMSCs after non-viral gene transfection, a 3D pellet culture was chosen to mimic the cellular condensation associated with chondrogenesis (Yoo et al., 1998). To confirm sustained transfection in this pellet model, cells were transfected with the optimised RALA-pGFP complexes and imaged prior to pellet formation and after pellet formation for 14 days (Fig.5.3.D), confirming the presence of pGFP positive cells at each time point (Fig.5.3.D).
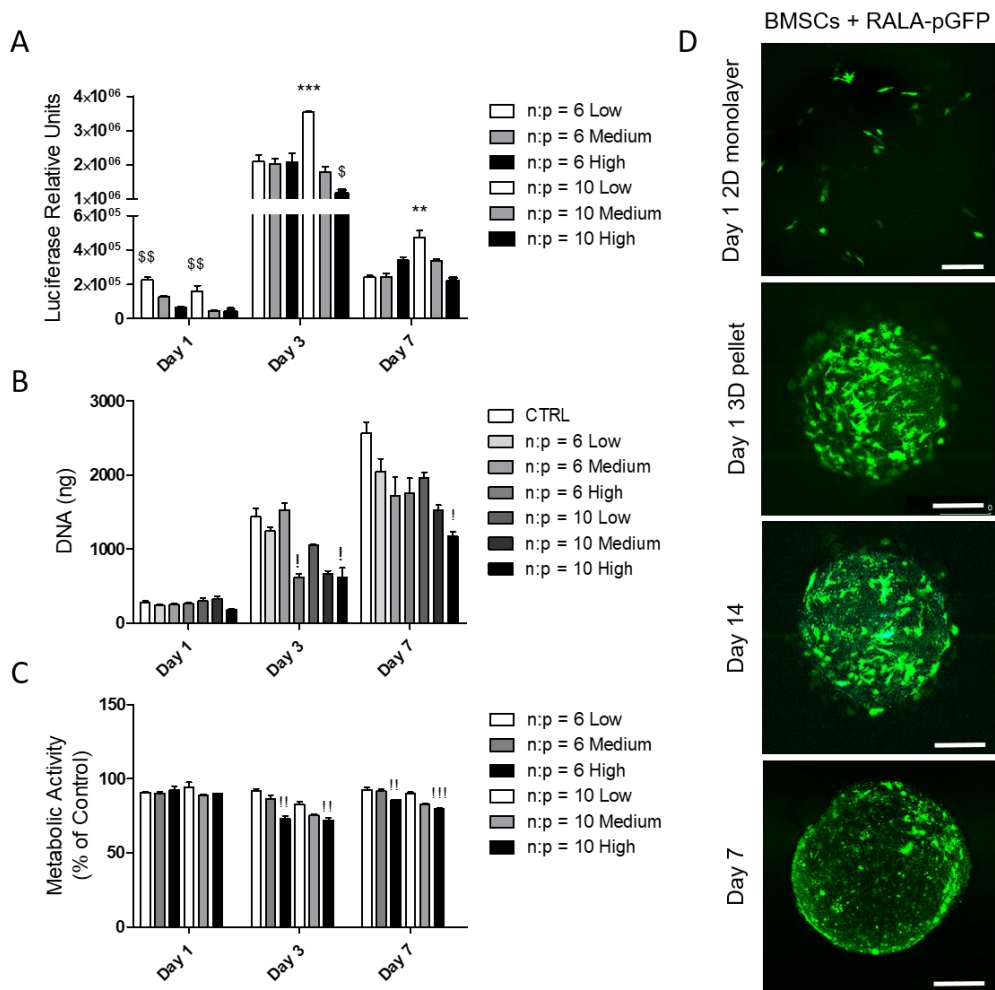
Fig.5.3. Optimisation of the amount of pDNA of 0.2 µg/cm^2 (low), 0.5 µg/cm^2 (medium), and 1 µg/cm^2 (high) in RLA-pDNA complexes at n:p ratio of 6 and 10 for BMSC transfection. (A) Quantification of luciferase expression in culture media at day 1, 3 and 7 after transfection. (B) Quantification of DNA (ng) of the control and transfected cells at day 1, 3 and 7 after transfection. (C) Cell metabolic activity as a % of the control at day 1, 3 and 7 after transfection. (D) Fluorescent imaging of BMSCs one day after RALA-pGFP transfection prior pellet formation and after pellet formation at day 1, 7 and 14. Scale bar = 250 µm. (**) Denotes significance (n=4, p<0.01) to all the groups at the same time point; (***) denotes significance (n=4, p<0.001) to all the groups at the same time point; ($) denotes significance (n=4, p<0.05) to medium and high groups at the same time point; ($$) denotes significance (n=4, p<0.01) to medium and high groups at the same time point; (!) denotes significance (n=3, p<0.05) to control, and all low groups at the same time point; (!!) denotes significance (n=4, p<0.01) to control, and all low groups at the same time point; (!!!) denotes significance (n=4, p<0.001) to control, and all low groups at the same time point.

5.3.2. RALA mediated delivery of therapeutic genes to BMSCs

After optimisation of the n:p ratio and the concentration of pDNA per cm^2 with reporter genes, therapeutic pDNA encoding for chondrogenic growth (pTGF-β3, BMP2 and BMP7) and regulatory (pCHM1, pGREM1, pHDAC4 and pSOX9) factors were delivered to BMSCs. At day 3 after RALA-mediated transfection, cells were lysed and the expression of the aforementioned genes was quantified. All RALA-pDNA complexes were shown to promote overexpression of the encoded genes (Fig.5.4.A-G).

Fig.5.4. Gene overexpression of therapeutic genes and pellet formation after RALA-pGFP transfection. Relative expression (to non-transfected control, fold change = 1) levels of TGF-β3 (A), BMP2 (B), BMP7 (C), CHM1 (D), GREM1 (E), HDAC4 (F) and SOX9 (G) at day 3 after monolayer RALA-mediated transfection of BMSCs. (***) Denotes significance (n=4, p<0.001) to the pGFP transfected control.

5.3.3. Combinatorial gene delivery of growth factors promotes robust chondrogenesis of MSCs

In order to assess the effect of RALA-mediated gene delivery of different growth factors on BMSC chondrogenesis, BMSCs were transfected with RALA-pDNA complexes encoding for either TGF-β3 (pTGF), BMP2 (pBMP2) or BMP7 (pBMP7) and the combinations between them (pTGF-pBMP2, pTGF-pBMP7 and pBMP2-pBMP7). Pellets were formed with the transfected and non-transfected (CTRL-) BMSCs and cultured *in vitro* for 28 days at 5% pO_2 in chemically defined media without additional growth factor supplementation. As a positive control (CTRL+), non-transfected BMSCs were pelleted and maintained in recombinant TGF-β3 supplemented media for 7 days, after which media was replaced by chemically defined media without growth factor.

After 28 days of *in vitro* culture, cell proliferation and matrix deposition were analysed (Fig.5.5). RALA-mediated co-delivery of pTGF-β3 and pBMP2 resulted in significantly higher levels of DNA and GAG in comparison to all other groups (Fig.5.5.A and B). Delivery of pBMP2 and co-delivery of pBMP2 and pBMP7 also enhanced GAG synthesis compared to the positive control of recombinant TGF-β3 stimulation (Fig.5.5.B). MSCs transfected with pBMP2, pTGF-pBMP2 and pBMP2-pBMP7 produced significantly higher levels of collagen than the other groups (Fig.5.5.C). Significantly higher levels of calcium deposition were observed in the pBMP2 and the pBMP2-pBMP7 transfected groups (Fig.5.5.D). Histological analysis of GAG, collagen and calcification was also performed, confirming the results of the biochemical assays (Fig.5.5.E). Immunohistochemical assessment demonstrated the presence of collagen type I and II in the CTRL+, pBMP2, pTGF-pBMP2 and pBMP2-pBMP7 groups. Non-negligible collagen type X staining was only observed in the positive control group (Fig.5.5.E).

Fig.5.5. Combinatorial gene delivery of growth factors for BMSCs chondrogenesis. Total DNA (A), GAG (B), collagen (C) and Calcium (D) deposition (µg/pellet) after 28 days of in vitro culture. (E) Histological (GAG, collagen and calcium) and immunohistochemical (collagen type I, II and X) of the pellets after 28 days of in vitro culture. Scale bar = 100 µm for the 20x images and 1 mm for the 4x images. (*) Denotes significance (n=4, p<0.05) to all the groups at the same time point; (**) denotes significance (n=3, p<0.01) to all the groups at the same time point; (***) denotes significance (n=3, p<0.001) to all the groups at the same time point; (!!) denotes significance (n=3, p<0.01) to the CTRL-, CTRL+, pGFP, pTGF, pBMP2 and pBMP2-pBMP7; (!!!) denotes significance (n=3, p<0.001) to the CTRL-, CTRL+, pGFP, pTGF, pBMP2 and pBMP2-pBMP7. ($) denotes significance (n=3, p<0.05) to the CTRL-, pGFP, pTGF, pBMP7, pTGF-pBMP7; ($$$) denotes significance (n=4, p<0.001) to the CTRL-, pGFP, pTGF, pBMP7, pTGF-pBMP7.
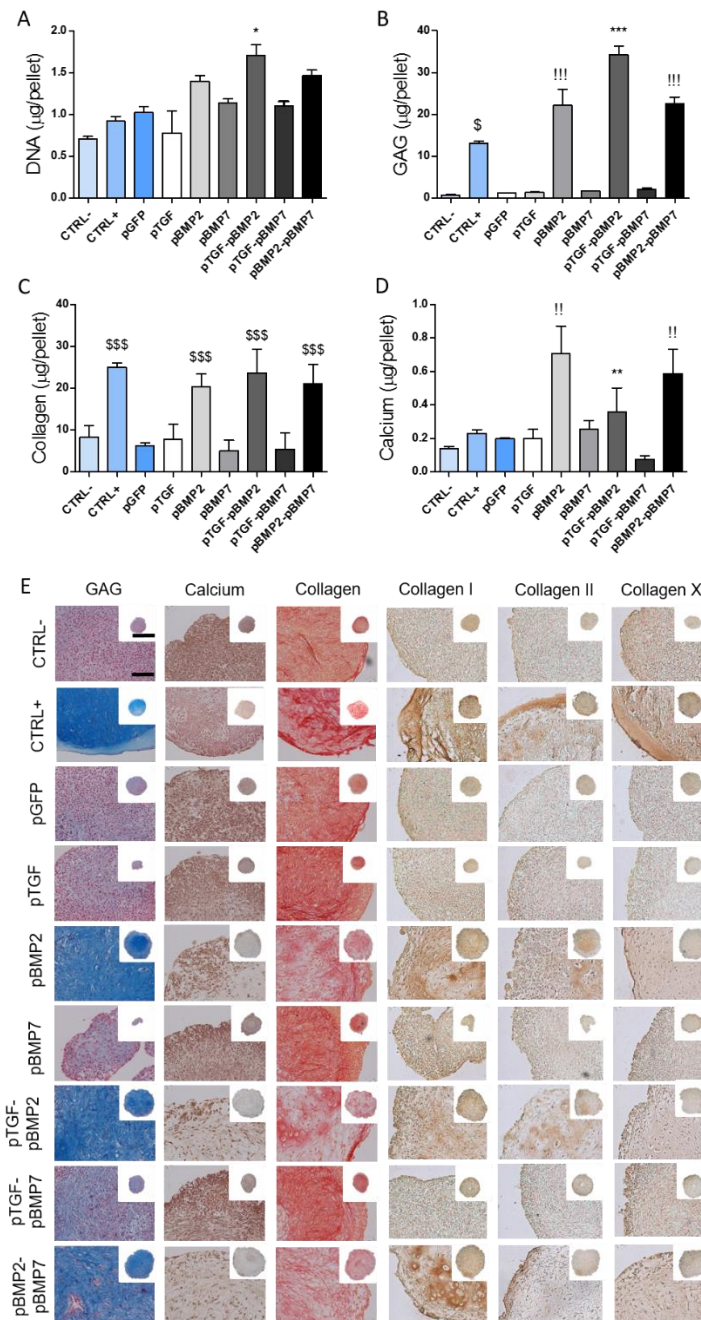
5.3.4. Gene delivery of chondrogenic regulatory factors did not promote robust chondrogenesis of MSCs

The low oxygen culture conditions utilized to date are known to supress hypertrophy and endochondral ossification of chondrogenically primed MSCs (Hirao et al., 2006; Sheehy et al., 2012), however such control of environmental conditions cannot be guaranteed in a regenerative context *in vivo*. We therefore sought to examine chondrogenesis and hypertrophy of MSCs in normoxic conditions (20% pO_2), and furthermore if combinatorial gene delivery of growth and regulatory factors could promote robust chondrogenesis of MSCs whilst suppressing progression along an endochondral pathway. To this end, RALA-pDNA complexes encoding for CHM1 (pCHM1), GREM1 (pGREM1), HDAC4 (pHDAC4) and SOX9 (pSOX9) were first used to transfect BMSCs which were pelletized and cultured *in vitro* at 20% pO_2 in chemically defined medium without exogenous growth factor supplementation. MSCs transfected with pCHM1, pHDAC4 and pSOX9 proliferated at a faster rate than the negative and pGFP controls (Fig.5.6.A). Also, significantly higher levels of GAG deposition were observed in the pGREM1, pHDAC4 and pSOX9 than the negative and pGFP control groups (Fig.5.6.B). No differences between groups were observed in terms of collagen or calcium deposition (Fig.5.6.C and D). Histological analysis revealed negligible GAG staining in the transfected groups, and immunohistochemistry of the pellets did not show any positive staining for collagen type II in any of the groups (Fig.5.6.E), indicating that these regulatory factors in isolation were unable to drive chondrogenesis of MSCs.
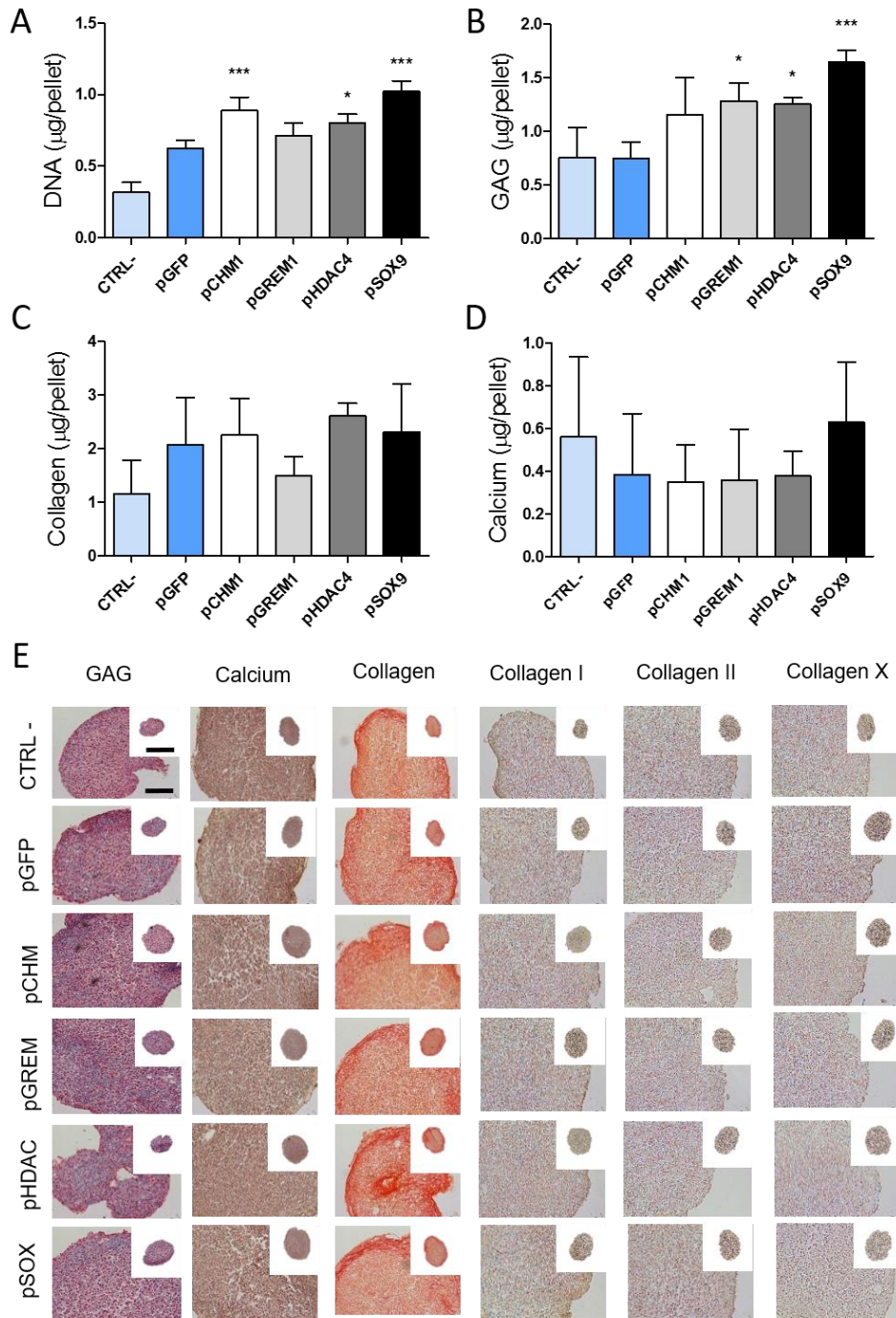
Fig.5.6. RALA-mediated gene delivery of chondrogenesis regulatory factors to BMSCs. Total DNA (A), GAG (B), collagen (C) and Calcium (D) deposition (µg/pellet) after 28 days of in vitro culture. (E) Histological (GAG, collagen and calcium) and immunohistochemical (collagen type I, II and X) of the pellets after 28 days of in vitro culture. Scale bar = 100 µm for the 20x images and 1 mm for the 4x images. (*) Denotes significance (n=4, p<0.05) to the CTRL- and pGFP groups; (***) denotes significance (n=4, p<0.001) to the CTRL- and pGFP groups.

5.3.5. Combinatorial gene delivery of growth and regulatory factors is able to promote chondrogenesis of MSCs with limited evidence of hypertrophy

Combinatorial gene delivery of growth and regulatory factors was next studied for induction of MSC chondrogenesis in normoxic culture conditions. RALA-mediated co-delivery of pTGF-β3 and pBMP2 (pTGF-pBMP2) was combined with either pCHM1 (pTGF-pBMP-pCHM), pGREM1 (pTGF-pBMP-pGREM), pHDAC4 (pTGF-pBMP-pHDAC) or pSOX9 (pTGF-pBMP-pSOX). The DNA content of all experimental pellet groups was higher than the negative control (CTRL-) group after 28 days of culture (Fig.5.7.A). Delivery of pTGF-pBMP-pSOX resulted in the development of pellets with significantly higher levels of DNA than all other groups (Fi.5.7.A), indicating a more proliferative phenotype. MSCs transfected with pTGF-pBMP2 contained significantly higher levels of sGAG compared to all other groups (Fig.5.7.B). Surprisingly, very low levels of GAG were measured in the pTGF-pBMP-pHDAC group, similar to those of the negative control (CTRL-) (Fig.5.7.B). Collagen deposition was similar in the transfected and CTRL+ groups, except for the pTGF-pBMP-pHDAC and CTRL- groups where low levels of collagen synthesis were observed (Fig.5.7.C). Significantly higher levels of calcium were detected in the CTRL+ and pTGF-pBMP2 pellets compared to all other groups (Fig.5.7.D). Histological analysis confirmed the biochemical assessment of GAG, collagen and calcium deposition (Fig.5.7.E). Immunohistochemical analysis of the pellets (Fig.5.7.E) showed intense collagen type I and II in all the pellets except the pTGF-pBMP-pHDAC group, with non-negligible collagen type X staining only observed in the CTRL+ and pTGF-pBMP2 groups.

To further confirm the observed effects of the combinatorial gene delivery of chondrogenic inducer and regulatory factors were due to the factor delivery and not due to the lower concentrations of the individual pDNAs (0.067 µg pDNA/cm^2 per pDNA in the groups transfected with 3 different pDNAs in comparison to 0.1 µg pDNA/cm^2 per pDNA in the groups transfected with 2 pDNAs), pTGF-pBMP2 transfection of BMSCs was compared to pTGF-pBMP-pGFP (Fig.A.2). After 28 days of *in vitro* culture under the same conditions as in the previous experiment, no differences were observed in the levels of DNA, GAG, collagen and calcium deposition (Fig.A.2.A-F) between the 2 groups.
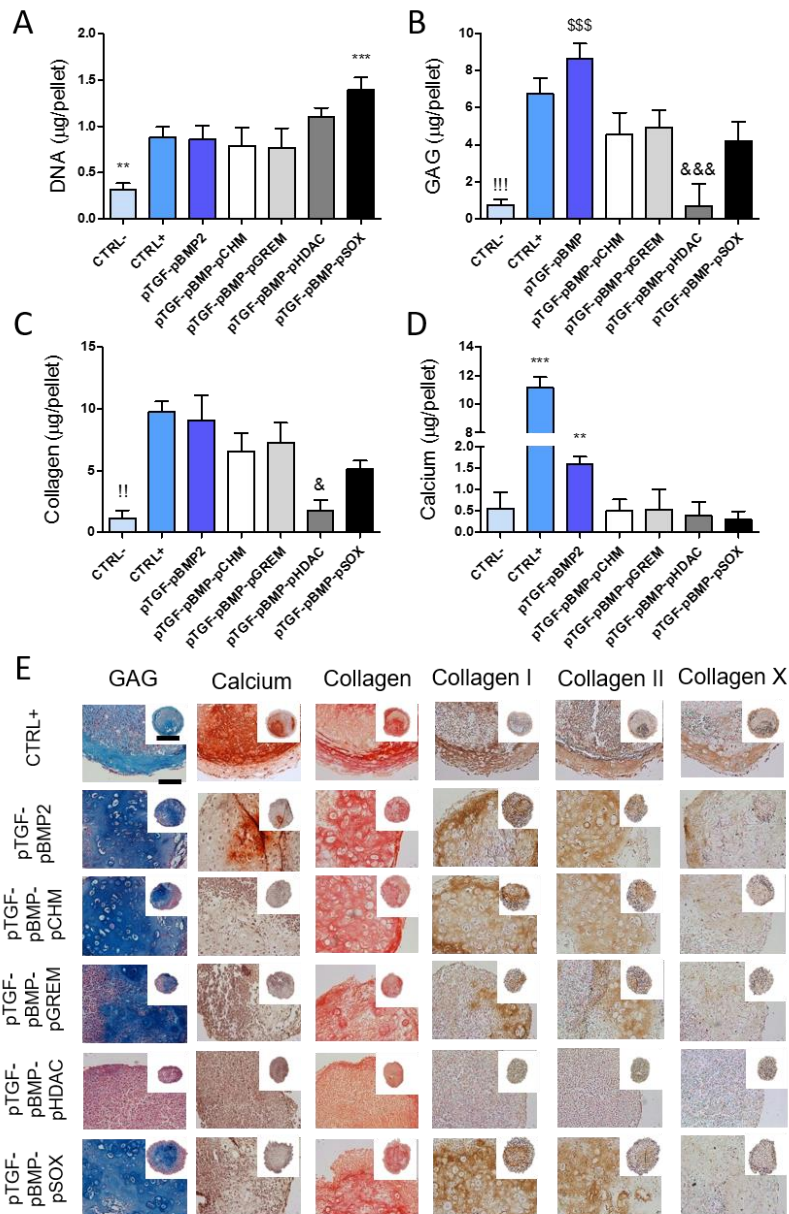
Fig.5.7. Combinatorial gene delivery of chondrogenic growth and regulatory factors to BMSCs. Total DNA (A), GAG (B), collagen (C) and Calcium (D) deposition (µg/pellet) after 28 days of in vitro culture. (E) Histological (GAG, collagen and calcium) and immunohistochemical (collagen type I, II and X) of the pellets after 28 days of in vitro culture. Scale bar = 100 µm for the 20x images and 1 mm for the 4x images. (**) Denotes significance (n=4, p<0.01) in comparison to all the groups; (***) denotes significance (n=4, p<0.001) to all the groups; (!!) denotes significance (n=4, p<0.01) in comparison to all the groups except pTGF-pBMP-pHDAC; (!!!) denotes significance (n=4, p<0.001) in comparison to all the groups except pTGF-pBMP-pHDAC; ($$$) denotes significance (n=4, p<0.001) in comparison to all the groups except CTRL+; (&) denotes significance (n=4, p<0.05) in comparison to all the groups except CTRL-. (&&&) Denotes significance (n =4, p<0.001) in comparison to all the groups except CTRL-.

5.4. Discussion

The goal of this study was to evaluate combinatorial non-viral gene delivery of chondrogenic inducers (growth factors) and regulatory factors to promote robust chondrogenic differentiation of BMSCs and to supress their tendency to progress along an endochondral pathway. The RALA peptide was selected as a non-viral vector for the transfection of BMSCs based on favourable comparisons to other established vectors performed in the previous chapter. After the RALA transfection parameters were optimised to reach high levels of transfection without compromising cell viability, the peptide was used to deliver therapeutic relevant chondrogenic factors to BMSCs. Combinatorial gene delivery of the growth factors TGF-β3 and BMP2 in hypoxic conditions was sufficient to induce chondrogenesis of BMSCs with little evidence of hypertrophy. As such ideal environmental conditions for stable chondrogenesis cannot be guaranteed *in vivo*, the effect of gene delivery of the chondrogenic regulators CHM1, GREM1, HDAC4 and SOX9 to BMSCs in normoxic culture conditions, less conducive to stable chondrogenesis, were next assessed. The delivery of these factors alone failed to promote robust chondrogenesis of MSCs, thus they were co-delivered with pTGF-β3 and pBMP2. In normoxic culture conditions, the co-delivery of pTGF-β3 and pBMP2 promoted GAG and collagen type II deposition, but it also promoted pellet mineralisation and collagen type X production. Delivery of either CHM1, GREM1 or SOX9, together with TGF-β3 and BMP2, reduced calcium and collagen type X deposition, pointing to a suppression of the endochondral phenotype in chondrogenically primed BMSCs.

Chemical-mediated non-viral gene delivery into primary cells, such as BMSCs, is characterized by low transfection efficiencies and by cell toxicity. In this study, a novel amphipathic peptide, RALA, was used for the transfection of BMSCs. RALA is a 30 amino acid peptide which, due to the presence of positively charged amino groups in the arginine residues, is able to complex to pDNA to form cationic nanoparticles capable of intracellular DNA delivery (Bennett et al., 2015; McCarthy et al., 2014). In this study, RALA-mediated pDNA delivery to BMSCs was optimized to maximize transfection and minimize cytotoxicity. One of the most important factors when using vectors with cationic amino groups is the n:p ratio, which influences the size and surface charge of

the vector-pDNA complexes. RALA-pDNA complexes produced using a n:p ratio of 10 offered the highest transfection efficiencies of around 40% 1 and 3 days after transfection, with no negative effects over cell viability in comparison to the control and complexes produced using lower ratios. McCarthy *et al.* (2014) showed 60% of transfection efficiency of NCTC-929 cells when using RALA-pDNA at n:p of 10, with nearly 100% of cell viability, compared to commercially available Lipofectamine 2000 which showed similar transfection efficiencies and a 60% decrease in cell viability (McCarthy et al., 2014). This could have been due to a smaller size and lower Z potential of the RALA-pDNA complexes when the n:p ratio was increased (McCarthy et al., 2014). The observed transfection efficiencies of around 40% are superior to previously reported MSC transfection efficiencies when using other cationic vectors such as PEI (~25%) (Tierney et al., 2013) and chitosan (~20%) (Malakooty Poor et al., 2014), and similar to those reported when Lipofectamine 2000 was used, but without the cytotoxicity associated with this vector (Curtin et al., 2012; Malakooty Poor et al., 2014). The concentration of pDNA per cm^2 was also assessed, showing the highest luciferase expression levels when the lowest concentration (0.2 $\mu g/cm^2$) was used. Higher concentrations of pDNA did not result in increased transgene expression, possibly due to a significant decrease in cell viability.

Once the transfection parameters were optimized, RALA was used to transfect BMSCs with therapeutically relevant chondrogenic factors. Gene delivery of the growth factors TGF-β3, BMP2 and BMP7 was explored to induce chondrogenesis of BMSCs, while CHM1, GREM1, HDAC4 and SOX9 were selected as regulators of chondrogenesis and endochondral ossification. After confirming effective transfection of BMSCs and transgene overexpression of all the factors, they were used alone, or in combination, in an attempt to promote stable chondrogenesis of MSCs. Recombinant protein supplementation of members of the TGF-β superfamily such as TGF-β3, BMP2 and BMP7 have been extensively explored to drive chondrogenesis of MSCs (Barry et al., 2001; Johnstone et al., 1998; Lee et al., 2008; Schmitt et al., 2003). In this study, gene co-delivery of BMP2 and TGF-β3 in hypoxia promoted stable chondrogenic differentiation of BMSCs, with higher levels of GAG and positive staining of collagen type II in comparison to the delivery of the single factors. In an early comparative study of the

effects of recombinant TGF-β3 and BMP2 supplementation on human BMSCs aggregates, both growth factors alone initiated stable BMSC chondrogenesis, but when supplemented together, higher levels of type II collagen were observed (Schmitt et al., 2003). Similar results were reported by Shen *et al.* (2009) who found that BMP2 enhanced TGF-β3 mediated chondrogenesis of BMSCs through the mothers against the DPP homolog (SMAD) and mitogen-activated protein kinase (MAPK) pathways, but that supplementation of both factors also enhanced collagen type X expression (Shen et al., 2009), a marker of chondrocyte hypertrophy. In low oxygen conditions we found that transfected MSCs did not stain positive for collagen type X, suggesting that hypertrophy and progression towards endochondral ossification was arrested. This is in agreement with previous studies that explored the use of recombinant BMP2 and/or TGF-β3 to promote chondrogenesis of MSCs in hypoxic conditions (Gómez-Leduc et al., 2017). In contrast with the stable chondrogenesis observed in the transfected groups, transient recombinant TGF-β3 supplementation for 1 week resulted in lower GAG deposition than the gene delivery of BMP2 alone or combined with either TGF-β3 or BMP7, with pellets staining positive for collagen type X, suggesting progression along an endochondral pathway as has been previously reported following recombinant TGF-β3 supplementation (Bian et al., 2011; Sheehy et al., 2012, 2013).

Despite successful overexpression of the transgene, pTGF-β3 delivery alone did not induce robust chondrogenesis of MSCs. This might be due to post-transcriptional regulation which leads to low protein levels (Fierro et al., 2011), as recombinant TGF-β3 concentrations lower than the traditionally used 10 ng/ml (Johnstone et al., 1998) have failed to promote robust chondrogenesis of BMSCs (Cals et al., 2012). Although previous studies have identified the co-delivery of recombinant TGF-β3 and BMP7 to promote chondrogenesis of MSCs (Crecente-Campo et al., 2017), we found that gene delivery of both factors in isolation or combination failed to induce chondrogenic differentiation.

As previously discussed, oxygen tension is a potent regulator of MSC chondrogenesis and endochondral ossification (Buckley et al., 2010; Sheehy et al., 2012). In a normal knee joint, the oxygen levels in articular cartilage have been reported to be between 5% and 1% (Lafont, 2010). But in diseased joints suffering from OA, vascular invasion of articular cartilage is accelerated, potentially increasing local oxygen levels

and promoting hypertrophic differentiation, subchondral bone remodeling and cartilage mineralization (Leijten et al., 2012b; Pesesse et al., 2013). Many factors, such as CHM1, GREM1, HDAC4 and SOX9, have been studied to suppress endochondral ossification by targeting diverse pathological processes. CHM1 and GREM1 are abundant proteins in superficial articular cartilage and regulate endochondral ossification by inhibiting vascular invasion and antagonizing BMP signaling respectively (Chen et al., 2016; Klinger et al., 2011; Leijten et al., 2012a; Shukunami et al., 1999). In contrast, HDAC4 and SOX9 act transcriptionally at the gene expression level, by inhibiting the expression of the transcription factor RUNX2, in the case of HDAC4 (Vega et al., 2004), and by suppressing vascularization, cartilage resorption and trabecular bone formation (due to the transcriptional inhibition of VEGF, RUNX2 and MMP13 expression) in the case of SOX9 (Hattori et al., 2010b). In the present study, the overexpression of these factors alone failed to induce robust chondrogenesis of BMSC aggregates. Although BMSCs transfected with GREM1, HDAC4 and SOX9 showed significantly higher levels of GAG deposition in comparison to non-transfected and GFP transfected controls, no positive staining for collagen type II was observed. In previous reports, adenoviral transduction of BMSCs with the CHM1 and SOX9 genes was shown to be sufficient to enhance aggrecan and collagen type II expression without the use of other stimuli (Cao et al., 2011; Chen et al., 2016), suggesting that the non-viral delivery of these factors, as in this study, is not sufficient to drive BMSC chondrogenesis. Other studies have reported that gene delivery of CHM1 alone to progenitor cells was not able to upregulate the expression of SOX9 or collagen type II *in vitro* (Klinger et al., 2011; Xing et al., 2015), and that gene delivery of SOX9 to MSCs *in vitro* resulted in levels of GAG deposition and collagen type II expression similar to those in GFP transfected controls (Liao et al., 2014). To the best of our knowledge, HDAC4 and GREM1 gene delivery has not been reported to be able to initiate chondrogenesis of MSCs. Adenoviral gene delivery of HDAC4 failed to drive chondrogenesis of MSCs, but when recombinant TGF-β1 was supplemented in the media, HDAC4 transduced cells expressed higher levels of collagen type II with increased deposition of GAGs (Pei et al., 2009). Recombinant supplementation of the GREM1 protein after 3 weeks of TGF-β3 mediated MSC differentiation has previously been shown to reduce ALP and collagen type X expression and mineralization, but also GAG deposition (Leijten et al., 2012a).

Chondrogenic differentiation and progression along an endochondral pathway are complex processes involving the action of multiple factors. The overexpression of a single factor might not be enough to develop a successful strategy for engineering functional, phenotypically stable articular cartilage. Therefore, it was hypothesized that the combined gene delivery of chondrogenic and regulatory factors could induce chondrogenesis of MSCs and suppress terminal endochondral differentiation. To this end, RALA-mediated gene co-delivery of TGF-β3 and BMP2 was combined with pDNAs encoding for the hypertrophy regulators CHM1, GREM1, HDAC4 and SOX9. To challenge the potential of this strategy to drive robust chondrogenesis and suppress hypertrophy, transfected cell pellets were cultured *in vitro* at 20% pO_2 for 28 days. After the culture period, co-delivery of TGF-β3 and BMP2 induced chondrogenesis of BMSCs but also promoted collagen type X deposition and tissue mineralization. In contrast, the co-delivery of these growth factors together with either CHM1, GREM1 or SOX9 suppressed mineralization and collagen type X deposition, however this was accompanied by a small decrease in GAG deposition. This might be explained, at least in part, by the fact that genes involved in the terminal differentiation of MSCs have also been identified as chondrogenic regulators. The osteoblastic transcription factor RUNX2, the expression of which has been shown to be directly downregulated by the action of CHM1 (Zhang et al., 2016), SOX9 (Cao et al., 2011) and HDAC4 (Vega et al., 2004), and indirectly by GREM1 (Leijten et al., 2012a), has been reported to be present at the initiation of MSC chondrogenesis (Musumeci et al., 2014), and Indian hedgehog (IHH)-mediated upregulation of RUNX2 has been shown to be necessary to initiate chondrogenesis of MSCs (Kim et al., 2013). Thus, temporal control of gene delivery to overexpress regulatory factors in the later stages of chondrogenesis might be preferable strategy. In the case of GREM1 overexpression, as a BMP antagonist, this protein could have hindered the effects of BMP2 overexpression which was integral to initiating chondrogenesis in this study. Combined gene delivery of TGF-β3, BMP2 and HDAC4 failed to induce chondrogenesis of MSCs, suggesting HDAC4 expression may be important for initiating chondrogenesis.

5.5. Conclusion

In conclusion, combinatorial gene delivery of growth and regulatory factors was able to promote stable chondrogenesis of MSCs after 4 weeks of *in vitro* culture in normoxia, demonstrating decreased mineralisation and collagen type X deposition in comparison to the co-delivery of the TGF-β3 and BMP2 genes and transient recombinant growth factor media stimulation. These results also confirm that RALA peptide-mediate gene delivery is a rapid and simple way for the simultaneous delivery of different pDNAs encoding for diverse chondrogenic factors to primary BMSCs, which could be of therapeutic importance for the treatment of cartilage defects and to limit or prevent progression towards OA.

In this chapter, the third objective of this thesis was assessed. RALA-mediated gene delivery was selected, based in the results from previous chapter, to drive chondrogenesis of MSCs. RALA-mediated transfection of MSCs was optimised and the best gene combinations for stable chondrogenic differentiation were identified. Also, the best culture conditions for chondrogenesis of MSCs were assessed, with hypoxia found to enhance cartilage specific matrix deposition and to prevent progression along an endochondral pathway. The results of this chapter will be used in following chapters to effectively drive chondrogenesis of MSCs in the cartilage layer of a multiphasic ostechondral construct.

CHAPTER 6

3D Bioprinting of PCL Reinforced Gene Activated Bioinks for Bone Tissue Engineering

Abstract

Regeneration of complex bone defects remains a significant clinical challenge. Multi-tool biofabrication has permitted the combination of various biomaterials to create multifaceted composites with tailorable mechanical properties and spatially controlled biological function. In this study we sought to use bioprinting to engineer non-viral gene activated constructs reinforced by polymeric micro-filaments. A gene activated bioink was developed using RGD-γ-irradiated alginate and nano-sized particles of hydroxyapatite (nHA) complexed to plasmid DNA (pDNA). This ink was combined with bone marrow-derived mesenchymal stem cells (MSCs) and then co-printed with a polycaprolactone (PCL) supporting mesh to provide mechanical stability to the construct. Reporter genes were first used to demonstrate successful cell transfection using this system, with sustained expression of the transgene detected over 14 days post bioprinting. Delivery of a combination of therapeutic genes encoding for BMP2 and TGF-β3 promoted robust osteogenesis of encapsulated MSCs *in vitro*, with enhanced levels of matrix deposition and mineralisation observed following the incorporation of therapeutic pDNA. These results validate the use of a gene activated bioink to impart biological functionality to 3D bioprinted constructs.

6.1. Introduction

While in previous chapters we focused on the identification of an appropriate vector and gene combination to promote stable chondrogenesis of MSCs, the reported nHA osteoinductive capacity was leverage in this chapter to promote endochondral bone formation *in vivo*. Also, alginate, that was able to support chondrogenesis and osteogenesis of MSCs in the first experimental chapter, was used as 3D printable bioink to support nHA-mediated gene delivery. Therefore, in this chapter the fourth objective of this thesis was addressed: to investigate the use of alginate hydrogels as gene activated bioinks for the 3D printing of mechanically robust constructs for bone TE which can be relevant for the regeneration of the subchondral bone layer in an osteochondral defect

Tissue engineering and regenerative medicine approaches can be augmented through the strategic use of gene therapy (Evans, 2014). Non-viral gene delivery can facilitate endogenous expression of desired therapeutic proteins, which can provide a stimulus to cells, resulting in enhanced levels of matrix production and tissue formation (Li and Huang, 2007; Santos et al., 2011). As demonstrated in chapter 1, nanohydroxyapatite (nHA) based cell transfection has been shown to be a safe and easy technique capable of yielding robust osteogenesis following administration of plasmid DNA (pDNA) encoding for relevant proteins, such as bone morphogenic protein (BMP2) and transforming growth factor (TGF-β3). Despite a relatively low transfection efficiency, nHA-pDNA complexes have been shown to be proficient at inducing a sustained expression of target proteins, both in 2D culture and when incorporated into 3D constructs to form gene activated matrices (Choi et al., 2013; Curtin et al., 2012). However, to address the need for regenerating larger and challenging anatomical defects, emerging methods such as 3D bioprinting may be required to generate suitably complex solutions (Daly et al., 2016b, 2017; Melchels et al., 2016; Murphy and Atala, 2014). An effective gene activated bioink could be integrated into such a biofabrication approach to provide biological functionality to a composite construct.

The degree of customised control offered by 3D bioprinting has enabled the production of scaled up, mechanically reinforced materials for musculoskeletal tissue engineering (Malda et al., 2013; Visser et al., 2015). Another attractive feature of this spatial control is the ability to deposit specific biological cues in relevant locations, to drive complex tissue formation (Cooper et al., 2010). An efficient gene activated bioink would be particularly beneficial in this regard as successful cell transfection could produce localised, sustained protein expression; something that is not as easily achieved through the use of growth factors as they can diffuse easily and cause non-localised effects (Bonadio et al., 1999). Calcium phosphate has been successfully used as a delivery vector within a 3D bioprinted alginate hydrogel previously, leading to elevated BMP2 expression and ALP production *in vitro* (Krebs et al., 2010; Loozen et al., 2013). However, no bone formation was observed after six weeks following subcutaneous implantation of this approach. In addition, more demanding defects such as load bearing bone defects may require more mechanical integrity than can be provided by a gene activated hydrogel alone (Billiet et al., 2012). Hydrogels have previously been combined with various polymeric support structures in order to fabricate composite materials with both biological and mechanical functionality (Boere et al., 2014; Xu et al., 2013). These constructs are typically cell-laden and cultured *in vitro* to engineer a mature tissue which can promote bone repair following implantation (Daly et al., 2016b; Schuurman et al., 2013). The inclusion of a gene activated bioink may permit the bioprinting of a material that can be implanted directly post fabrication, inducing sustained therapeutic protein expression *in vivo* and hence accelerating regeneration.

In this work we developed a gene activated bioink by combining a printable alginate hydrogel with nHA-pDNA complexes and co-printing this ink with a reinforcing polycaprolactone (PCL) scaffold to produce a gene activated 3D construct. Bone marrow-derived mesenchymal stem cells (MSCs) were combined with the bioink directly before printing. The capacity of this strategy to successfully transfect MSCs was first assessed using reporter genes, before utilizing a combination of therapeutic genes encoding for BMP2 and TGF-β3 in an attempt to induce osteogenesis of MSCs *in vitro*. The developed approach could potentially be used at the point of care to develop personalised gene activated implants for treating complex bone defects.
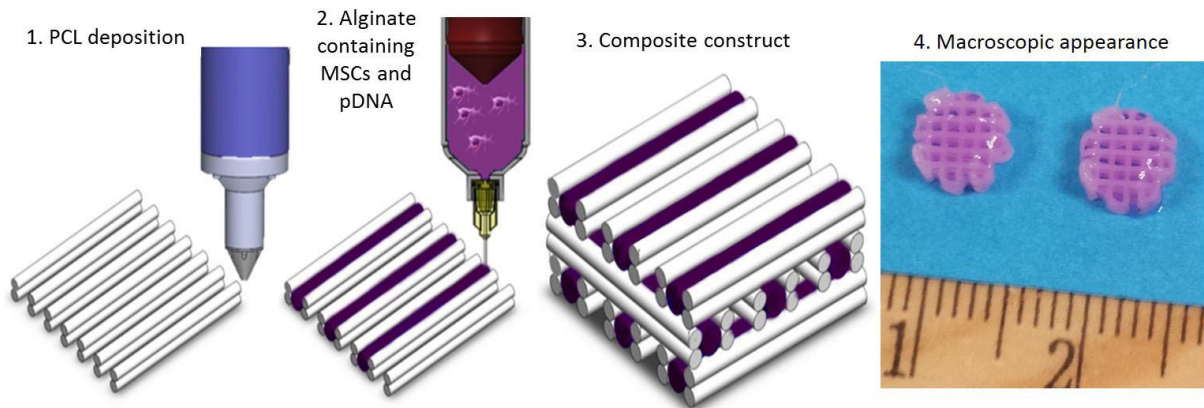
Fig.6.1. Schematic representation of the bioprinting process, with co-deposition of PCL and the gene activated bioink comprising of alginate, nHA-pDNA complexes and MSCs, and the macroscopic appearance of the constructs prior to implantation.

6.2. Materials and methods

6.2.1. Plasmid propagation

Four different plasmids were used in the current study: two plasmids encoding for the reporter genes red fluorescent protein (pRFP, also called pTomato, kind donation from Prof. Gerhart Ryffel through Addgene) and luciferase (pLUC, pGaussia luciferase; New England Biolabs, Massachusetts, USA), and another two encoding for the therapeutic genes BMP2 (kind donation from Prof. Kazihusa Bessho, Kyoto University, Japan) and TGF-β3 (InvivoGen, Ireland). Plasmid amplification was performed by transforming chemically competent E-coli bacterial cells (One Shot TOP10; Biosciences, Ireland) according to the manufacturer's protocol. The transformed bacteria were cultured on LB plates with 100 mg/L ampicillin (Sigma-Aldrich, Ireland) as the selective antibiotic for the four plasmids. Bacterial colonies were harvested and inoculated in LB broth (Sigma-Aldrich, Ireland) and incubated overnight for further amplification. The harvested bacterial cells were then lysed, and the respective pDNA samples were purified using Qiagen plasmid kit (MaxiPrep Kit; Qiagen, Ireland). Nucleic acid concentration (ng/μl) was determined by analyzing the 260:280 ratio and 230 nm measurement using NanoDrop spectrophotometer (Labtech International, Uckfield, UK).

6.2.2. Preparation of nano hydroxyapatite (nHA)-pDNA complexes

The synthesis of the nano hydroxyapatite (nHA) particles was performed as previously described (Cunniffe et al., 2010). Briefly, a solution of 12 mM sodium phosphate (Sigma-Aldrich, Ireland), containing 0.017% DARVAN 821A (RTVanderbilt, Norwalk, USA) was added to an equal volume of a 20 mM chloride solution (Sigma-Aldrich, Ireland) and filtered through a 0.2 mm filter (Curtin et al., 2012). nHA-pDNA complexes were prepared by adding 1845 µl of the nHA solution to 125 µg of pBMP2 (in 250 µl), and 125 µg of pTGF-β3 (in 105 µl) pre-treated with 300 µl 250 mM CaCl$_2$ (Sigma-Aldrich, Ireland). This 2.5 ml solution was then added to 50 x 10^6 MSCs and alginate as described below.

6.2.3. Gene activated bioink

Low molecular weight sodium alginate (γ alginate, 58 000 g mol−1) was prepared by irradiating sodium alginate (Protanal LF20/40, 196 000 g/mol, Pronova Biopolymers, Oslo, Norway) at a gamma dose of 5 Mrad, as previously described (Alsberg et al., 2003). RGD-modified alginates were prepared by coupling the GGGGRGDSP to the alginate using standard carbodiimide chemistry. Briefly, 10 g alginate was dissolved in 1 L MES Buffer (0.1 M MES, 0.3 M NaCl, and pH 6.5). 274 mg sulfo-NHS (Pierce, Rockford, IL), 484 mg EDC (Sigma), and 100 mg GGGGRGDSP peptide (AIBioTech, Richmond, VA) were then added into alginate solution. The reaction was stopped by addition of hydroxylamine (0.18 mg/ml, Sigma), and the solution was purified by dialysis against ultrapure deionized water (MWCO 3500, Spectrum Laboratories Inc., Rancho Dominguez, CA) at 4 °C for 3 days, treated with activated charcoal (5 g/L, 50-200 mesh, Fisher Scientific Inc., Pittsburgh, PA) for 30 min, filtered (0.22 µm filter) and lyophilized (Jeon et al., 2010).

Bone marrow-derived MSCs were isolated from the femoral shaft of 4 month old pigs and expanded to passage 2 in standard culture media (high glucose Dulbecco's modified eagle's medium GlutaMAX (hgDMEM), 10% (v/v) foetal bovine serum (FBS), 100 U mL^{-1} penicillin per 100 µg mL^{-1} streptomycin) prior to transfection. The nHA-pDNA complexes (2.5 ml) were prepared immediately before transfection, and added to a suspension of MSCs in 1 ml of standard expansion media. After 1 h of incubation,

alginate was added to the cells and nHA-pDNA complexes to yield a final volume of 5 mls, containing a concentration of 10 million cells/ml in 1% alginate. Then the solution was mixed until a homogenous mixture was obtained.

6.2.4. Bioprinting gene activated constructs

Gene activated polymer/bioink scaffolds were fabricated using the 3D Discovery multi-head bioprinting system (Regen HU, Switzerland). The 3D Discovery was set up to allow for co-printing of a pneumatic driven syringes containing the bioinks alongside a fused deposition modeler (FDM) allowing for deposition of molten polycaprolactone (PCL, Sigma, Mn 45 000). First the RGD-γ alginate bioink was dissolved at 3.5 wt% and mixed thoroughly using a luer lock system with the MSCs in either nHA solution (nHA alone control) or the nHA-pDNA complexes (both containing 50 mM $CaCl_2$) to yield a gene activated bioink with 1% final alginate concentration [41]. To ensure homogeneity the suspension was mixed between syringes 25 times. The gene activated bioink solution was loaded into the pressure driven piston system and co-printed alongside PCL melted at 60°C (Fig.6.1). A pressure of 0.2 MPa and a 25 Gauge needle were used to deposit the bioink strands, using an orthogonal 90 degree angle print pattern to build the constructs to the pre-designed height. Following this, the constructs were immersed in a 100 mM $CaCl_2$ solution for 15 min to fully crosslink the bioink. The 3D Discovery was operated within a laminar flow hood to ensure sterility throughout the biofabrication process.

Constructs of dimensions 10 x 2 mm (diameter x height) were printed for *in vitro* evaluation. *In vitro* analysis was conducted over 28 days in either control medium (high glucose Dulbecco's modified eagle's medium GlutaMAX (hgDMEM), 10% (v/v) foetal bovine serum (FBS), 100 U mL^{-1} penicillin per 100 µg mL^{-1} streptomycin) or osteogenic culture conditions (high glucose Dulbecco's modified eagle's medium GlutaMAX (hgDMEM), 100 nM dexamethasone, 10 mM β-glycerol phosphate, and 0.05 mM ascorbic acid (all from Sigma-Aldrich, Ireland) at 20% oxygen.

6.2.5. Live/dead confocal microscopy

Cell viability was assessed 24 h after bioprinting using a LIVE/DEAD viability/cytotoxicity assay kit (Invitrogen, Bio-science, Ireland). Briefly, constructs were cut in half, washed in PBS followed by incubation for 1 h in PBS containing 2 µM calcein AM (green fluorescence of membrane for live cells) and 4 µM ethidium homodimer-1 (red fluorescence of DNA for dead cells). Sections were again washed in PBS, imaged at magnification ×10 with an Olympus FV-1000 Point-Scanning Confocal Microscope (Southend-on-Sea, UK) at 515 and 615 nm channels and analysed using FV10-ASW 2.0 Viewer software. Live/dead-based semi-quantification on n≥4 separate regions, chosen at random, was carried out using Image J.

6.2.6. Biochemical analysis

To perform biochemical analysis, constructs were digested with papain (125 mg/mL, pH 6.5) in 0.1 M sodium acetate, 5 nM L-cysteine HCl, and 0.05 M EDTA (all Sigma-Aldrich, Ireland) at 60 °C under constant rotation for 18 h. Calcium content was determined using a Sentinel Calcium Kit (Alpha Laboratories Ltd, UK) after digestion in 1 M HCl at 110 °C for 48 h. Proteoglycan content was estimated by quantifying the amount of sulfated glycosaminoglycan (sGAG) in the constructs using the dimethylmethylene blue (DMMB) dye-binding assay (Blyscan, Biocolor Ltd. Northern Ireland), with a chondroitin sulfate standard. Total collagen content was determined by measuring the hydroxyproline content. Samples were hydrolyzed at 110 °C for 18 h in concentrated HCl 38%, allowed to dry, and analyzed using a chloramine-T assay (Hollander and Hatton, 2003) with a hydroxyproline-to-collagen ratio of 1:7.69 (Ignat'eva et al., 2007). Four samples per group were analyzed for each biochemical assay.

6.2.7. Reporter gene detection

RFP expression was detected using Leica SP8 scanning confocal microscope (Leica Microsystems, Ireland) 24 hours post bioprinting. Luciferase expression was imaged using a real time bioluminescence imaging system (PhotonImager, Biospace lab, France) to visualise the spatial distribution of luminescence over time. Luciferase

expression in the culture media was also quantified using a Pierce Gaussia Luciferase Flash Assay Kit (ThermoFisher, Ireland) at different time points up to 14 days.

6.2.8. Micro-computed tomography

Micro-computed tomography (microCT) scans were performed using a Scanco Medical 40 microCT system (Scanco Medical, Bassersdorf, Switzerland) with a 70 kVp X-ray source at 114 µA. N=3 samples were scanned and analysed at a threshold of 100, corresponding to 120.81 mg hydroxyapatite/cm^3 for the *in vitro* study. Reconstructed 3D images were generated from the scans and used to visualise mineral distribution throughout the constructs.

6.2.9. Statistical analysis

Statistical analysis was carried out using GraphPad software. The results are reported as means ± standard deviation and groups were analysed using Student's two-tailed t-tests or by a general linear model for analysis of variance with groups of factors. Tukey's post-hoc test was used to compare conditions. Significance was accepted at a level of $p < 0.05$.

6.3. Results

6.3.1 Gene activated bioinks support sustained expression of reporter genes following co-printing with PCL filaments

To establish that the gene activated bioink would remain functional following 3D bioprinting with a PCL support structure, reporter genes (pLUC and pRFP) were utilised to validate successful transfection of MSCs encapsulated within the bioinks at the time of bioprinting. The viability of MSCs printed within the gene activated bioink was not affected by the presence of the pDNA encoding for luciferase, however, some cell death was observed due to co-printing the cell-laden bioink with PCL (nHA-alone 64 ± 10%, nHA-pLUC 69 ± 2%, Fig.6.2, Fig.A.3). By 14 days, the DNA content remained at the same

level as that quantified at day 1 and almost 100% of cells within the construct were observed to be viable using live/dead staining.
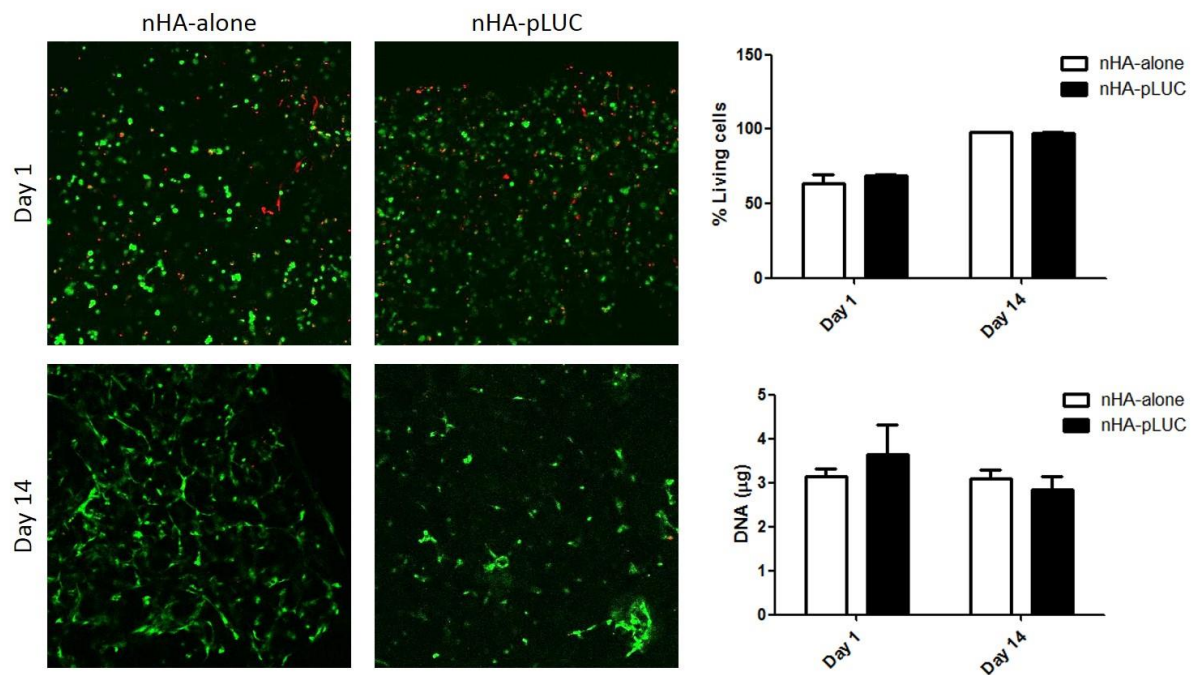
Fig.6.2. Cell viability is maintained following pDNA incorporation. Live/dead images demonstrate the presence of viable cells (green) at both day 1 and day 14 post bioprinting, while quantification of DNA indicated no difference between groups cultured with or without pDNA encoding for luciferase.

Reporter gene analysis using red fluorescent protein (RFP) and luciferase indicated that successful transfection of bioprinted MSCs was achieved within the gene activated bioink (Fig.6.3). RFP was observed 24 hours post bioprinting using fluorescent microscopy to provide an initial validation of successful pDNA uptake and protein expression. Luciferase was then employed to investigate temporal expression of a reporter protein. Luciferase was found to increase in expression over 14 days of culture, as assessed both by quantifying the luciferase expressed and released into the media (Fig.6.3.B) and qualitatively by imaging the protein remaining within the constructs (Fig.6.3.C).
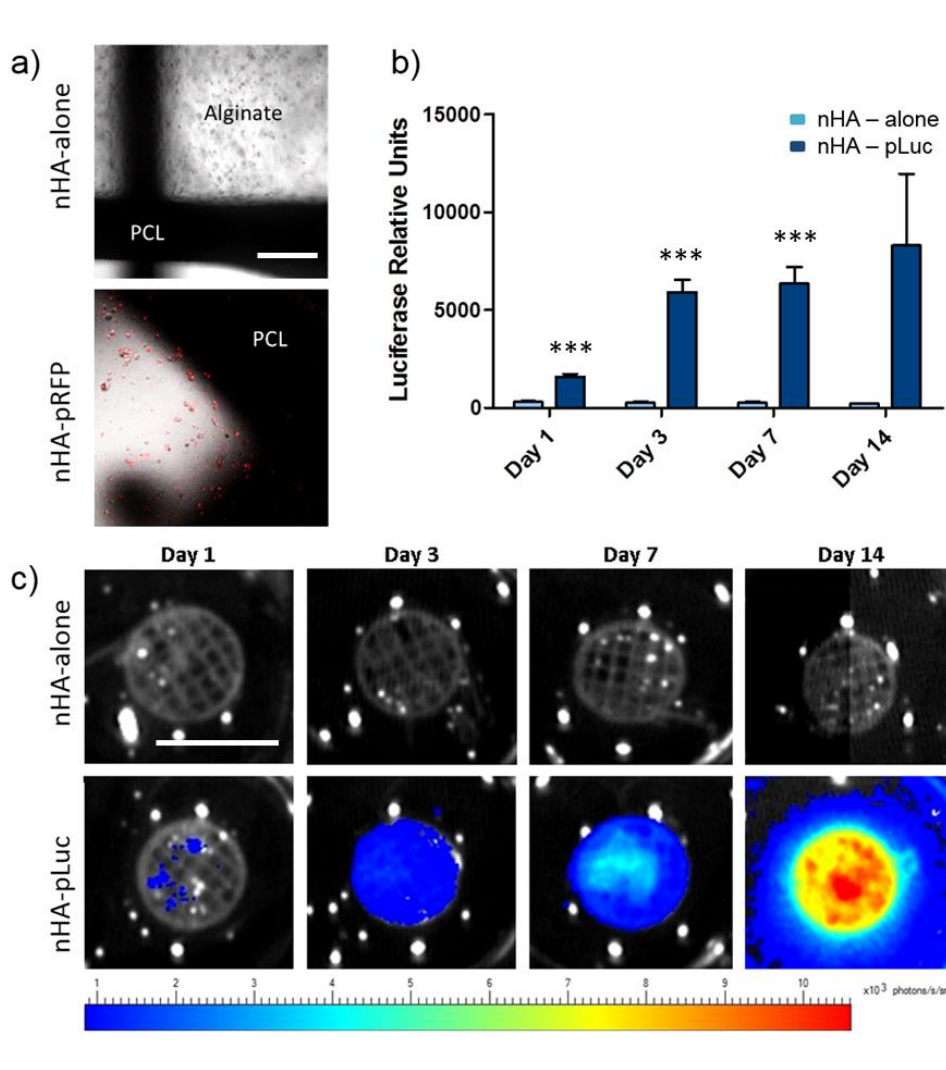
Fig.6.3. (A) Positive expression of red fluorescent protein (RFP) was detected 24 hours post bioprinting. Scale bar = 200 μm. (B, C) Luciferase expression was quantified and imaged for 14 days post bioprinting, demonstrating a sustained and increasing expression profile over time. Scale bar = 10 mm. (***p<0.001).

6.3.2 Therapeutic gene delivery enhanced osteogenesis of MSCs *in vitro*

Following validation of successful transfection using reporter genes, a combination of therapeutic genes encoding for BMP2 and TGF-β3 was incorporated into the bioink system. These combinations of genes were chosen as delivery of recombinant BMP2 and TGF-β protein from MSC-laden alginate hydrogels has previously been shown to promote bone formation *in vivo* (Simmons et al., 2004). Constructs were bioprinted and cultured for 28 days in either control medium or osteogenic culture conditions. Macroscopically, evidence of matrix deposition can be observed in all groups at this time

point relative to constructs at day 0 (Fig.6.4). Biochemical quantification indicated that significantly higher levels of DNA and deposition of glycosaminoglycan (GAG) and collagen was achieved in both culture conditions following inclusion of pDNA within the bioink. Live/dead quantification at day 1 and day 14 for the constructs transfected with therapeutic genes (Fig.A.3) had not indicated any differential response in DNA content between the transfected and non-transfected control groups.
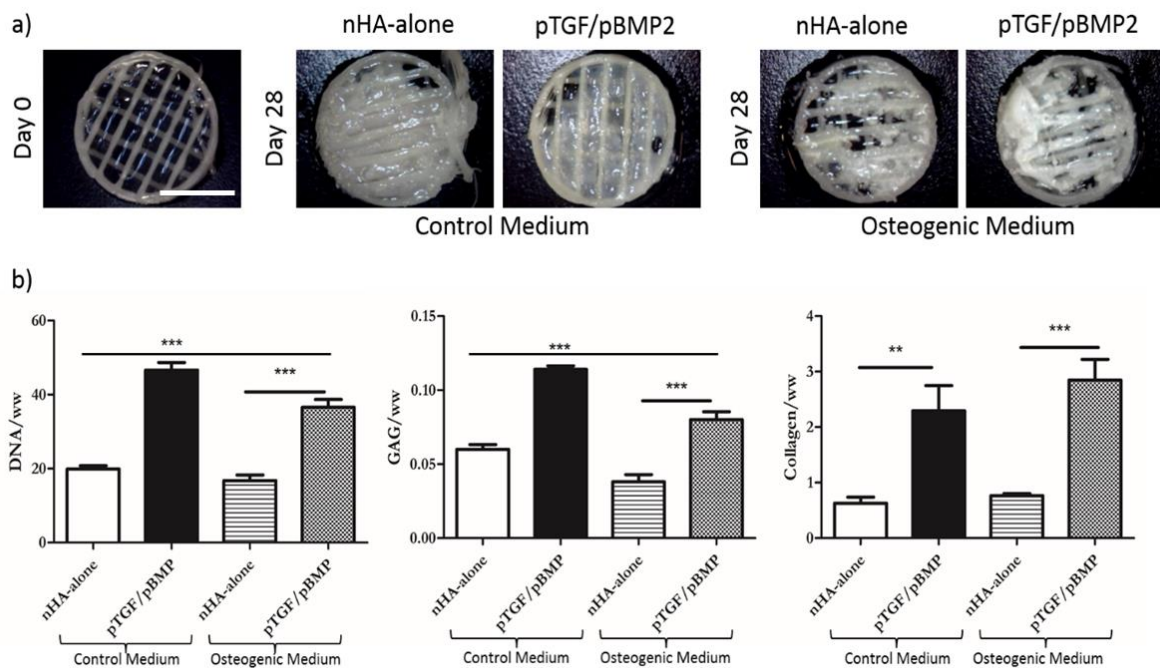
Fig.6.4. (A) Macroscopic appearance of bioprinted constructs immediately post bioprinting, and following 28 days in either control or osteogenic media. Scale bar = 5 mm. (B) Biochemical analysis revealed significantly higher levels of DNA in addition to glycosaminoglycan (GAG) and collagen deposition was achieved following pDNA incorporation vs. nHA-alone controls. (**p<0.01, ***p<0.001).

Upon quantification of calcium content, the matrix was found to be mineralised, indicating the onset of osteogenesis (Fig.6.5). Significantly higher levels of mineral deposition were observed within the pDNA containing bioinks in control medium, and this effect was greatly amplified following culture in osteogenic supplemented medium. 3D reconstructed microCT images demonstrated the homogeneity of the mineral distribution throughout the cultured constructs.
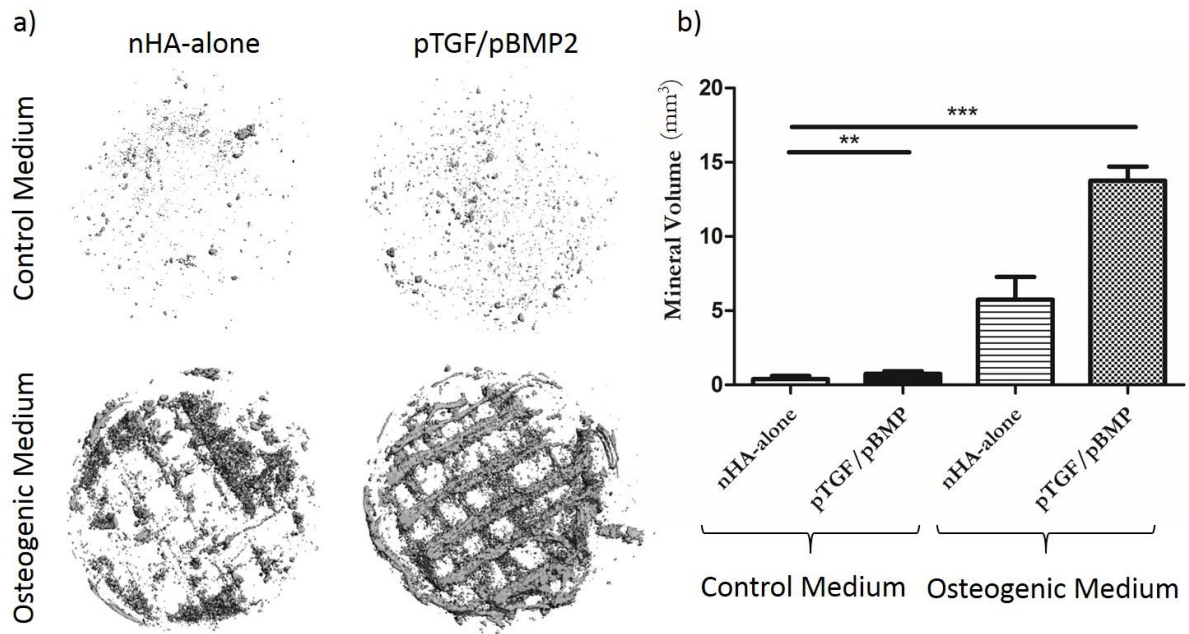
Fig.6.5. (A) 3D reconstructed images and (B) quantification of mineral deposition over 28 days in vitro demonstrating superior deposition was detected in the pDNA containing groups. (**p<0.01, ***p<0.001).

6.4. Discussion

This study describes the successful development of a gene activated bioink capable of transfecting mesenchymal stem cells post 3D bioprinting. These MSC-laden bioinks were co-deposited alongside a reinforcing PCL network to produce composite constructs suitable for bone tissue engineering applications. Reporter genes indicated that protein expression was detected after 24 hours and that protein expression could be sustained, and in fact continued to increase, over 14 days of *in vitro* culture. Transfection with therapeutic genes encoding for BMP2 and TGF-β3 promoted enhanced osteogenesis *in vitro* compared to non-transfected controls containing only the nHA vector, implying that this gene activated bioink system could induce the expression of biologically functional proteins. These findings support the continued development of 3D printed gene activated scaffolds as putative 'point-of-care' treatment options for a range of musculoskeletal defects.

184

The choice of material for the gene activated bioink was motivated by a number of factors, including the printability of the alginate hydrogel, the presence of the RGD ligand to allow cell spreading, the ability to facilitate calcium phosphate based gene delivery and established capacity to enable the osteogenic differentiation of MSCs (Cunniffe et al., 2015a; Daly et al., 2016b; Krebs et al., 2010; Kundu et al., 2015; Wegman et al., 2011). Previous studies from our lab have demonstrated that reinforcement of MSC-laden alginate hydrogels with printed PCL microfibers results in dramatic improvements in the mechanical properties of the construct (Daly et al., 2016b). Polymeric scaffolds are typically inert and may require supplementation with various factors in order to induce a favourable biological response, often provided through the addition of extracellular matrix components, or exogenous growth factors (Pati et al., 2015; Sadr et al., 2012; Shim et al., 2014). A number of publications have also reported superior biological activity solely due to the addition of alginate hydrogel to PCL scaffolds (Kim and Kim, 2015). Furthermore, alginate has a tunable degradation rate, tailorable mechanical properties, and already has FDA approval for other indications (Jeon et al., 2010).

The temporal production of gene product observed over 14 days of culture clearly demonstrates the potential of this gene activated bioink approach for sustained therapeutic protein delivery, especially when compared to the burst release profiles typically observed with traditional growth factor delivery hydrogels. By employing the cells themselves to express the desired protein, limitations with protein delivery including rapid degradation of potentially supra-physiological, toxic doses, and dispersion of the drug to dangerous locations can be overcome (Wegman et al., 2013). The bioprinting process itself, or the fact that the bioinks were co-deposited alongside molten PCL, does not seem to detract from the ability of the non-viral delivery vector nHA to successfully transfect cells. In fact, the intensity of luciferase signal increased over 14 days of culture, suggesting sustained transfection of encapsulated MSCs following the bioprinting process.

Having demonstrated it was possible to bioprint gene activated constructs reinforced by a network of PCL micro-filaments, the capacity of this system to promote MSC differentiation along the osteogenic pathway was then tested. Alginate is

commonly used as a biomaterial in bone regeneration strategies (Lee and Mooney, 2012; Sheehy et al., 2014a), and more recently has been used as a bioink for bone and cartilage bioprinting (Daly et al., 2017). In the absence of osteogenic supplements, the co-delivery of BMP2 and TGFβ3 pDNA within these MSC-laden alginate bioinks resulted in the deposition of a mineralised matrix, with the differences compared to non-transfected controls becoming particularly apparent when cultured in osteogenic conditions. The nHA particles used to deliver the plasmids may be providing an osteogenic stimulus, although the concentration used to deliver pDNA is relatively low compared to that used previously to induce mineralisation (Cunniffe et al., 2015a; Curtin et al., 2015). Furthermore, it has previously been shown that while nHA transfects cells with lower efficiencies to other vectors, its use still promotes higher overall levels of osteogenesis (Curtin et al., 2015). Previously in the first experimental chapter, we observed that nHA-mediated delivery of TGF-β3 and BMP2 in an alginate hydrogel promoted a more chondrogenic rather than osteogenic stimulus. This may be explained by the conditions (normoxia and osteogenic media) and the RGD modification of the alginate which we implemented in this study to promote direct osteogenic differentiation of encapsulated MSCs. Therefore, in the basal (control) medium, gene delivery may be promoting a more endochondral phenotype compared to a more intramembranous phenotype in the osteogenic media, although further studies are required to confirm this. Regardless, these findings support the use of alginate hydrogels containing pDNA-nHA complexes as gene activated bioinks for bone tissue engineering. These results also agree with previous *in vivo* studies delivering a combination of BMP2 and TGF-β3, either as recombinant proteins or through the use of gene delivery (Oest et al., 2007; Simmons et al., 2004).

6.5. Conclusion

The treatment of challenging fractures and large osseous defects presents a formidable clinical problem. Multi-tool biofabrication has permitted combination of various materials to create complex composite implants with tailorable mechanical properties and spatially controlled biological function. This study validated the efficiency

of a gene activated bioink to induce cell transfection within a 3D bioprinted PCL-bioink composite construct. Sustained protein expression was achieved for up to 14 days post bioprinting, and the combined delivery of the therapeutic genes BMP2 and TGF-β3 led to enhanced osteogenesis of MSCs *in vitro.* These results demonstrate an effective platform technology to enrich biofabrication techniques with gene activated bioinks for musculoskeletal applications.

In the following final experimental chapter, nHA-mediated gene delivery in alginate hydrogels was used as osteogenic layer in a bi-phasic osteochondral construct to spatially promote osteogenesis, mineralisation and vascularisation of encapsulated MSCs.

CHAPTER 7

Pore-forming bioinks to enable spatiotemporally defined non-viral gene delivery for osteochondral tissue engineering

Abstract

The regeneration of complex tissues and organs remains a major clinical challenge. With a view towards bioprinting such tissues, we developed a new class of pore-forming bioink to spatially and temporally control the presentation of therapeutic genes within bioprinted tissues. By blending sacrificial and stable hydrogels, we were able to produce bioinks whose porosity increased following printing. When combined with complexes of plasmids and cell penetrating peptides, these bioinks supported enhanced non-viral gene transfer to stem cells *in vitro*, and *in vivo* facilitated accelerated transfection of either host or transplanted cells. To demonstrate the utility of these bioinks for engineering spatially complex tissues, they were next used to spatially position stem cells and plasmids encoding for BMP2 only (*osteo* region) or a combination of TGF-β3, BMP2 and SOX9 (chondral region) within networks of printed thermoplastic fibers to produce mechanically reinforced osteochondral constructs. *In vivo*, these printed tissues supported the development of a vascularized, bony tissue overlaid by a layer of stable cartilage. When combined with multiple-tool biofabrication strategies, these gene-activated bioinks can enable the bioprinting of a wide range of spatially complex tissues.

In this final chapter, the final two objectives of this thesis were addressed. Gene delivery in alginate-methylcellulose hybrid gels were explored to develop gene activated pore-forming bionks for enhanced gene delivery, and the capacity of these constructs to support cartilage and bone development was assessed *in vitro* and *in vivo*. Also, the optimization of gene carrier, gene combination and bulk material developed in previous chapters, together with these pore-forming hydrogel bioinks, were used to engineer a biphasic mechanically robust gene activated construct for zonal differentiation of MSCs and recapitulation of compositional gradients present in osteochondral tissue.

7.1. Introduction

Tissue engineering has been shown successful for the regeneration of simple tissues, but the engineering of complex tissues and organs, such as the osteochondral unit, remains challenging. 3D bioprinting of cells and growth factors could be a potential solution, as this approach offers fine layer-by-layer spatial control of cells, regulatory factors and biomaterials. Delivery of biological cues at specific locations may allow for phenotypic regulation of host and transplanted cells and guide tissue and organ regeneration (Chen et al., 2010). However, the presentation of signaling molecules such as growth factors, can be challenging as hydrogels commonly used as bioinks show diffusive transport characteristics (Daly et al., 2017). Additionally, monolithic polymeric networks possess burst release kinetics (Huang and Brazel, 2001), limiting the drug availability in the site of injury and its therapeutic effect. Furthermore, in order to overcome these limitations, the use of high concentrations of these factors is needed, which might cause cytotoxicity and undesired side-effects (Chen et al., 2010; Kearney and Mooney, 2013).

Engineering cells to locally produce growth and transcription factors through gene delivery may enable a more precise spatial control within 3D printed constructs (Daly et al., 2017). Also, genetic modification allows for cell-mediated expression of proteins with authentic post-translational modifications and increased biological activity in comparison to their recombinant counterparts (Evans, 2014). Different approaches have been explored in order to apply gene therapy into regenerative medicine. *Ex vivo* gene transfer of cells and subsequent transplantation *in vivo* within a 3D scaffold has been shown to offer high levels of protein expression over prolonged periods of time (Glass et al., 2014; Madry et al., 2012; Venkatesan et al., 2013). However, this strategy is limited by the survival of the transfected cells and their immobilization at the site of action (Capito and Spector, 2007). In contrast, the incorporation of the gene of interest and its delivery vector into a biodegradable scaffold, to form a gene activated matrix (GAM), offers a promising platform for localized and sustained gene delivery to transplanted and host cells for the repair of orthopaedic tissues *in situ*. Hydrogel-based materials extensively used in additive manufacturing, such as alginate (Loozen et al., 2013; Stilhano et al., 2016), agarose (Meilander-Lin et al., 2005), fibrin (Kidd et al., 2012)

and gelatin (Lin et al., 2017), have been explored as platforms for viral and non-viral gene delivery. Alginate is a natural occurring polymer which due to its biocompatibility, low-cost and mild gelation conditions (Lee and Mooney, 2012), has been widely employed in musculoskeletal tissue bioprinting (Axpe and Oyen, 2016; Daly et al., 2016b; Fedorovich et al., 2012). But its slow degradation, limited adhesion and mobility of encapsulated cells, and an average pore size in the nanometer range (Boontheekul et al., 2005), might limit the cellular uptake of entrapped gene therapeutics, specially of those complexed to nanoparticles larger than 10 nm (Kearney et al., 2015).

To solve these issues and gain temporal control over gene delivery, the opening of micro-pores in alginate hydrogels have been shown to facilitate the on-demand release of encapsulated non-viral vector-pDNA complexes (Huebsch et al., 2014). Methylcellulose, previously used to increase the printability of alginate, can also be used as a sacrificial material to increase the micro-porosity of the bulk alginate gel, with no negative effect on cell viability (Markstedt et al., 2015; Schütz et al., 2015). The modulation of alginate microporous structure, through the incorporation of methylcellulose, could not only provide fine spatial control of cells and gene therapeutics by increasing the printability of the bulk gel, but also to facilitate nanoparticle-mediated gene delivery within a 3D printed construct.

The overall aims of this study were thus to develop gene-activated pore-forming bioinks for enhanced gene delivery, and assess the capacity of these constructs to support cartilage and bone development within a mechanically robust osteochondral construct. Firstly, the microstructure and printability of alginate-methylcellulose (ALG-MC) hybrid gels were assessed to valid their potential as bioinks for high precision bioprinting. Next, temporal non-viral gene delivery within the ALG-MC gels was characterized *in vitro* and *in vivo*. Finally, zonal gene delivery of chondrogenic and osteogenic factors was explored to spatially control stem cell behavior and engineer a mechanically reinforced osteochondral construct of therapeutic relevance.

7.2. Materials and methods

7.2.1. Alginate-methylcellulose hydrogel preparation and characterization

Methylcellulose (Sigma-Aldrich, Ireland), with a molecular weight of 40,000 Mn and a viscosity of 400,000 Cp, was added in a ratio of 1:1 or 1:2 to a solution of 2% alginate (Pronova FMC BioPolymer, Norway). The alginate only and ALG-MC hydrogels were crosslinked using a 3% agarose/100 nM $CaCl_2$ (both from Sigma-Aldrich, Ireland) to form cylindrical constructs (Ø5 x H4 mm).

After fabrication and incubation of the gels at room temperature (RT) in ultrapure water (UPW), their macroscopic and microscopic structure was analysed. For histological analysis, constructs were processed as previously described (Sheehy et al., 2014a) and stained with hematoxylin and eosin (H&E) (Sigma-Aldrich, Ireland). The microstructure of hydrogel-based constructs was characterized using cryogenic SEM (cryoSEM) methods. Samples were prepared for imaging by mounting onto standard SEM stubs, then subsequently plunged into liquid nitrogen slush, freeze fractured and lightly sputter coated before transferring to the SEM chamber (Quorum Technologies, UK). Samples were imaged at 5 kV using a Carl Zeiss Ultra SEM (Carl Zeiss, Germany). Pore size was analysed using ImageJ analysis and calculated using Feret´s diameter (Merkus, 2009). The percentage of wet weight (w/w) loss was calculated by weighting the constructs immediately after fabrication and after 7 days of incubation in UPW at RT.

7.2.2. Mechanical testing

Constructs were mechanically tested (n=4) in unconfined compression using a standard material testing machine with a 5N load cell (Zwick Roell Z005). Briefly, constructs were kept hydrated through immersion in DMEM (Gibco Biosciences, Ireland) bath maintained at RT. A preload of 0.01 N was applied to ensure that the construct surface was in direct contact with the impermeable loading platens. Stress relaxation tests were performed consisting of a ramp displacement of 1 m/s up to 10% strain. A relaxation period of 30 min was used.

7.2.3. Rheological assessment

MCR 301 rheometer (Anton Paar GmbH, Austria) was used for the rheological assessment of the hydrogels. A 50 mm parallel plate with a measurement gap of 0.55 mm was used. Strain sweeps in the range of 0.1% to 100% at the frequency of 1 Hz was carried out in order to determine the linear viscoelastic range of the samples. A recovery test was also carried out where the hydrogels were subjected to 1% shear rate for 60 s, 100% shear rate for 10 s and 1% shear rate for 60 s to simulate the printing process, and to assess the recovery of the viscosity of the materials. The 100% shear rate is estimated to be the maximum shear rate experienced by the hydrogel during printing process. This test also informs the thixotropic property of the hydrogels and thus, how quickly the hydrogel can recover its viscosity immediately after printing.

7.2.4. 3D printing process and printability assessment

A 3D Discovery multi-head (Regen HU, Switzerland) 3D plotter was used for printing. For hydrogel printing, pneumatic driven syringes with 25 Gauge (G) needles were used at extrusion pressures between 0.1 and 0.2 MPa. The filament spreading ratio, defined as the width of the printed filament divided by the needle diameter, was used as a measure of printability as previously described (Daly et al., 2016a). For polycaprolactone (PCL) (Mw = 45,000 Mn, Sigma-Aldrich, Ireland) printing, fused deposition modeler (FDM) was used to deposit filaments of molten PCL. To characterize the filament size and separation between fibers, PCL scaffolds were placed onto SEM stubs and Au/Pd sputter coated before imaging. SEM characterization was conducted on a Carl Zeiss Supra SEM, aligned at 5 kV (Carl Zeiss, Germany).

7.2.5. Isolation and expansion of bone marrow-derived MSCs, and chondrogenic differentiation

Bone marrow-derived MSCs were isolated from the femora of porcine donors (3–4 months, >50 kg) within 3 h of sacrifice according to a modified method developed for human MSCs (Lennon and Caplan, 2006). Mononuclear cells were plated at a seeding density of 5×10^3 cells/cm^2 in standard culture media, high glucose Dulbecco's modified

Eagle's medium (4.5 mg/mL D-glucose and 200 mM L-glutamine; hgDMEM) supplemented with 10% fetal bovine serum (FBS) and penicillin-streptomycin (100 U/mL) (all from Gibco, Biosciences, Ireland), and expanded in a humidified atmosphere at 37 °C, 5% CO_2, and 20% pO_2. MSCs at passage 2-3 were used for all experiments.

For chondrogenic differentiation of MSCs, MSCs were trypsinized and encapsulated at a concentration of 20 x 10^6 cells/mL, in either pre-crosslinked alginate hydrogels or ALG-MC hybrid gels. The cell laden bioinks were printed to form cylindrical constructs that were further crosslinked in a 100 mM $CaCl_2$ bath for 5-10 min. After crosslinking The gels were cultured for 4 weeks at 5% PO_2 in chondrogenically defined media consisting of DMEM GlutaMAX supplemented with 100 U/mL penicillin/streptomycin (both Gibco), 100 µg/mL sodium pyruvate, 40 µg/mL L-proline, 50 µg/mL L-ascorbic acid 2-phosphate, 4.7 µg/mL linoleic acid, 1.5 mg/mL bovine serum albumin, 1x insulin–transferrin–selenium, 100 nM dexamethasone (all from Sigma–Aldrich) and 10 ng/mL human TGF-β3 (PrepoTech, UK).

7.2.6. Plasmid propagation

Six different plasmids were used in the current study: three plasmids encoding for the reporter genes green fluorescent protein (pGFP, Amaxa, Lonza Cologne AG, Germany) and luciferase (pLUC, pGaussia Luciferase; New England Biolabs, Massachusetts, USA), and dtTomato (pTomato, kind donation from Prof. Gerhart Ryffel through Addgene), and another three encoding for the therapeutic genes BMP2 (pBMP2, kind donation from Prof. Kazihusa Bessho, Kyoto University, Japan), TGF-β3 (pTGF-β3, InvivoGen, Ireland) and SOX9 (pSOX9, kind donation from Prof. Dr. Gun-Il Im, Dongguk University, South Korea). Plasmid amplification was performed by transforming chemically competent *Escherichia coli* bacterial cells (One Shot TOP10; Biosciences, Ireland) according to the manufacturer's protocol. The transformed bacteria were cultured on LB plates with 50 mg/L kanamycin (Sigma-Aldrich, Ireland) as the selective antibiotic for pGFP and pSOX9, and 100 mg/L ampicillin (Sigma-Aldrich, ireland) as the selective antibiotic for pLUC, pTGF-β3, pBMP2 and pTomato. Bacterial colonies were harvested and inoculated in LB broth (Sigma-Aldrich, Ireland) and incubated overnight for further amplification. The harvested bacterial cells were then

lysed, and the respective pDNA samples were purified using qiagen plasmid kit (MaxiPrep Kit; Qiagen, Ireland). Nucleic acid concentration (ng/mL) was determined by analyzing the 260:280 ratio and 230 nm measurement using NanoDrop spectrophotometer (Labtech International, UK).

7.2.7. Preparation of delivery vectors, vector-pDNA complexes

The synthesis of the nHA particles was performed as previously described (Cunniffe et al., 2010). nHA-pDNA complexes were prepared by adding 150 mL of the nHA solution to 2 mg of pDNA pretreated with 0.25 M $CaCl_2$ (Sigma-Aldrich, Ireland) as previously optimized (Castaño et al., 2014; Curtin et al., 2012). The RALA peptide was produced as previously described (McCarthy et al., 2014), and complexed with pDNA at an n:p ratio of 10 for 30 min at RT.

7.2.8. Monolayer transfection and 3D printing of pre-transfected cells

For monolayer transfection, MSCs were seeded in T175 flasks at a seeding density of 5×10^4 cells/cm^2 and cultured for 72 h in standard culture media prior to transfection. RALA and nHA-pDNA complexes were prepared immediately before transfection. For the RALA-pDNA transfections, the plated cells were washed twice with PBS and incubated in 10 mL of Opti-MEM (Life Technologies, Ireland) for 2 h. After the incubation time, complexes were suspended in 5 mL of Opti-MEM and added to the MSCs to a density of 0.2 μg of pDNA/cm^2. For nHA-pDNA transfection, complexes were suspended in 5 mL of standard media and added to the MSCs at the same density as the RALA-pDNA complexes. Following incubation for 4-6 h with both RALA and nHA-pDNA complexes, the cells were washed with PBS and standard culture media was added. 3 days after transfection, cells were trypsinized and encapsulated in pre-crosslinked alginate or ALG-MC paste to a final concentration of 20×10^6 cells/mL. Once encapsulated, cell laden gels were printed simultaneously using different pneumatic heads of the 3D Discovery system.

7.2.9. Preparation of gene activated bioinks and *in vitro* culture of gene activated constructs

For 1 mL of pre-crosslinked $CaCl_2$ and ALG-Mc bioinks, 20 μg of pDNA were complexed to either nHA (0.0125 μL nHA/μg pDNA) or RALA (N:P ratio of 10) and added to a suspension of MSCs (20 x 10^6 cells/mL bioink) in either 0.5 mL of standard media for nHA or 0.5 mL of Opti-MEM for RALA transfection. After 1 h of incubation, the nHA-pDNA containing groups were spun down to retire excess of $CaCl_2$ and mixed with $CaCl_2$ (50 mM) and alginate added in a 7:3 ratio until a homogenous mixture of a final 2% alginate was obtained. For the RALA-pDNA containing groups, the 0.5mL of cell and complex suspension were mixed with 0.5 mL of 4% ALG-MC paste (1:2 ratio) until a homogenous mixture of a final 2% alginate was obtained.

After 3D printing and crosslinking of the constructs in a 100 mM $CaCl_2$ bath for 5-10 min, RALA-pDNA containing 3D printed hydrogels were incubated for 4-6 hours in Opti-MEM. In contrast, after crosslinking, nHA-pDNA containing gels were directly cultured in the desired media. For reporter gene expression, constructs were incubated at 37 °C and 20% PO_2 in standard culture media. For therapeutic gene delivery, constructs were incubated at 37 °C and 5% PO_2 in chemically defined chondrogenic media without recombinant TGF-β3 supplementation.

7.2.10. Characterisation of RALA-pDNA encapsulation and release in ALG-MC hydrogels

RALA-pDNA complexes (n:p ratio of 10) were formed and encapsulated in alginate and ALG-MC cells at a concentration of 0.5 μg/mL. To assess the complex encapsulation efficiency, after crosslink in a 3% agarose/100 nM $CaCl_2$ mold to form cylindrical constructs, they were homogenized in citrate buffer for 1 h at 37 °C and the amount of pDNA per gel was quantified with a nanodrop. To characterize complex release, after crosslinking, gels were incubated in UPW at RT. The UPW was collected and changed after 12 h, 24 h, 3 days, 7 days and 10 days, and the quantity of pDNA in the UPW was analysed with a nanodrop.

7.2.11. Reporter and therapeutic gene expression analysis.

For gels containing pGFP, transfected cells were assessed using a Leica SP8 scanning confocal microscope (Leica Microsystems, Ireland). Luciferase expression was assessed in the culture media using a Pierce Gaussia Luciferase Flash Assay Kit (ThermoFisher, Ireland) at different time points up to 10 or 14 days. The levels of BMP2 and TGF-β3 were quantified in the culture medium using ELISAs (R&D Systems) according to the manufacturer's instructions.

7.2.12. Live dead analysis

Cell viability was assessed using a LIVE/DEAD viability/cytotoxicity assay kit (Invitrogen, Bio-science, Ireland). Briefly, constructs were cut in half, washed in phosphate-buffered saline (PBS) followed by incubation for 1 h in PBS containing 2 mM calcein and 4 mM ethidium homodimer-1. Sections were again washed in PBS, imaged using a Leica SP8 scanning confocal microscope.

7.2.13. Subcutaneous *in vivo* construct implantation and *in vivo* luciferase analysis

Control and gene activated 3D printed constructs were implanted subcutaneously into the back of nude mice (Balb/c; Harlan, United Kingdom) as previously described with 2 samples from the same group inserted in each of two pockets (Cunniffe et al., 2015b). The constructs were harvested after 3 weeks for the *in vivo* luciferase expression study, and after 4 weeks for the therapeutic genes studies. Mice were euthanized by CO_2 inhalation and the animal protocol was reviewed and approved by the Ethics Committee of Trinity College Dublin and the Health Products Regulatory Authority (HPRA).

For the *in vivo* luciferase imaging, a protocol previously developed by Tannous et al (2009) was followed (Tannous, 2009). Briefly, previous to administration, coelenterazine (Gold Biotechnology, USA), prepared in acid methanol at a concentration of 5 mg/mL, was dissolved in PBS to a final concentration of 0.5 mg/mL under minimal light conditions, immediate after the mice were anesthetized using isoflurane, 50 μL of

the coelenterazine mix were injected in each of the pockets. Immediately after coelenterazine injection, photon counts were acquired using a real-time bioluminescence imaging system (PhotonImager; Biospace lab, France) over 5 minutes.

7.2.14. Micro-computed tomography analysis

Micro-computed tomography (microCT) scans were performed using a Scanco Medical 40 microCT system (Scanco Medical, Switzerland) with a 70 kVp X-ray source at 114 µA. Quantification was performed by setting a threshold of 200, corresponding to a density of 411.98 mg hydroxyapatite/cm^3 and the mineral volume (mm^3) was recorded. Reconstructed 3D images were generated from the scans and used to visualize mineral distribution throughout the constructs.

7.2.15. Bilayer construct fabrication

Control or gene activated hydrogels were cast into 3D printed PCL constructs (6 mm diameter x 5 mm height) inserted in 3% agarose/100 nM CaCl$_2$, to form cylindrical constructs (6 mm diameter x 6 mm height) comprising of an osteogenic layer (4 mm height) and a chondrogenic layer (2 mm height). The osteogenic layer was formed by either MSC-laden pre-crosslinked alginate gel for the control groups or MSC-laden pre-crosslinked alginate gel containing nHA-pBMP2 complexes for the gene activated groups. The chondrogenic layer was formed by either MSC-laden ALG-MC (1:2 ratio) hybrid gels for the control groups, or MSC-laden ALG-MC hybrid gels containing either RALA-pTGF-β3-pBMP2 (pTGF-pBMP) or RALA-pTGF-β3-pBMP2-pSOX9 (pTGF-pBMP-pSOX) gene combinations.

7.2.16. Biochemical analysis

DNA and sGAG content were quantified biochemically using the Hoechst Bisbenzimide 33258 dye assay and the dimethyl methylene blue dye-binding (DMMB) assay respectively, as previously described (Sheehy et al., 2012). To exclude any background absorbance from the alginate, the PH of the DMMB was adjusted to 1.35. Total collagen content was determined by measuring the hydroxyproline content using the dimethylaminobenzaldehyde and chloramine T assay and a hydroxyproline to

collagen ratio of 1:7.69. Calcium content was determined using a Sentinel Calcium Kit (Alpha Laboratories Ltd, UK) after digestion in 1 M HCl at 110 ℃ for 48 h.

7.2.17. Histological and Immunohistochemical Analysis

Constructs were processed for histological analysis as previously described (Sheehy et al., 2014a). The sections were stained with H&E to assess bone and blood vessel formation, aldehyde fuschin/alcian blue to assess sGAG content, picrosirius red to assess collagen content and alizarin red to assess calcification. Collagen types I, II, and X were evaluated using a standard immunohistochemical technique as previously described (Sheehy et al., 2014b). The presence of vascular structures was quantified by counting distinct areas of red blood cell activity as a blood vessel. The number of blood vessels across a whole cross section was then counted.

7.2.18. Statistical analysis

Statistical analyses were performed using GraphPad Prism (version 5) software. Statistical differences were determined by analysis of variance (ANOVA) followed by Tukey's multiple comparison test or Student's t-test where appropriate. Numerical and graphical results are displayed as mean ± standard deviation. Significance was accepted at a level of $p < 0.05$. Sample size (n) is indicated within the corresponding figure legends.

7.3. Results

7.3.1. Addition of methylcellulose to alginate hydrogels increases the porosity and printability of alginate hydrogels

To generate bioinks whose porosity increases post-printing, alginate and methylcellulose (as a sacrificial component) were mixed at alginate:methylcellulose weight ratios of 1:0, 1:1 and 1:2 (Fig.7.1.A). These composites formed stable hydrogels (Fig.7.1.B), but one day post-fabrication clearly differed in both their macro- (Fig.7.1.C) and micro-structure (Fig.7.1.D) to normal alginate hydrogels. Methylcellulose (1:1 and 1:2) containing hydrogels contained larger pores than alginate only hydrogels (Fig.7.1.G), with the pore diameter increasing with increases in methylcellulose content. This correlated with a faster reduction in the wet weight (w/w) of methylcellulose containing hydrogels (Fig.7.1.E). Furthermore, methylcellulose containing hydrogels showed a lower bulk Young's modulus one day post-fabrication (Fig.7.1.F).
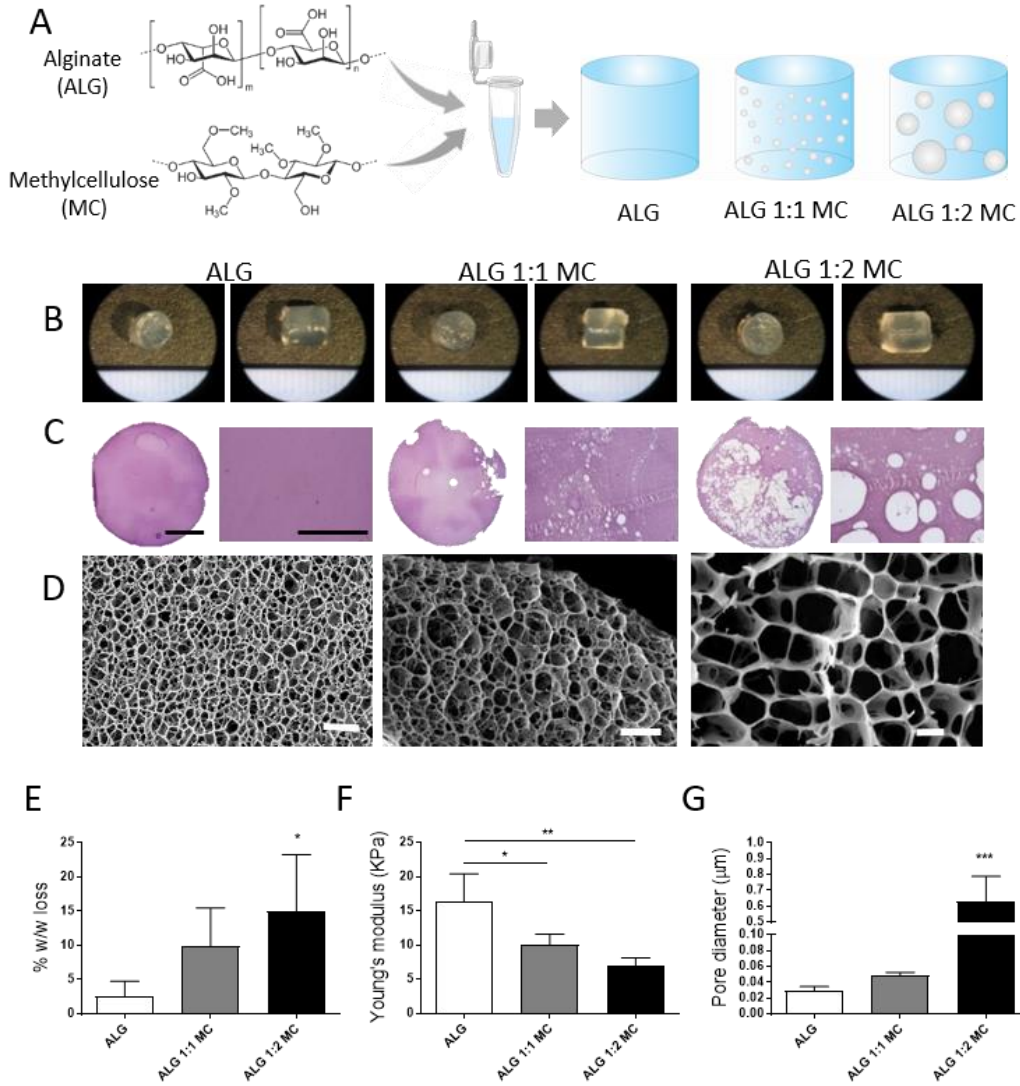
Fig.7.1. Development and characterization of ALG-MC gels. (A) Schematic of the fabrication of the ALG-MC gels. (B) Macroscopic appearance of cylindrical gels fabricated with alginate and ALG-MC at 1:1 and 1:2 alginate-methylcellulose ratios (C) Histological analysis through H&E staining of the structure of the alginate and ALG-MC gels, scale bar = 1 mm in the lower magnification images and 0.2 mm in the higher magnification images. (D) CryoSEM analysis of the micro-porosity of alginate and ALG-MC gels, scale bar = 1 μm. (E) Percentage of wet weight loss in the alginate and ALG-MC gels after 7 days in aqueous solution. (F) Young´s modulus of the alginate and ALG-MC gels after 1 day of fabrication. (G) Pore diameter calculation based on the cryoSEM imaging of the alginate and alginate-MC gels. (*) Denotes significance (n=4, p<0.05) in comparison to the rest of the groups; (**) denotes significance (n=4, p<0.01) in comparison to the rest of the groups; (***) denotes significance (n=4, p<0.001) in comparison to the rest of the groups.

To assess the printability of the alginate and ALG-MC hydrogels, the rheological properties of the different materials were assessed. The addition of methylcellulose significantly increased the viscosity of alginate, with these composites also exhibiting shear thinning properties (Fig.7.2.A). Also, a viscosity recovery test was performed at a steady shear rate to determine if the hydrogel is thixotropic (property of certain gels having a viscosity that decreases when a stress is applied) and thus better suited to bioprinting applications. The viscosity of the alginate was very low (0.180 Pa.s) and did not exhibit appreciable changes with increases in the shear rate (Fig.7.2.B). However, the ALG-MC (1:1 and 1:2) gels exhibited thixotropic behaviour when the shear rate was reduced from 100 to 1 1/s (Fig.7.2.B). Assuming an average shear rate of 100 1/s during the printing process (pressure of 0.1 Bar and printing velocity of 2-8 mm/s), and based on the relationship between shear rate and printing velocity described by Li *et al.* (2016), the thixotropic properties of the analysed bioinks should be preserved when 3D bioprinted (Li *et al.*, 2016). To confirm this observation, the printability of $CaCl_2$ pre-crosslinked alginate (ALG-Ca) and ALG-MC gels was assessed by measuring the spreading ratio post-printing (Fig.7.2.C). The ALG-MC gels (1:2) (Fig.7.2.G) showed similar printability to alginate pre-crosslinked with $CaCl_2$ (Fig.7.2.E), demonstrating a significantly lower spreading ratio than the ALG-MC 1:1 (Fig.7.2.F) and alginate alone (Fig.7.2.D).

To confirm that such bioinks could be used to produce constructs with spatially defined gradients of cell populations, previously nanoparticle-transfected MSCs with pDNA encoding for GFP (green) and dtTomato (red) were encapsulated in ALG-Ca and alginate 1:2 methylcellulose hybrid bioinks respectively (Fig.7.2.H). Both gels were simultaneously printed, using a multi-head printing system, in different patterns. After ionic crosslinking, the prints were imaged under a fluorescent confocal microscope showing defined spatial distribution of both cell populations (Fig.7.2.I).
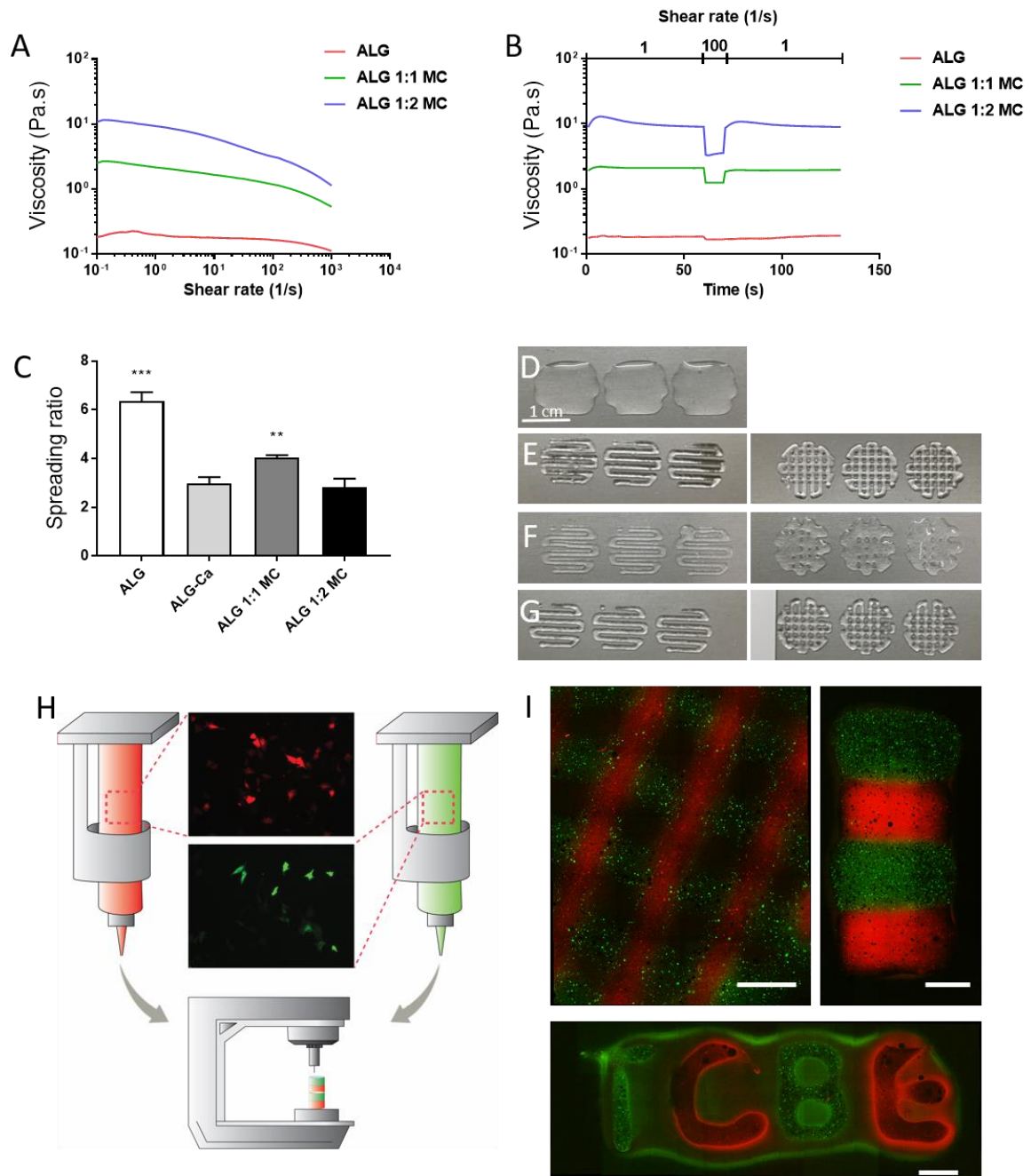
Fig.7.2. Printability of ALG-MC hybrid gels. (A) Viscosity of ALG-Ca and ALG-MC gels (ALG 1:1 MC and ALG 1:2 MC) as a function of shear rate. (B) Viscosity recovery test as a function of shear rate. (C) Spreading ratio of the alginate, ALG-Ca and ALG-MC gels. Images of printed patterns of the alginate (D), ALG-Ca (E), ALG-MC 1:1 (F) and ALG-MC 1:2 (G), scale bar = 1 cm. (H) Schematic of the printing of ALG-Ca gels containing GFP transfected MSCs and the ALG-MC 1:2 containing dtTomato transfected MSCs. (I) 3D printed patterns with the ALG-Ca bioink containing GFP transfected cells and the ALG-MC 1:2 bioink containing dtTomato transfected cells, scale bar = 2 mm. (**) Denotes significance (n=4, p<0.01) in comparison to the rest of the groups; (***) denotes significance (n=4, p<0.001).

7.3.2. 3D printed alginate-methylcellulose hybrid gels were able to support chondrogenesis of encapsulated MSCs *in vitro*

MSCs were encapsulated in ALG-Ca and ALG-MC hybrid gels and then printed to form cylindrical constructs (Fig.7.3.A). Live/dead semi-quantitative analysis of cell viability in the 3D printed constructs 1 day after printing was performed (Fig.7.3.B). The percentage of living cells was shown to be significantly higher in the ALG-MC gels in comparison to the ALG-Ca pre-crosslinked gels (Fig.7.3.C). These MSC-laden 3D printed constructs were then cultured *in vitro* in chondrogenic media for 28 days and the chondrogenic differentiation of the encapsulated stem cells was analysed in both groups. Biochemical analysis of the levels of DNA (Fig.7.3.D), GAGs (Fig.7.3.E) and collagen (Fig.7.3.F) revealed no significant differences between groups. However, analysis of the calcium content (Fig.7.3.G) showed significantly higher levels of mineralization in the ALG-Ca group. Histological analysis also showed similar staining levels of GAG and collagen (Fig.7.3.H), but although immunohistochemical analysis of collagen type I and II showed similar levels of staining between the two groups, only the ALG-Ca gels showed positive collagen type X staining (Fig.7.3.H), a marker of endochondral ossification.
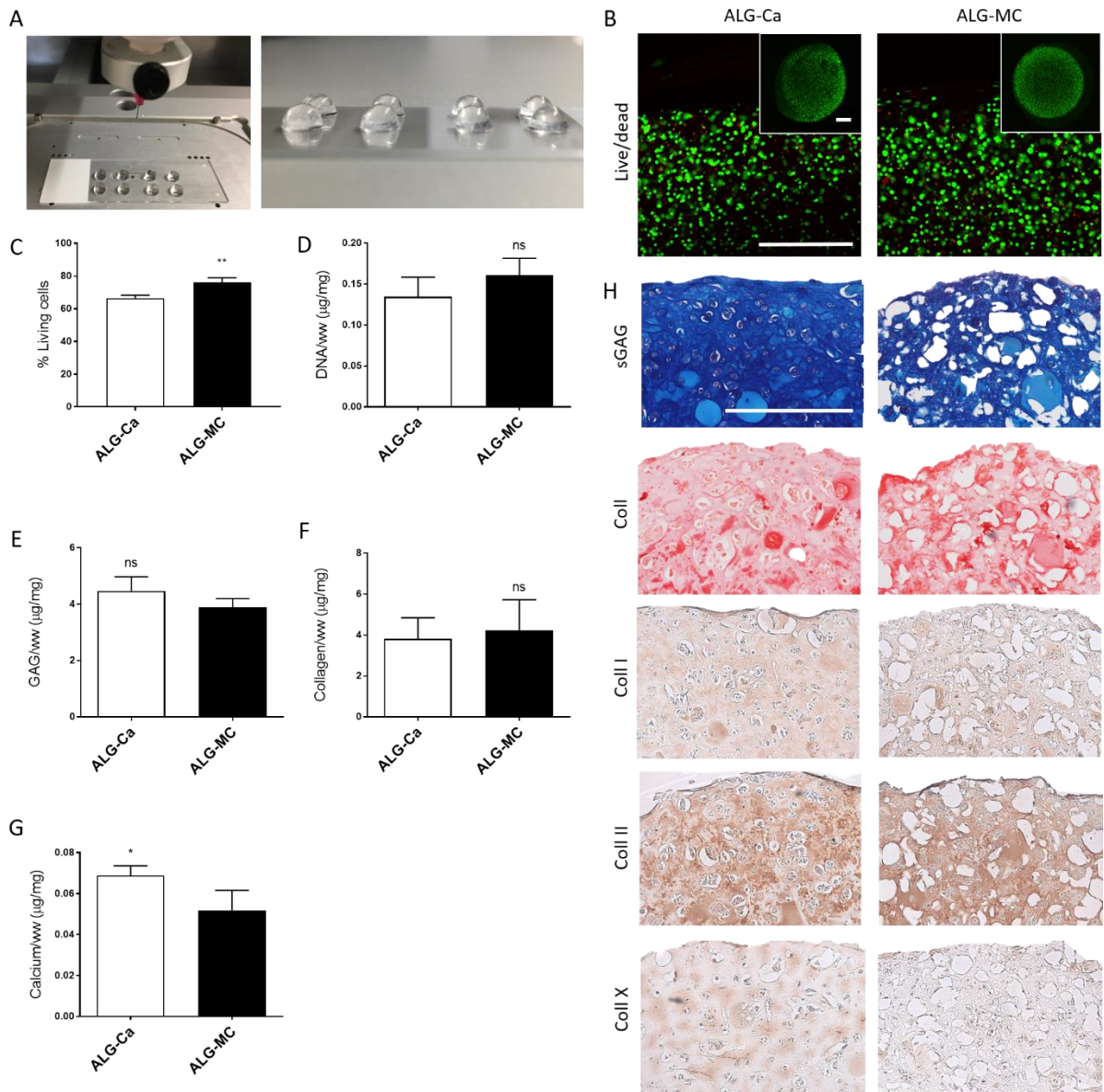
Fig.7.3. Chondrogenesis of 3D printed cell-laden hydrogels. (A) 3D printing process and macroscopic appearance of the constructs after printing. (B) Live/dead images of the encapsulated MSCs 1 day after printing (living cells are stained in green, dead are red). Scale bar = 1 mm for lower magnification images and 0.5 mm for the higher magnification images. (C) Percentage of living cells in the printed gels 1 day after fabrication. Quantification of DNA/ww (D), GAG/ww (E), collagen/ww (F) and calcium/ww (G) in the 3D printed gels after 28 days of in vitro culture in chondrogenic media. (H) Histological and immunohistochemical analysis of the 3D printed gels after 28 days of in vitro culture. (Scale bar = 0.5 mm). (*) Denotes significance (n=4, $p<0.05$); (**) denotes significance (n=4, $p<0.01$).

7.3.3. Pore-forming hydrogel bioinks enhance nanoparticle-mediated reporter gene delivery to encapsulated MSCs *in vitro*

Before assessing the capacity of printed bioinks to support non-viral gene delivery, we first assessed the capacity of cast hydrogels to transfect encapsulated MSCs. RALA-pDNA nanoparticle complexes were encapsulated in alginate and in ALG-MC hybrid gels with different ratios of methylcellulose (1:1 and 1:2), to form gene activated hydrogels. After hydrogel crosslinking, the presence of the RALA-pDNA complexes was analysed through cryoSEM, confirming the presence of the non-viral complexes in all the groups (Fig.7.4.A). The encapsulation efficiency (Fig.7.4.B) of the complexes into the hydrogels was also analysed showing no significant differences between the groups. The analysis of pDNA released from the hydrogels during 10 days in aqueous solution (Fig.7.4.C), showed a significant increased release as the amount of methylcellulose was incremented. MSCs were also encapsulated in the gene activated hydrogels together with RALA-pGFP complexes, allowing for transfection of the encapsulated MSCs over 10 days in all the groups (Fig.7.4.D). The encapsulation of RALA-pLUC complexes allowed for temporal quantification of cell transfection, showing increased expression of the transgene as the amount of methylcellulose in the gels was increased (Fig.7.4.E). We could also observe a sustained luciferase expression over 11 days, suggesting continuous transfection of MSCs within the hydrogels (Fig.7.4.D). In addition, the DNA content inside the gels was analysed as a measure of cell viability showing no significant differences between the groups at every time point (Fig.7.4.F).

Fig.7.4. Characterization of temporal RALA-pDNA release and transfection of encapsulated MCS in the alginate and ALG-MC gels. (A) CryoSEM images of the encapsulated RALA-pDNA complexes in the alginate and ALG-MC (1:1 and 1:2) gels. Scale bar = 200 μm. (B) Encapsulation efficiency of the RALA-pDNA complexes in the different gels. (C) Percentage of the released RALA-pDNA complexes in the different gels at 12 h, 24 h, day 3, 7 and 10. (D) GFP positive encapsulated MSCs in the alginate and ALG-MC containing RALA-pGFP complexes at day 1, 3, 7 and 10 after fabrication. Scale bar = 250 μm. (E) Luciferase quantification in the media of cell laden alginate and ALG-MC gels containing RALA-pLUC complexes at day 1, 3, 7 and 11. (D) DNA quantification in the cell laden alginate and ALG-MC gels containing RALA-pLUC complexes at day 1, 3, 7 and 11. (*) Denotes significance (n=4, p<0.05) in comparison to the rest of the groups at the same time point; (**) denotes significance (n=4, p<0.01) in comparison to the rest of the groups at the same time point; (ns) denotes no significance (n=4, p>0.05).

Gene delivery of reporter genes to encapsulated MSCs was also assessed in 3D printed constructs (Fig.7.5.A). MSCS and RALA-pLUC complexes were encapsulated in ALG-Ca and in the ALG-MC hybrid bioinks and printed to form discs (Fig.4.5.B). One day after printing, live/dead analysis of the encapsulated MSCs was performed, demonstrating limited cell dead in the all the printed constructs (Fig.7.5.C, D and E). Furthermore, the DNA content within the printed gene activated printed constructs was at least comparable to the non-transfected controls over 14 days in culture (Fig.7.5.F). Temporal luciferase gene expression was also assessed, which revealed a 10 fold increase in luciferase expression in the printed pore-forming ALG-MC constructs in comparison to the ALG-Ca constructs (Fig.7.5.G). Luciferase expression was maintained over time in the gene activated groups suggesting continuous cell uptake (Fig.7.5.G). This finding was also observed for other gene delivery vectors, as when nHA-pLUC complexes were encapsulated in the pore-forming ALG-MC bioink, an increase in gene expression was also observed at all time-points in comparison to the ALG-Ca hydrogels (Fig.A.4.B), with no negative effects on cell viability (Fig.A.4.A).

Fig.7.5. In vitro RALA-mediated gene delivery in 3D printed ALG-CA and ALG-MC gels. (A) Schematic of the encapsulation of MSCs and RALA-pLUC complexes into the alginate-based bioinks and 3D printing to produced gene activated constructs in which transfection could be monitored through measuring the luciferase in the culture media. (B) Macroscopic pictures of the 3D printed gene activated gels. Live/dead staining in the ALG-Ca control (CTRL) (C), ALG-Ca RALA-pLUC (RALA-pLUC Ca) containing gels (D) and ALG-MC RALA-pLUC (RALA-pLUC MC) containing gels (E) 1 day after fabrication. Scale bar = 1 mm for the large magnification pictures and 250 µm for the higher magnification. (F) DNA quantification in the CTRL, RALA-pLUC Ca and RALA-pLUC MC gels at different time points. (G) Luciferase quantification in the culture media of the tested gels at day 1, 3, 7 and 14 after fabrication. (*) Denotes significance (n=4, p<0.05) in comparison to the rest of the groups at the same time point; (**) denotes significance (n=4, p<0.01) in comparison to the rest of the groups at the same time point; (***) denotes significance (n=4, p<0.001) in comparison to the rest of the groups at the same time point.

7.3.4. Pore-forming bioinks enhance nanoparticle-mediated reporter gene delivery *in vivo* to recruited cells and transplanted MSCs

Acellular or MSC-laden ALG-Ca and pore-forming ALG-MC bioinks containing RALA-pLUC complexes were used to print cylindrical discs which were implanted subcutaneously in nude mice, with luciferase expression analysed *in vivo* over 3 weeks using an IBIS system (Fig. 7.5.A). Luciferase expression analysis of the acellular RALA-pLUC constructs demonstrated distinct luciferase expression profiles (Fig.7.6.B-D and H), suggesting that the bioink formulation influenced the release of RALA-pLUC complexes *in vivo* and/or the ability of host cells to uptake the RALA-pLUC complexes. Luciferase expression peaked early and decreased over time in the pore-forming ALG-MC constructs, while a more sustained expression was observed in the ALG-Ca constructs (Fig.7.6.H). Similar trends were seen when nHA-pLUC complexes were encapsulated in the printed hydrogels (Fig.A.4.C). When MSCs were encapsulated in the printed constructs, increased luciferase expression was observed in the ALG-MC constructs at day 3 and 7 compared to the ALG-Ca constructs (Fig.7.6.E-G and I). While luciferase expression was noticeably higher in the cell laden gels, it did not stay constant and decreased more dramatically over time (Fig.7.6.I). In contrast, when nHA-pLUC complexes were encapsulated in cellular gels, the ALG-MC group did not show enhanced transgene expression in comparison to the ALG-Ca gels (Fig.A.4.D).
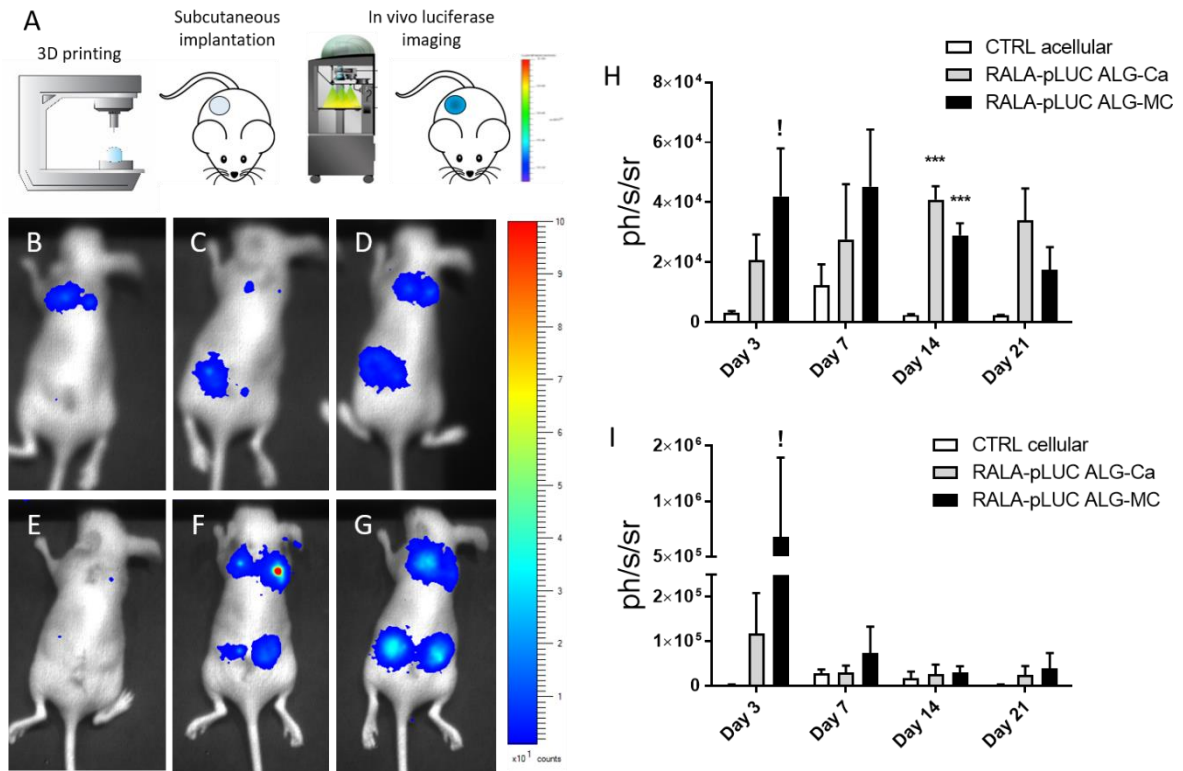
Fig.7.6. In vivo RALA-mediated gene delivery in 3D printed ALG-Ca and ALG-MC gels. (A) Schematic of alginate-based bioinks and 3D printing and mouse subcutaneous implantation to assess the in vivo luciferase expression. Macroscopic images of the nude mice during the bioluminescence imaging protocol in the acellular (B (top nHA-pLUC in ALG-MC and bottom CTRL acellular), C (top RALA-pLUC in ALG-Ca and bottom nHA-pLUC in ALG-Ca) and D (top RALA-pLUC in ALG-Ca and bottom RALA-pLUC in ALG-MC)) and cell laden (E (top CTRL acellular, bottom CTRL cellular), F (top nHA-pLUC in ALG-Ca and bottom nHA-pLUC in ALG-MC) and G (top RALA-pLUC in ALG-Ca and bottom RALA-pLUC in ALG-MC) gene activated gels at day 3 after implantation. Bioluminescence quantification (ph/s/sr) of the acellular (H) and cell laden (I) gene activated gels. (!) Denotes significance (n=6, p<0.05) in comparison to the non-transfected control (CTRL) at the same time point; (***) denotes significance (n=>4, p<0.001) in comparison to the rest of the groups at the same time point.

After 21 days of *in vivo* subcutaneous implantation, the mineralization of the implanted constructs was also assessed. Acellular ALG-Ca constructs were noticeably more calcified than the ALG-MC gels (Fig.A.5.A and C), which can potentially be attributed to the higher calcium content of the ALG-Ca implants. The MSC-laden constructs underwent higher mineralization than their acellular counterparts (Fig.A.5.B and C), with the ALG-Ca constructs containing nHA-pLUC undergoing the highest level of calcification in comparison to the rest of the gene activated groups.

7.3.5. Therapeutic gene delivery within the 3D printed hydrogels can modulate stem cell fate towards either the osteogenic or chondrogenic pathway *in vitro* and *in vivo*

With the vision to engineer an osteochondral construct with spatial gene delivery to zonally direct stem cell fate, RALA-pDNA containing ALG-MC hybrid gels were explored for the delivery of chondrogenic factors; whereas the nHA nanoparticles entrapped in ALG-Ca bioinks were used for the delivery of osteogenic genes due to its superior mineralization *in vivo* and previous results in the sixth chapter. To drive osteogenesis of MSCs within ALG-Ca bioinks, we delivered pDNA encoding for BMP2 using nHA vectors. To induce chondrogenesis of MSCs within ALG-MC bioinks, two gene combinations were analysed. The first combination gene combination comprised the delivery of TGF-β3 and BMP2 genes, while in the second combination pDNA encoding for SOX9 was co-delivered with the TGF-β3 and BMP2 genes.

After MSC and vector-pDNA encapsulation, constructs were 3D printed and maintained *in vitro* for 4 weeks. BMP2 and TGF-β3 levels in the media were measured, which demonstrated that RALA and nHA were able to successfully deliver the pDNA to alginate encapsulated MSCs (Fig.A.6.A and B). After 28 days of *in vitro* culture, nHA-mediated BMP2 gene delivery in the ALG-Ca was able to significantly increase GAG deposition in comparison to the non-transfected control (Fig.7.7.B), and increased construct calcification in comparison to all the control and gene activated groups (Fig.7.7.D). In contrast, RALA-mediated gene delivery of both chondrogenic gene combinations (pTGF-pBMP2 and pTGF-pBMP2-pSOX9) resulted in significantly higher GAG and collagen deposition (Fig.7.7.B and C) and significantly lower levels of calcification (Fig.7.7.D) in comparison with all the other groups. The Young's (Fig.7.7.E) and Equilibrium modulus (Fig.7.7.F) of the constructs containing chondrogenic gene combinations were significantly higher than other groups. These results were confirmed through histological examination of GAG, collagen and calcium deposition (Fig.7.7.G). Immunohistochemistry revealed higher collagen type II deposition in the gels containing both chondrogenic combinations (Fig.7.7.G), whereas collagen type I staining was only present in gels containing the pTGF-pBMP2 combination (Fig.7.7.G).
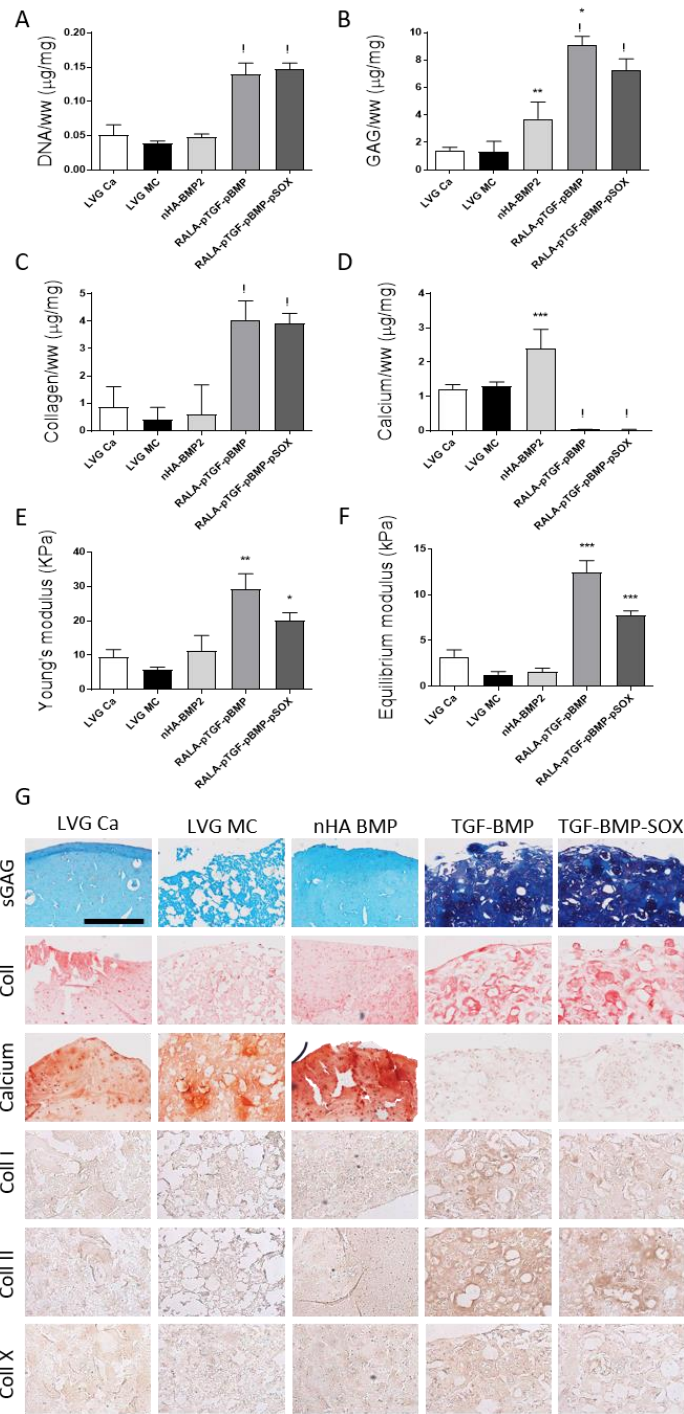
Fig.7.7. In vitro therapeutic gene delivery in 3D printed gels. Quantification of DNA (A), GAG (B), collagen (C), and calcium (D) deposition after 28 days of in vitro culture in the control and gene activated hydrogels. Young´s modulus (E) and Equilibrium modulus (F) of the control and gene activated gels after 28 days of in vitro culture. (G) Histological and immunohistochemical examination of the control and gene activated constructs after 28 days of in vitro culture. Scale bar = 0.5 mm. (*) Denotes significance (n=4, p<0.05) in comparison to the rest of the groups; (**) denotes significance (n=4, p<0.01) in comparison to the rest of the groups; (***) denotes significance (n=4, p<0.001) in comparison to the rest of the groups; (!) denotes significance (n=4, p<0.05) in comparison to the ALG-Ca, ALG-MC and nHA-pBMP2 groups.

After 4 weeks of subcutaneous implantation in a nude mouse model, mineralization and matrix deposition in the control and gene activated 3D printed gels were assessed. In the ALG-Ca gels, microCT examination revealed high mineralization of the control and nHA-BMP2 containing groups (Fig.7.8.A), while very little calcification was present in all the ALG-MC groups (Fig.7.8.A). H&E staining revealed the presence of blood vessels in the nHA-pBMP2 containing gels and in the ALG-MC control gels (Fig.7.8.B). In the gene activated ALG-MC groups, H&E staining showed the presence of soft tissue aggregates which stained intensely for GAG (Fig.7.8.C) and collagen (Fig.7.8.D). Immunohistochemistry showed intense staining for collagen type II (Fig.7.8.E) in the aggregates observed in these gene activated gels, but only the pTGF-pBMP2 group was positive for collagen type X (Fig.7.8.F). Staining for collagen type II and X was also observed in the control and nHA-pBMP2 containing ALG-Ca gels (Fig.7.8.E and F).
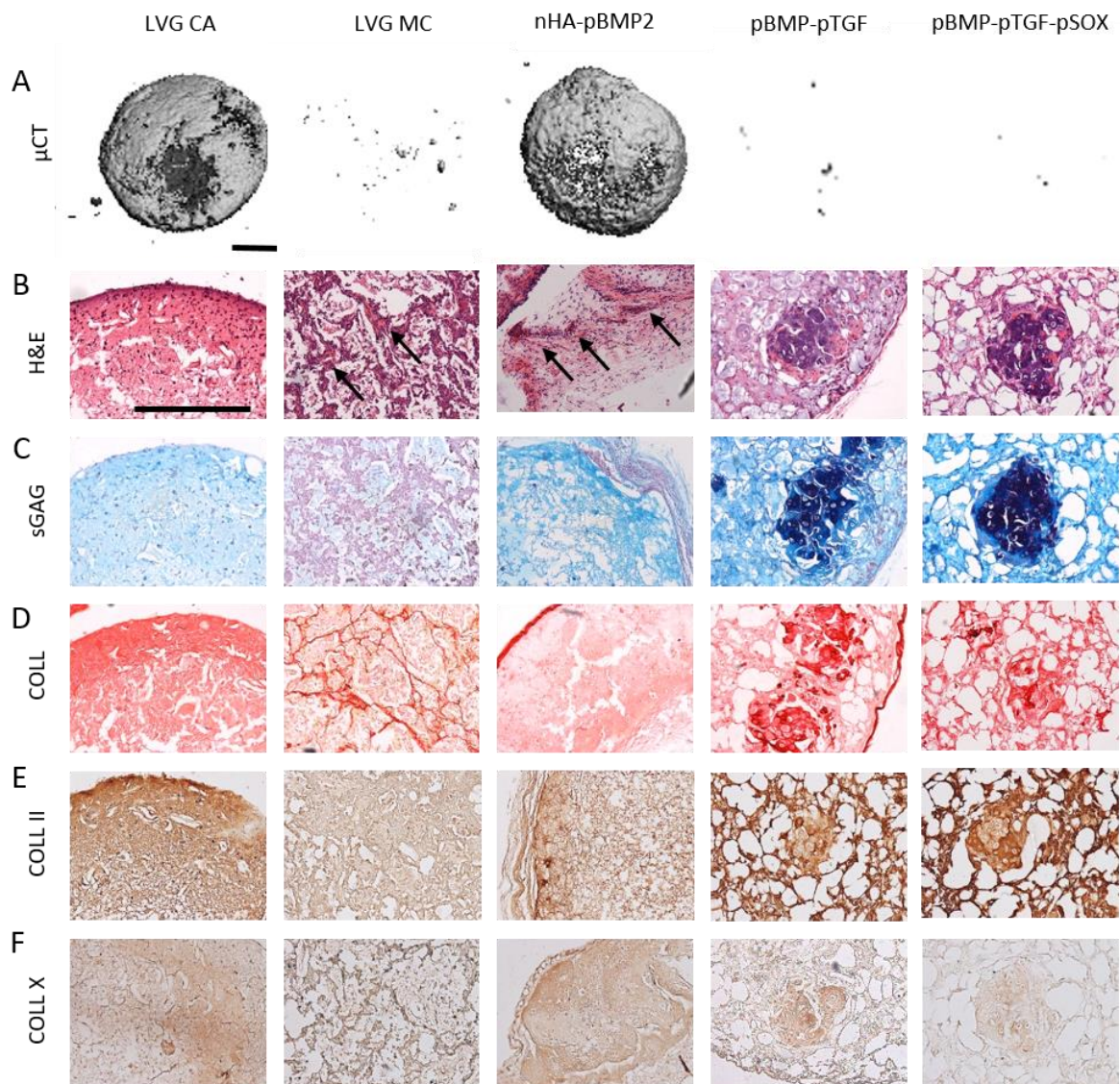
Fig.7.8. In vivo therapeutic gene delivery in 3D printed gels after 4 weeks of subcutaneous implantation. (A) MicroCT images of the implanted groups after 4 weeks of in vivo implantation. (B) H&E histological examination of the implanted constructs, black arrows indicate areas of blood vessel activity. Histological examination of GAG (C) and collagen (D) deposition in the implanted gels. Immunohistochemical examination of collagen type II (E) and type X (E). Scale bar = 1 mm for A and 0.5 mm in B-F.

7.3.6. Spatially patterned therapeutic gene delivery within mechanically reinforced osteochondral gene activated hydrogels can modulate stem cell fate zonally *in vitro* and *in vivo*

Cylindrical PCL porous constructs of 6 mm diameter by 6 mm height (Fig.7.9.A) were 3D printed using fused deposition modeling. SEM imaging of these constructs showed a fiber diameter of 159.71 +/- 34.79 µm (Fig.7.9.B) and a lateral spacing between fibers of 246.77 +/- 47.9 µm (Fig.7.9.C). Alginate and ALG-MC hybrid gels containing 1:1 and 1:2 ratio of alginate to methylcellulose were cast into the PCL scaffold (Fig.7.9.A) to produce mechanically reinforced composites. The Young´s modulus of the empty PCL and the composites was significantly higher than the non-reinforced gels (Fig.7.9.D). These PCL-hydrogel composites also showed mechanical properties similar to porcine cartilage (Fig.7.9.D). MSCs and RALA-pGFP complexes were encapsulated in the alginate (Fig.7.9.E) and ALG-MC hybrid gels (Fig.7.9.F and G) and cast into the PCL scaffolds. Successful transfection of the encapsulated cells was observed at day 7 after fabrication (Fig.7.9.E, F and G).
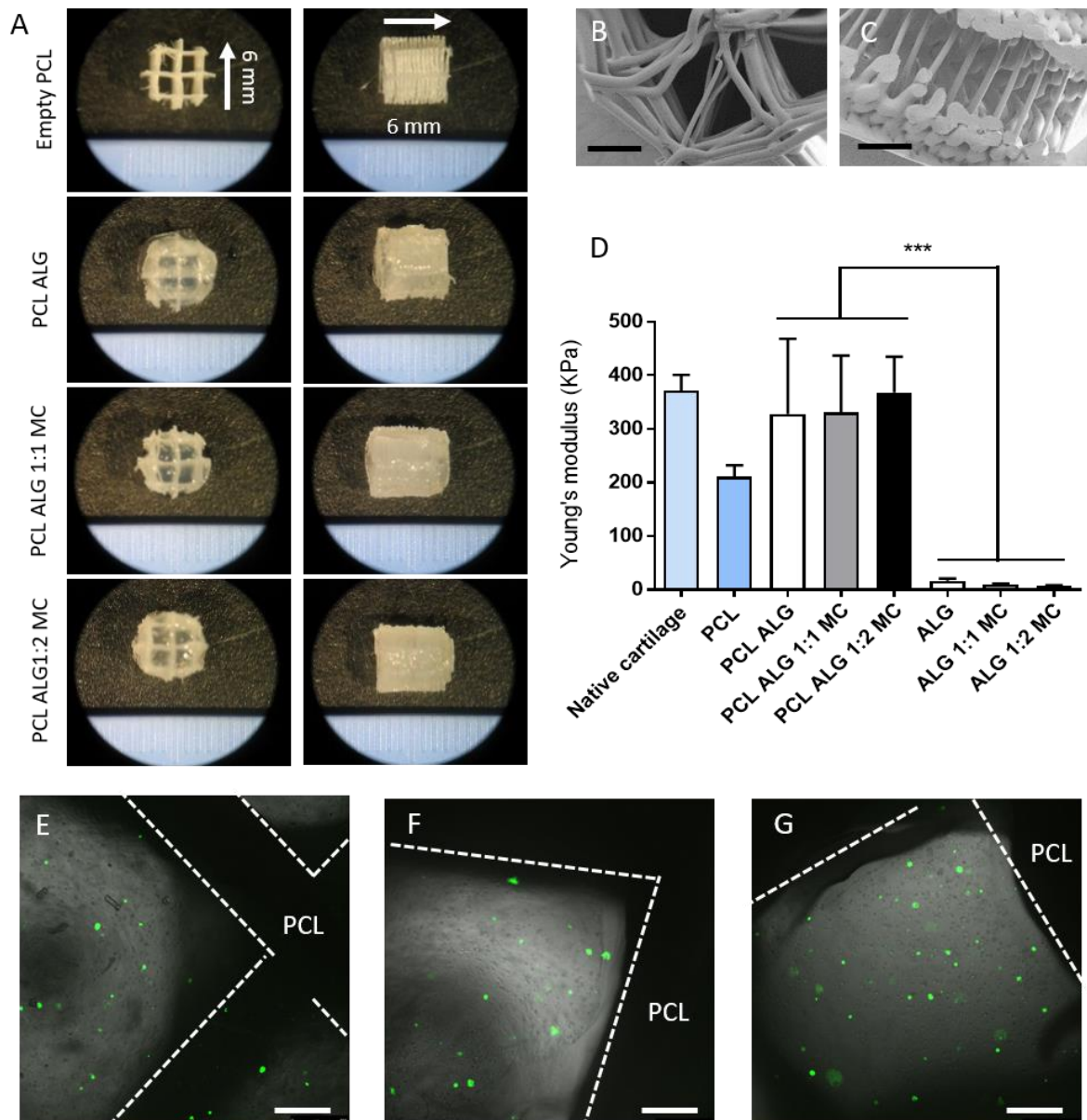
Fig.7.9. Alginate-PCL mechanically reinforced constructs. (A) Macroscopic examination of the PCL constructs alone and cast with alginate (PCL ALG) and ALG-MC (1:1 and 1:2) gels. SEM images of the top (B) and lateral (C) of the PCL constructs. (D) Young´s modulus of the PCL empty constructs, PCL reinforced gels and empty gels in comparison to native porcine cartilage. Fluorescent imaging of MSC-laden PCL reinforced alginate (E), ALG-MC 1:1 (F) and ALG-MC 1:2 (G) gels containing RALA-pGFP complexes at day 7 after fabrication. Scale bar = 500 μm for B and C and 250 μm for E, F and G. (***) Denotes significance (n=4, p<0.001).

Having assessed the mechanical properties of alginate-PCL composites, PCL porous constructs of 6 mm in diameter by 5 mm in height (Fig.A.7.A) were 3D printed and cast with the developed hydrogels to form osteochondral bilayer constructs. The osseous region was filled with either control or gene activated ALG-Ca bioinks containing MSCs and nHA-pBMP2 complexes. The cartilaginous region was filled with either ALG-MC control or with gene activated ALG-MC bioinks containing either pTGF-pBMP2 or pTGF-pBMP2-pSOX9 chondrogenic gene combinations.

These mechanically reinforced gene activated bilayers were cultured *in vitro* for 4 weeks and analysed for their biochemical and histological composition (Fig.7.10). The control group (Fig.7.10.A) showed similar levels of GAG (Fig.7.10.A and E), collagen (Fig.7.10.A and F) and calcium (Fig.7.10.A and G) in both the *chondro* and *osteo* layer. In contrast, significant differences between the levels of GAG (Fig.7.10.E), collagen (Fig.7.10.F) and calcium (Fig.7.10.G), could be observed between the *chondro* and *osteo* layer of both, pTGF-pBMP (Fig.7.10.B) and pTGF-pBMP-pSOX groups (Fig.7.10.C). While the *chondro* layer of both gene activated groups showed significant higher levels of GAG (Fig.7.10.B, C and E) and collagen (Fig.7.10.B,C and F) in comparison to their *osteo* layer and both layers of the control groups, it showed reduced levels of calcification (Fig.7.10.B, C and G). Immunohistochemical examination of the *chondro* layers of all the 3 groups (Fig.7.10.H) revealed higher collagen type II staining in the *chondro* layers of both gene activated groups, and collagen type I staining in the pTGF-pBMP group.
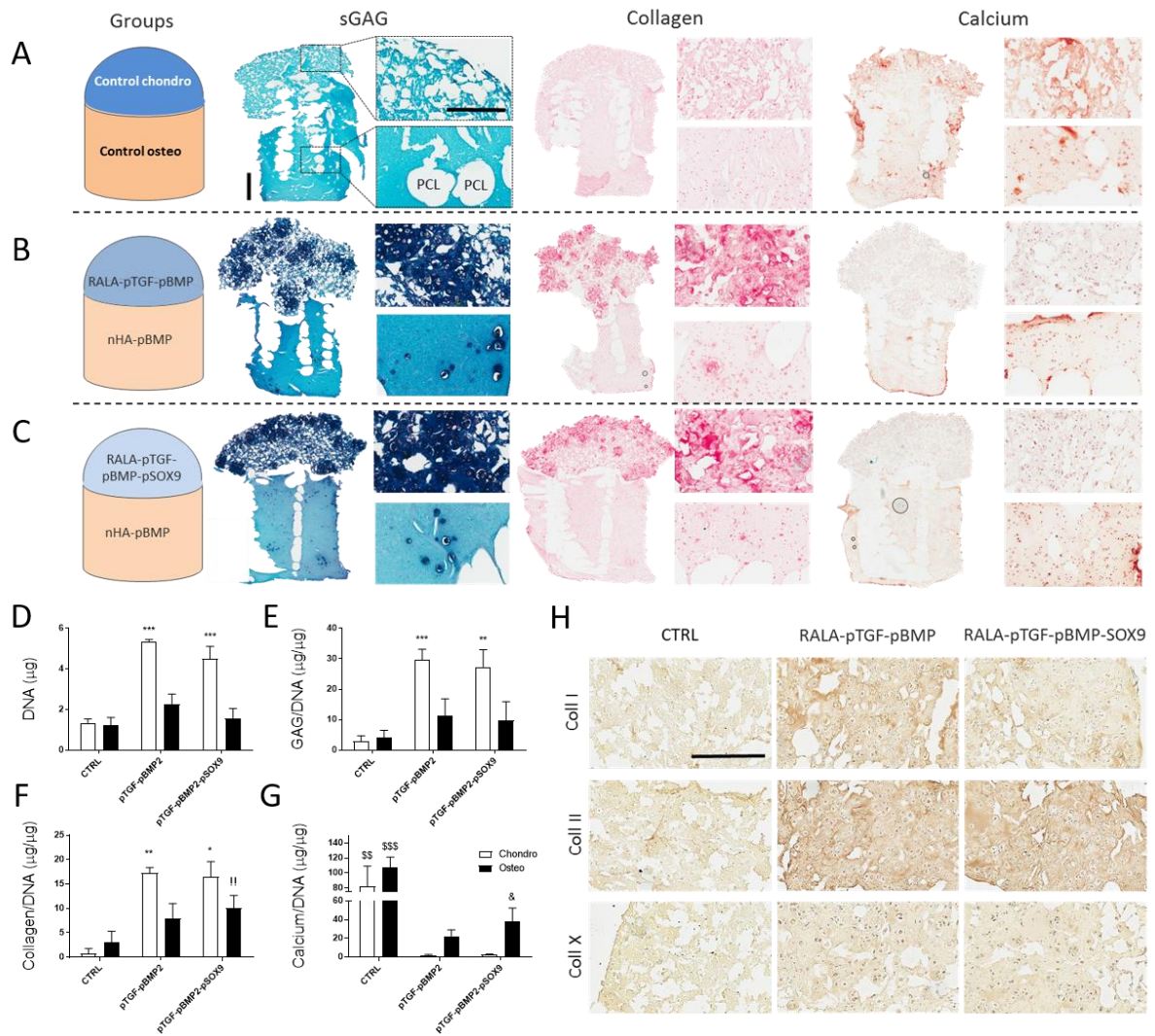
Fig.7.10. Spatial therapeutic gene delivery in mechanically reinforced alginate gels in vitro. Histological analysis of GAG, collagen and calcium of the control (A), nHA-pBMP/RALA-pTGF-pBMP (B) and nHA-pBMP/RALA-pTGF-pBMP-pSOX (C) groups after 28 days of in vitro culture. Quantification of levels of DNA (D), GAG/DNA (E), collagen/DNA (F) and calcium/DNA (G) in the chondro and osteo layers of the control and gene activated groups after 28 days of in vitro culture. (H) Immunohistochemical analysis of the chondro layers of the control and gene activated hydrogels. Scale bar = 1 mm in the high magnification images and 0.2 mm in the rest of the images. (*) Denotes significance (n=4, p<0.05) in comparison to the rest of the groups; (**) denotes significance (n=4, p<0.01) in comparison to the rest of the groups; (***) denotes significance (n=4, p<0.001) in comparison to the rest of the groups; (!!) denotes significance (n=4, p<0.01) in comparison to the osteo layer of the control; ($$) denotes significance (n=4, p<0.01) in comparison to the gene activated groups; ($$$) denotes significance (n=4, p<0.001) in comparison to the gene activated groups; (&) denotes significance (n=4, p<0.05) in comparison to the chondro layers of both gene activated groups.

In order to assess the *in vivo* therapeutic potential of the developed bilayered constructs, the day after fabrication, mechanically reinforced control and gene activated constructs were implanted subcutaneously in a nude mouse model. After 4 weeks *in vivo*, the mineralization and histological composition of the constructs was analysed. MicroCT scans of the implants showed increased mineralization (Fig.7.11.D) in the *osteo* and *chondro* layer of both the control (Fig.7.11.A) and pTGF-pBMP (Fig.7.11.B) groups, in comparison to the pTGF-pBMP-pSOX9 group (Fig.7.11.C), with mineralization localized to the *osteo* layer in all the implanted constructs. H&E staining also revealed significantly higher vascularization of the *osteo* layers of both gene activated groups (Fig.7.11.B, C and E) in comparison to their condro layers and both layers of the control group (Fig.7.11.A and E). GAG staining of the constructs showed intense staining of cell aggregates in the pTGF-pBMP-pSOX group (Fig.7.11.C) which also stained positive for collagen type II (Fig.7.11.F) and negative for collagen type X (Fig.7.11.G). In contrast, the *osteo* layers of all the groups stained positive for collagen type II and X (Fig.7.11.F and G), and the *chondro* layer of the pTGF-pBMP group showed positive collagen type X staining (Fig.7.11.G).
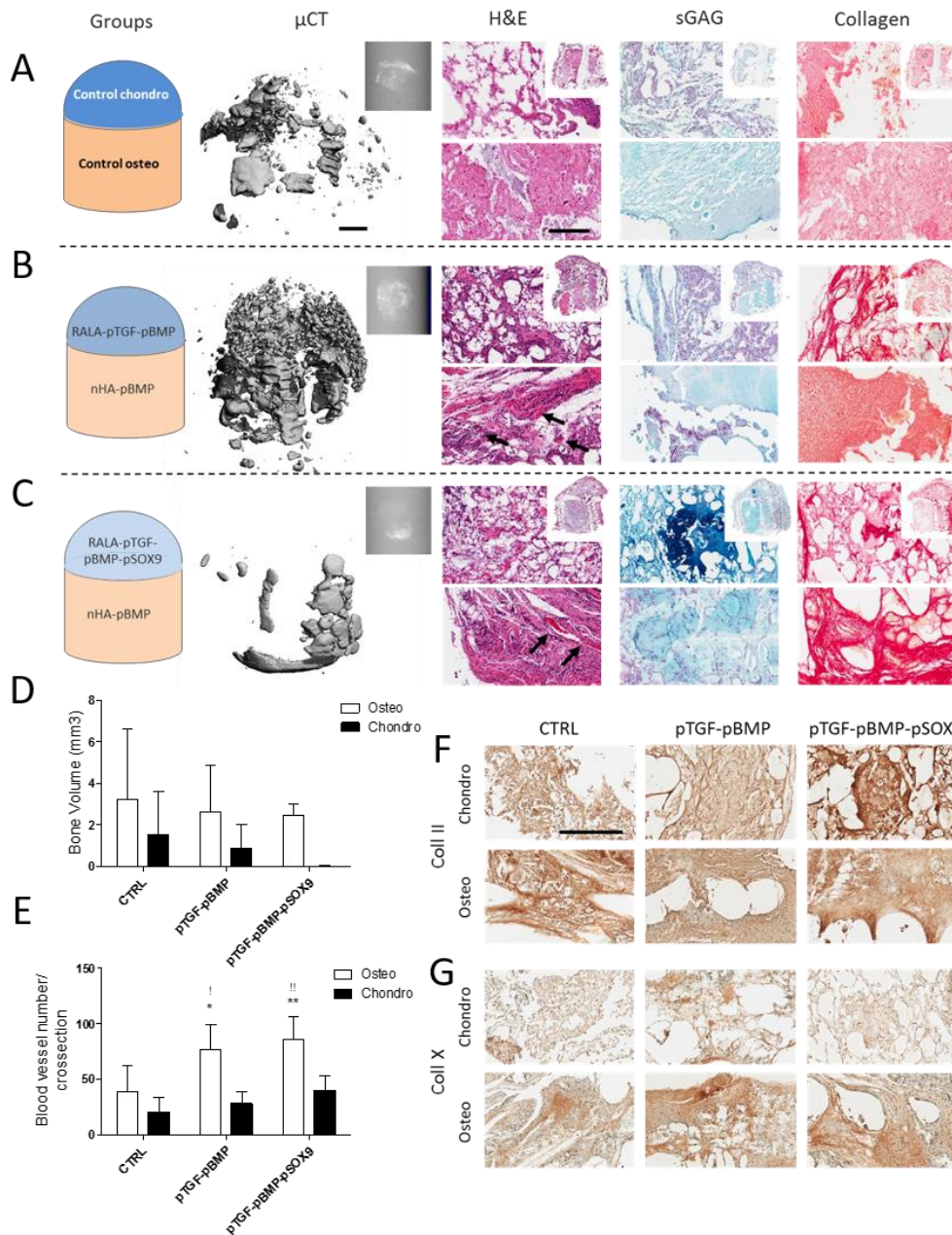
Fig.7.11. Spatial therapeutic gene delivery in mechanically reinforced alginate gels in vivo. MicroCT, Histological analysis of H&E, GAG, collagen and calcium staining of the control (A), nHA-pBMP/RALA-pTGF-pBMP (B) and nHA-pBMP/RALA-pTGF-pBMP-pSOX (C) groups after 4 weeks of in vivo implantation. Black arrows highlight areas of blood vessel activity. Quantification of levels of bone volume (D) and blood vessels (E) in the chondro and osteo layers of the control and gene activated groups after 4 weeks of in vivo implantation. Immunohistochemical analysis of the chondro and osteo layers collagen type II (F) and type X (G) content of the control and gene activated hydrogels after 4 weeks of in vivo implantation. Scale bar = 1 mm in the high magnification images and 0.2 mm in the rest of the images. (*) Denotes significance (n=4, p<0.05) in comparison to chondro layer of all the groups; (**) denotes significance (n=4, p<0.01) in comparison to the chondro layer of all the groups; (!) denotes significance (n=4, p<0.05) in comparison to the osteo layer of the control; (!!) denotes significance (n=4, p<0.01) in comparison to the osteo layer of the control.

7.4. Discussion

The overall objective of this study was to 3D print a mechanically robust, gene activated construct capable of controlling the spatial differentiation of stem cells to enable the engineering of an osteochondral tissue. To this end, a pore-forming bioink was first developed by blending alginate and methylcellulose. Secondly, reporter gene delivery in this pore-forming bioink was explored, which enabled accelerated release of non-viral vector-pDNA complexes and an enhanced capacity to transfect encapsulated MSCs over time. These gene activated hydrogels were also tested *in vivo*, highlighting the capacity of these gels to transfect host and transplanted cells. Next, therapeutic gene delivery was assessed to modulate MSC phenotype. RALA-mediated gene delivery in 3D printed ALG-MC gels of two different chondrogenic gene combinations (pTGF-pBMP and pTGF-pBMP-pSOX) resulted in enhanced chondrogenesis of MSCs *in vitro* and *in vivo*. In contrast, nHA-mediated gene delivery of pBMP2 in ALG-Ca gels promoted calcification *in vitro* and vascularization *in vivo*. Finally, the nHA and RALA gene activated alginate-based hydrogels were spatially cast into a mechanically functional 3D printed PCL scaffold, forming bilayered constructs able to zonally direct the differentiation of encapsulated MSCs. *In vitro*, increased deposition of GAG and collagen were observed in the chondrogenic layers of the gene activated constructs, while calcification was observed only in the osteogenic layer. *In vivo* subcutaneous implantation of the gene activated constructs resulted in stable chondrogenesis in the chondrogenic layer containing pTGF-pBMP-pSOX genes, whereas vascularization and mineralization of this construct was generally confined to the osteogenic layer, recapitulating key aspects of the biochemical gradients present in the native osteochondral unit.

Methylcellulose is the simplest cellulose derivative, synthetized by the etherification of cellulose (Nasatto et al., 2015). The hydroxyl groups in the methylcellulose molecular structure (Fig.7.1.A) provide high solubility in aqueous solutions, while the methyl groups prevent aggregation and crystallization (Nasatto et al., 2015). Due to its inverse thermal gelling nature, this biopolymer can also gel at high temperatures depending on its molecular weight, concentration and the presence of salts (Nasatto et al., 2015; Schütz et al., 2015; Thirumala et al., 2013). Precisely, the lack of gelling of the methylcellulose in the ALG-MC paste, due to the need of higher

temperatures than those used during fabrication and *in vitro* culture (Nasatto et al., 2015; Thirumala et al., 2013), allowed for the methylcellulose to be released from the ALG-MC constructs. One day after fabrication, histological and cryoSEM analysis of the hybrid hydrogels revealed dramatic changes on their macro structure (Fig.7.1.C) and increased micro-porosity (Fig.7.1.D and G). In addition, the wet weight of the hybrid gels decreased by about 20% (Fig.7.1.E).

Hydrogels, such as alginate, although considered as promising bioinks for 3D bioprinting (Malda et al., 2013), usually lack sufficient viscosity to be able to extrude continuous filaments when 3D printed and maintain their structural integrity after the printing process (Daly et al., 2017; Malda et al., 2013). Partial gelation of alginate, usually through the addition of divalent cations such as Ca^{2+}, has been explored to satisfy the rheological requirements for extrusion printing (Chung et al., 2013; Ozbolat and Hospodiuk, 2016). But poor ink homogeneity due to uncontrolled gelation (Chung et al., 2013; Kuo and Ma, 2001) and possible effects of high concentrations of calcium ions on stem cell viability (Cao et al., 2012a), might hinder the application of this strategy for 3D bioprinting. To solve these issues, the development of hybrid multicomponent gels through the addition of biopolymers which do not contribute to hydrogel crosslinking, and therefore can be washed away after construct fabrication, such as cellulose, in the form of methylcellulose or nanofibrillated cellulose, has been previously explored (Markstedt et al., 2015; Müller et al., 2017; Schütz et al., 2015). In this study, the addition of methylcellulose to alginate to form printable ALG-MC hybrid gels resulted in increased rheological properties (Fig.7.2.A and B) which enable an accurate fiber deposition, and a comparable printability to partially crosslinked alginate (Fig.7.2.C and D-G), similar to previous reports (Schütz et al., 2015). Furthermore, the encapsulation of either GFP or dtTomato genetically modified MSCs in ALG-Ca and ALG-MC gels respectively, resulted in defined spatial patterns of both cell populations (Fig.7.2.I) when simultaneously printed using a multi-head system, thus enabling the engineering of integrated multiphase tissues.

According to the shift in the biofabrication window proposed by Malda et al. (2013), bioinks must not only be printable but also they must be cytocompatible and allow for cell differentiation and tissue formation (Malda et al., 2013). 3D printing of

stem cell laden ALG-MC hybrid constructs showed significantly higher cell viability in comparison to ALG-Ca (Fig.7.3.B and C), similar to previous reports which showed higher cell dead in ALG-Ca bioinks (Cao et al., 2012a). Also, *in vitro* chondrogenic differentiation of the encapsulated cells showed similar levels of chondrogenesis in both bioinks. However, statistically significant calcium deposition (Fig.7.3.G) and positive collagen type X staining (Fig.7.3.H) was observed in the ALG-Ca gels suggesting chondrocyte hypertrophy and endochondral progression. In a recent study by Müller et al. (2017), chondrocyte laden alginate-nanocellulose gels were assessed for the maintenance of hyaline cartilage phenotype, resulting in a fibrocartilage phenotype with high collagen type I deposition (Müller et al., 2017). In contrast, the observed stable chondrogenic phenotype in the ALG-MC gels, characterized by high deposition and homogenous distribution of collagen type II, could be due to the decrease in Young´s modulus of these hybrid gels (Fig.7.1.F), as soft substrates have been reported to promote TGF-β-mediated MSC differentiation (Park et al., 2011); whereas stiffer substrates have been shown to enhance MSC osteogenic differentiation and chondrocyte hypertrophy (Navarrete et al., 2017). Also, enhanced cell condensation due to the release of the methylcellulose and increased gel macro porosity, as evident in the histological examination (Fig.7.3.H), might have influenced stem cell chondrogenic differentiation (Ghosh et al., 2009). Further reasons for the development of stable chondrogenesis in the ALG-MC bioink in comparison to the fibrocartilage observed in the alginate-nanocellulose gels by Müller et al. (2017) might be the use of sulfated alginate which promoted cell adhesion and spreading and a more fibroblastic phenotype (Müller et al., 2017).

Driving *in vivo* stem cell differentiation towards a specific phenotype remains challenging in tissue engineering and, in particular, within 3D printed tissues. While recombinant protein administration presents many limitations, genetically engineering cells to act as factories for the production of growth and transcription factors has been hypothesized as a promising alternative option to direct the phenotype of host and transplanted cells at the site of injury (Evans, 2014; Heyde et al., 2007). Moreover, the addition of gene therapeutics in the form of non-viral nanoparticle-gene complexes to bioinks might allow for spatial distribution of the gene product to drive zonal MSC

differentiation and recapitulate the biochemical gradients found in native tissues (Daly et al., 2017). Nanoparticle-based vectors such as RALA and nHA have been previously explored for sustained matrix-based gene delivery for different applications (Ali et al., 2017; Castaño et al., 2014; Curtin et al., 2012, 2015). Previously, in the fourth chapter of this thesis, transfection of MSCs with reporter and therapeutic genes, revealed the effects of these two nanoparticles on MSC chondrogenic and osteogenic differentiation. While RALA-pDNA complexes enhanced chondrogenic differentiation of transfected MSCs, nHA drove mineralization of MSCs and endochondral ossification. Although the entrapment of these nanoparticle-pDNA complexes into 3D printable hydrogels could finely localize their delivery *in vivo*, their release and availability to transplanted and host cells would be limited by the slow degradation profile of easy printable high molecular weight alginates (Alsberg et al., 2003; Daly et al., 2017). Modulating micro-porosity of alginate hydrogels may provide temporal control over the release and uptake of encapsulated non-viral gene therapeutics (Huebsch et al., 2014).

In the current study, the addition of methylcellulose to gene activated alginate hydrogels enhanced the release of the nanoparticle-pDNA complexes over time, and facilitated complex uptake by encapsulated MSCs as evidenced by higher luciferase expression in the 1:1 and 1:2 ratio ALG-MC gels in comparison to the alginate control (Fig.7.4). The luciferase overexpression was maintained over 10 days, suggesting continuous RALA-pLUC uptake by encapsulated cells, in comparison to monolayer transfection as shown in the fourth and fifth chapter, in which luciferase production peaked at day 3 after transfection and significantly decreased at day 7. The observed enhanced release and transfection could be due to the higher pore diameter of around 700 nm (Fig.7.1.D and G) in the ALG-MC group, which might have facilitated the uptake of RALA-pDNA complexes, of around 60 nm in diameter (McCarthy et al., 2014), in comparison to the pores in the bulk alginate gel which were shown to be around 20 nm (Fig.7.1.D and G). 3D printed ALG-MC cell laden gene activated constructs also showed same transfection trends when RALA-pDNA and nHA-pDNA complexes were delivered (Fig.7.5.G and Fig.A.4), in comparison to ALG-Ca. In this group, gene delivery could have been hindered not only due to the pore size of the alginate matrix, but also by the $CaCl_2$ used to partially crosslink the hydrogels. Although, calcium cations have been shown to

directly interact with pDNA, facilitating liposome-mediated pDNA delivery at $CaCl_2$ concentrations between 5 and 25 mM, $CaCl_2$ concentrations of 50 mM and higher were shown to have an opposite effect and significantly diminish transfection (Lam and Cullis, 2000). Thus, the $CaCl_2$ concentrations used for alginate pre-crosslinking could have had a negative effect on cell transfection.

ALG-MC 3D printed gels were also tested as a platform for gene delivery *in vivo*. When implanted subcutaneously, delivery of RALA and nHA-pLUC complexes in acellular ALG-MC gels showed early transfection of host cells that peaked at day 7 and decreased progressively until day 21 (Fig.7.6.H). In contrast, ALG-Ca hydrogels offered a peak of transgene expression at day 14 which was maintained until day 21 (Fig.7.6.H). MSC-laden ALG-MC gene-activated constructs also showed increased transfection *in vivo* in comparison to ALG-Ca gels. But, although levels of transgene expression were higher in the cell laden groups than in the acellular, luciferase expression in the MSC containing gels peaked at day 3 and decreased until day 21 (Fig.7.6.E-G and I). The observed decrease could be due to short lifespan of transplanted MSCs as previously reported in literature (Deschepper et al., 2011; Eggenhofer et al., 2014; Logeart-Avramoglou et al., 2010). Mineralization of these constructs after implantation was also assessed showing higher calcification of the ALG-Ca gels in comparison to ALG-MC constructs (Fig.A.5.2). $CaCl_2$ crosslinked alginate constructs have been previously shown to calcified upon *in vivo* implantation (Davey et al., 2000), due to phosphate interaction and hydroxyapatite crystals formation (Lee et al., 2010). Lack of mineralization of ALG-MC constructs, possibly due to disruption of the alignment of alginate polysaccharide chains (Lee et al., 2010), highlights the therapeutic relevance of this approach for soft tissue engineering.

Once reporter gene delivery was assessed in the ALG-MC hybrid constructs *in vitro* and *in vivo*, therapeutic gene delivery was investigated to modulate MSC differentiation towards either osteogenic or chondrogenic phenotype. BMP2 nHA-mediated gene delivery was used in 3D printed ALG-Ca gels to promote MSC osteogenesis, while two different gene combinations, pTGF-pBMP and pTGF-pBMP-pSOX, were tested, in combination with ALG-MC gels, to promote chondrogenesis. nHA-mediated delivery of pBMP2 promoted *in vitro* calcification (Fig.7.7.D and G), and enhanced mineralization and vascularization *in vivo*, in comparison to the ALG-MC

groups (Fig.7.8). In contrast, the RALA-mediated co-delivery of pTGF-pBMP and pTGF-pBMP-pSOX promoted chondrogenesis of MSCs *in vitro* and *in vivo* (Fig.7.7 and 7.8). Even though both chondrogenic combinations were shown to promote GAG and collagen type II deposition, pTGF-pBMP co-delivery revealed positive staining for collagen type I *in vitro* (Fig.7.7.G) and for collagen type X *in vivo* (Fig.7.8.F), suggesting the progression of encapsulated MSCs towards the endochondral ossification pathway (Lyama et al., 1991). The addition of SOX9 to BMP2 and TGF-β3 overexpression, as a regulator of chondrocyte hypertrophy, offered a more stable hyaline cartilage phenotype, probably due to the inhibition of RUNX2 transactivation as previously described (Liao et al., 2014; Yamashita et al., 2009).

Native biological tissues and organs are not homogenous, they exhibit fine spatial organization of cell types, extracellular matrix (ECM) components and bioactive cues. Successful tissue engineering strategies should aim to recapitulate this structural complexity for the fabrication of functional musculoskeletal tissues. In addition, the need of mechanically robust constructs, able to withstand the mechanical stresses once implanted, poses an additional challenge for the success of tissue engineered orthopedic devices. Due to the aforementioned issues, we aimed to engineer a gene activated, mechanically reinforced bilayer construct for the recapitulation of the osteochondral unit, comprising a superficial layer of hyaline cartilage over an underlying osseous layer (Martini et al., 2009). PCL printed constructs, with bulk mechanical properties similar to those of articular cartilage (Fig.7.9), were used as scaffolding for the spatial distribution of the developed nHA and RALA gene activated bioinks. *In vitro*, nHA-mediated delivery of pBMP2 to the *osteo* layer and co-delivery of either pTGF-pBMP2 or pTGF-pBMP-pSOX for the *chondro* layer, resulted in the zonal distribution of calcified and cartilaginous tissues which did not occur in the non-transfected controls (Fig.7.10). After 4 weeks of *in vivo* implantation, this bioprinted construct promoted mineralisation and vascularisation of the osteogenic layer, and the formation of GAG and Collagen type II rich cell clusters in the chondrogenic layer (Fig.7.11), thus spatially guiding cell differentiation and spatial ECM deposition, and highlighting the potential of this approach for *in vivo* osteochondral repair.

7.5. Conclusion

3D printable alginate-based materials could be used to zonally deliver pDNA encoding for growth and transcription factors, guiding spatial stem cell differentiation *in vitro* and *in vivo*. This study highlights the potential of biomaterial-guided gene delivery to engineer spatially complex musculoskeletal tissues that could be of clinical relevance for the treatment of injuries and disorders involving disruption of biological interfaces.

In this final experimental chapter, the optimization of the gene delivery vector, gene combination and bulk material presented in previous chapters, enabled the engineering of a multiphasic construct to spatially direct the differentiation of MSCs *in vitro* and *in vivo*, thus condensing all previous results into a tissue engineering strategy of therapeutic relevance for the treatment of osteochondral defects.

CHAPTER 8

Discussion

8.1. Summary

The objective of this thesis was to explore the combination of nanoparticle-based non-viral gene delivery and biofabrication techniques to develop a multiphasic gene activated construct for osteochondral TE. Non-viral gene delivery of therapeutic genes is a promising approach to direct MSC differentiation, but the success of this technique ultimately depends on the choice of gene delivery vector. Different non-viral gene carriers were assessed to this end, with results identifying nHA and the RALA peptide as optimal for osteogenesis and chondrogenesis of MSCs respectively. Also, delivery of genes encoding for different growth and regulatory factors, alone or in combination, was explored to identify the best gene combination to successfully direct MSCs differentiation towards the desired phenotype. To gain spatiotemporal control over gene transfection and MSC differentiation, these delivery vectors were then incorporated into alginate-based bioinks that were able to transfect transplanted MSCs and host cells *in vivo* and to support MSC differentiation and *de novo* tissue formation. While nHA-pDNA complexes entrapped in ionically pre-crosslinked alginate were shown successful to drive endochondral ossification of MSCs, alginate-methylcellulose hybrid gels containing RALA-pDNA complexes were observed to support stable non-hypertrophic chondrogenesis of MSCs. Finally, both gene activated bioinks were employed, in combination with PCL, to engineer a mechanically robust bi-phasic osteochondral construct, capable of spatially directing MSC differentiation and tissue production to recapitulate key biochemical aspects found in the native osteochondral unit.

This thesis began by investigating the capacity of nHA to transfect MSCs encapsulated in alginate hydrogels for bone and cartilage TE (chapter 3). nHA has been previously explored for bone tissue engineering due to its osteoinductive nature (Cunniffe, Curtin, Thompson, Dickson, & O'Brien, 2016), enhanced transfection efficiency in comparison to commercial CaP, and high biocompatibility, offering better

cell viability than Lipofectamine 2000 (Curtin et al., 2012). Gene therapeutics can be combined with biomaterials for a prolonged, sustained and localized *in situ* production of a protein of interest. This approach may overcome the limitations associated with 2D transfection (Dinser et al., 2001; Madry et al., 2003) and direct injection which are not ideal for targeting a specific tissue or cell type (Madry and Cucchiarini, 2014). Therefore, after confirming successful nHA-mediated transfection of MSCs in 2D, nHA-pDNA complexes were entrapped in 3D alginate gels and the delivery of reporter and therapeutic genes to MSCs was analysed. Characterization of reporter gene expression and nHA-pDNA complex uptake confirmed effective sustained transfection of MSCs over time. Therapeutic gene delivery of TGF-β3 and BMP2 promoted sGAG and collagen type II production when the two genes were delivered in combination, or calcification and collagen type X deposition when these genes were delivered in isolation. This capacity of nHA-mediated gene delivery to enhance osteogenesis and hypertrophy of MSCs was explored in later chapters to enhance *in vivo* bone formation and for the osseous layer of a multiphasic osteochondral gene activated construct. In contrast, the use of nHA might be limited for cartilage tissue engineering by its inherent osteogenicity. The addition of low concentrations of nHA to collagen scaffolds has been reported to significantly enhance bone repair in a rat cranial defect, thus demonstrating its osteoinductivity (Cunniffe, Curtin, Thompson, Dickson, & O'Brien, 2016). Also, *in vivo* nHA-mediated transfection in a collagen scaffold exhibited higher vascularization and bone repair than the use of PEI as gene delivery vector, suggesting a synergistic effect between nHA and the overexpression of BMP2 and VEGF (Curtin et al., 2015). Therefore, recognizing the limitations of nHA as a gene delivery vector for stable chondrogenesis of MSCs, different non-viral nanoparticle-based vectors were assessed in the following chapter for this purpose.

In chapter 4 novel and established non-viral vectors were compared for chondrogenic and osteogenic differentiation of MSCs. Cationic polymers (PEI), inorganic nanoparticles (nHA) and amphipathic peptides (RALA peptide) were assessed for the modulation of stem cell fate after reporter and therapeutic gene delivery. Cationic polymeric gene delivery vectors such as PEI have been traditionally used as gold standard for non-viral gene delivery (Santos et al., 2011). However, their potential

cytotoxicity (Lv et al., 2006; Yin et al., 2014) and sensitivity to media supplementation with serum and antibiotics (Baker et al., 1997) limit their use in tissue engineering. Inorganic particles, such as nHA, and different classes of peptides, such as the RALA amphipathic peptide could be promising alternatives to cationic lipids and polymeric vectors due to their excellent biocompatibility, long term stability and low cell toxicity (Curtin et al., 2012; McCarthy et al., 2014). Although the three gene carriers offered comparable transfection efficiencies, they exerted unique effects on metabolic activity, cellular morphology and the phenotype of MSCs. Moreover, when reporter genes were delivered, MSCs transfected with PEI underwent adipogenesis, whereas MSCs transfected with nHA and RALA underwent osteogenesis when cells were cultured in osteo-adipo media. These differential phenotypes could be due to the observed transfection-induced morphological and cytoskeletal tension changes. Increased cytoskeletal tension and focal adhesions (as seen when nHA and RALA were used) have been reported to enhance osteogenesis of MSCs, while a more rounded morphology (as observed when PEI was used) can lead to a switch towards the adipogenic pathway (Feng et al., 2010; Kilian et al., 2010; Rodríguez et al., 2004; Sonowal et al., 2013). In order to understand the influence of the delivery vector when complexed with therapeutic genes, we next evaluated the delivery of pDNA encoding for the growth factors TGF-β3 and BMP2, in combination or in isolation, on MSC differentiation. While nHA promoted significantly lower transgene expression than the other vectors, it induced MSC mineralization in 2D and accelerated MSC hypertrophy and endochondral ossification in 3D pellet culture. In contrast, RALA exhibited a reduced osteogenic potential and promoted a more stable hyaline cartilage-like phenotype in pellet culture. The PEI treated MSCs failed to undergo either osteogenesis or chondrogenesis in 2D and 3D pellet culture despite high levels of therapeutic protein production. These results further confirmed the osteogenic potential of nHA-mediated gene delivery to induce MSC osteogenesis and hypertrophy, and highlighted RALA as a promising option for the stable chondrogenesis of MSCs and cartilage tissue engineering.

Having identified RALA as a promising gene delivery vector for cartilage tissue engineering, in chapter 5 RALA-mediated gene delivery of chondrogenic growth and regulatory factors was explored, in both normoxic and hypoxic culture conditions, to

promote chondrogenesis of MSCs and to suppress hypertrophy and endochondral ossification. Bone marrow-derived MSCs (BMSCs) are the most common type of MSC used for musculoskeletal tissue engineering applications (Goldberg et al., 2017). Although BMSCs are able to differentiate *in vitro* into chondrocytes, they typically terminally differentiate along an endochondral route, which presents a significant challenge for the engineering of stable articular cartilage (Hellingman et al., 2011; Mueller and Tuan, 2008; Pelttari et al., 2006; Vinardell et al., 2012). While delivery of genes encoding for growth factors such as TGF-β3, BMP2 and BMP7 has been explored for chondrogenesis of MSCs (Hao et al., 2008; Mason et al., 1998; Zachos et al., 2007), the risk of hypertrophy still persists. Following RALA 2D transfection optimisation to maximise transfection efficiency and minimise cell death, pDNAs encoding for TGF-β3, BMP2 and BMP7 were delivered in combination or isolation to BMSCs in hypoxia. The co-delivery of TGF-β3 and BMP2 was shown to initiate robust *in vitro* chondrogenesis of MSCs, showing higher levels of GAG deposition and collagen type II but no collagen type X. As oxygen levels are a determinant factor to influence stable BMSC differentiation, gene delivery of the chondrogenic regulators CHM1, GREM1, HDAC4 and SOX9 was assessed on BMSCs in normoxia. In 20% pO_2, MSCs transfected with both TGF-β3 and BMP2 exhibited high levels of GAG and collagen type II deposition but also mineralisation and collagen type X, suggesting endochondral progression. In contrast, when either CHM1, GREM1 or SOX9 genes were co-delivered with TGFβ3 and BMP2 absence of calcium deposition or collagen type X was observed, suppressing endochondral progression of BMSCs. The results of this chapter confirmed the therapeutic potential of RALA-mediated combinatorial gene delivery for the stable chondrogenesis of MSCs. In later chapters, the reported hypertrophy effects of the overexpression of TGF-β3 and BMP2 in normoxia were leveraged in combination with nHA to drive endochondral bone formation *in vivo*, while the RALA-mediated co-delivery of TGF-β3, BMP2 and SOX9 was explored for stable chondrogenic induction in the cartilage layer of a gene activated osteochondral construct.

In chapter 6, we sought to explore the osteogenic potential of nHA-mediated transfection confirmed in chapter 4, and the gene activated alginate hydrogels in chapter 3, to engineer gene activated bioinks for the 3D printing of mechanically robust

constructs for *in vivo* bone TE. Emerging biofabrication techniques, such as 3D bioprinting, are promising solutions to produce scaled up, mechanically reinforced composites for musculoskeletal tissue engineering (Daly et al., 2016, 2017). Furthermore, 3D bioprinting allows for the deposition of specific biological cues in relevant locations, to drive complex tissue formation (Cooper et al., 2010). But, this is not easily achieved through the use of recombinant proteins, as hydrogels commonly used as bioinks show diffusive transport characteristics (Daly et al., 2017), and might cause non-localised effects (Bonadio et al., 1999). In contrast, engineering cells to locally produce growth and transcription factors through gene delivery may enable a more precise spatial control within 3D printed constructs. Therefore, MSC-laden gene activated hydrogels, containing nHA-pDNA complexes, were co-printed simultaneously with reinforcing PCL to engineer mechanically reinforced constructs for bone TE. Reporter gene delivery in these gene activated constructs, confirmed sustained temporal overexpression of the transgene for 14 days. Therapeutic co-delivery of the TGF-β3 and BMP2 genes in the gene activated 3D printed constructs enhanced GAG, collagen and mineral deposition when cultured *in vitro*. These results correlate with the results in previous chapters, in which nHA-mediated transfection enhanced osteogenesis of MSCs and the overexpression of TGF-β3 and BMP2 promoted progression of MSC phenotype towards the endochondral route. These MSC-laden gene activated 3D bioprinted constructs were then implanted subcutaneously *in vivo,* exhibiting increased mineralisation and vascularisation at 4 and 12 weeks post-implantation in comparison to acellular constructs, thus highlighting the therapeutic potential of bioink-based nHA-mediated gene delivery for bone TE. The developed bioink, capable of *de novo* bone tissue generation *in vivo* was explored in the last experimental chapter for the osseous layer of an osteochondral construct.

In the last experimental chapter, the final two objectives of this thesis were addressed. Alginate-methylcellulose (ALG-MC) hybrid gels were explored as gene-activated pore-forming bionks for enhanced gene delivery, and the capacity of these constructs to support cartilage and bone development was assessed. Also, the optimization of gene carrier, gene combination and bulk material developed in previous chapters, together with the assessment of ALG-MC hydrogels, were used to engineer a

biphasic mechanically robust gene activated construct for zonal differentiation of MSCs and recapitulation of the biochemical gradients present in osteochondral tissue. As previously discussed, the incorporation of non-viral gene delivery into 3D printable bioinks could be a promising approach to gain fine spatial control over the overexpression of a gene of interest. But the characteristics of alginate hydrogels could limit the cellular uptake of entrapped gene therapeutics, specially of those complexed to nanoparticles larger than 10 nm (Kearney et al., 2015). Therefore, we initially investigated the addition of methylcellulose to alginate gels in order to modulate their microposity so as to gain temporal control over the release and uptake of encapsulated non-viral gene therapeutics. ALG-MC hybrid gels showed enhanced microporosity and printability in comparison to alginate alone, and the hybrid gels also exhibited increased gene delivery *in vitro* and *in vivo* to encapsulated MSCs. But in terms of *in vivo* mineralization, these ALG-MC hybrid gels showed lower mineral deposition in comparison to the $CaCl_2$ pre-crosslinked hydrogels used in chapter 6, thus suggesting the potential of the ALG-MC bioinks for cartilage TE. Following reporter gene delivery characterization, combinatorial delivery of TGF-β3, BMP2 and SOX9 genes using the RALA peptide as delivery vector (combination identified in chapter 5) in ALG-MC, and BMP2 using nHA as the delivery vector in $CaCl_2$ pre-crosslinked gels, were used to engineer bi-phasic mechanically robust osteochondral constructs able to spatially direct MSC differentiation *in vitro* and *in vivo*. Also, it should be noted that RALA co-delivery of TGF-β3, BMP2 and SOX9 genes, resulted in a more stable chondrogenesis of MSCs than the co-delivery of just TGF-β3 and BMP2 *in vitro* and *in vivo*, without the reduction in GAG and collagen levels observed in chapter 5, possibly due to a more sustained biomaterial-mediated transfection of the 3 genes in comparison to direct 2D transfection.

In conclusion, the optimisation of gene delivery vector, gene combination and carrier material developed in the chapters of this thesis, allowed for the achievement of the main objective of this thesis, the engineering of novel 3D bioprinted gene activated constructs therapeutically relevant for osteochondral tissue regeneration.

8.2. Limitations

The BMSCs used in this thesis were isolated from skeletally immature, 3-4 months old porcine donors. And although pigs have been considered as a suitable animal model for evaluation of stem cell therapies for regenerative medicine (Bharti et al., 2016), differences still remain between progenitor cells of porcine and human origin (Noort et al., 2012). Also, results from cells isolated from young and healthy animal donors might not be comparable to results obtained from more therapeutically relevant aged and diseased human donors. A recent study showed that human MSCs from elderly patients exhibited slower proliferation rates, decreased chondrogenic and osteogenic potential, and increased senescence (Marędziak et al., 2016). Also, BMSCs from adult rabbit donors showed impaired proliferation, senescence, and chondrogenesis in comparison to juvenile cells (Beane et al., 2014). Therefore, the use of adult human cells and the comparison between different human and animal donors could validate the therapeutic impact of this thesis. Also, the choice of porcine BMSCs as model for non-viral gene transfection could limit the translation of the results presented in this thesis as transfection efficiency has been shown to vary between species (Curtin et al., 2012).

In this thesis, all *in vivo* studies were performed in an athymic mice subcutaneous, or ectopic, model. While subcuatenous implantation of TE constructs allow for their initial evaluation in a living organism, this model presents many limitations as these animals are immunocompromised and the subcutaneous implantation doesn´t recapitulate the mechanical stresses present in a knee joint. Orthopic evaluation of the therapies explored in this thesis in larger animal models might be more suitable for assessing the clinical relevance of these results. Therefore, further studies are required to assess the efficacy of this approach.

Regarding the delivery of different combinations of therapeutic genes to BMSCs, we focused on the tissue engineering outputs of the overexpression of these factors, while the molecular mechanisms behind their action were not analysed in depth. Although we hypothesised the possible molecular action based on previous literature, elucidation of the actual events would be of interest for the understanding of BMSC differentiation pathways. Also, despite demonstrating in chapter 5 that combinatorial

delivery of TGF-β3 and BMP2 genes together with either CHM1, GREM1 and SOX9 suppressed hypertrophy of MSCs, the combination of TGF-β3, BMP2 and SOX9 genes was chosen in the final experimental chapter as optimal for stable chondrogenesis of MSCs. This was selected based on previous literature reports as SOX9 has been extensively explored as a regulator of MSC chondrogenesis in combination with factors of the TGF-β superfamily (Liao et al., 2014; Park et al., 2012). The other identified combinations should be further assessed in future studies.

In the final chapter, temporal control of gene delivery was achieved through the inclusion of methylcellulose as a sacrificial material in alginate bioinks. Although the addition of different concentration of methylcellulose help to modulate vector-pDNA release and cellular uptake of the nanoparticle-gene complexes, a more controlled on-demand delivery might allow more finely controlled sequential delivery of therapeutic genes.

8.3. Concluding remarks

- The incorporation of nHA-pDNA complexes into alginate hydrogels to form gene activated constructs, allowed sustained transfection of encapsulated MSCs, leading to increased transgene expression over at least 14 days of culture. This was capable of modulating stem cell fate toward either a chondrogenic or an osteogenic/endochondral phenotype.

- Different classes of commonly used non-viral vectors are not inert and the chemical and physical characteristics of these nanomaterials have a strong effect on cell morphology, stress fiber formation and gene transcription in MSCs, which modulates their capacity to differentiate along the osteogenic, adipogenic and chondrogenic lineages. RALA-mediated transfection was able to promote chondrogenesis of MSCs, while nHA-mediated gene delivery enhanced osteogenic capacity of MSCs and promoted terminal endochondral differentiation.

- Non-viral gene delivery vectors are a promising tool for combinatorial gene therapy, offering a rapid and simple way for the simultaneous delivery of multiple genes capable of promoting chondrogenesis of MSCs and suppression of hypertrophy.

- Gene activated alginate-based bioinks using nHA-mediated transfection of MSCs, were used for the 3D printing of mechanically reinforced composite constructs. These were capable of successful therapeutic gene transfection leading to enhanced osteogenesis of MSCs *in vitro* and formation of a vascularized and mineralized tissue upon subcutaneous implantation *in vivo*.

- The development of alginate-methylcellulose hybrid bioinks resulted in pore-forming hydrogels capable of enhanced non-viral gene delivery *in vitro* and *in vivo.*

- The developed nHA-alginate and RALA-alginate-methylcellulose bioinks were spatially deposited into mechanically robust PCL 3D printed constructs to form bi-phasic osteochondral constructs capable of zonal MSC differentiation and the recapitulation of the biochemical gradients found in native osteochondral tissue.

8.4. Future work

As previously discussed, the *in vivo* results in this thesis were obtained through subcutaneous implantation in an athymic mice model. Future work should explore the therapeutic potential of this gene activated approaches in orthotopic defects. The developed nHA gene activated bioink could be used for improved bone formation in a femoral defect, while the osteochondral multiphasic constructs could be assessed for the repair of osteochondral defects in a large animal model. Also, the 3D printing methodologies used in this thesis to engineer multiphasic constructs could be applied to investigate the engineering of anatomically accurate gene activated materials for total knee regeneration.

The developed gene activated bioinks were also shown capable of host cell transfection *in vivo*, offering the possibility of the implantation of cell-free 3D printed constructs to modulate host cell differentiation without the need of allogenic cell transplantation.

An important factor for the repair of cartilage injuries in the context of an osteoarthritic knee is the inflammatory conditions that might hinder the regenerative efforts and the reestablishment of cartilage homeostasis. A promising approach that could be explored to favour cartilage repair in a pro-inflammatory environment might be the co-delivery of pro-regenerative and immunomodulatory factors that may offer a more complete approach for the regeneration of diseased articulations. Gene co-delivery of TGF-β1 and the anti-inflammatory factor interleukin 1 receptor antagonist (IL-1RA) into a rabbit OA disease model resulted in disease reversal and improved tissue repair (Zhang et al., 2015b). This promising approach could be explored in combination with the developed gene activated bioinks for the localised *in situ* repair of osteoarthritic joints.

BIBLIOGRAPHY

Adair, J.H., Parette, M.P., Altinoğlu, E.I., and Kester, M. (2010). Nanoparticulate alternatives for drug delivery. ACS Nano *4*, 4967–4970.

Ahn, H.H., Lee, J.H.Y., Kim, K.S., Lee, J.H.Y., Kim, M.S., Khang, G., Lee, I.W., and Lee, H.B. (2008). Polyethyleneimine-mediated gene delivery into human adipose derived stem cells. Biomaterials *29*, 2415–2422.

Akhtar, S. (2006). Non-viral cancer gene therapy: beyond delivery. Gene Ther. *13*, 739–740.

Akiyama, H. (2008). Control of chondrogenesis by the transcription factor Sox9. Mod. Rheumatol. *18*, 213–219.

Ali, A.A., McCrudden, C.M., McCaffrey, J., McBride, J.W., Cole, G., Dunne, N.J., Robson, T., Kissenpfennig, A., Donnelly, R.F., and McCarthy, H.O. (2017). DNA vaccination for cervical cancer; a novel technology platform of RALA mediated gene delivery via polymeric microneedles. Nanomedicine Nanotechnology, Biol. Med. *13*, 921–932.

Almeida, H. V, Liu, Y., Cunniffe, G.M., Mulhall, K.J., Matsiko, A., Buckley, C.T., O'Brien, F.J., and Kelly, D.J. (2014). Controlled release of transforming growth factor-β3 from cartilage-extra-cellular-matrix-derived scaffolds to promote chondrogenesis of human-joint-tissue-derived stem cells. Acta Biomater. *10*, 4400–4409.

Alsberg, E., Anderson, K.W., Albeiruti, A., Franceschi, R.T., and Mooney, D.J. (2001). Cell-interactive alginate hydrogels for bone tissue engineering. J. Dent. Res. *80*, 2025–2029.

Alsberg, E., Kong, H.J., Hirano, Y., Smith, M.K., Albeiruti, A., and Mooney, D.J. (2003). Regulating bone formation via controlled scaffold degradation. J Dent Res *82*, 903–908.

Armstrong, J.P.K., Burke, M., Carter, B.M., Davis, S.A., and Perriman, A.W. (2016). 3D Bioprinting Using a Templated Porous Bioink. Adv. Healthc. Mater. *5*, 1724–1730.

Ateshian, G.A., and Mow, V.C. (2005). Basic Orthopaedic Biomechanics and Mechano-Biology. Frict. Lubr. Wear Articul. Cartil. Diarthrodial Joints 447–494.

Atoui, R., and Chiu, R.C.J. (2012). Concise Review: Immunomodulatory Properties of Mesenchymal Stem Cells in Cellular Transplantation: Update, Controversies, and Unknowns. Stem Cells Transl. Med. *1*, 200–205.

Axpe, E., and Oyen, M.L. (2016). Applications of Alginate-Based Bioinks in 3D Bioprinting. Int. J. Mol. Sci. *17*.

Baker, A., Saltik, M., Lehrmann, H., Killisch, I., Mautner, V., Lamm, G., Christofori, G., and Cotten, M. (1997). Polyethylenimine (PEI) is a simple, inexpensive and effective reagent for condensing and linking plasmid DNA to adenovirus for gene delivery. Gene Ther. *4*, 773–782.

Baldo, B.A. (2014). Side Effects of Cytokines Approved for Therapy. Drug Saf. *37*, 921–943.

Ballarín-González, B., and Howard, K.A. (2012). Polycation-based nanoparticle delivery of RNAi therapeutics: Adverse effects and solutions. Adv. Drug Deliv. Rev. *64*, 1717–1729.

Bangham, A.D., Standish, M.M., and Watkins, J.C. (1965). Diffusion of univalent ions across the lamellae of swollen phospholipids. J. Mol. Biol. *13*, 238–252.

De Bari, C., Dell'Accio, F., Vanlauwe, J., Eyckmans, J., Khan, I.M., Archer, C.W., Jones, E.A., McGonagle, D., Mitsiadis, T.A., Pitzalis, C., et al. (2006). Mesenchymal multipotency of adult

human periosteal cells demonstrated by single-cell lineage analysis. Arthritis Rheum. *54*, 1209–1221.

Barry, F., Boynton, R.E., Liu, B., and Murphy, J.M. (2001). Chondrogenic differentiation of mesenchymal stem cells from bone marrow: differentiation-dependent gene expression of matrix components. Exp. Cell Res. *268*, 189–200.

Baum, C., Kustikova, O., Modlich, U., Li, Z., and Fehse, B. (2006). Mutagenesis and oncogenesis by chromosomal insertion of gene transfer vectors. Hum. Gene Ther. *17*, 253–263.

Beane, O.S., Fonseca, V.C., Cooper, L.L., Koren, G., and Darling, E.M. (2014). Impact of aging on the regenerative properties of bone marrow-, muscle-, and adipose-derived mesenchymal stem/stromal cells. PLoS One *9*.

Bedi, A., Feeley, B.T., and Williams, R.J. (2010). Management of articular cartilage defects of the knee. J. Bone Joint Surg. Am. *92*, 994–1009.

Bennett, R., Yakkundi, A., McKeen, H.D., McClements, L., McKeogh, T.J., McCrudden, C.M., Arthur, K., Robson, T., and McCarthy, H.O. (2015). RALA-mediated delivery of FKBPL nucleic acid therapeutics. Nanomedicine (Lond). *10*, 1–30.

Benoit, D.S.W., Schwartz, M.P., Durney, A.R., and Anseth, K.S. (2008). Small functional groups for controlled differentiation of hydrogel-encapsulated human mesenchymal stem cells. Nat. Mater. *7*, 816–823.

Benya, P.D., and Shaffer, J.D. (1982). Dedifferentiated chondrocytes reexpress the differentiated collagen phenotype when cultured in agarose gels. Cell *30*, 215–224.

Bessis, N., GarciaCozar, F.J., and Boissier, M.-C. (2004). Immune responses to gene therapy vectors: influence on vector function and effector mechanisms. Gene Ther. *11 Suppl 1*, S10-7.

Bez, M., Sheyn, D., Tawackoli, W., Avalos, P., Shapiro, G., Giaconi, J.C., Da, X., David, S. Ben, Gavrity, J., Awad, H.A., et al. (2017). In situ bone tissue engineering via ultrasound-mediated gene delivery to endogenous progenitor cells in mini-pigs. Sci. Transl. Med. *9*.

Bharali, D.J., Klejbor, I., Stachowiak, E.K., Dutta, P., Roy, I., Kaur, N., Bergey, E.J., Prasad, P.N., and Stachowiak, M.K. (2005). Organically modified silica nanoparticles: a nonviral vector for in vivo gene delivery and expression in the brain. Proc. Natl. Acad. Sci. U. S. A. *102*, 11539–11544.

Bharti, D., Shivakumar, S.B., Subbarao, R.B., and Rho, G.-J. (2016). Research Advancements in Porcine Derived Mesenchymal Stem Cells. Curr. Stem Cell Res. Ther. *11*, 78–93.

Bian, L., Zhai, D.Y., Tous, E., Rai, R., Mauck, R.L., and Burdick, J.A. (2011). Enhanced MSC chondrogenesis following delivery of TGF-β3 from alginate microspheres within hyaluronic acid hydrogels in vitro and in vivo. Biomaterials *32*, 6425–6434.

Bijlsma, J.W.J., Berenbaum, F., and Lafeber, F.P.J.G. (2011). Osteoarthritis: an update with relevance for clinical practice. Lancet *377*, 2115–2126.

Billiet, T., Vandenhaute, M., Schelfhout, J., Van Vlierberghe, S., Dubruel, P., Schelfhout, J., and Dubruel, P. (2012). A review of trends and limitations in hydrogel-rapid prototyping for tissue engineering. Biomaterials *33*, 6020–6041.

Boere, K.W.M., Visser, J., Seyednejad, H., Rahimian, S., Gawlitta, D., van Steenbergen, M.J., Dhert, W.J. a, Hennink, W.E., Vermonden, T., and Malda, J. (2014). Covalent attachment of a three-dimensionally printed thermoplast to a gelatin hydrogel for mechanically enhanced cartilage constructs. Acta Biomater. *10*, 2602–2611.

Bonadio, J., Smiley, E., Patil, P., and Goldstein, S. (1999). Localized, direct plasmid gene delivery in vivo: prolonged therapy results in reproducible tissue regeneration. Nat. Med. *5*, 753–759.

Boontheekul, T., Kong, H.-J.J., and Mooney, D.J. (2005). Controlling alginate gel degradation utilizing partial oxidation and bimodal molecular weight distribution. Biomaterials *26*, 2455–2465.

Bose, S., and Tarafder, S. (2012). Calcium phosphate ceramic systems in growth factor and drug delivery for bone tissue engineering: A review. Acta Biomater. *8*, 1401–1421.

Boskey, A.L. (2013). Bone composition: relationship to bone fragility and antiosteoporotic drug effects. Bonekey Rep. *2*, 447.

Bouard, D., Alazard-Dany, D., and Cosset, F.-L. (2009). Viral vectors: from virology to transgene expression. Br. J. Pharmacol. *157*, 153–165.

Boussif, O., Lezoualc'h, F., Zanta, M.A., Mergny, M.D., Scherman, D., Demeneix, B., and Behr, J.P. (1995). A versatile vector for gene and oligonucleotide transfer into cells in culture and in vivo: polyethylenimine. Proc. Natl. Acad. Sci. U. S. A. *92*, 7297–7301.

Brew, K., Dinakarpandian, D., and Nagase, H. (2000). Tissue inhibitors of metalloproteinases: evolution, structure and function. Biochim. Biophys. Acta *1477*, 267–283.

Brittberg, M., Lindahl, A., Nilsson, A., Ohlsson, C., Isaksson, O., and Peterson, L. (1994). Treatment of deep cartilage defects in the knee with autologous chondrocyte transplantation. N. Engl. J. Med. *331*, 889–895.

Brooks, P.M. (2002). Impact of osteoarthritis on individuals and society: how much disability? Social consequences and health economic implications. Curr. Opin. Rheumatol. *14*, 573–577.

Browne, S., Fontana, G., Rodriguez, B.J., and Pandit, A. (2012). A protective extracellular matrix-based gene delivery reservoir fabricated by electrostatic charge manipulation. Mol. Pharm. *9*, 3099–3106.

Brundin, M., Figdor, D., Sundqvist, G., and Sjögren, U. (2013). DNA binding to hydroxyapatite: a potential mechanism for preservation of microbial DNA. J. Endod. *39*, 211–216.

Brunger, J.M., Huynh, N.P.T., Guenther, C.M., Perez-Pinera, P., Moutos, F.T., Sanchez-Adams, J., Gersbach, C. a, and Guilak, F. (2014). Scaffold-mediated lentiviral transduction for functional tissue engineering of cartilage. Proc. Natl. Acad. Sci. U. S. A. *111*, E798-806.

Buckley, C.T., Vinardell, T., and Kelly, D.J. (2010). Oxygen tension differentially regulates the functional properties of cartilaginous tissues engineered from infrapatellar fat pad derived MSCs and articular chondrocytes. Osteoarthr. Cartil. *18*, 1345–1354.

Buckwalter, J.A., and Mankin, H.J. (1998). Articular cartilage: degeneration and osteoarthritis, repair, regeneration, and transplantation. Instr. Course Lect. *47*, 487–504.

Buckwalter, J. a, and Martin, J. a (2006). Osteoarthritis. Adv. Drug Deliv. Rev. *58*, 150–167.

Burridge, K., and Wennerberg, K. (2004). Rho and Rac Take Center Stage. Cell *116*, 167–179.

C.H. Evans, S.C. Ghivizzani, and P.D.R. (2012). Orthopaedic gene therapy-Lost in translation? J. Cell. Physiol. *227*, 416–420.

Cals, F.L.J., Hellingman, C.A., Koevoet, W., Baatenburg de Jong, R.J., and van Osch, G.J.V.M. (2012). Effects of transforming growth factor-β subtypes on in vitro cartilage production and mineralization of human bone marrow stromal-derived mesenchymal stem cells. J. Tissue Eng. Regen. Med. *6*, 68–76.

Cao, L., Yang, F., Liu, G., Yu, D., Li, H., Fan, Q., Gan, Y., Tang, T., and Dai, K. (2011). The promotion of cartilage defect repair using adenovirus mediated Sox9 gene transfer of rabbit bone marrow mesenchymal stem cells. Biomaterials *32*, 3910–3920.

Cao, N., Chen, X.B., and Schreyer, D.J. (2012a). Influence of Calcium Ions on Cell Survival and Proliferation in the Context of an Alginate Hydrogel. ISRN Chem. Eng. *2012*, 1–9.

Cao, X., Deng, W., Wei, Y., Yang, Y., Su, W., Wei, Y., Xu, X., and Yu, J. (2012b). Incorporating pTGF-β1/calcium phosphate nanoparticles with fibronectin into 3-dimensional collagen/chitosan scaffolds: efficient, sustained gene delivery to stem cells for chondrogenic differentiation. Eur. Cell. Mater. *23*, 81–93.

Capito, R.M., and Spector, M. (2007). Collagen scaffolds for nonviral IGF-1 gene delivery in articular cartilage tissue engineering. Gene Ther. *14*, 721–732.

Caplan, A.I., and Correa, D. (2011). PDGF in bone formation and regeneration: New insights into a novel mechanism involving MSCs. J. Orthop. Res. *29*, 1795–1803.

Carragee, E.J., Hurwitz, E.L., and Weiner, B.K. (2011). A critical review of recombinant human bone morphogenetic protein-2 trials in spinal surgery: emerging safety concerns and lessons learned. Spine J. *11*, 471–491.

Castaño, I.M., Curtin, C.M., Shaw, G., Mary Murphy, J., Duffy, G.P., and O'Brien, F.J. (2014). A novel collagen-nanohydroxyapatite microRNA-activated scaffold for tissue engineering applications capable of efficient delivery of both miR-mimics and antagomiRs to human mesenchymal stem cells. J. Control. Release *200*, 42–51.

Cha, B.-H., Kim, J.-H., Kang, S.-W., Do, H.-J., Jang, J.-W., Choi, Y.R., Park, H., Kim, B.-S., and Lee, S.-H. (2013). Cartilage tissue formation from dedifferentiated chondrocytes by codelivery of BMP-2 and SOX-9 genes encoding bicistronic vector. Cell Transplant. *22*, 1519–1528.

Charalambous, C.P. (2014). Articular cartilage. Part II: Degeneration and osteoarthrosis, repair, regeneration, and transplantation. In Classic Papers in Orthopaedics, pp. 389–391.

Chen, F.M., Zhang, M., and Wu, Z.F. (2010). Toward delivery of multiple growth factors in tissue engineering. Biomaterials *31*, 6279–6308.

Chen, J., Chen, H., Li, P., Diao, H., Zhu, S., Dong, L., Wang, R., Guo, T., Zhao, J., and Zhang, J. (2011). Simultaneous regeneration of articular cartilage and subchondral bone in vivo using MSCs induced by a spatially controlled gene delivery system in bilayered integrated scaffolds. Biomaterials *32*, 4793–4805.

Chen, S., Fu, P., Cong, R., Wu, H.S., and Pei, M. (2015). Strategies to minimize hypertrophy in cartilage engineering and regeneration. Genes Dis. *2*, 76–95.

Chen, Z., Wei, J., Zhu, J., Liu, W., Cui, J., Li, H., and Chen, F. (2016). Chm-1 gene-modified bone marrow mesenchymal stem cells maintain the chondrogenic phenotype of tissue-engineered cartilage. Stem Cell Res. Ther. *7*, 70.

Cheong, H., Kim, K.-H., Park, Y.-J., Kim, T.-I., Lee, Y.-M., Ku, Y., Rhyu, I.-C., Lee, D.-S., Lee, S.-J., Chung, C.-P., et al. (2007). Osteogenic effects of polyethyleneimine-condensed BMP-2 genes in vitro and in vivo. J. Korean Acad. Periodontol. *37*, 859.

Chernousova, S., Klesing, J., Soklakova, N., and Epple, M. (2013). A genetically active nano-calcium phosphate paste for bone substitution, encoding the formation of BMP-7 and VEGF-A. RSC Adv. *3*, 11155–11161.

Chew, S.A., Kretlow, J.D., Spicer, P.P., Edwards, A.W., Baggett, L.S., Tabata, Y., Kasper, F.K., and

Mikos, A.G. (2011). Delivery of plasmid DNA encoding bone morphogenetic protein-2 with a biodegradable branched polycationic polymer in a critical-size rat cranial defect model. Tissue Eng. Part A *17*, 751–763.

Cho, J., Kim, T., Park, Y., Shin, J., Kang, S., and Lee, B. (2016). A Phase III Clinical Trial of a Cell and Gene Therapy, Invossa™, for the Treatment of Osteoarthritis. Cytotherapy *18*, S10.

Choi, S., Yu, X., Jongpaiboonkit, L., Hollister, S.J., and Murphy, W.L. (2013). Inorganic coatings for optimized non-viral transfection of stem cells. Sci. Rep. *3*.

Chung, J.H.Y., Naficy, S., Yue, Z., Kapsa, R., Quigley, A., Moulton, S.E., and Wallace, G.G. (2013). Bio-ink properties and printability for extrusion printing living cells. Biomater. Sci. *1*, 763–773.

Clements, B.A., Incani, V., Kucharski, C., Lavasanifar, A., Ritchie, B., and Uludağ, H. (2007). A comparative evaluation of poly-l-lysine-palmitic acid and Lipofectamine ™ 2000 for plasmid delivery to bone marrow stromal cells. Biomaterials *28*, 4693–4704.

Cohen-Sacks, H., Elazar, V., Gao, J., Golomb, A., Adwan, H., Korchov, N., Levy, R.J., Berger, M.R., and Golomb, G. (2004). Delivery and expression of pDNA embedded in collagen matrices. J. Control. Release *95*, 309–320.

Cooper, G.M., Miller, E.D., DeCesare, G.E., Usas, A., Lensie, E.L., Bykowski, M.R., Huard, J., Weiss, L.E., Losee, J.E., and Campbell, P.G. (2010). Inkjet-Based Biopatterning of Bone Morphogenetic Protein-2 to Spatially Control Calvarial Bone Formation. Tissue Eng. Part A *16*, 1749–1759.

Corsi, K., Chellat, F., Yahia, L., and Fernandes, J.C. (2003). Mesenchymal stem cells, MG63 and HEK293 transfection using chitosan-DNA nanoparticles. Biomaterials *24*, 1255–1264.

Crecente-Campo, J., Borrajo, E., Vidal, A., and Garcia-Fuentes, M. (2017). New scaffolds encapsulating TGF-β3/BMP-7 combinations driving strong chondrogenic differentiation. Eur. J. Pharm. Biopharm. *114*, 69–78.

Crystal, R.G. (1995). Transfer of genes to humans: early lessons and obstacles to success. Science *270*, 404–410.

Cucchiarini, M., Thurn, T., Weimer, A., Kohn, D., Terwilliger, E.F., and Madry, H. (2007). Restoration of the extracellular matrix in human osteoarthritic articular cartilage by overexpression of the transcription factor SOX9. Arthritis Rheum. *56*, 158–167.

Cucchiarini, M., Terwilliger, E.F., Kohn, D., and Madry, H. (2009). Remodelling of human osteoarthritic cartilage by FGF-2, alone or combined with Sox9 via rAAV gene transfer. J. Cell. Mol. Med. *13*, 2476–2488.

Cui, X., Dean, D., Ruggeri, Z.M., and Boland, T. (2010). Cell damage evaluation of thermal inkjet printed Chinese hamster ovary cells. Biotechnol. Bioeng. *106*, 963–969.

Cunniffe, G.M., O'Brien, F.J., Partap, S., Levingstone, T.J., Stanton, K.T., and Dickson, G.R. (2010). The synthesis and characterization of nanophase hydroxyapatite using a novel dispersant-aided precipitation method. J. Biomed. Mater. Res. Part A *95A*, 1142–1149.

Cunniffe, G.M., Vinardell, T., Thompson, E.M., Daly, A.C., Matsiko, A., O'Brien, F.J., and Kelly, D.J. (2015a). Chondrogenically primed mesenchymal stem cell-seeded alginate hydrogels promote early bone formation in critically-sized defects. Eur. Polym. J. *72*, 464–472.

Cunniffe, G.M., Vinardell, T., Murphy, J.M., Thompson, E.M., Matsiko, A., O'Brien, F.J., and Kelly, D.J. (2015b). Porous decellularized tissue engineered hypertrophic cartilage as a scaffold for large bone defect healing. Acta Biomater. *23*, 82–90.

Cunniffe, G.M., Curtin, C.M., Thompson, E.M., Dickson, G.R., and O'Brien, F.J. (2016a). Content-dependent osteogenic response of nano-hydroxyapatite; an in vitro and in vivo assessment within collagen-based scaffolds. ACS Appl. Mater. Interfaces *8*, 23477–23488.

Cunniffe, G.M., Curtin, C.M., Thompson, E.M., Dickson, G.R., and O'Brien, F.J. (2016b). Content-Dependent Osteogenic Response of Nanohydroxyapatite: An in Vitro and in Vivo Assessment within Collagen-Based Scaffolds. ACS Appl. Mater. Interfaces *8*, 23477–23488.

Curtin, C.M., Cunniffe, G.M., Lyons, F.G., Bessho, K., Dickson, G.R., Duffy, G.P., and O'Brien, F.J. (2012). Innovative collagen nano-hydroxyapatite scaffolds offer a highly efficient non-viral gene delivery platform for stem cell-mediated bone formation. Adv. Mater. *24*, 749–754.

Curtin, C.M., Tierney, E.G., McSorley, K., Cryan, S.-A., Duffy, G.P., and O'Brien, F.J. (2015). Combinatorial gene therapy accelerates bone regeneration: non-viral dual delivery of VEGF and BMP2 in a collagen-nanohydroxyapatite scaffold. Adv. Healthc. Mater. *4*, 223–227.

D'Mello, S.R., Elangovan, S., Hong, L., Ross, R.D., Sumner, D.R., and Salem, A.K. (2015). A Pilot Study Evaluating Combinatorial and Simultaneous Delivery of Polyethylenimine-Plasmid DNA Complexes Encoding for VEGF and PDGF for Bone Regeneration in Calvarial Bone Defects. Curr. Pharm. Biotechnol. *16*, 655–660.

Daly, A.C., Critchley, S.E., Rensock, E.M., Kelly, D.J., Rencsok, E.M., and Kelly, D.J. (2016a). A Comparison of Different Bioinks for 3D Bioprinting of Fibrocartilage and Hyaline Cartilage. Biofabrication *8*, 1–25.

Daly, A.C., Cunniffe, G.M., Sathy, B.N., Jeon, O., Alsberg, E., and Kelly, D.J. (2016b). 3D Bioprinting of Developmentally Inspired Templates for Whole Bone Organ Engineering. Adv. Healthc. Mater. *5*, 2353–2362.

Daly, A.C., Freeman, F.E., Gonzalez-Fernandez, T., Critchley, S.E., Nulty, J., and Kelly, D.J. (2017). 3D Bioprinting for Cartilage and Osteochondral Tissue Engineering. Adv. Healthc. Mater. *6*.

Dang, J.M., and Leong, K.W. (2006). Natural polymers for gene delivery and tissue engineering. Adv. Drug Deliv. Rev. *58*, 487–499.

Davey, R.B., Sparnon, A.L., and Byard, R.W. (2000). Unusual donor site reactions to calcium alginate dressings. Burns *26*, 393–398.

Delalande, A., Gosselin, M.P., Suwalski, A., Guilmain, W., Leduc, C., Berchel, M., Jaffr??s, P.A., Baril, P., Midoux, P., and Pichon, C. (2015). Enhanced Achilles tendon healing by fibromodulin gene transfer. Nanomedicine Nanotechnology, Biol. Med. *11*, 1735–1744.

Deng, B., Chen, C., Gong, X., Guo, L., Chen, H., Yin, L., Yang, L., and Wang, F. (2017). Chondromodulin-I expression and correlation with angiogenesis in human osteoarthritic cartilage. Mol. Med. Rep. *16*, 2142–2148.

Deschepper, M., Oudina, K., David, B., Myrtil, V., Collet, C., Bensidhoum, M., Logeart-Avramoglou, D., and Petite, H. (2011). Survival and function of mesenchymal stem cells (MSCs) depend on glucose to overcome exposure to long-term, severe and continuous hypoxia. J. Cell. Mol. Med. *15*, 1505–1514.

Diao, H., Wang, J., Shen, C., Xia, S., Guo, T., Dong, L., Zhang, C., Chen, J., Zhao, J., and Zhang, J. (2009). Improved cartilage regeneration utilizing mesenchymal stem cells in TGF-beta1 gene-activated scaffolds. Tissue Eng. Part A *15*, 2687–2698.

DiFranco, M., Quinonez, M., Capote, J., and Vergara, J. (2009). DNA Transfection of Mammalian Skeletal Muscles using *In Vivo* Electroporation. J. Vis. Exp.

Dinser, R., Kreppel, F., Zaucke, F., Blank, C., Paulsson, M., Kochanek, S., and Maurer, P. (2001). Comparison of long-term transgene expression after non-viral and adenoviral gene transfer into primary articular chondrocytes. Histochem. Cell Biol. *116*, 69–77.

Dixon, J.E., Osman, G., Morris, G.E., Markides, H., Rotherham, M., Bayoussef, Z., El Haj, A.J., Denning, C., and Shakesheff, K.M. (2016). Highly efficient delivery of functional cargoes by the synergistic effect of GAG binding motifs and cell-penetrating peptides. Proc. Natl. Acad. Sci. U. S. A. *113*, E291-9.

Dizaj, S., Jafari, S., and Khosroushahi, A. (2014). A sight on the current nanoparticle-based gene delivery vectors. Nanoscale Res. Lett. *9*, 252.

Dorozhkin, S. V, and Epple, M. (2002). Biological and medical significance of calcium phosphates. Angew. Chem. Int. Ed. Engl. *41*, 3130–3146.

Dudics, V., Kunstár, A., Kovács, J., Lakatos, T., Géher, P., Gömör, B., Monostori, E., and Uher, F. (2009). Chondrogenic potential of mesenchymal stem cells from patients with rheumatoid arthritis and osteoarthritis: measurements in a microculture system. Cells. Tissues. Organs *189*, 307–316.

Eggenhofer, E., Luk, F., Dahlke, M.H., and Hoogduijn, M.J. (2014). The life and fate of mesenchymal stem cells. Front. Immunol. *5*.

Elangovan, S., D'Mello, S.R., Hong, L., Ross, R.D., Allamargot, C., Dawson, D. V, Stanford, C.M., Johnson, G.K., Sumner, D.R., and Salem, A.K. (2014). The enhancement of bone regeneration by gene activated matrix encoding for platelet derived growth factor. Biomaterials *35*, 737–747.

Elmallah, R.K., Cherian, J.J., Jauregui, J.J., Pierce, T.P., Beaver, W.B., and Mont, M. a (2015). Genetically modified chondrocytes expressing TGF-β1: a revolutionary treatment for articular cartilage damage? Expert Opin. Biol. Ther. *15*, 455–464.

Elsler, S., Schetting, S., Schmitt, G., Kohn, D., Madry, H., and Cucchiarini, M. (2012). Effective , safe nonviral gene transfer to preserve the chondrogenic differentiation potential of human mesenchymal stem cells. J. Gene Med. *14*, 501–511.

Emadedin, M., Liastani, M.G., Fazeli, R., Mohseni, F., Moghadasali, R., Mardpour, S., Hosseini, S.E., Niknejadi, M., Moeininia, F., Fanni, A.A., et al. (2015). Long-term follow-up of intra-articular injection of autologous mesenchymal stem cells in patients with knee, ankle, or hip osteoarthritis. Arch. Iran. Med. *18*, 336–344.

Endo, M., Kuroda, S., Kondo, H., Maruoka, Y., Ohya, K., and Kasugai, S. (2006). Bone regeneration by modified gene-activated matrix: effectiveness in segmental tibial defects in rats. Tissue Eng. *12*, 489–497.

Euliss, L.E., DuPont, J.A., Gratton, S., DeSimone, J., Rao, C.N.R., Kulkarni, G.U., Thomas, P.J., Edwards, P.P., Euliss, L.E., Grancharov, S.G., et al. (2006). Imparting size, shape, and composition control of materials for nanomedicine. Chem. Soc. Rev. *35*, 1095.

Evans, C. (2014). Using genes to facilitate the endogenous repair and regeneration of orthopaedic tissues. Int. Orthop. *38*, 1761–1769.

Evans, C.H., and Huard, J. (2015). Gene therapy approaches to regenerating the musculoskeletal system. Nat. Rev. Rheumatol. *11*, 234–242.

Evans, C.H., Robbins, P.D., Ghivizzani, S.C., Wasko, M.C., Tomaino, M.M., Kang, R., Muzzonigro, T.A., Vogt, M., Elder, E.M., Whiteside, T.L., et al. (2005). Gene transfer to human joints: progress toward a gene therapy of arthritis. Proc. Natl. Acad. Sci. U. S. A. *102*, 8698–8703.

Fang, J., Zhu, Y.-Y., Smiley, E., Bonadio, J., Rouleaut, J.P., Goldsteint, S.A., Mccauleyt, L.K., Davidson, B.L., Roessler, B.J., and Deluca, H.F. (1996). Stimulation of new bone formation by direct transfer of osteogenic plasmid genes (gene transfer/rat osteotomy model/bone formation/repair fibroblast/wound healing). *93*, 5753–5758.

Farrell, E., Both, S.K., Odörfer, K.I., Koevoet, W., Kops, N., O'Brien, F.J., Baatenburg de Jong, R.J., Verhaar, J.A., Cuijpers, V., Jansen, J., et al. (2011). In-vivo generation of bone via endochondral ossification by in-vitro chondrogenic priming of adult human and rat mesenchymal stem cells. BMC Musculoskelet. Disord. *12*, 31.

Fedorovich, N.E., Schuurman, W., Wijnberg, H.M., Prins, H.-J., van Weeren, P.R., Malda, J., Alblas, J., and Dhert, W.J. a. (2012). Biofabrication of Osteochondral Tissue Equivalents by Printing Topologically Defined, Cell-Laden Hydrogel Scaffolds. Tissue Eng. Part C Methods *18*, 33–44.

Feeley, B.T., Conduah, A.H., Sugiyama, O., Krenek, L., Chen, I.S.Y., and Lieberman, J.R. (2006). In vivo molecular imaging of adenoviral versus lentiviral gene therapy in two bone formation models. J. Orthop. Res. *24*, 1709–1721.

Feng, T., Szabo, E., Dziak, E., and Opas, M. (2010). Cytoskeletal disassembly and cell rounding promotes adipogenesis from ES cells. Stem Cell Rev. Reports *6*, 74–85.

Fibel, K.H., Hillstrom, H.J., and Halpern, B.C. (2015). State-of-the-Art management of knee osteoarthritis. World J. Clin. Cases *3*, 89–101.

Fierro, F.A., Kalomoiris, S., Sondergaard, C.S., and Nolta, J.A. (2011). Effects on proliferation and differentiation of multipotent bone marrow stromal cells engineered to express growth factors for combined cell and gene therapy. Stem Cells *29*, 1727–1737.

Fisher, D.M., Wong, J.M.-L., Crowley, C., and Khan, W.S. (2013). Preclinical and clinical studies on the use of growth factors for bone repair: a systematic review. Curr. Stem Cell Res. Ther. *8*, 260–268.

Florea, B.I., Meaney, C., Junginger, H.E., and Borchard, G. (2002). Transfection efficiency and toxicity of polyethylenimine in differentiated Calu-3 and nondifferentiated COS-1 cell cultures. AAPS PharmSci *4*, E12.

Foerg, C., Ziegler, U., Fernandez-Carneado, J., Giralt, E., and Merkle, H.P. (2007). Differentiation restricted endocytosis of cell penetrating peptides in MDCK cells corresponds with activities of Rho-GTPases. Pharm. Res. *24*, 628–642.

Fortune, J.A., Chemistry, B.A., and Essigmann, J.M. (2010). SPECIFIC AND EFFICIENT IN VIVO DELIVERY OF DNA AND siRNA BY POLYETHYLENIMINE AND ITS DERIVATIVES LIBRARIES Thesis Supervisor.

Frisch, J., Rey-Rico, A., Venkatesan, J.K., Schmitt, G., Madry, H., and Cucchiarini, M. (2016). rAAV-mediated overexpression of sox9, TGF-β and IGF-I in minipig bone marrow aspirates to enhance the chondrogenic processes for cartilage repair. Gene Ther. *23*, 247–255.

Frisch, J., Orth, P., Rey-Rico, A., Venkatesan, J.K., Schmitt, G., Madry, H., Kohn, D., and Cucchiarini, M. (2017). Peripheral blood aspirates overexpressing IGF-I via rAAV gene transfer undergo enhanced chondrogenic differentiation processes. J. Cell. Mol. Med. *21*, 2748–2758.

Fu, H., Hu, Y., McNelis, T., and Hollinger, J.O. (2005). A calcium phosphate-based gene delivery system. J. Biomed. Mater. Res. Part A *74A*, 40–48.

Gao, F., Chiu, S.M., Motan, D.A.L., Zhang, Z., Chen, L., Ji, H.-L., Tse, H.-F., Fu, Q.-L., and Lian, Q.

(2016). Mesenchymal stem cells and immunomodulation: current status and future prospects. Cell Death Dis. *7*, e2062.

Gao, L., McBeath, R., and Chen, C.S. (2010). Stem cell shape regulates a chondrogenic versus myogenic fate through rac1 and N-cadherin. Stem Cells *28*, 564–572.

Gao, Y., Lim, J., Teoh, S.-H., and Xu, C. (2015). Emerging translational research on magnetic nanoparticles for regenerative medicine. Chem. Soc. Rev. *44*, 6306–6329.

Geiger, F., Bertram, H., Berger, I., Lorenz, H., Wall, O., Eckhardt, C., Simank, H.-G., and Richter, W. (2005). Vascular endothelial growth factor gene-activated matrix (VEGF165-GAM) enhances osteogenesis and angiogenesis in large segmental bone defects. J. Bone Miner. Res. *20*, 2028–2035.

Gelse, K., Mühle, C., Franke, O., Park, J., Jehle, M., Durst, K., Göken, M., Hennig, F., von der Mark, K., and Schneider, H. (2008). Cell-based resurfacing of large cartilage defects: long-term evaluation of grafts from autologous transgene-activated periosteal cells in a porcine model of osteoarthritis. Arthritis Rheum. *58*, 475–488.

Gerich, T.G., Ghivizani, S., Fu, F.H., Robbins, P.D., and Evans, C.H. (1997). [Gene transfer into the patellar tendon of rabbits: a preliminary study of locoregional expression of growth factors]. Wien. Klin. Wochenschr. *109*, 384–389.

Gerstenfeld, L.C., Cullinane, D.M., Barnes, G.L., Graves, D.T., and Einhorn, T.A. (2003). Fracture healing as a post-natal developmental process: molecular, spatial, and temporal aspects of its regulation. J. Cell. Biochem. *88*, 873–884.

Ghosh, S., Laha, M., Mondal, S., Sengupta, S., and Kaplan, D.L. (2009). In vitro model of mesenchymal condensation during chondrogenic development. Biomaterials *30*, 6530–6540.

Glass, K.A., Link, J.M., Brunger, J.M., Moutos, F.T., Gersbach, C.A., and Guilak, F. (2014). Tissue-engineered cartilage with inducible and tunable immunomodulatory properties. Biomaterials *35*, 5921–5931.

Glyn-Jones, S., Palmer, a J.R., Agricola, R., Price, a J., Vincent, T.L., Weinans, H., and Carr, a J. (2015). Osteoarthritis. Lancet *6736*, 1–12.

Godbey, W.T., Wu, K.K., and Mikos, A.G. (2001). Poly(ethylenimine)-mediated gene delivery affects endothelial cell function and viability. Biomaterials *22*, 471–480.

Goldberg, A., Mitchell, K., Soans, J., Kim, L., and Zaidi, R. (2017). The use of mesenchymal stem cells for cartilage repair and regeneration: a systematic review. J. Orthop. Surg. Res. *12*, 39.

Goldring, M.B. (2000). Osteoarthritis and cartilage: the role of cytokines. Curr. Rheumatol. Rep. *2*, 459–465.

Gómez-Leduc, T., Desancé, M., Hervieu, M., Legendre, F., Ollitrault, D., de Vienne, C., Herlicoviez, M., Galéra, P., and Demoor, M. (2017). Hypoxia is a critical parameter for chondrogenic differentiation of human umbilical cord blood mesenchymal stem cells in type I/III collagen sponges. Int. J. Mol. Sci. *18*.

Gonzalez, M.A., Gonzalez-Rey, E., Rico, L., Buscher, D., and Delgado, M. (2009). Treatment of experimental arthritis by inducing immune tolerance with human adipose-derived mesenchymal stem cells. Arthritis Rheum. *60*, 1006–1019.

Goomer, R.S., Maris, T.M., Gelberman, R., Boyer, M., Silva, M., and Amiel, D. (2000). Nonviral in vivo gene therapy for tissue engineering of articular cartilage and tendon repair. Clin. Orthop. Relat. Res. S189-200.

Goomer, R.S., Deftos, L.J., Terkeltaub, R., Maris, T., Lee, M.C., Harwood, F.L., and Amiel, D. (2001). High-efficiency non-viral transfection of primary chondrocytes and perichondrial cells for ex-vivo gene therapy to repair articular cartilage defects. Osteoarthr. Cartil. *9*, 248–256.

Gorbunoff, M.J. (1984). The interaction of proteins with hydroxyapatite. I. Role of protein charge and structure. Anal. Biochem. *136*, 425–432.

Goren, A., Dahan, N., Goren, E., Baruch, L., and Machluf, M. (2010). Encapsulated human mesenchymal stem cells: a unique hypoimmunogenic platform for long-term cellular therapy. FASEB J. *24*, 22–31.

Gossen, M., and Bujard, H. (1992). Tight control of gene expression in mammalian cells by tetracycline-responsive promoters. Proc. Natl. Acad. Sci. U. S. A. *89*, 5547–5551.

Grande, D.A., Mason, J., Light, E., and Dines, D. (2003). Stem cells as platforms for delivery of genes to enhance cartilage repair. J. Bone Joint Surg. Am. *85–A Suppl*, 111–116.

Gratton, S.E. a, Ropp, P. a, Pohlhaus, P.D., Luft, J.C., Madden, V.J., Napier, M.E., and DeSimone, J.M. (2008). The effect of particle design on cellular internalization pathways. Proc. Natl. Acad. Sci. U. S. A. *105*, 11613–11618.

Gresch, O., Engel, F.B., Nesic, D., Tran, T.T., England, H.M., Hickman, E.S., Körner, I., Gan, L., Chen, S., Castro-Obregon, S., et al. (2004). New non-viral method for gene transfer into primary cells. Methods *33*, 151–163.

Grosse, S., Aron, Y., Thévenot, G., Monsigny, M., and Fajac, I. (2007). Cytoskeletal involvement in the cellular trafficking of plasmid/PEI derivative complexes. J. Control. Release *122*, 111–117.

Gründer, T., Gaissmaier, C., Fritz, J., Stoop, R., Hortschansky, P., Mollenhauer, J., and Aicher, W.K. (2004). Bone morphogenetic protein (BMP)-2 enhances the expression of type II collagen and aggrecan in chondrocytes embedded in alginate beads. Osteoarthritis Cartilage *12*, 559–567.

Guo, C.-A., Liu, X.-G., Huo, J.-Z., Jiang, C., Wen, X.-J., and Chen, Z.-R. (2007). Novel gene-modified-tissue engineering of cartilage using stable transforming growth factor-β1-transfected mesenchymal stem cells grown on chitosan scaffolds. J. Biosci. Bioeng. *103*, 547–556.

Guo, X., Du, J., Zheng, Q., Yang, S., Liu, Y., Duan, D., and Yi, C. (2002). Expression of transforming growth factor beta 1 in mesenchymal stem cells: potential utility in molecular tissue engineering for osteochondral repair. J. Huazhong Univ. Sci. Technolog. Med. Sci. *22*, 112–115.

Guo, X., Zheng, Q., Kulbatski, I., Yuan, Q., Yang, S., Shao, Z., Wang, H., Xiao, B., Pan, Z., and Tang, S. (2006). Bone regeneration with active angiogenesis by basic fibroblast growth factor gene transfected mesenchymal stem cells seeded on porous β-TCP ceramic scaffolds. Biomed. Mater. *1*, 93–99.

Gupta, B., Levchenko, T.S., and Torchilin, V.P. (2005). Intracellular delivery of large molecules and small particles by cell-penetrating proteins and peptides. Adv. Drug Deliv. Rev. *57*, 637–651.

Gurusinghe, S., and Strappe, P. (2014). Gene modification of mesenchymal stem cells and articular chondrocytes to enhance chondrogenesis. Biomed Res. Int. *2014*.

Ha, C.-W., Noh, M.J., Choi, K.B., and Lee, K.H. (2012). Initial phase I safety of retrovirally transduced human chondrocytes expressing transforming growth factor-beta-1 in degenerative arthritis patients. Cytotherapy *14*, 247–256.

Habraken, W., Habibovic, P., Epple, M., and Bohner, M. (2016). Calcium phosphates in biomedical applications: materials for the future? Mater. Today *19*, 69–87.

Haleem-Smith, H., Derfoul, A., Okafor, C., Tuli, R., Olsen, D., Hall, D.J., and Tuan, R.S. (2005). Optimization of high-efficiency transfection of adult human mesenchymal stem cells in vitro. Mol. Biotechnol. *30*, 9–20.

Hamid, R., Rotshteyn, Y., Rabadi, L., Parikh, R., and Bullock, P. (2004). Comparison of alamar blue and MTT assays for high through-put screening. Toxicol. Vitr. *18*, 703–710.

Hao, J., Yao, Y., Varshney, R.R., Wang, L., Prakash, C., Li, H., and Wang, D.-A. (2008). Gene transfer and living release of transforming growth factor-beta3 for cartilage tissue engineering applications. Tissue Eng. Part C. Methods *14*, 273–280.

Hattori, T., Müller, C., Gebhard, S., Bauer, E., Pausch, F., Schlund, B., Bösl, M.R., Hess, A., Surmann-Schmitt, C., von der Mark, H., et al. (2010a). SOX9 is a major negative regulator of cartilage vascularization, bone marrow formation and endochondral ossification. Development *137*, 901–911.

Hattori, T., Muller, C., Gebhard, S., Bauer, E., Pausch, F., Schlund, B., Bosl, M.R., Hess, A., Surmann-Schmitt, C., von der Mark, H., et al. (2010b). SOX9 is a major negative regulator of cartilage vascularization, bone marrow formation and endochondral ossification. Development *137*, 901–911.

Häuselmann, H.J., Masuda, K., Hunziker, E.B., Neidhart, M., Mok, S.S., Michel, B.A., and Thonar, E.J. (1996). Adult human chondrocytes cultured in alginate form a matrix similar to native human articular cartilage. Am. J. Physiol. *271*, 742–752.

He, C.-X., Zhang, T.-Y., Miao, P.-H., Hu, Z.-J., Han, M., Tabata, Y., Hu, Y.-L., and Gao, J.-Q. (2012). TGF-β1 gene-engineered mesenchymal stem cells induce rat cartilage regeneration using nonviral gene vector. Biotechnol. Appl. Biochem. *59*, 163–169.

Heiligenstein, S., Cucchiarini, M., Laschke, M.W., Bohle, R.M., Kohn, D., Menger, M.D., and Madry, H. (2011). In vitro and in vivo characterization of nonbiomedical- and biomedical-grade alginates for articular chondrocyte transplantation. Tissue Eng. Part C. Methods *17*, 829–842.

Heitz, F., Morris, M.C., and Divita, G. (2009). Twenty years of cell-penetrating peptides: from molecular mechanisms to therapeutics. Br. J. Pharmacol. *157*, 195–206.

Hellingman, C.A., Davidson, E.N.B., Koevoet, W., Vitters, E.L., van den Berg, W.B., van Osch, G.J.V.M., and van der Kraan, P.M. (2011). Smad Signaling Determines Chondrogenic Differentiation of Bone-Marrow-Derived Mesenchymal Stem Cells: Inhibition of Smad1/5/8P Prevents Terminal Differentiation and Calcification. Tissue Eng. Part A *17*, 1157–1167.

Heo, D.N., Ko, W.-K., Bae, M.S., Lee, J.B., Lee, D.-W., Byun, W., Lee, C.H., Kim, E.-C., Jung, B.-Y., Kwon, I.K., et al. (2014). Enhanced bone regeneration with a gold nanoparticle–hydrogel complex. J. Mater. Chem. B *2*, 1584–1593.

Heyde, M., Partridge, K.A., Oreffo, R.O.C., Howdle, S.M., Shakesheff, K.M., and Garnett, M.C. (2007). Gene therapy used for tissue engineering applications. J. Pharm. Pharmacol. *59*, 329–350.

Hidaka, C., Goodrich, L.R., Chen, C.T., Warren, R.F., Crystal, R.G., and Nixon, A.J. (2003). Acceleration of cartilage repair by genetically modified chondrocytes over expressing bone morphogenetic protein-7. J. Orthop. Res. *21*, 573–583.

Hirao, M., Tamai, N., Tsumaki, N., Yoshikawa, H., and Myoui, A. (2006). Oxygen tension regulates chondrocyte differentiation and function during endochondral ossification. J. Biol. Chem. *281*, 31079–31092.

Hjelle, K., Solheim, E., Strand, T., Muri, R., and Brittberg, M. (2002). Articular cartilage defects in 1,000 knee arthroscopies. Arthroscopy *18*, 730–734.

Ho, A., Schwarze, S.R., Mermelstein, S.J., Waksman, G., and Dowdy, S.F. (2001). Synthetic protein transduction domains: enhanced transduction potential in vitro and in vivo. Cancer Res. *61*, 474–477.

Hollander, A.P., and Hatton, P. V. (2003). Biopolymer Methods in Tissue Engineering (New Jersey: Humana Press).

Hong, J.W., Park, J.H., Huh, K.M., Chung, H., Kwon, I.C., and Jeong, S.Y. (2004). PEGylated polyethylenimine for in vivo local gene delivery based on lipiodolized emulsion system. J. Control. Release *99*, 167–176.

Hootman, J.M., and Helmick, C.G. (2006). Projections of US prevalence of arthritis and associated activity limitations. Arthritis Rheum. *54*, 226–229.

Hortensius, R.A., Becraft, J.R., Pack, D.W., and Harley, B.A.C. (2015). The effect of glycosaminoglycan content on polyethylenimine-based gene delivery within three-dimensional collagen-GAG scaffolds. Biomater. Sci *3*.

Houchin-Ray, T., Whittlesey, K.J., and Shea, L.D. (2007). Spatially patterned gene delivery for localized neuron survival and neurite extension. Mol. Ther. *15*, 705–712.

Huang, X., and Brazel, C.S. (2001). On the importance and mechanisms of burst release in matrix-controlled drug delivery systems. J. Control. Release *73*, 121–136.

Huang, Y.-C., Simmons, C., Kaigler, D., Rice, K.G., and Mooney, D.J. (2005a). Bone regeneration in a rat cranial defect with delivery of PEI-condensed plasmid DNA encoding for bone morphogenetic protein-4 (BMP-4). Gene Ther. *12*, 418–426.

Huang, Y.-C., Riddle, K., Rice, K.G., and Mooney, D.J. (2005b). Long-term in vivo gene expression via delivery of PEI-DNA condensates from porous polymer scaffolds. Hum. Gene Ther. *16*, 609–617.

Huard, J., and Fu, F.H. (2000). Gene Therapy and Tissue Engineering in Orthopaedic and Sports Medicine (Birkhäuser Boston).

Huard, J., Li, Y., Peng, H., and Fu, F.H. (2003). Gene therapy and tissue engineering for sports medicine. J. Gene Med. *5*, 93–108.

Huebsch, N., Kearney, C.J., Zhao, X., Kim, J., Cezar, C.A., Suo, Z., and Mooney, D.J. (2014). Ultrasound-triggered disruption and self-healing of reversibly cross-linked hydrogels for drug delivery and enhanced chemotherapy. Proc. Natl. Acad. Sci. *111*, 9762–9767.

Igarashi, T., Iwasaki, N., Kasahara, Y., and Minami, A. (2010). A cellular implantation system using an injectable ultra-purified alginate gel for repair of osteochondral defects in a rabbit model. J. Biomed. Mater. Res. A *94*, 844–855.

Ignat'eva, N.Y., Danilov, N.A., Averkiev, S. V., Obrezkova, M. V., Lunin, V. V., and Sobol', E.N. (2007). Determination of hydroxyproline in tissues and the evaluation of the collagen content of the tissues. J. Anal. Chem. *62*, 51–57.

Ikeda, T., Kamekura, S., Mabuchi, A., Kou, I., Seki, S., Takato, T., Nakamura, K., Kawaguchi, H., Ikegawa, S., and Chung, U. (2004). The combination of SOX5, SOX6, and SOX9 (the SOX trio) provides signals sufficient for induction of permanent cartilage. Arthritis Rheum. *50*, 3561–3573.

Im, G.-I., and Kim, H.-J. (2011). Electroporation-mediated gene transfer of SOX trio to enhance

chondrogenesis in adipose stem cells. Osteoarthr. Cartil. *19*, 449–457.

Im, G.-I., Kim, H.-J., and Lee, J.H. (2011). Chondrogenesis of adipose stem cells in a porous PLGA scaffold impregnated with plasmid DNA containing SOX trio (SOX-5,-6 and -9) genes. Biomaterials *32*, 4385–4392.

Itaka, K., Ohba, S., Miyata, K., Kawaguchi, H., Nakamura, K., Takato, T., Chung, U.-I., and Kataoka, K. (2007). Bone Regeneration by Regulated In Vivo Gene Transfer Using Biocompatible Polyplex Nanomicelles. Mol. Ther. *15*, 1655–1662.

Ivkovic, A., Pascher, A., Hudetz, D., Maticic, D., Jelic, M., Dickinson, S., Loparic, M., Haspl, M., Windhager, R., and Pecina, M. (2010). Articular cartilage repair by genetically modified bone marrow aspirate in sheep. Gene Ther. *17*, 779–789.

Iyama, K., Ninomiya, Y., Olsen, B.R., Linsenmayer, T.F., Trelstad, R.L., and Hayashi, M. (1991). Spatiotemporal pattern of type X collagen gene expression and collagen deposition in embryonic chick vertebrae undergoing endochondral ossification. Anat. Rec. *229*, 462–472.

Jackson, D.W., Simon, T.M., and Aberman, H.M. (2001). Symptomatic articular cartilage degeneration: the impact in the new millennium. Clin. Orthop. Relat. Res. S14-25.

Jang, J.-H., and Shea, L.D. (2003). Controllable delivery of non-viral DNA from porous scaffolds. J. Control. Release *86*, 157–168.

Jang, J.-H., Bengali, Z., Houchin, T.L., and Shea, L.D. (2006). Surface adsorption of DNA to tissue engineering scaffolds for efficient gene delivery. J. Biomed. Mater. Res. A *77*, 50–58.

Jeon, M., Shin, Y., Jung, J., Jung, U.-W., Lee, J.-H., Moon, J.-S., Kim, I., Shin, J.-S., Lee, S.-K., and Song, J.S. (2017). HIF1A overexpression using cell-penetrating DNA-binding protein induces angiogenesis in vitro and in vivo. Mol. Cell. Biochem. 1–9.

Jeon, O., Powell, C., Ahmed, S.M., and Alsberg, E. (2010). Biodegradable, Photocrosslinked Alginate Hydrogels with Independently Tailorable Physical Properties and Cell Adhesivity. Tissue Eng. Part A *16*, 2915–2925.

Jeon, O., Krebs, M., and Alsberg, E. (2011). Controlled and sustained gene delivery from injectable, porous PLGA scaffolds. J. Biomed. Mater. Res. A *98*, 72–79.

Jeon, S.Y., Park, J.S., Yang, H.N., Woo, D.G., and Park, K.-H. (2012). Co-delivery of SOX9 genes and anti-Cbfa-1 siRNA coated onto PLGA nanoparticles for chondrogenesis of human MSCs. Biomaterials *33*, 4413–4423.

Jo, J., Hong, S., Choi, W.Y., and Lee, D.R. (2014). Cell-penetrating peptide (CPP)-conjugated proteins is an efficient tool for manipulation of human mesenchymal stromal cells. Sci. Rep. *4*, 4378.

Johnstone, B., Hering, T.M., Caplan, A.I., Goldberg, V.M., and Yoo, J.U. (1998). In vitro chondrogenesis of bone marrow-derived mesenchymal progenitor cells. Exp. Cell Res. *238*, 265–272.

Joydeep, D., Choi, Y.-J., Yasuda, H., Han, J.W., Park, C., Song, H., Bae, H., and Kim, J.-H. (2016). Efficient delivery of C/EBP beta gene into human mesenchymal stem cells via polyethylenimine-coated gold nanoparticles enhances adipogenic differentiation. Sci. Rep. *6*, 33784.

Kafienah, W., Al-Fayez, F., Hollander, A.P., and Barker, M.D. (2003). Inhibition of cartilage degradation: a combined tissue engineering and gene therapy approach. Arthritis Rheum. *48*, 709–718.

Kaitsuka, T., and Tomizawa, K. (2015). Cell-Penetrating Peptide as a Means of Directing the Differentiation of Induced-Pluripotent Stem Cells. Int. J. Mol. Sci. *16*, 26667–26676.

Kapoor, M., and Burgess, D.J. (2012). Efficient and safe delivery of siRNA using anionic lipids: Formulation optimization studies. Int. J. Pharm. *432*, 80–90.

Katayama, R., Wakitani, S., Tsumaki, N., Morita, Y., Matsushita, I., Gejo, R., and Kimura, T. (2004). Repair of articular cartilage defects in rabbits using CDMP1 gene-transfected autologous mesenchymal cells derived from bone marrow. Rheumatology *43*, 980–985.

Kaul, G., Cucchiarini, M., Arntzen, D., Zurakowski, D., Menger, M.D., Kohn, D., Trippel, S.B., and Madry, H. (2006). Local stimulation of articular cartilage repair by transplantation of encapsulated chondrocytes overexpressing human fibroblast growth factor 2 (FGF-2) in vivo. J. Gene Med. *8*, 100–111.

Kawai, M., Bessho, K., Kaihara, S., Sonobe, J., Oda, K., Iizuka, T., and Maruyama, H. (2003). Ectopic Bone Formation by Human Bone Morphogenetic Protein-2 Gene Transfer to Skeletal Muscle Using Transcutaneous Electroporation. Hum. Gene Ther. *14*, 1547–1556.

Kawai, M., Bessho, K., Maruyama, H., Miyazaki, J.-I., and Yamamoto, T. (2005). Human BMP-2 gene transfer using transcutaneous in vivo electroporation induced both intramembranous and endochondral ossification. Anat. Rec. Part A Discov. Mol. Cell. Evol. Biol. *287A*, 1264–1271.

Kay, M.A. (2011). State-of-the-art gene-based therapies: the road ahead. Nat. Rev. Genet. *12*, 316–328.

Kayabaşi, G.K., Aydin, R.S.T., and Gümüşderelioğlu, M. (2013). In vitro chondrogenesis by BMP6 gene therapy. J. Biomed. Mater. Res. A *101*, 1353–1361.

Kearney, C.J., and Mooney, D.J. (2013). Macroscale delivery systems for molecular and cellular payloads. Nat. Mater. *12*, 1004–1017.

Kearney, C.J., Skaat, H., Kennedy, S.M., Hu, J., Darnell, M., Raimondo, T.M., and Mooney, D.J. (2015). Switchable Release of Entrapped Nanoparticles from Alginate Hydrogels. Adv. Healthc. Mater. *4*, 1634–1639.

Keeney, M., van den Beucken, J.J.J.P., van der Kraan, P.M., Jansen, J.A., and Pandit, A. (2010). The ability of a collagen/calcium phosphate scaffold to act as its own vector for gene delivery and to promote bone formation via transfection with VEGF165. Biomaterials *31*, 2893–2902.

Keller, B., Yang, T., Chen, Y., Munivez, E., Bertin, T., Zabel, B., and Lee, B. (2011). Interaction of TGFbeta and BMP Signaling Pathways during Chondrogenesis. PLoS One *6*, e16421.

Khoury, M., Bigey, P., Louis-Plence, P., Noel, D., Rhinn, H., Scherman, D., Jorgensen, C., and Apparailly, F. (2006). A comparative study on intra-articular versus systemic gene electrotransfer in experimental arthritis. J. Gene Med. *8*, 1027–1036.

Kidd, M.E., Shin, S., and Shea, L.D. (2012). Fibrin hydrogels for lentiviral gene delivery in vitro and in vivo. J. Control. Release *157*, 80–85.

Kilian, K.A., Bugarija, B., Lahn, B.T., and Mrksich, M. (2010). Geometric cues for directing the differentiation of mesenchymal stem cells. Proc. Natl. Acad. Sci. U. S. A. *107*, 4872–4877.

Kim, Y.B., and Kim, G.H. (2015). PCL/Alginate Composite Scaffolds for Hard Tissue Engineering: Fabrication, Characterization, and Cellular Activities. ACS Comb. Sci. *17*, 87–99.

Kim, E.J., Cho, S.W., Shin, J.O., Lee, M.J., Kim, K.S., and Jung, H.S. (2013). Ihh and Runx2/Runx3 Signaling Interact to Coordinate Early Chondrogenesis: A Mouse Model. PLoS One *8*, e55296.

King, W.J., Kouris, N.A., Choi, S., Ogle, B.M., and Murphy, W.L. (2012). Environmental parameters influence non-viral transfection of human mesenchymal stem cells for tissue engineering applications. Cell Tissue Res. *347*, 689–699.

Klinger, P., Surmann-Schmitt, C., Brem, M., Swoboda, B., Distler, J.H., Carl, H.D., Von Der Mark, K., Hennig, F.F., and Gelse, K. (2011). Chondromodulin 1 stabilizes the chondrocyte phenotype and inhibits endochondral ossification of porcine cartilage repair tissue. Arthritis Rheum. *63*, 2721–2731.

Kock, L., van Donkelaar, C.C., and Ito, K. (2012). Tissue engineering of functional articular cartilage: the current status. Cell Tissue Res. *347*, 613–627.

Kotlarz, H., Gunnarsson, C.L., Fang, H., and Rizzo, J. a (2009). Insurer and out-of-pocket costs of osteoarthritis in the US: evidence from national survey data. Arthritis Rheum. *60*, 3546–3553.

van der Kraan, P., Vitters, E., and van den Berg, W. (1992). Differential effect of transforming growth factor beta on freshly isolated and cultured articular chondrocytes. J. Rheumatol. *19*, 140–145.

Krebs, M.D., Salter, E., Chen, E., Sutter, K. a, and Alsberg, E. (2010). Calcium phosphate-DNA nanoparticle gene delivery from alginate hydrogels induces in vivo osteogenesis. J. Biomed. Mater. Res. A *92*, 1131–1138.

Kruskal, B.A., Shak, S., and Maxfield, F.R. (1986). Spreading of human neutrophils is immediately preceded by a large increase in cytoplasmic free calcium. Proc. Natl. Acad. Sci. U. S. A. *83*, 2919–2923.

Kundu, J., Shim, J.-H., Jang, J., Kim, S.-W., and Cho, D.-W. (2015). An additive manufacturing-based PCL-alginate-chondrocyte bioprinted scaffold for cartilage tissue engineering. J. Tissue Eng. Regen. Med. *9*, 1286–1297.

Kuo, C.K., and Ma, P.X. (2001). Ionically crosslinked alginate hydrogels as scaffolds for tissue engineering: Part 1. Structure, gelation rate and mechanical properties. Biomaterials *22*, 511–521.

Labek, G., Thaler, M., Janda, W., Agreiter, M., and Stockl, B. (2011). Revision rates after total joint replacement: CUMULATIVE RESULTS FROM WORLDWIDE JOINT REGISTER DATASETS. Bone Joint J. *93–B*, 293–297.

Lafont, J.E. (2010). Lack of oxygen in articular cartilage: Consequences for chondrocyte biology. Int. J. Exp. Pathol. *91*, 99–106.

Lai, Q.-G., Yuan, K.-F., Xu, X., Li, D., Li, G.-J., Wei, F.-L., Yang, Z.-J., Luo, S.-L., Tang, X.-P., and Li, S. (2011). Transcription factor osterix modified bone marrow mesenchymal stem cells enhance callus formation during distraction osteogenesis. Oral Surgery, Oral Med. Oral Pathol. Oral Radiol. Endodontology *111*, 412–419.

Lam, A.M.I., and Cullis, P.R. (2000). Calcium enhances the transfection potency of plasmid DNA–cationic liposome complexes. Biochim. Biophys. Acta - Biomembr. *1463*, 279–290.

Lamartina, S., Silvi, L., Roscilli, G., Casimiro, D., Simon, A.J., Davies, M.-E., Shiver, J.W., Rinaudo, C.D., Zampaglione, I., Fattori, E., et al. (2003). Construction of an rtTA2(s)-m2/tts(kid)-based transcription regulatory switch that displays no basal activity, good inducibility, and high responsiveness to doxycycline in mice and non-human primates. Mol. Ther. *7*, 271–280.

De Laporte, L., and Shea, L.D. (2007). Matrices and scaffolds for DNA delivery in tissue engineering. Adv. Drug Deliv. Rev. *59*, 292–307.

Larsen, A.K., Hunter, A.C., Parhamifar, L., Moghimi, S.M., and Andresen, T.L. (2010). Polycation cytotoxicity: a delicate matter for nucleic acid therapy—focus on polyethylenimine. Soft Matter *6*, 4001.

Latchman, D.S. (1997). Transcription factors: an overview. Int. J. Biochem. Cell Biol. *29*, 1305–1312.

Ledley, F.D., McNamee, L.M., Uzdil, V., and Morgan, I.W. (2014). Why commercialization of gene therapy stalled; examining the life cycles of gene therapy technologies. Gene Ther. *21*, 188–194.

Lee, K.Y., and Mooney, D.J. (2012). Alginate: properties and biomedical applications. Prog. Polym. Sci. *37*, 106–126.

Lee, C.S.D., Moyer, H.R., Gittens I., R.A., Williams, J.K., Boskey, A.L., Boyan, B.D., and Schwartz, Z. (2010). Regulating in vivo calcification of alginate microbeads. Biomaterials *31*, 4926–4934.

Lee, H.-P., Rey-Rico, A., Cucchiarini, M., and Madry, H. (2014). Nonviral gene transfer into human meniscal cells. Part II: effect of three-dimensional environment and overexpression of human fibroblast growth factor 2. Int. Orthop. *38*, 1931–1936.

Lee, J.-S., Lee, J.-M., and Im, G.-I. (2011). Electroporation-mediated transfer of Runx2 and Osterix genes to enhance osteogenesis of adipose stem cells. Biomaterials *32*, 760–768.

Lee, M.-H., Kim, Y.-J., Kim, H.-J., Park, H.-D., Kang, A.-R., Kyung, H.-M., Sung, J.-H., Wozney, J.M., and Ryoo, H.-M. (2003). BMP-2-induced Runx2 expression is mediated by Dlx5, and TGF-beta 1 opposes the BMP-2-induced osteoblast differentiation by suppression of Dlx5 expression. J. Biol. Chem. *278*, 34387–34394.

Lee, S.Y., Nakagawa, T., and Reddi, A.H. (2008). Induction of chondrogenesis and expression of superficial zone protein (SZP)/lubricin by mesenchymal progenitors in the infrapatellar fat pad of the knee joint treated with TGF-beta1 and BMP-7. Biochem. Biophys. Res. Commun. *376*, 148–153.

Lefebvre, V., Li, P., and de Crombrugghe, B. (1998). A new long form of Sox5 (L-Sox5), Sox6 and Sox9 are coexpressed in chondrogenesis and cooperatively activate the type II collagen gene. EMBO J. *17*, 5718–5733.

Lei, P., Padmashali, R.M., and Andreadis, S.T. (2009). Cell-controlled and spatially arrayed gene delivery from fibrin hydrogels. Biomaterials *30*, 3790–3799.

Leijten, J.C.H., Emons, J., Sticht, C., van Gool, S., Decker, E., Uitterlinden, a, Rappold, G., Hofman, a, Rivadeneira, F., Scherjon, S., et al. (2012a). Gremlin 1, frizzled-related protein, and Dkk-1 are key regulators of human articular cartilage homeostasis. Arthritis Rheum. *64*, 3302–3312.

Leijten, J.C.H., Moreira Teixeira, L.S., Landman, E.B.M., van Blitterswijk, C.A., and Karperien, M. (2012b). Hypoxia Inhibits Hypertrophic Differentiation and Endochondral Ossification in Explanted Tibiae. PLoS One *7*.

Lennon, D.P., and Caplan, A.I. (2006). Isolation of human marrow-derived mesenchymal stem cells. Exp. Hematol. *34*, 1604–1605.

Li, S.-D., and Huang, L. (2007). Non-viral is superior to viral gene delivery. J. Control. Release *123*, 181–183.

Li, B., Yang, J., Ma, L., Li, F., Tu, Z., and Gao, C. (2013). Fabrication of poly(lactide-co-glycolide) scaffold filled with fibrin gel, mesenchymal stem cells, and poly(ethylene oxide)-b-poly(L - lysine)/TGF-beta1 plasmid DNA complexes for cartilage restoration in vivo. J. Biomed. Mater. Res. - Part A *101*, 3097–3108.

Li, B., Li, F., Ma, L., Yang, J., Wang, C., Wang, D., and Gao, C. (2014). Poly(lactide-co-glycolide)/fibrin gel construct as a 3D model to evaluate gene therapy of cartilage in vivo. Mol. Pharm. *11*, 2062–2070.

Li, R., Stewart, D.J., von Schroeder, H.P., Mackinnon, E.S., and Schemitsch, E.H. (2009). Effect of cell-based VEGF gene therapy on healing of a segmental bone defect. J. Orthop. Res. *27*, 8–14.

Liao, J., Hu, N., Zhou, N., Lin, L., Zhao, C., Yi, S., Fan, T., Bao, W., Liang, X., Chen, H., et al. (2014). Sox9 potentiates BMP2-induced chondrogenic differentiation and inhibits BMP2-induced osteogenic differentiation. PLoS One *9*, e89025.

Lin, C.-Y.Y., Chang, Y.-H.H., Li, K.-C.C., Lu, C.-H.H., Sung, L.-Y.Y., Yeh, C.-L.L., Lin, K.-J.J., Huang, S.-F.F., Yen, T.-C.C., and Hu, Y.-C.C. (2013). The use of ASCs engineered to express BMP2 or TGF-β3 within scaffold constructs to promote calvarial bone repair. Biomaterials *34*, 9401–9412.

Lin, H., Tang, Y., Lozito, T.P., Oyster, N., Kang, R.B., Fritch, M.R., Wang, B., and Tuan, R.S. (2017). Projection Stereolithographic Fabrication of BMP-2 Gene-activated Matrix for Bone Tissue Engineering. Sci. Rep. *7*, 11327.

Liu, K., Zhou, G.D., Liu, W., Zhang, W.J., Cui, L., Liu, X., Liu, T.Y., and Cao, Y. (2008). The dependence of in vivo stable ectopic chondrogenesis by human mesenchymal stem cells on chondrogenic differentiation in vitro. Biomaterials *29*, 2183–2192.

Livak, K.J., and Schmittgen, T.D. (2001). Analysis of Relative Gene Expression Data Using Real-Time Quantitative PCR and the 2−ΔΔCT Method. Methods *25*, 402–408.

Locatelli, P., Olea, F.D., Hnatiuk, A., Sepúlveda, D., Pérez Sáez, J.M., Argüello, R., and Crottogini, A. (2013). Efficient plasmid-mediated gene transfection of ovine bone marrow mesenchymal stromal cells. Cytotherapy *15*, 163–170.

Loebel, C., Czekanska, E.M., Bruderer, M., Salzmann, G., Alini, M., and Stoddart, M.J. (2015). In vitro osteogenic potential of human mesenchymal stem cells is predicted by Runx2/Sox9 ratio. Tissue Eng. Part A *21*, 115–123.

Logeart-Avramoglou, D., Oudina, K., Bourguignon, M., Delpierre, L., Nicola, M.-A., Bensidhoum, M., Arnaud, E., and Petite, H. (2010). In vitro and in vivo bioluminescent quantification of viable stem cells in engineered constructs. Tissue Eng. Part C. Methods *16*, 447–458.

Loozen, L.D., Wegman, F., Öner, F.C., Dhert, W.J. a., and Alblas, J. (2013). Porous bioprinted constructs in BMP-2 non-viral gene therapy for bone tissue engineering. J. Mater. Chem. B *1*, 6619–6626.

Loozen, L.D., van der Helm, Y.J.M., Öner, F.C., Dhert, W.J. a., Kruyt, M.C., and Alblas, J. (2015). Bone Morphogenetic Protein-2 Nonviral Gene Therapy in a Goat Iliac Crest Model for Bone Formation. Tissue Eng. Part A *21*, 1672–1679.

Lopa, S., and Madry, H. (2014). Bioinspired Scaffolds for Osteochondral Regeneration. Tissue Eng. Part A *20*, 2052–2076.

Lv, H., Zhang, S., Wang, B., Cui, S., and Yan, J. (2006). Toxicity of cationic lipids and cationic polymers in gene delivery. J. Control. Release *114*, 100–109.

Ma, H.-L., Hung, S.-C., Lin, S.-Y., Chen, Y.-L., and Lo, W.-H. (2003). Chondrogenesis of human mesenchymal stem cells encapsulated in alginate beads. J. Biomed. Mater. Res. A *64*, 273–281.

Mackay, A.M., Beck, S.C., Murphy, J.M., Barry, F.P., Chichester, C.O., and Pittenger, M.F. (1998). Chondrogenic differentiation of cultured human mesenchymal stem cells from marrow. Tissue Eng. *4*, 415–428.

Macri, L., Silverstein, D., and Clark, R.A.F. (2007). Growth factor binding to the pericellular matrix and its importance in tissue engineering. Adv. Drug Deliv. Rev. *59*, 1366–1381.

Madry, H., and Cucchiarini, M. (2014). Tissue-engineering strategies to repair joint tissue in osteoarthritis: nonviral gene-transfer approaches. Curr. Rheumatol. Rep. *16*, 450.

Madry, H., Cucchiarini, M., Stein, U., Remberger, K., Menger, M.D., Kohn, D., and Trippel, S.B. (2003). Sustained transgene expression in cartilage defects in vivo after transplantation of articular chondrocytes modified by lipid-mediated gene transfer in a gel suspension delivery system. J. Gene Med. *5*, 502–509.

Madry, H., Kaul, G., Cucchiarini, M., Stein, U., Zurakowski, D., Remberger, K., Menger, M.D., Kohn, D., and Trippel, S.B. (2005). Enhanced repair of articular cartilage defects in vivo by transplanted chondrocytes overexpressing insulin-like growth factor I (IGF-I). Gene Ther. *12*, 1171–1179.

Madry, H., Orth, P., Kaul, G., Zurakowski, D., Menger, M.D., Kohn, D., and Cucchiarini, M. (2010). Acceleration of articular cartilage repair by combined gene transfer of human insulin-like growth factor I and fibroblast growth factor-2 in vivo. Arch Orthop Trauma Surg *130*, 1311–1322.

Madry, H., Kaul, G., Zurakowski, D., Vunjak-Novakovic, G., and Cucchiarini, M. (2012). Cartilage constructs engineered from chondrocytes overexpressing IGF-I improve the repair of osteochondral defects in a rabbit model. Eur. Cells Mater. *25*, 229–247.

Malakooty Poor, E., Baghaban Eslaminejad, M., Gheibi, N., Bagheri, F., and Atyabi, F. (2014). Chitosan–pDNA nanoparticle characteristics determine the transfection efficacy of gene delivery to human mesenchymal stem cells. Artif. Cells, Nanomedicine, Biotechnol. *42*, 376–384.

Malda, J., Visser, J., Melchels, F.P., Jüngst, T., Hennink, W.E., Dhert, W.J. a, Groll, J., and Hutmacher, D.W. (2013). 25th anniversary article: Engineering hydrogels for biofabrication. Adv. Mater. *25*, 5011–5028.

Mansouri, S., Lavigne, P., Corsi, K., Benderdour, M., Beaumont, E., and Fernandes, J.C. (2004). Chitosan-DNA nanoparticles as non-viral vectors in gene therapy: strategies to improve transfection efficacy. Eur. J. Pharm. Biopharm. *57*, 1–8.

Marędziak, M., Marycz, K., Tomaszewski, K.A., Kornicka, K., and Henry, B.M. (2016). The Influence of Aging on the Regenerative Potential of Human Adipose Derived Mesenchymal Stem Cells. Stem Cells Int. *2016*, 1–15.

Margadant, C., Cremers, L., Sonnenberg, A., and Boonstra, J. (2013). MAPK uncouples cell cycle progression from cell spreading and cytoskeletal organization in cycling cells. Cell. Mol. Life Sci. *70*, 293–307.

Markstedt, K., Mantas, A., Tournier, I., Martínez Ávila, H., Hägg, D., and Gatenholm, P. (2015). 3D bioprinting human chondrocytes with nanocellulose-alginate bioink for cartilage tissue engineering applications. Biomacromolecules *16*, 1489–1496.

Martin, M.E., and Rice, K.G. (2007). Peptide-guided gene delivery. AAPS J. *9*, E18-29.

Martini, F., Nath, J., and Bartholomew, E. (2009). Fundamentals of anatomy and physiology.

Mason, J.M., Grande, D. a, Barcia, M., Grant, R., Pergolizzi, R.G., and Breitbart, a S. (1998). Expression of human bone morphogenic protein 7 in primary rabbit periosteal cells: potential utility in gene therapy for osteochondral repair. Gene Ther. *5*, 1098–1104.

Mastrobattista, E., Bravo, S.A., van der Aa, M., and Crommelin, D.J.A. (2005). Nonviral gene delivery systems: From simple transfection agents to artificial viruses. Drug Discov. Today.

Technol. *2*, 103–109.

Mathieu, P.S., and Loboa, E.G. (2012). Cytoskeletal and focal adhesion influences on mesenchymal stem cell shape, mechanical properties, and differentiation down osteogenic, adipogenic, and chondrogenic pathways. Tissue Eng. Part B. Rev. *18*, 436–444.

Matsumoto, T., Okazaki, M., Inoue, M., Yamaguchi, S., Kusunose, T., Toyonaga, T., Hamada, Y., and Takahashi, J. (2004). Hydroxyapatite particles as a controlled release carrier of protein. Biomaterials *25*, 3807–3812.

McBeath, R., Pirone, D.M., Nelson, C.M., Bhadriraju, K., and Chen, C.S. (2004). Cell shape, cytoskeletal tension, and RhoA regulate stem cell lineage commitment. Dev. Cell *6*, 483–495.

McCaffrey, J., McCrudden, C.M., Ali, A.A., Massey, A.S., McBride, J.W., McCrudden, M.T.C., Vicente-Perez, E.M., Coulter, J.A., Robson, T., Donnelly, R.F., et al. (2016). Transcending epithelial and intracellular biological barriers; A prototype DNA delivery device. J. Control. Release *226*, 238–247.

McCarthy, H.O., McCaffrey, J., McCrudden, C.M., Zholobenko, A., Ali, A. a, McBride, J.W., Massey, A.S., Pentlavalli, S., Chen, K.-H., Cole, G., et al. (2014). Development and characterization of self-assembling nanoparticles using a bio-inspired amphipathic peptide for gene delivery. J. Control. Release *189C*, 141–149.

McKiernan, P.J., Cunningham, O., Greene, C.M., Cryan, S.-A., McKiernan, P.J., Cunningham, and Greene, C.M. (2013). Targeting miRNA-based medicines to cystic fibrosis airway epithelial cells using nanotechnology. Int. J. Nanomedicine *8*, 3907–3915.

Mease, P.J., Wei, N., Fudman, E.J., Kivitz, A.J., Schechtman, J., Trapp, R.G., Hobbs, K.F., Greenwald, M., Hou, A., Bookbinder, S.A., et al. (2010). Safety, tolerability, and clinical outcomes after intraarticular injection of a recombinant adeno-associated vector containing a tumor necrosis factor antagonist gene: results of a phase 1/2 Study. J. Rheumatol. *37*, 692–703.

Mehlhorn, a T., Niemeyer, P., Kaschte, K., Muller, L., Finkenzeller, G., Hartl, D., Sudkamp, N.P., and Schmal, H. (2007). Differential effects of BMP-2 and TGF-beta1 on chondrogenic differentiation of adipose derived stem cells. Cell Prolif. *40*, 809–823.

Meilander-Lin, N.J., Cheung, P.J., Wilson, D.L., and Bellamkonda, R. V. (2005). Sustained in Vivo Gene Delivery from Agarose Hydrogel Prolongs Nonviral Gene Expression in Skin. Tissue Eng. *11*, 546–555.

Meinel, L., Hofmann, S., Betz, O., Fajardo, R., Merkle, H.P., Langer, R., Evans, C.H., Vunjak-Novakovic, G., and Kaplan, D.L. (2006). Osteogenesis by human mesenchymal stem cells cultured on silk biomaterials: comparison of adenovirus mediated gene transfer and protein delivery of BMP-2. Biomaterials *27*, 4993–5002.

Melchels, F.P.W., Blokzijl, M.M., Levato, R., Peiffer, Q.C., Ruijter, M. De, Hennink, W.E., Vermonden, T., and Malda, J. (2016). Hydrogel-based reinforcement of 3D bioprinted constructs. Biofabrication *8*.

Mellott, A.J., Forrest, M.L., and Detamore, M.S. (2013). Physical non-viral gene delivery methods for tissue engineering. Ann. Biomed. Eng. *41*, 446–468.

Merkus, H.G. (2009). Particle Size Measurements.

Mhanna, R., Kashyap, A., Palazzolo, G., Vallmajo-Martin, Q., Becher, J., Möller, S., Schnabelrauch, M., and Zenobi-Wong, M. (2014). Chondrocyte culture in three dimensional alginate sulfate hydrogels promotes proliferation while maintaining expression of chondrogenic markers. Tissue

Eng. Part A *20*, 1454–1464.

Mi, Z., Ghivizzani, S.C., Lechman, E., Glorioso, J.C., Evans, C.H., and Robbins, P.D. (2003). Adverse effects of adenovirus-mediated gene transfer of human transforming growth factor beta 1 into rabbit knees. Arthritis Res. Ther. *5*, R132-9.

Michael, A. (1996). Financing gene therapy beyond phase II. Gene Ther. *3*, 1035–1038.

Michlits, W., Mittermayr, R., Schäfer, R., Redl, H., and Aharinejad, S. (2007). Fibrin-embedded administration of VEGF plasmid enhances skin flap survival. Wound Repair Regen. *15*, 360–367.

Mir, L.M., Bureau, M.F., Gehl, J., Rangara, R., Rouy, D., Caillaud, J.M., Delaere, P., Branellec, D., Schwartz, B., and Scherman, D. (1999). High-efficiency gene transfer into skeletal muscle mediated by electric pulses. Proc. Natl. Acad. Sci. U. S. A. *96*, 4262–4267.

Moghimi, S.M., Symonds, P., Murray, J.C., Hunter, A.C., Debska, G., and Szewczyk, A. (2005). A two-stage poly(ethylenimine)-mediated cytotoxicity: implications for gene transfer/therapy. Mol. Ther. *11*, 990–995.

Monteiro, N., Martins, A., Reis, R.L., and Neves, N.M. (2014a). Liposomes in tissue engineering and regenerative medicine. J. R. Soc. Interface *11*.

Monteiro, N., Ribeiro, D., Martins, A., Faria, S., Fonseca, N.A., Moreira, J.N., Reis, R.L., and Neves, N.M. (2014b). Instructive nanofibrous scaffold comprising runt-related transcription factor 2 gene delivery for bone tissue engineering. ACS Nano *8*, 8082–8094.

Mooney, D.J., Shea, L.D., Smiley, E., and Bonadio, J. (1999). DNA delivery from polymer matrices for tissue engineering. Nat. Biotechnol. *17*, 551–554.

Morales, T.I. (1991). Transforming growth factor-beta 1 stimulates synthesis of proteoglycan aggregates in calf articular cartilage organ cultures. Arch. Biochem. Biophys. *286*, 99–106.

Morris, M., Vidal, P., Chaloin, L., Heitz, F., and Divita, G. (1997). A new peptide vector for efficient delivery of oligonucleotides into mammalian cells. Nucleic Acids Res. *25*, 2730–2736.

Mueller, M.B., and Tuan, R.S. (2008). Functional characterization of hypertrophy in chondrogenesis of human mesenchymal stem cells. Arthritis Rheum. *58*, 1377–1388.

Müller, M., Öztürk, E., Arlov, Ø., Gatenholm, P., and Zenobi-Wong, M. (2017). Alginate Sulfate–Nanocellulose Bioinks for Cartilage Bioprinting Applications. Ann. Biomed. Eng. *45*, 210–223.

Murphy, S. V, and Atala, A. (2014). 3D bioprinting of tissues and organs. Nat. Biotechnol. *32*, 773–785.

Musumeci, G., Mobasheri, A., Trovato, F.M., Szychlinska, M.A., Graziano, A.C.E., Lo Furno, D., Avola, R., Mangano, S., Giuffrida, R., and Cardile, V. (2014). Biosynthesis of collagen I, II, RUNX2 and lubricin at different time points of chondrogenic differentiation in a 3D in vitro model of human mesenchymal stem cells derived from adipose tissue. Acta Histochem. *116*, 1407–1417.

Nabiev, I., Mitchell, S., Davies, A., Williams, Y., Kelleher, D., Moore, R., Gun'ko, Y.K., Byrne, S., Rakovich, Y.P., Donegan, J.F., et al. (2007). Nonfunctionalized nanocrystals can exploit a cell's active transport machinery delivering them to specific nuclear and cytoplasmic compartments. Nano Lett. *7*, 3452–3461.

Nasatto, P.L., Pignon, F., Silveira, J.L.M., Duarte, M.E.R., Noseda, M.D., and Rinaudo, M. (2015). Methylcellulose, a cellulose derivative with original physical properties and extended applications. Polymers (Basel). *7*, 777–803.

Nauta, A.J., and Fibbe, W.E. (2007). Immunomodulatory properties of mesenchymal stromal

cells. Blood *110*, 3499–3506.

Navarrete, R.O., Lee, E.M., Smith, K., Hyzy, S.L., Doroudi, M., Williams, J.K., Gall, K., Boyan, B.D., and Schwartz, Z. (2017). Substrate stiffness controls osteoblastic and chondrocytic differentiation of mesenchymal stem cells without exogenous stimuli. PLoS One *12*.

Needham, C.J., Shah, S.R., Dahlin, R.L., Kinard, L. a, Lam, J., Watson, B.M., Lu, S., Kasper, F.K., and Mikos, A.G. (2014). Osteochondral tissue regeneration through polymeric delivery of DNA encoding for the SOX trio and RUNX2. Acta Biomater. *10*, 4103–4112.

Ng, C.P., Goodman, T.T., Park, I.-K., and Pun, S.H. (2009). Bio-mimetic surface engineering of plasmid-loaded nanoparticles for active intracellular trafficking by actin comet-tail motility. Biomaterials *30*, 951–958.

Nguyen, L.H., Kudva, A.K., Saxena, N.S., and Roy, K. (2011). Engineering articular cartilage with spatially-varying matrix composition and mechanical properties from a single stem cell population using a multi-layered hydrogel. Biomaterials *32*, 6946–6952.

Nigg, E.A. (1997). Nucleocytoplasmic transport: signals, mechanisms and regulation. Nature *386*, 779–787.

Nishida, K., Doita, M., Takada, T., Kakutani, K., Miyamoto, H., Shimomura, T., Maeno, K., and Kurosaka, M. (2006). Sustained Transgene Expression in Intervertebral Disc Cells In Vivo Mediated by Microbubble-Enhanced Ultrasound Gene Therapy. Spine (Phila. Pa. 1976). *31*, 1415–1419.

Nomikou, N., Feichtinger, G.A.A., Saha, S., Nuernberger, S., Heimel, P., Redl, H., and Mchale, A.P.P. (2017). Ultrasound-responsive gene-activated matrices for osteogenic gene therapy using matrix-assisted sonoporation. J. Tissue Eng. Regen. Med.

Nooeaid, P., Salih, V., Beier, J.P., and Boccaccini, A.R. (2012). Osteochondral tissue engineering: scaffolds, stem cells and applications. J. Cell. Mol. Med. *16*, 2247–2270.

Noort, W.A., Oerlemans, M.I.F.J., Rozemuller, H., Feyen, D., Jaksani, S., Stecher, D., Naaijkens, B., Martens, A.C., Bühring, H.J., Doevendans, P.A., et al. (2012). Human versus porcine mesenchymal stromal cells: Phenotype, differentiation potential, immunomodulation and cardiac improvement after transplantation. J. Cell. Mol. Med. *16*, 1827–1839.

O'Brien, F.J. (2011). Biomaterials & scaffolds for tissue engineering. Mater. Today *14*, 88–95.

O'Brien, F.J., Harley, B.A., Yannas, I. V, and Gibson, L.J. (2005). The effect of pore size on cell adhesion in collagen-GAG scaffolds. Biomaterials *26*, 433–441.

Oba, M., Demizu, Y., Yamashita, H., Kurihara, M., and Tanaka, M. (2015). Plasmid DNA delivery using fluorescein-labeled arginine-rich peptides. Bioorg. Med. Chem. *23*, 4911–4918.

Oest, M.E., Dupont, K.M., Kong, H.J., Mooney, D.J., and Guldberg, R.E. (2007). Quantitative assessment of scaffold and growth factor-mediated repair of critically sized bone defects. J. Orthop. Res. *25*, 941–950.

Okazaki, M., Yoshida, Y., Yamaguchi, S., Kaneno, M., and Elliott, J.C. (2001). Affinity binding phenomena of DNA onto apatite crystals. Biomaterials *22*, 2459–2464.

Ono, I., Yamashita, T., Jin, H.-Y., Ito, Y., Hamada, H., Akasaka, Y., Nakasu, M., Ogawa, T., and Jimbow, K. (2004). Combination of porous hydroxyapatite and cationic liposomes as a vector for BMP-2 gene therapy. Biomaterials *25*, 4709–4718.

Orth, P., Kaul, G., Cucchiarini, M., Zurakowski, D., Menger, M.D., Kohn, D., and Madry, H. (2011).

Transplanted articular chondrocytes co-overexpressing IGF-I and FGF-2 stimulate cartilage repair in vivo. Knee Surgery, Sport. Traumatol. Arthrosc. *19*, 2119–2130.

Ozbolat, I.T., and Hospodiuk, M. (2016). Current advances and future perspectives in extrusion-based bioprinting (Elsevier Ltd).

Pagnotto, M.R., Wang, Z., Karpie, J.C., Ferretti, M., Xiao, X., and Chu, C.R. (2007). Adeno-associated viral gene transfer of transforming growth factor-beta1 to human mesenchymal stem cells improves cartilage repair. Gene Ther. *14*, 804–813.

Palmer, G.D., Steinert, A., Pascher, A., Gouze, E., Gouze, J.N., Betz, O., Johnstone, B., Evans, C.H., and Ghivizzani, S.C. (2005). Gene-induced chondrogenesis of primary mesenchymal stem cells in vitro. Mol. Ther. *12*, 219–228.

Park, J., Ries, J., Gelse, K., Kloss, F., von der Mark, K., Wiltfang, J., Neukam, F.W., and Schneider, H. (2003). Bone regeneration in critical size defects by cell-mediated BMP-2 gene transfer: a comparison of adenoviral vectors and liposomes. Gene Ther. *10*, 1089–1098.

Park, J., Lutz, R., Felszeghy, E., Wiltfang, J., Nkenke, E., Neukam, F.W., and Schlegel, K.A. (2007). The effect on bone regeneration of a liposomal vector to deliver BMP-2 gene to bone grafts in peri-implant bone defects. Biomaterials *28*, 2772–2782.

Park, J.S., Na, K., Woo, D.G., Yang, H.N., Kim, J.M., Kim, J.H., Chung, H.-M., and Park, K.-H. (2010). Non-viral gene delivery of DNA polyplexed with nanoparticles transfected into human mesenchymal stem cells. Biomaterials *31*, 124–132.

Park, J.S., Chu, J.S., Tsou, A.D., Diop, R., Tang, Z., Wang, A., and Li, S. (2011). The effect of matrix stiffness on the differentiation of mesenchymal stem cells in response to TGF-beta. Biomaterials *32*, 3921–3930.

Park, J.S., Yang, H.N., Woo, D.G., Jeon, S.Y., and Park, K.-H. (2012). SOX9 gene plus heparinized TGF-β 3 coated dexamethasone loaded PLGA microspheres for inducement of chondrogenesis of hMSCs. Biomaterials *33*, 7151–7163.

Park, J.S., Yi, S.W., Kim, H.J., Kim, S.M., Kim, J.-H., and Park, K.-H. (2017). Construction of PLGA Nanoparticles Coated with Polycistronic *SOX5* , *SOX6* , and *SOX9* Genes for Chondrogenesis of Human Mesenchymal Stem Cells. ACS Appl. Mater. Interfaces *9*, 1361–1372.

Pascher, A., Palmer, G., Steinert, A., Oligino, T., Gouze, E., Gouze, J.-N., Betz, O., Spector, M., Robbins, P., Evans, C., et al. (2004). Gene delivery to cartilage defects using coagulated bone marrow aspirate. Gene Ther. *11*, 133–141.

Pati, F., Song, T.H., Rijal, G., Jang, J., Kim, S.W., and Cho, D.W. (2015). Ornamenting 3D printed scaffolds with cell-laid extracellular matrix for bone tissue regeneration. Biomaterials *37*, 230–241.

Patnaik, S., and Gupta, K.C. (2013). Novel polyethylenimine-derived nanoparticles for *in vivo* gene delivery. Expert Opin. Drug Deliv. *10*, 215–228.

Pei, M., Chen, D., Li, J., and Wei, L. (2009). Histone deacetylase 4 promotes TGF-beta1-induced synovium-derived stem cell chondrogenesis but inhibits chondrogenically differentiated stem cell hypertrophy. Differentiation *78*, 260–268.

Pelttari, K., Winter, A., Steck, E., Goetzke, K., Hennig, T., Ochs, B.G., Aigner, T., and Richter, W. (2006). Premature induction of hypertrophy during in vitro chondrogenesis of human mesenchymal stem cells correlates with calcification and vascular invasion after ectopic transplantation in SCID mice. Arthritis Rheum. *54*, 3254–3266.

Peng, L., Cheng, X., Zhuo, R., Lan, J., Wang, Y., Shi, B., and Li, S. (2009). Novel gene-activated matrix with embedded chitosan/plasmid DNA nanoparticles encoding PDGF for periodontal tissue engineering. J. Biomed. Mater. Res. Part A *90A*, 564–576.

Peng, L.-H., Niu, J., Zhang, C.-Z., Yu, W., Wu, J.-H., Shan, Y.-H., Wang, X.-R., Shen, Y.-Q., Mao, Z.-W., Liang, W.-Q., et al. (2014). TAT conjugated cationic noble metal nanoparticles for gene delivery to epidermal stem cells. Biomaterials *35*, 5605–5618.

Pesesse, L., Sanchez, C., Delcour, J.-P.P., Bellahc??ne, A., Baudouin, C., Msika, P., Henrotin, Y., Bellahcène, A., Baudouin, C., Msika, P., et al. (2013). Consequences of chondrocyte hypertrophy on osteoarthritic cartilage: Potential effect on angiogenesis. Osteoarthr. Cartil. *21*, 1913–1923.

Pi, Y., Zhang, X., Shi, J., Zhu, J., Chen, W., Zhang, C., Gao, W., Zhou, C., and Ao, Y. (2011). Targeted delivery of non-viral vectors to cartilage in vivo using a chondrocyte-homing peptide identified by phage display. Biomaterials *32*, 6324–6332.

Plank, C., Zelphati, O., and Mykhaylyk, O. (2011). Magnetically enhanced nucleic acid delivery. Ten years of magnetofection-progress and prospects. Adv. Drug Deliv. Rev. *63*, 1300–1331.

Plonka, A.B., Khorsand, B., Yu, N., Sugai, J. V, Salem, A.K., Giannobile, W. V, and Elangovan, S. (2017). Effect of sustained PDGF nonviral gene delivery on repair of tooth-supporting bone defects. Gene Ther. *24*, 31–39.

Premaraj, S., Mundy, B., Parker-Barnes, J., Winnard, P., and Moursi, A. (2005). Collagen gel delivery of Tgf-β3 non-viral plasmid DNA in rat osteoblast and calvarial culture. Orthod. & Craniofacial Res. *8*, 320–322.

Qiao, C., Zhang, K., Jin, H., Miao, L., Shi, C., Liu, X., Yuan, A., Liu, J., Li, D., Zheng, C., et al. (2013). Using poly(lactic-co-glycolic acid) microspheres to encapsulate plasmid of bone morphogenetic protein 2/polyethylenimine nanoparticles to promote bone formation in vitro and in vivo. Int. J. Nanomedicine *8*, 2985–2995.

Radomsky, M.L., Thompson, A.Y., Spiro, R.C., and Poser, J.W. (1998). Potential role of fibroblast growth factor in enhancement of fracture healing. Clin. Orthop. Relat. Res. S283-93.

Raftery, R., O'Brien, F.J., and Cryan, S.-A. (2013). Chitosan for gene delivery and orthopedic tissue engineering applications. Molecules *18*, 5611–5647.

Raftery, R.M., Tierney, E.G., Curtin, C.M., Cryan, S.A., and O'Brien, F.J. (2015). Development of a gene-activated scaffold platform for tissue engineering applications using chitosan-pDNA nanoparticles on collagen-based scaffolds. J. Control. Release *210*, 84–94.

Raisin, S., Belamie, E., and Morille, M. (2016). Non-viral gene activated matrices for mesenchymal stem cells based tissue engineering of bone and cartilage. Biomaterials *104*, 223–237.

Reginster, J.Y. (2002). The prevalence and burden of arthritis. Rheumatology (Oxford). *41 Supp 1*, 3–6.

Rey-Rico, A., Babicz, H., Madry, H., Concheiro, A., Alvarez-Lorenzo, C., and Cucchiarini, M. (2017). Supramolecular polypseudorotaxane gels for controlled delivery of rAAV vectors in human mesenchymal stem cells for regenerative medicine. Int. J. Pharm. *531*, 492–503.

Riley, M.K., Vermerris, W., and Vermerris, W. (2017). Recent Advances in Nanomaterials for Gene Delivery-A Review. Nanomater. (Basel, Switzerland) *7*.

Rizk, A., and Rabie, B.M. (2013). Electroporation for Transfection and Differentiation of Dental Pulp Stem Cells. Biores. Open Access *2*, 155–162.

Rodríguez, J.P., González, M., Ríos, S., and Cambiazo, V. (2004). Cytoskeletal organization of human mesenchymal stem cells (MSC) changes during their osteogenic differentiation. J. Cell. Biochem. *93*, 721–731.

Roman-Blas, J.A., Stokes, D.G., and Jimenez, S.A. (2007). Modulation of TGF-beta signaling by proinflammatory cytokines in articular chondrocytes. Osteoarthritis Cartilage *15*, 1367–1377.

Ronzière, M.C., Perrier, E., Mallein-Gerin, F., and Freyria, A.-M. (2010). Chondrogenic potential of bone marrow- and adipose tissue-derived adult human mesenchymal stem cells. Biomed. Mater. Eng. *20*, 145–158.

Roy, K., Wang, D., Hedley, M.L., and Barman, S.P. (2003). Gene delivery with in-situ crosslinking polymer networks generates long-term systemic protein expression. Mol. Ther. *7*, 401–408.

Sadr, N., Pippenger, B.E., Scherberich, A., Wendt, D., Mantero, S., Martin, I., and Papadimitropoulos, A. (2012). Enhancing the biological performance of synthetic polymeric materials by decoration with engineered, decellularized extracellular matrix. Biomaterials *33*, 5085–5093.

Samorezov, J.E., and Alsberg, E. (2015). Spatial regulation of controlled bioactive factor delivery for bone tissue engineering. Adv. Drug Deliv. Rev. *84*, 45–67.

Sano, A. (2003). Atelocollagen for protein and gene delivery. Adv. Drug Deliv. Rev. *55*, 1651–1677.

Santos, J.L., Pandita, D., Rodrigues, J., Pêgo, A.P., Granja, P.L., and Tomás, H. (2011). Non-viral gene delivery to mesenchymal stem cells: methods, strategies and application in bone tissue engineering and regeneration. Curr. Gene Ther. *11*, 46–57.

Saraf, A., and Mikos, A.G. (2006). Gene delivery strategies for cartilage tissue engineering. Adv. Drug Deliv. Rev. *58*, 592–603.

Sathy, B.N., Olvera, D., Gonzalez-Fernandez, T., Inne, G., Cunniffe, M., Pentlavalli, S., Chambers, P., Jeon, O., Alsberg, E., Mccarthy, H.O., et al. (2017). RALA complexed a-TCP nanoparticle delivery to mesenchymal stem cells induces bone formation in tissue engineered constructs in vitro and in vivo. J. Mater. Chem. B *5*, 1753–1764.

Scharstuhl, A., Schewe, B., Benz, K., Gaissmaier, C., Bühring, H.-J., and Stoop, R. (2007). Chondrogenic potential of human adult mesenchymal stem cells is independent of age or osteoarthritis etiology. Stem Cells *25*, 3244–3251.

Schillinger, U., Wexel, G., Hacker, C., Kullmer, M., Koch, C., Gerg, M., Vogt, S., Ueblacker, P., Tischer, T., Hensler, D., et al. (2008). A Fibrin Glue Composition as Carrier for Nucleic Acid Vectors. Pharm. Res. *25*, 2946–2962.

Schliephake, H. (2010). Application of bone growth factors—the potential of different carrier systems. Oral Maxillofac. Surg. *14*, 17–22.

Schmitt, B., Ringe, J., Häupl, T., Notter, M., Manz, R., Burmester, G.R., Sittinger, M., and Kaps, C. (2003). BMP2 initiates chondrogenic lineage development of adult human mesenchymal stem cells in high-density culture. Differentiation *71*, 567–577.

Schulz, R.M., Zscharnack, M., Hanisch, I., Geiling, M., Hepp, P., and Bader, A. (2008). Cartilage tissue engineering by collagen matrix associated bone marrow derived mesenchymal stem cells. Biomed. Mater. Eng. *18*, S55-70.

Schütz, K., Placht, A.-M., Paul, B., Brüggemeier, S., Gelinsky, M., and Lode, A. (2015). Three-dimensional plotting of a cell-laden alginate/methylcellulose blend: towards biofabrication of

tissue engineering constructs with clinically relevant dimensions. J. Tissue Eng. Regen. Med. *4*, n/a-n/a.

Schuurman, W., Levett, P.A., Pot, M.W., van Weeren, P.R., Dhert, W.J.A. a, Hutmacher, D.W., Melchels, F.P.W.W., Klein, T.J., and Malda, J. (2013). Gelatin-methacrylamide hydrogels as potential biomaterials for fabrication of tissue-engineered cartilage constructs. Macromol. Biosci. *13*, 551–561.

Schwabe, P., Greiner, S., Ganzert, R., Eberhart, J., Dähn, K., Stemberger, A., Plank, C., Schmidmaier, G., Wildemann, B., and Wildemann, B. (2012). Effect of a Novel Nonviral Gene Delivery of BMP-2 on Bone Healing. Sci. World J. *2012*, 1–9.

Scotti, C., Piccinini, E., Takizawa, H., Todorov, A., Bourgine, P., Papadimitropoulos, A., Barbero, A., Manz, M.G., and Martin, I. (2013). Engineering of a functional bone organ through endochondral ossification. Proc. Natl. Acad. Sci. U. S. A. *110*, 3997–4002.

Segura, T., Chung, P.H., and Shea, L.D. (2005). DNA delivery from hyaluronic acid-collagen hydrogels via a substrate-mediated approach. Biomaterials *26*, 1575–1584.

Shanmugarajan, T.S., Kim, B., Lee, H., and Im, G. (2011). Growth Factors and Signaling Pathways in the Chondrogenic Differentiation of Mesenchymal Stem Cells. Tissue Eng. Regen. Med. *8*, 292–299.

Shapiro, G., Kallai, I., Sheyn, D., Tawackoli, W., Koh, Y. Do, Bae, H., Trietel, T., Goldbart, R., Kost, J., Gazit, Z., et al. (2014). Ultrasound-mediated transgene expression in endogenous stem cells recruited to bone injury sites. Polym. Adv. Technol. *25*, 525–531.

Sheehy, E.J., Buckley, C.T., and Kelly, D.J. (2012). Oxygen tension regulates the osteogenic, chondrogenic and endochondral phenotype of bone marrow derived mesenchymal stem cells. Biochem. Biophys. Res. Commun. *417*, 305–310.

Sheehy, E.J., Vinardell, T., Buckley, C.T., and Kelly, D.J. (2013). Engineering osteochondral constructs through spatial regulation of endochondral ossification. Acta Biomater. *9*, 5484–5492.

Sheehy, E.J., Mesallati, T., Vinardell, T., and Kelly, D.J. (2014a). Engineering cartilage or endochondral bone: A comparison of different naturally derived hydrogels. Acta Biomater. *13*, 245–253.

Sheehy, E.J., Vinardell, T., Toner, M.E., Buckley, C.T., and Kelly, D.J. (2014b). Altering the architecture of tissue engineered hypertrophic cartilaginous grafts facilitates vascularisation and accelerates mineralisation. PLoS One *9*.

Shen, B., Wei, A., Tao, H., Diwan, A.D., and Ma, D.D.F. (2009). BMP-2 enhances TGF-beta3-mediated chondrogenic differentiation of human bone marrow multipotent mesenchymal stromal cells in alginate bead culture. Tissue Eng. Part A *15*, 1311–1320.

Shi, J., Zhang, X., Zhu, J., Pi, Y., Hu, X., Zhou, C., and Ao, Y. (2013). Nanoparticle delivery of the bone morphogenetic protein 4 gene to adipose-derived stem cells promotes articular cartilage repair in vitro and in vivo. Arthroscopy *29*, 2001–2011.

Shim, J.-H., Kim, S.E., Park, J.Y., Kundu, J., Kim, S.W., Kang, S.S., and Cho, D.-W. (2014). Three-Dimensional Printing of rhBMP-2-Loaded Scaffolds with Long-Term Delivery for Enhanced Bone Regeneration in a Rabbit Diaphyseal Defect. Tissue Eng. Part A *20*, 1980–1992.

Shimomura, K., Moriguchi, Y., Murawski, C.D., Yoshikawa, H., and Nakamura, N. (2014). Osteochondral tissue engineering with biphasic scaffold: current strategies and techniques.

Tissue Eng. Part B. Rev. *20*, 468–476.

Shukunami, C., Iyama, K., Inoue, H., and Hiraki, Y. (1999). Spatiotemporal pattern of the mouse chondromodulin-I gene expression and its regulatory role in vascular invasion into cartilage during endochondral bone formation. Int J Dev Biol *43*, 39–49.

Simmons, C. a., Alsberg, E., Hsiong, S., Kim, W.J., and Mooney, D.J. (2004). Dual growth factor delivery and controlled scaffold degradation enhance in vivo bone formation by transplanted bone marrow stromal cells. Bone *35*, 562–569.

Smith, B.D., and Grande, D.A. (2015). The current state of scaffolds for musculoskeletal regenerative applications. Nat. Rev. Rheumatol. *11*, 213–222.

Somia, N., and Verma, I.M. (2000). Gene therapy: trials and tribulations. Nat. Rev. Genet. *1*, 91–99.

Somoza, R.A., Welter, J.F., Correa, D., and Caplan, A.I. (2014). Chondrogenic differentiation of Mesenchymal Stem Cells: challenges and unfulfilled expectations. Tissue Eng. Part B. Rev. *20*, 1–50.

Sonowal, H., Kumar, A., Bhattacharyya, J., Gogoi, P.K., and Jaganathan, B.G. (2013). Inhibition of actin polymerization decreases osteogeneic differentiation of mesenchymal stem cells through p38 MAPK pathway. J. Biomed. Sci. *20*, 71.

Steinert, A.F., Ghivizzani, S.C., Rethwilm, A., Tuan, R.S., Evans, C.H., and Nöth, U. (2007). Major biological obstacles for persistent cell-based regeneration of articular cartilage. Arthritis Res. Ther. *9*, 213.

Steinmetz, N.J., Aisenbrey, E.A., Westbrook, K.K., Qi, H.J., and Bryant, S.J. (2015). Mechanical loading regulates human MSC differentiation in a multi-layer hydrogel for osteochondral tissue engineering. Acta Biomater. *21*, 142–153.

Stilhano, R.S., Madrigal, J.L., Wong, K., Williams, P.A., Martin, P.K.M., Yamaguchi, F.S.M., Samoto, V.Y., Han, S.W., and Silva, E.A. (2016). Injectable alginate hydrogel for enhanced spatiotemporal control of lentivector delivery in murine skeletal muscle. J. Control. Release *237*, 42–49.

Stoeger, T., Proetzel, G.E., Welzel, H., Papadimitriou, A., Dony, C., Balling, R., and Hofmann, C. (2002). In situ gene expression analysis during BMP2-induced ectopic bone formation in mice shows simultaneous endochondral and intramembranous ossification. Growth Factors *20*, 197–210.

Street, J., Bao, M., deGuzman, L., Bunting, S., Peale, F. V, Ferrara, N., Steinmetz, H., Hoeffel, J., Cleland, J.L., Daugherty, A., et al. (2002). Vascular endothelial growth factor stimulates bone repair by promoting angiogenesis and bone turnover. Proc. Natl. Acad. Sci. U. S. A. *99*, 9656–9661.

Suh, J.S., Lee, J.Y., Choi, Y.S., Chong, P.C., and Park, Y.J. (2013). Peptide-mediated intracellular delivery of miRNA-29b for osteogenic stem cell differentiation. Biomaterials *34*, 4347–4359.

Suh, J.S., Lee, J.Y., Choi, Y.J., You, H.K., Hong, S.-D., Chung, C.P., and Park, Y.J. (2014). Intracellular delivery of cell-penetrating peptide-transcriptional factor fusion protein and its role in selective osteogenesis. Int. J. Nanomedicine *9*, 1153–1166.

Sun, X.D., Jeng, L., Bolliet, C., Olsen, B.R., and Spector, M. (2009). Non-viral endostatin plasmid transfection of mesenchymal stem cells via collagen scaffolds. Biomaterials *30*, 1222–1231.

Suri, S., and Walsh, D.A. (2012). Osteochondral alterations in osteoarthritis. Bone *51*, 204–211.

Taddei, L., Chiarugi, P., Brogelli, L., Cirri, P., Magnelli, L., Raugei, G., Ziche, M., Granger, H.J., Chiarugi, V., and Ramponi, G. (1999). Inhibitory Effect of Full-Length Human Endostatin on in Vitro Angiogenesis. Biochem. Biophys. Res. Commun. *263*, 340–345.

Tannous, B.A. (2009). Gaussia luciferase reporter assay for monitoring of biological processes in culture and in vivo. Nat. Protoc. *4*, 582–591.

Tchetina, E. V, Antoniou, J., Tanzer, M., Zukor, D.J., and Poole, a R. (2006). Transforming growth factor-beta2 suppresses collagen cleavage in cultured human osteoarthritic cartilage, reduces expression of genes associated with chondrocyte hypertrophy and degradation, and increases prostaglandin E(2) production. Am. J. Pathol. *168*, 131–140.

Tchetverikov, I., Verzijl, N., Huizinga, T.W., TeKoppele, J.M., Hanemaaijer, R., and DeGroot, J. Active MMPs captured by alpha 2 macroglobulin as a marker of disease activity in rheumatoid arthritis. Clin. Exp. Rheumatol. *21*, 711–718.

Thirumala, S., Gimble, J., and Devireddy, R. (2013). Methylcellulose Based Thermally Reversible Hydrogel System for Tissue Engineering Applications. Cells *2*, 460–475.

Thomas, M., and Klibanov, A.M. (2002). Enhancing polyethylenimine's delivery of plasmid DNA into mammalian cells. Proc. Natl. Acad. Sci. U. S. A. *99*, 14640–14645.

Thomas, C.E., Ehrhardt, A., and Kay, M. a (2003). Progress and problems with the use of viral vectors for gene therapy. Nat. Rev. Genet. *4*, 346–358.

Thomas, M., Lu, J.J., Zhang, C., Chen, J., and Klibanov, A.M. (2007). Identification of novel superior polycationic vectors for gene delivery by high-throughput synthesis and screening of a combinatorial library. Pharm. Res. *24*, 1564–1571.

Thompson, E.M., Matsiko, A., Farrell, E., Kelly, D.J., and O'Brien, F.J. (2014). Recapitulating endochondral ossification: a promising route to in vivo bone regeneration. J. Tissue Eng. Regen. Med. *9*, 889–902.

Tierney, E.G., Duffy, G.P., Hibbitts, A.J., Cryan, S.-A., and O'Brien, F.J. (2012). The development of non-viral gene-activated matrices for bone regeneration using polyethyleneimine (PEI) and collagen-based scaffolds. J. Control. Release *158*, 304–311.

Tierney, E.G., McSorley, K., Hastings, C.L., Cryan, S.-A., O'Brien, T., Murphy, M.J., Barry, F.P., O'Brien, F.J., and Duffy, G.P. (2013). High levels of ephrinB2 over-expression increases the osteogenic differentiation of human mesenchymal stem cells and promotes enhanced cell mediated mineralisation in a polyethyleneimine-ephrinB2 gene-activated matrix. J. Control. Release *165*, 173–182.

Tortorella, M.D., Arner, E.C., Hills, R., Easton, A., Korte-Sarfaty, J., Fok, K., Wittwer, A.J., Liu, R.-Q., and Malfait, A.-M. (2004). Alpha2-macroglobulin is a novel substrate for ADAMTS-4 and ADAMTS-5 and represents an endogenous inhibitor of these enzymes. J. Biol. Chem. *279*, 17554–17561.

Trentin, D., Hall, H., Wechsler, S., and Hubbell, J.A. (2006). Peptide-matrix-mediated gene transfer of an oxygen-insensitive hypoxia-inducible factor-1alpha variant for local induction of angiogenesis. Proc. Natl. Acad. Sci. U. S. A. *103*, 2506–2511.

Tuan, R.S., Boland, G., and Tuli, R. (2003). Adult mesenchymal stem cells and cell-based tissue engineering. Arthritis Res. Ther. *5*, 32–45.

Türk, M., Dinçer, S., and Pişkin, E. (2007). Smart and cationic poly(NIPA)/PEI block copolymers as non-viral vectors:in vitro andin vivo transfection studies. J. Tissue Eng. Regen. Med. *1*, 377–

388.

Uccelli, A., Moretta, L., and Pistoia, V. (2008). Mesenchymal stem cells in health and disease. Nat. Rev. Immunol. *8*, 726–736.

Ueblacker, P., Wagner, B., Krüger, a, Vogt, S., DeSantis, G., Kennerknecht, E., Brill, T., Hillemanns, M., Salzmann, G.M., Imhoff, a B., et al. (2004). Inducible nonviral gene expression in the treatment of osteochondral defects. Osteoarthritis Cartilage *12*, 711–719.

Ueblacker, P., Wagner, B., Vogt, S., Salzmann, G., Wexel, G., Krüger, A., Plank, C., Brill, T., Specht, K., Hennig, T., et al. (2007). In vivo analysis of retroviral gene transfer to chondrocytes within collagen scaffolds for the treatment of osteochondral defects. Biomaterials *28*, 4480–4487.

Urello, M.A., Kiick, K.L., and Sullivan, M.O. (2014). A CMP-based method for tunable, cell-mediated gene delivery from collagen scaffolds. J. Mater. Chem. B *2*, 8174–8185.

Vahle, J.L., Sato, M., Long, G.G., Young, J.K., Francis, P.C., Engelhardt, J.A., Westmore, M.S., Ma, Y.L., and Nold, J.B. (2002). Skeletal Changes in Rats Given Daily Subcutaneous Injections of Recombinant Human Parathyroid Hormone (1-34) for 2 Years and Relevance to Human Safety. Toxicol. Pathol. *30*, 312–321.

Vangsness, C.T., Farr, J., Boyd, J., Dellaero, D.T., Mills, C.R., and LeRoux-Williams, M. (2014). Adult Human Mesenchymal Stem Cells Delivered via Intra-Articular Injection to the Knee Following Partial Medial Meniscectomy. J. Bone Jt. Surgery-American Vol. *96*, 90–98.

Vega, A., Martín-Ferrero, M.A., Del Canto, F., Alberca, M., García, V., Munar, A., Orozco, L., Soler, R., Fuertes, J.J., Huguet, M., et al. (2015). Treatment of Knee Osteoarthritis With Allogeneic Bone Marrow Mesenchymal Stem Cells: A Randomized Controlled Trial. Transplantation *99*, 1681–1690.

Vega, R.B., Matsuda, K., Oh, J., Barbosa, A.C., Yang, X., Meadows, E., McAnally, J., Pomajzl, C., Shelton, J.M., Richardson, J.A., et al. (2004). Histone deacetylase 4 controls chondrocyte hypertrophy during skeletogenesis. Cell *119*, 555–566.

Venkatesan, J.K., Ekici, M., Madry, H., Schmitt, G., Kohn, D., and Cucchiarini, M. (2012). SOX9 gene transfer via safe, stable, replication-defective recombinant adeno-associated virus vectors as a novel, powerful tool to enhance the chondrogenic potential of human mesenchymal stem cells. Stem Cell Res. Ther. *3*, 22.

Venkatesan, J.K., Rey-Rico, A., Schmitt, G., Wezel, A., Madry, H., and Cucchiarini, M. (2013). rAAV-mediated overexpression of TGF-β stably restructures human osteoarthritic articular cartilage in situ. J. Transl. Med. *11*, 211.

Veronesi, F., Giavaresi, G., Tschon, M., Borsari, V., Nicoli Aldini, N., and Fini, M. (2013). Clinical Use of Bone Marrow, Bone Marrow Concentrate, and Expanded Bone Marrow Mesenchymal Stem Cells in Cartilage Disease. Stem Cells Dev. *22*, 181–192.

Vial, S., Reis, R.L., and Oliveira, J.M. (2017). Recent advances using gold nanoparticles as a promising multimodal tool for tissue engineering and regenerative medicine. Curr. Opin. Solid State Mater. Sci. *21*, 92–112.

Vinardell, T., Sheehy, E.J., Buckley, C.T., and Kelly, D.J. (2012). A comparison of the functionality and in vivo phenotypic stability of cartilaginous tissues engineered from different stem cell sources. Tissue Eng. Part A *18*, 1161–1170.

Visser, J., Melchels, F.P.W., Jeon, J.E., van Bussel, E.M., Kimpton, L.S., Byrne, H.M., Dhert, W.J.A., Dalton, P.D., Hutmacher, D.W., and Malda, J. (2015). Reinforcement of hydrogels using three-

dimensionally printed microfibres. Nat. Commun. *6*, 6933.

Vo, T.T.N., Kasper, F.K., and Mikos, A.G.A. (2012). Strategies for controlled delivery of growth factors and cells for bone regeneration. Adv. Drug Deliv. Rev. *64*, 1292–1309.

de Vries-van Melle, M.L., Tihaya, M.S., Kops, N., Koevoet, W.J.L.M., Murphy, J.M., Verhaar, J.A.N., Alini, M., Eglin, D., and van Osch, G.J.V.M. (2014). Chondrogenic differentiation of human bone marrow-derived mesenchymal stem cells in a simulated osteochondral environment is hydrogel dependent. Eur. Cell. Mater. *27*, 112–123.

W. Mark Saltzman (1999). Delivering tissue regeneration. Nat. Biotechnol. *17*, 534–535.

Wadia, J.S., and Dowdy, S.F. (2002). Protein transduction technology. Curr. Opin. Biotechnol. *13*, 52–56.

Waehler, R., Russell, S.J., and Curiel, D.T. (2007). Engineering targeted viral vectors for gene therapy. Nat. Rev. Genet. *8*, 573–587.

Wagner, D.E., and Bhaduri, S.B. (2012). Progress and Outlook of Inorganic Nanoparticles for Delivery of Nucleic Acid Sequences Related to Orthopedic Pathologies: A Review. Tissue Eng. Part B Rev. *18*, 1–14.

Wallace, I.J., Worthington, S., Felson, D.T., Jurmain, R.D., Wren, K.T., Maijanen, H., Woods, R.J., and Lieberman, D.E. (2017). Knee osteoarthritis has doubled in prevalence since the mid-20th century. Proc. Natl. Acad. Sci. *114*, 9332–9336.

Walsh, D.P., Heise, A., O'Brien, F.J., and Cryan, S.-A. (2017). An efficient, non-viral dendritic vector for gene delivery in tissue engineering. Gene Ther. *24*, 681–691.

Wang, Q.-W., Chen, Z.-L., and Piao, Y.-J. (2005). Mesenchymal stem cells differentiate into tenocytes by bone morphogenetic protein (BMP) 12 gene transfer. J. Biosci. Bioeng. *100*, 418–422.

Wang, Q.F., Huang, Y., He, G.C., Wang, H.S., Chen, Z.H., Cai, X.H., Xie, Y.H., and Liu, Q. (2017). Osteoblast differentiation of rabbit adipose-derived stem cells by polyethylenimine-mediated BMP-2 gene transfection in vitro. Genet. Mol. Res. *16*.

Wang, W., Li, B., Li, Y., Jiang, Y., Ouyang, H., and Gao, C. (2010). In vivo restoration of full-thickness cartilage defects by poly(lactide-co-glycolide) sponges filled with fibrin gel, bone marrow mesenchymal stem cells and DNA complexes. Biomaterials *31*, 5953–5965.

Wang, W., Li, W., Ou, L., Flick, E., Mark, P., Nesselmann, C., Lux, C.A., Gatzen, H.H., Kaminski, A., Liebold, A., et al. (2011). Polyethylenimine-mediated gene delivery into human bone marrow mesenchymal stem cells from patients. J. Cell. Mol. Med. *15*, 1989–1998.

Wang, W., Li, W., Ma, N., and Steinhoff, G. (2013). Non-viral gene delivery methods. Curr. Pharm. Biotechnol. *14*, 46–60.

Wang, X., Hélary, C., and Coradin, T. (2015). Local and sustained gene delivery in silica-collagen nanocomposites. ACS Appl. Mater. Interfaces *7*, 2503–2511.

Wegman, F., Bijenhof, A., Schuijff, L., Oner, F.C., Dhert, W.J. a, and Alblas, J. (2011). Osteogenic differentiation as a result of BMP-2 plasmid DNA based gene therapy in vitro and in vivo. Eur. Cell. Mater. *21*, 230–242.

Wegman, F., van der Helm, Y., Öner, F.C., Dhert, W.J. a, and Alblas, J. (2013). Bone morphogenetic protein-2 plasmid DNA as a substitute for bone morphogenetic protein-2 protein in bone tissue engineering. Tissue Eng. Part A *19*, 2686–2692.

Wegman, F., Geuze, R.E., van der Helm, Y.J., Cumhur Öner, F., Dhert, W.J.A., and Alblas, J. (2014). Gene delivery of bone morphogenetic protein-2 plasmid DNA promotes bone formation in a large animal model. J. Tissue Eng. Regen. Med. *8*, 763–770.

Wehling, P., Reinecke, J., Baltzer, A.W.A., Granrath, M., Schulitz, K.P., Schultz, C., Krauspe, R., Whiteside, T.W., Elder, E., Ghivizzani, S.C., et al. (2009). Clinical responses to gene therapy in joints of two subjects with rheumatoid arthritis. Hum. Gene Ther. *20*, 97–101.

Wehrhan, F., Amann, K., Molenberg, A., Lutz, R., Neukam, F.W., and Schlegel, K.A. (2012). PEG matrix enables cell-mediated local BMP-2 gene delivery and increased bone formation in a porcine critical size defect model of craniofacial bone regeneration. Clin. Oral Implants Res. *23*, 805–813.

Weimer, A., Madry, H., Venkatesan, J.K., Schmitt, G., Frisch, J., Wezel, A., Jung, J., Kohn, D., Terwilliger, E.F., Trippel, S.B., et al. (2012). Benefits of recombinant adeno-associated virus (rAAV)-mediated insulinlike growth factor I (IGF-I) overexpression for the long-term reconstruction of human osteoarthritic cartilage by modulation of the IGF-I axis. Mol. Med. *18*, 346–358.

Welzel, T., Radtke, I., Meyer-Zaika, W., Heumann, R., and Epple, M. (2004). Transfection of cells with custom-made calcium phosphate nanoparticles coated with DNA. J. Mater. Chem. *14*, 2213–2217.

Whittlesey, K.J., and Shea, L.D. (2006). Nerve growth factor expression by PLG-mediated lipofection. Biomaterials *27*, 2477–2486.

Williams, D.A., and Thrasher, A.J. (2014). Concise review: lessons learned from clinical trials of gene therapy in monogenic immunodeficiency diseases. Stem Cells Transl. Med. *3*, 636–642.

Wong, G.C., Tang, J.X., Lin, A., Li, Y., Janmey, P.A., and Safinya, C.R. (2000). Hierarchical self-assembly of F-actin and cationic lipid complexes: stacked three-layer tubule networks. Science *288*, 2035–2039.

Woolf, A.D., and Pfleger, B. (2003). Burden of major musculoskeletal conditions. Bull. World Health Organ. *81*, 646–656.

Wübbenhorst, D., Dumler, K., Wagner, B., Wexel, G., Imhoff, A., Gansbacher, B., Vogt, S., and Anton, M. (2010). Tetracycline-regulated bone morphogenetic protein 2 gene expression in lentivirally transduced primary rabbit chondrocytes for treatment of cartilage defects. Arthritis Rheum. *62*, 2037–2046.

Wyman, T.B., Nicol, F., Zelphati, O., Scaria, P. V., Plank, C., and Szoka, F.C. (1997). Design, Synthesis, and Characterization of a Cationic Peptide That Binds to Nucleic Acids and Permeabilizes Bilayers [†]. Biochemistry *36*, 3008–3017.

Xiang, S., Su, J., Tong, H., Yang, F., Tong, W., Yuan, W., Wu, F., Wang, C., Jin, T., Dai, K., et al. (2012). Biscarbamate cross-linked low molecular weight PEI for delivering IL-1 receptor antagonist gene to synoviocytes for arthritis therapy. Biomaterials *33*, 6520–6532.

Xing, S.-C., Liu, Y., Feng, Y., Jiang, C., Hu, Y.-Q., Sun, W., Wang, X.-H., Wei, Z.-Y., Qi, M., Liu, J., et al. (2015). Chondrogenic differentiation of ChM-I gene transfected rat bone marrow-derived mesenchymal stem cells on 3-dimensional poly (L-lactic acid) scaffold for cartilage engineering. Cell Biol. Int. *39*, 300–309.

Xu, Y., and Szoka, F.C. (1996). Mechanism of DNA release from cationic liposome/DNA complexes used in cell transfection. Biochemistry *35*, 5616–5623.

Xu, T., Binder, K.W., Albanna, M.Z., Dice, D., Zhao, W., Yoo, J.J., and Atala, A. (2013). Hybrid printing of mechanically and biologically improved constructs for cartilage tissue engineering applications. Biofabrication *5*, 15001.

Xu, X., Qiu, S., Zhang, Y., Yin, J., and Min, S. (2017). PELA microspheres with encapsulated arginine–chitosan/pBMP-2 nanoparticles induce pBMP-2 controlled-release, transfected osteoblastic progenitor cells, and promoted osteogenic differentiation. Artif. Cells, Nanomedicine, Biotechnol. *45*, 330–339.

Xu, Z.P., Zeng, Q.H., Lu, G.Q., and Yu, A.B. (2006). Inorganic nanoparticles as carriers for efficient cellular delivery. Chem. Eng. Sci. *61*, 1027–1040.

Yamashita, S., Andoh, M., Ueno-Kudoh, H., Sato, T., Miyaki, S., and Asahara, H. (2009). Sox9 directly promotes Bapx1 gene expression to repress Runx2 in chondrocytes. Exp. Cell Res. *315*, 2231–2240.

Yan, M., Liu, X., Dang, Q., Huang, H., Yang, F., and Li, Y. (2017). Intra-Articular Injection of Human Synovial Membrane-Derived Mesenchymal Stem Cells in Murine Collagen-Induced Arthritis: Assessment of Immunomodulatory Capacity In Vivo. Stem Cells Int. *2017*, 1–12.

Yang, H.Y., Vonk, L.A., Licht, R., Van Boxtel, A.M.G., Bekkers, J.E.J., Kragten, A.H.M., Hein, S., Varghese, O.P., Howard, K.A., Cumhur Öner, F., et al. (2014). Cell type and transfection reagent-dependent effects on viability, cell content, cell cycle and inflammation of RNAi in human primary mesenchymal cells. Eur. J. Pharm. Sci. *53*, 35–44.

Yao, Y., He, Y., Guan, Q., and Wu, Q. (2014). A tetracycline expression system in combination with Sox9 for cartilage tissue engineering. Biomaterials *35*, 1898–1906.

Yelin, E., Weinstein, S., and King, T. (2016). The burden of musculoskeletal diseases in the United States. Semin. Arthritis Rheum. *46*, 259–260.

Yi, C., Liu, D., Fong, C.-C., Zhang, J., and Yang, M. (2010). Gold Nanoparticles Promote Osteogenic Differentiation of Mesenchymal Stem Cells through p38 MAPK Pathway. ACS Nano *4*, 6439–6448.

Yin, H., Kanasty, R.L., Eltoukhy, A. a, Vegas, A.J., Dorkin, J.R., and Anderson, D.G. (2014). Non-viral vectors for gene-based therapy. Nat. Rev. Genet. *15*, 541–555.

Ylä-Herttuala, S. (2012). Endgame: glybera finally recommended for approval as the first gene therapy drug in the European union. Mol. Ther. *20*, 1831–1832.

Yoo, J., Barthel, T., and Nishimura, K. (1998). The chondrogenic potential of human bone-marrow-derived mesenchymal progenitor cells. J. Bone Jt. Surg. *80A*, 1745–1759.

Yoon, B.S., Ovchinnikov, D.A., Yoshii, I., Mishina, Y., Behringer, R.R., and Lyons, K.M. (2005). Bmpr1a and Bmpr1b have overlapping functions and are essential for chondrogenesis in vivo. Proc. Natl. Acad. Sci. U. S. A. *102*, 5062–5067.

Yu, M., Lei, B., Gao, C., Yan, J., and Ma, P.X. (2017). Optimizing surface-engineered ultra-small gold nanoparticles for highly efficient miRNA delivery to enhance osteogenic differentiation of bone mesenchymal stromal cells. Nano Res. *10*, 49–63.

Yu, Y.Y., Lieu, S., Lu, C., and Colnot, C. (2010). Bone morphogenetic protein 2 stimulates endochondral ossification by regulating periosteal cell fate during bone repair. Bone *47*, 65–73.

Zachos, T., Diggs, A., Weisbrode, S., Bartlett, J., and Bertone, A. (2007). Mesenchymal stem cell-mediated gene delivery of bone morphogenetic protein-2 in an articular fracture model. Mol. Ther. *15*, 1543–1550.

Zara, J.N., Siu, R.K., Zhang, X., Shen, J., Ngo, R., Lee, M., Li, W., Chiang, M., Chung, J., Kwak, J., et al. (2011). High doses of bone morphogenetic protein 2 induce structurally abnormal bone and inflammation in vivo. Tissue Eng. Part A *17*, 1389–1399.

Zelenin, A. V, Kolesnikov, V.A., Tarasenko, O.A., Shafei, R.A., Zelenina, I.A., Mikhailov, V. V, Semenova, M.L., Kovalenko, D. V, Artemyeva, O. V, Ivaschenko, T.E., et al. (1997). Bacterial beta-galactosidase and human dystrophin genes are expressed in mouse skeletal muscle fibers after ballistic transfection. FEBS Lett. *414*, 319–322.

Zhang, F., Su, K., Fang, Y., Sandhya, S., and Wang, D.-A. (2015a). A mixed co-culture of mesenchymal stem cells and transgenic chondrocytes in alginate hydrogel for cartilage tissue engineering. J. Tissue Eng. Regen. Med. *9*, 77–84.

Zhang, H., Leng, P., and Zhang, J. (2009). Enhanced Meniscal Repair by Overexpression of hIGF-1 in a Full-thickness Model. Clin. Orthop. Relat. Res. *467*, 3165–3174.

Zhang, P., Zhong, Z.-H., Yu, H.-T., and Liu, B. (2015b). Exogenous expression of IL-1Ra and TGF-β1 promotes in vivo repair in experimental rabbit osteoarthritis. Scand. J. Rheumatol. *44*, 404–411.

Zhang, X., Prasadam, I., Fang, W., Crawford, R., and Xiao, Y. (2016). Chondromodulin-1 ameliorates osteoarthritis progression by inhibiting HIF-2α activity. Osteoarthr. Cartil. *24*, 1970–1980.

Zhao, L., Kutikov, A., Shen, J., Duan, C., Song, J., and Han, G. (2013). Stem cell labeling using polyethylenimine conjugated (α-NaYbF4:Tm3+)/CaF2 upconversion nanoparticles. Theranostics *3*, 249–257.

Zhao, Q.-Q., Chen, J.-L., Lv, T.-F., He, C.-X., Tang, G.-P., Liang, W.-Q., Tabata, Y., and Gao, J.-Q. (2009). N/P ratio significantly influences the transfection efficiency and cytotoxicity of a polyethylenimine/chitosan/DNA complex. Biol. Pharm. Bull. *32*, 706–710.

Zhao, X., Li, X., Zhao, Y., Cheng, Y., Yang, Y., Fang, Z., Xie, Y., Liu, Y., Chen, Y., Ouyang, Y., et al. (2017). Immune Activities of Polycationic Vectors for Gene Delivery. Front. Pharmacol. *8*, 510.

Zheng, J., Manuel, W.S., and Hornsby, P.J. (2000). Transfection of Cells Mediated by Biodegradable Polymer Materials with Surface-Bound Polyethyleneimine. Biotechnol. Prog. *16*, 254–257.

Zheng, Q., Wang, Y., and Gu, X. (2005). Wild-type Smad3 gene enhances the osteoblastic differentiation of rat bone marrow-derived mesenchymal stem cells in vitro. J. Huazhong Univ. Sci. Technolog. Med. Sci. *25*, 674–678.

Zou, B., Liu, Y., Luo, X., Chen, F., Guo, X., and Li, X. (2012). Electrospun fibrous scaffolds with continuous gradations in mineral contents and biological cues for manipulating cellular behaviors. Acta Biomater. *8*, 1576–1585.

Zuo, G., Wan, Y., Meng, X., Zhao, Q., Ren, K., Jia, S., and Wang, J. (2011). Synthesis and characterization of a lamellar hydroxyapatite/DNA nanohybrid. Mater. Chem. Phys. *126*, 470–475.
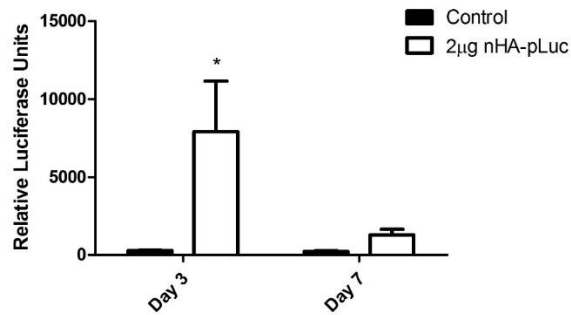
APPENDIX (A)

Fig.A.1. Luciferase expression at day 3 and 7 of MSCs transfected in 2D using nHA nanoparticles complexed to 2µg of pLuc; (*) denotes significance (n=3, p<0.05) in comparison to the non-transfected control.
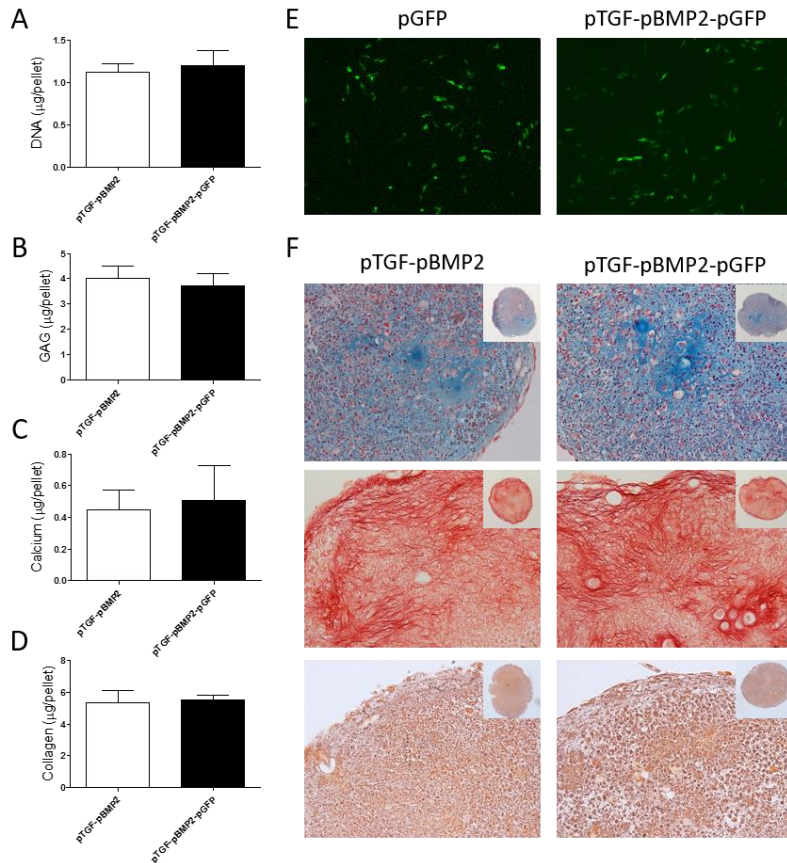

Fig.A.2. Comparison of gene delivery of pTGF-pBMP2 and pTGF-pBMP-pGFP in chondrogenesis of MSCs. Biochemical quantification of DNA (A), GAG (B), calcium (C) and collagen (D) deposition after 28 days of in vitro culture (µg/pellet). (E) Imaging of GFP positive cells in pGFP and pTGF-pBMP-pGFP transfected groups at day 1 after transfection. (F) Histological analysis of GAG, collagen and calcium deposition.
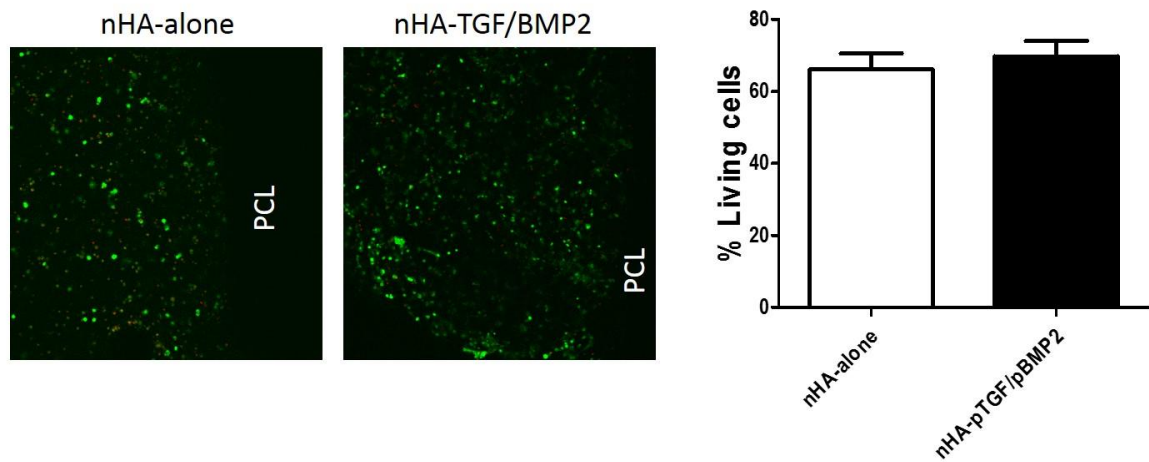
Fig.A.3. Cells remain viable within 3D bioprinted constructs containing pDNA encoding for TGF-β3 and BMP2. Quantification indicated approximately 68% viable cells 24 hours post bioprinting.
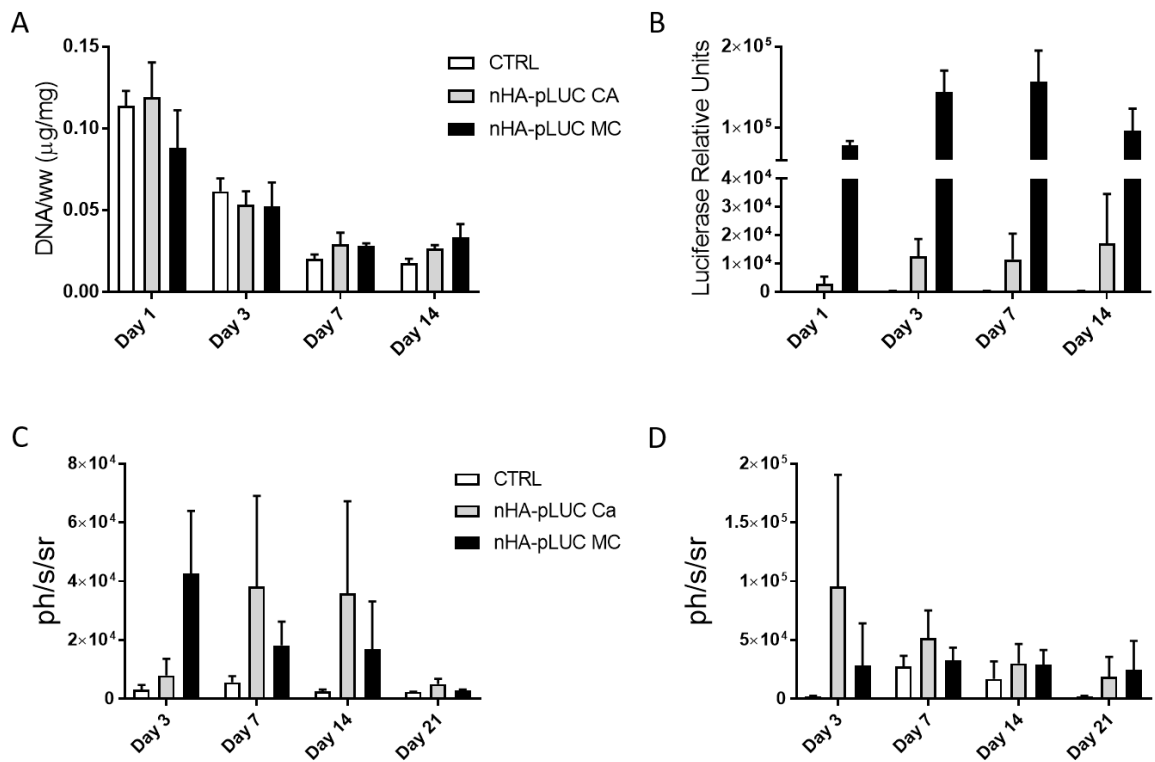

Fig.A.4. In vitro and in vivo nHA-pLUC gene delivery in ALG-MC and ALG-Ca gels. Quantification of DNA/ww (A) and luciferase expression (B) levels in 3D printed control and gene activated hydrogels at day 1, 3, 7 and 14 of in vitro culture. Quantification of bioluminescence in ph/s/sr in the acellular (C) and cell-laden (D) control and gene activated gels at day 3, 7, 14 and 21 after in vivo implantation.
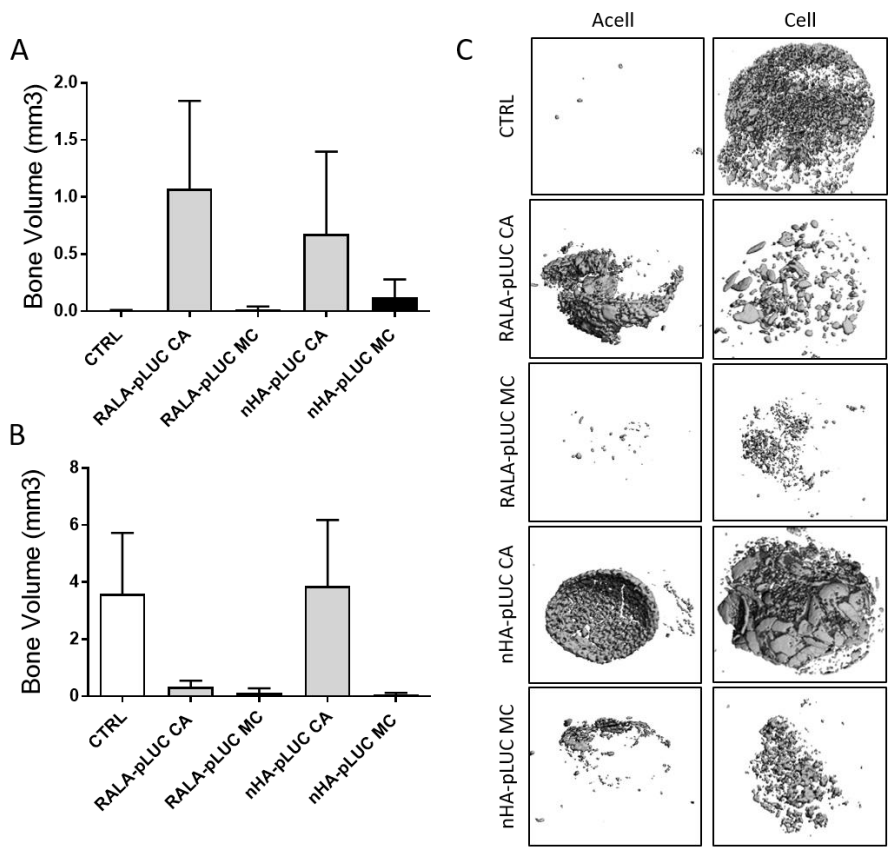
Fig.A.5. In vivo mineralization of the acellular and cell laden control and gene activated hydrogels. Bone volume quantification in the acellular (A) and cellular (B) control and gene activated constructs after 3 weeks of in vivo implantation. (C) MicroCT images of acellular and cellular control and gene activated constructs after 3 weeks of in vivo implantation.
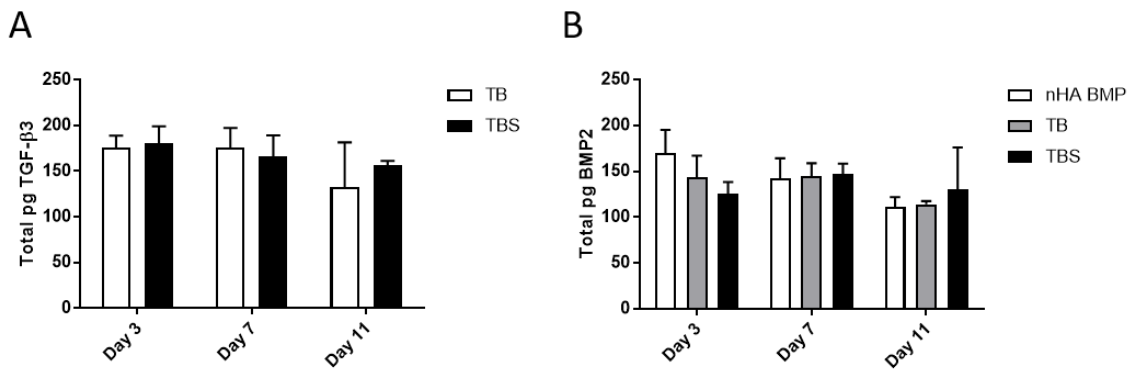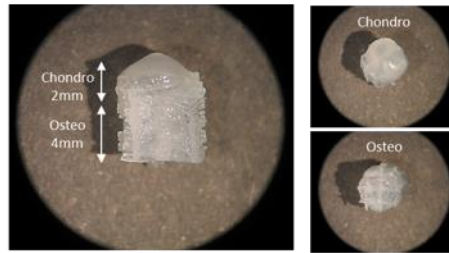

Fig.A.6. ELISA Protein expression quantification of TGF-ß3 (A) and BMP2 (B) in the media of gene activated 3D printed constructs containing MSCs and either nHA-pBMP2 (nHA-BMP), RALA-pTGF-pBMP2 (TB) or RALA-pTGF-pBMP2-pSOX9 (TBS).
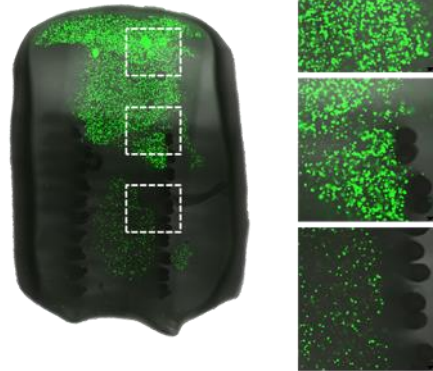
Fig.A.7. (A) Macroscopic appearance of the bilayer constructs at day 1 after fabrication. (B) Live/dead imaging of the bilayered constructs 1 day after fabrication.